

General Disclaimer

One or more of the Following Statements may affect this Document

- This document has been reproduced from the best copy furnished by the organizational source. It is being released in the interest of making available as much information as possible.
- This document may contain data, which exceeds the sheet parameters. It was furnished in this condition by the organizational source and is the best copy available.
- This document may contain tone-on-tone or color graphs, charts and/or pictures, which have been reproduced in black and white.
- This document is paginated as submitted by the original source.
- Portions of this document are not fully legible due to the historical nature of some of the material. However, it is the best reproduction available from the original submission.

AIRCRAFT GAS TURBINE LOW-POWER EMISSIONS REDUCTION TECHNOLOGY PROGRAM

FINAL REPORT

OCTOBER 1978

by

W.J. Dodds

C.C. Gleason

D.W. Bahr

GENERAL ELECTRIC COMPANY

(NASA-CR-135434) AIRCRAFT GAS TURBINE
LOW-POWER EMISSIONS REDUCTION TECHNOLOGY
PROGRAM Final Report (General Electric Co.)
161 p HC A08/MF A01 CSCL 21E

N78-32097

G3/07 31668
Unclas

Prepared For

National Aeronautics and Space Administration



NASA-Lewis Research Center
NAS3-20580

FOREWORD

The work described herein was conducted by General Electric Company, Aircraft Engine Group, under Contract NAS3-20580. The work was performed under the direction of the NASA Project Manager, Dr. Edward J. Mularz, Airbreathing Engines Division, NASA-Lewis Research Center.

Key General Electric contributors to this program were: A.L. Meyer, Program Manager; D.W. Bahr, Technical Program Manager; C.C. Gleason, Principal Investigator; W.J. Dodds, Combustor Evaluation; E.C. Vickers, Combustor Aerothermodynamic Design; H.M. Maclin, Combustor Mechanical Design; R.P. Crandall, Combustor Testing; and V.M. Cecil, Data Reduction and Graphics.

Subcontract support in catalytic reactor design and analysis was furnished by Engelhard Industries Division of Engelhard Minerals and Chemicals Corporation; key Engelhard contributors were Dr. R.V. Carrubba, Dr. R.M. Heck, Dr. I.T. Osgerby, and H. Hess.

PRECEDING PAGE BLANK NOT FILLED

TABLE OF CONTENTS

<u>Section</u>		<u>Page</u>
1.0	SUMMARY	1
2.0	INTRODUCTION	2
3.0	PROGRAM PLAN	4
4.0	DESIGN AND DEVELOPMENT APPROACHES	7
4.1	Combustor Concepts	7
4.1.1	Hot-Wall Liner Combustor	7
4.1.2	Recuperative-Cooled Liner Combustor	8
4.1.3	Catalytic Converter Combustor	11
4.1.4	Combustor Airflow Circuits	13
4.1.5	High-Power Operating Considerations	16
4.2	Baseline Combustor Descriptions	16
4.2.1	Common Design Features	18
4.2.2	Hot-Wall Combustor	28
4.2.3	Recuperative Combustor	28
4.2.4	Catalytic Combustor	34
4.3	Test Rig and Facilities	37
4.3.1	Combustor Rig	37
4.3.2	Combustor Test Facility	37
4.3.3	Emissions Sampling and Analysis System	39
4.3.4	Combustor Performance Instrumentation	44
4.4	Test Conditions and Procedures	47
4.4.1	Screening Test Point Matrix	47
4.4.2	Test Procedures	47
4.4.3	Data Acquisition Procedures	50
4.5	Data Reduction Procedures	51
4.5.1	Emissions Data Processing Procedure	51
4.5.2	Operating and Performance Data Processing	54
5.0	EXPERIMENTAL TEST RESULTS	56
5.1	Overall Test Summary	56
5.2	Screening Test Emissions Results	58
5.2.1	Hot-Wall Combustor	58
5.2.2	Recuperative Combustor	65
5.2.3	Catalytic Combustor	73
5.3	Screening Test Performance Results	82
5.3.1	General Performance	82
5.3.2	Low-Emissions Concept Performance	86

TABLE OF CONTENTS (Concluded)

<u>Section</u>	<u>Page</u>
5.4 Parametric Test Results	88
5.4.1 Emissions Results	92
5.4.2 Performance Results	101
6.0 ASSESSMENT OF RESULTS	107
6.1 Emissions Results	107
6.2 Performance Results	110
APPENDIX A - COMBUSTOR TEST CONFIGURATIONS	115
APPENDIX B - COMBUSTOR TEST RESULTS	120
APPENDIX C - CATALYTIC REACTOR DESIGN PROGRAM SUMMARY	142
APPENDIX D - SYMBOLS	149
APPENDIX E - REFERENCES	151

LIST OF ILLUSTRATIONS

<u>Figure</u>		<u>Page</u>
1.	Hot-Wall Liner Combustor Concept.	9
2.	Recuperative-Cooled Liner Combustor Concept.	10
3.	Recuperative-Cooled Liner Combustor Concept Variation.	12
4.	Catalytic Converter Combustor Concept.	14
5.	Combustor Airflow Circuits.	15
6.	Staged Combustion Systems.	17
7.	Baseline Combustor Flowpath.	19
8.	Baseline Combustor Designs.	21
9.	Common Dome Construction Details (Inlet Cowl and Swirlers Not Installed).	22
10.	Common Dome Assembly Details.	23
11.	Swirler Assembly.	25
12.	Common Combustor Aft Section (Sideplate Removed).	26
13.	CO Consumption Rates at Low-Power Operating Conditions.	29
14.	Baseline Hot-Wall Combustor Airflow and Pressure Distribution.	30
15.	Hot-Wall Combustor Cooling Circuit.	31
16.	Baseline Recuperative Combustor Airflow and Pressure Distribution.	32
17.	Recuperative Combustor Cooling Circuit.	33
18.	Baseline Catalytic Combustor Airflow and Pressure Distribution.	35
19.	Catalytic Reactor.	36
20.	CF6-50 60-Degree-Sector Combustor Test Rig.	38
21.	Control Console, Building 306 Advanced Combustion Laboratory.	40

LIST OF ILLUSTRATIONS (Continued)

<u>Figure</u>		<u>Page</u>
22.	Combination Thermocouple/Gas Sample/Total Pressure Rake.	41
23.	Combustor Exit Instrumentation Locations.	42
24.	Gas Sample/Exit Pressure Manifolding Diagram.	43
25.	Combustor Performance Instrumentation.	46
26.	LOPER Data Reduction Flowpath.	52
27.	Baseline Hot-Wall Combustor Emissions Characteristics.	62
28.	Effect of Swirler Airflow on Hot-Wall Combustor Emissions.	63
29.	Hot-Wall Combustor Swirler Modifications.	64
30.	Effect of Primary Zone Dilution Scheme on Hot-Wall Combustor Emissions.	66
31.	Effect of Swirler Airflow on Recuperative Combustor Emissions.	69
32.	Effect of Primary Zone Dilution Location on Recuperative Combustor Emissions.	71
33.	Effect of Airflow Distribution Variations on Recuperative Combustor Emissions.	72
34.	Catalytic Combustor Configurations.	76
35.	Catalytic Reactor Effectiveness.	77
36.	Effect of Airflow Distribution on Catalytic Combustor Emissions.	78
37.	Catalytic Combustor Swirler Modification.	80
38.	Effect of Increased Primary Zone Length and Swirler Modification on Catalytic Combustor Emissions.	81
39.	Resonance Damage to Forward Combustor Liner, Configuration III.	84
40.	Typical LOPER Resonance Limits.	85
41.	Recuperative Combustor Swirler Air Temperature Rise Correlation.	87

LIST OF ILLUSTRATIONS (Concluded)

<u>Figure</u>		<u>Page</u>
42.	Localized Catalyst Damage, Configuration C4.	89
43.	Catalyst Remnants After Collapse, Configuration C5.	90
44.	Modified Catalyst Mounting Scheme.	91
45.	Comparison of Hot-Wall Combustor Screening and Parametric Emission Test Results.	94
46.	Comparison of Recuperative Combustor Screening and Parametric Emission Test Results.	95
47.	Comparison of Catalytic Combustor Screening and Parametric Emission Test Results.	96
48.	Parametric Test Results, Comparison of Emissions at Design Point Inlet Conditions.	97
49.	Parametric Test Results, Comparison of Emissions at Most Severe Inlet Conditions.	100
50.	Parametric Test Results, Effect of Inlet Temperature and Pressure on Recuperative Combustor Emissions.	102
51.	Parametric Test Results, Effect of Reference Velocity on Recuperative Combustor Emissions.	103
52.	Parametric Test Results, Comparison of Combustor Exit Temperature Profiles.	105
53.	Comparison of Current Production, ECCP, and LOPER Combustor Idle Emission Levels.	111
54.	Dilution Hole Circumferential Locations.	119
55.	Catalyst Screening Test Configurations.	143
56.	Screening and Parametric Test Catalysts.	144
57.	Catalytic Conversion and Pressure Drop Predictions Based on Screening Test Results.	147
58.	Parametric Test Conversion Performance Catalyst.	148

LIST OF TABLES

<u>Table</u>		<u>Page</u>
I.	Pollutant Emission Level Goals of the NASA/GE LOPER Program.	5
II.	Combustor Design and Test Conditions of the NASA/GE LOPER Program.	6
III.	Combustor Design Parameters.	20
IV.	Baseline Combustor Airflow Distributions.	27
V.	Emission Instrument Calibration Gases.	45
VI.	Combustor Liner Thermocouple Locations.	48
VII.	Combustor Screening Test Point Matrix.	49
VIII.	Emissions Data Output Format.	53
IX.	Sample Test Summary Format.	55
X.	Combustor Design Parameter Summary.	57
XI.	Hot-Wall Combustor Configurations.	59
XII.	Hot-Wall Combustor Emissions Summary.	60
XIII.	Recuperative Combustor Configurations.	67
XIV.	Recuperative Combustor Emissions Summary.	68
XV.	Catalytic Combustor Configurations.	74
XVI.	Catalytic Combustor Emissions Summary.	75
XVII.	Primary Zone Airflow Comparison, Parametric Test Configurations.	99
XVIII.	Resonance Limits, Parametric Test Configurations.	106
XIX.	Comparison of Emission Levels, Most Promising Configurations.	108
XX.	Assessment of LOPER Idle Emission Reduction Design Features.	109

LIST OF TABLES (Continued)

<u>Table</u>	<u>Page</u>
XXI. Assessment of LOPER Combustor Design Concepts.	112
XXII. Hot-Wall Combustor Area/Airflow Distributions.	116
XXIII. Recuperative Combustor Area/Airflow Distributions.	117
XXIV. Catalytic Combustor Area/Airflow Distributions.	118
XXV. Test Summary, Combustor Configuration H1, Runs 4 and 5.	121
XXVI. Test Summary, Combustor Configuration H2, Run 11.	122
XXVII. Test Summary, Combustor Configuration H3, Run 18.	123
XXVIII. Test Summary, Combustor Configuration H4, Run 19.	124
XXIX. Test Summary, Combustor Configuration H5, Runs 20 and 21.	125
XXX. Test Summary, Combustor Configuration H6, Run 22.	126
XXXI. Test Summary, Combustor Configuration H7, Run 27.	127
XXXII. Test Summary, Combustor Configuration R1, Runs 6 and 7.	128
XXXIII. Test Summary, Combustor Configuration R2, Run 8.	129
XXXIV. Test Summary, Combustor Configuration R3, Runs 12 and 13.	130
XXXV. Test Summary, Combustor Configuration R4, Runs 14 and 15.	131
XXXVI. Test Summary, Combustor Configuration R5, Run 16.	132
XXXVII. Test Summary, Combustor Configuration R6, Run 17.	133
XXXVIII. Test Summary, Combustor Configuration R7, Run 28.	134
XXXIX. Test Summary, Combustor Configuration C1, Runs 1 and 2.	135
XL. Test Summary, Combustor Configuration C2, Run 3.	136
XLI. Test Summary, Combustor Configuration C3, Run 9.	137
XLII. Test Summary, Combustor Configuration C4, Run 10.	138
XLIII. Test Summary, Combustor Configuration C5, Run 23.	139

LIST OF TABLES (Concluded)

<u>Table</u>		<u>Page</u>
XLIV.	Test Summary, Combustor Configuration C6, Runs 24 and 25.	140
XLV.	Test Summary, Combustor Configuration C7, Run 26.	141
XLVI.	Nominal Catalyst Test Conditions .	146

1.0 SUMMARY

The objective of this experimental program was to evolve advanced aircraft gas turbine engine combustor technology for reducing low-power emissions of carbon monoxide (CO) and unburned hydrocarbons (HC) to levels significantly lower than those which can be achieved with current technology while not significantly increasing the emission levels of oxides of nitrogen (NO_x).

The program involved a series of screening and parametric tests of three low-emissions combustor design concepts in a 60-degree-sector rig. The first of these concepts was the Hot-Wall Liner Concept, which through the use of high-temperature refractory coated surfaces, was designed to eliminate regions where CO and HC consumption reactions might be quenched. The second concept was the Recuperative-Cooled Liner Concept, which was designed to reduce CO and HC levels by increasing the primary zone inlet air temperature. The third concept was the Catalytic Converter Concept featuring the use of a catalyst to permit more rapid and complete oxidation of residual CO and HC.

Twenty-one combustor configurations were tested in a modified CF6-50 engine size 60-degree-sector combustor rig over a range of combustor inlet conditions typical of aircraft turbine engine ground-idle operation. The best configurations of all three concepts produced emission levels which met or were well below the stringent program design point emission goals which were 10, 1, and 4 g/kg for CO, HC, and NO_x , respectively, at the design operating condition (inlet temperature 422 K, inlet pressure 304 kPa, reference velocity 23 m/s, fuel-air ratio 10.5 g/kg). While all three concepts essentially met all of the program emissions goals, the Hot-Wall Concept was favored slightly because of its relative simplicity and demonstrated performance.

2.0 INTRODUCTION

This report describes the results of a program to develop technology for reducing low-power emissions of CO and HC from aircraft gas turbine engines to levels which are significantly lower than can be achieved with current technology.

In response to provisions contained in the Clean Air Act Amendments of 1970, the U.S. Environmental Protection Agency (EPA) conducted studies to assess the impact of aircraft engine pollutant emissions on air quality. Based on the results of those studies the EPA concluded that for quantities of CO, HC, NO_x, and smoke emissions discharged by aircraft operating within or near airports, regulative standards were needed. Based on this finding, such standards were defined and issued in 1973 (Reference 1). Smoke standards became effective in January 1976. Gaseous emissions standards were to become effective in January 1979, but were recently postponed to January 1981, at which postponement a wide range of changes were proposed (Reference 2).

As a result of Government and industry efforts initiated more than 12 years ago, significant advances have been made in the development of smoke abatement technology for use in aircraft turbine engines. Modern aircraft gas turbine engines, such as the General Electric CF6 engines, operate with virtually invisible smoke levels and, thus, are already in compliance with the EPA-prescribed smoke emission standards. However, compliance with EPA-prescribed gaseous emission standards requires large reductions in the emission levels of all current-technology engines. Major combustor design technology advances are needed to obtain these significant reductions in gaseous pollutant emission levels.

To provide these needed combustor design technology advances, the Experimental Clean Combustor Program (ECCP) was initiated by the U.S. National Aeronautics and Space Administration (NASA) in 1972 (Reference 3). The overall objective of this major program was to define, develop, and demonstrate technology for the design of low pollutant emission combustors for use in advanced commercial CTOL aircraft engines with high-cycle pressure ratios in the range of 20 to 35. The NASA/General Electric Experimental Clean Combustor Program (References 4 and 5) was one of a number of programs that together comprised the overall program. Staged combustor design concepts were developed in order to reduce emissions generated primarily at low-power operating conditions (NO_x and smoke). Significant reductions (40 to 90%) in each of the gaseous emissions were demonstrated.

In 1976, NASA initiated a series of programs to provide technology needed to design combustors with further reduced levels of pollutant emissions that occur in both airport and high-altitude-cruise operation. The NASA/GE Aircraft Gas Turbine Engine Low-Power Emissions Reduction Technology (LOPER) Program was a part of this second-generation emissions reduction effort.

The LOPER program involved screening and parametric tests conducted in a sector rig of three low-emissions combustor design concepts which were

previously identified as having potential for meeting the program's very ambitious pollutant emission goals. Therefore, each of the concepts employed advanced features and were not merely applications of previous technology. One of the concepts incorporated thermal barrier coatings to provide hot walls, thereby minimizing wall quenching reactions. Another concept incorporated recuperatively heated combustor air to enhance reaction rates. The third concept incorporated a cleanup catalytic reactor developed under sub-contract by Engelhard Industries, Murray Hill, New Jersey. All three of the concepts were designed for and tested only at aircraft turbine engine low-power operating conditions, thereby simulating only the pilot stage of a multistage combustor and/or one setting of a variable geometry combustor. Full-range operation considerations were beyond the scope of this program.

3.0 PROGRAM PLAN

The purpose of the LOPER program was to develop technology for reducing low-power emissions of CO and HC to significantly lower levels than can be achieved with current technology. The pollutant emission-level goals of the program are shown in Table I. Although the program did not focus on NO_x reductions, a goal was specified in order that NO_x-CO trade offs would not be used. For comparison, idle emission goals of the ECCP and idle emission levels of the current production CF6-50 engine are also shown. The LOPER goals are much lower than the ECCP goals, which in turn are much lower than the current technology levels. The LOPER goals are, however, consistent with the proposed 1984 EPA emission standards for newly certified subsonic engines (Reference 2). The LOPER CO and HC emission index goals are equivalent to combustion efficiency of 99.7%.

The program involved design and evaluation of three combustor concepts which are described in the following sections. The combustors were each designed for installation into a common, representative, advanced turbofan engine combustor housing. The design point operating conditions, shown in Table II together with the range of test conditions, were also selected to be representative of advanced turbofan engine designs.

The experimental evaluations consisted of: (1) 18 screening tests (3 concepts and 6 configurations each) to identify the most promising configurations of each concept, followed by (2) verification parametric tests of the selected configurations of each concept. Each of these tests involved measurements of exhaust emissions and performance parameters over a range of combustor operating conditions selected from Table II. Combustor screening evaluations were planned to require approximately 75 test hours, and parametric testing was planned to involve approximately 25 additional test hours.

The program design efforts were initiated in November 1976; testing was completed in April 1978.

Table I. Pollutant Emission Level Goals of the NASA/GE LOPER Program.

<u>Pollutant</u>	Emission Index, g/kg at Engine Idle Operating Conditions			
	<u>LOPER Goals</u>	<u>ECCP Goals</u>	Current ⁽¹⁾ <u>CF6-50</u>	Current ⁽²⁾ <u>JT9D-7</u>
HC, Hydrocarbons (as CH ₄)	1	4	30	27
CO, Carbon Monoxide	10	20	73	58
NO _x , Oxide of Nitrogen (as NO ₂)	4	--	2.5	3.1

(1) Reference 4

(2) Reference 9

Table II. Combustor Design and Test Conditions of the NASA/GE JOPER Program.

<u>Parameter</u>	<u>Design Value</u>	<u>Range of Variation</u>
Inlet Pressure, kPa	304	203 to 405
Inlet Temperature, K	422	366 to 478
Reference Velocity, m/s	22.9	15.2 to 30.5
Fuel-Air Ratio, g/kg	10.5	5.0 to 15.5
Combustor Pressure Drop, $\Delta P_c/P_3$ %	5.0	---

4.0 DESIGN AND DEVELOPMENT APPROACHES

4.1 COMBUSTOR CONCEPTS

The three low-emissions combustor concepts considered in the LOPER program were (1) the Hot-Wall Liner concept, which, through the use of high-temperature refractory coated surfaces, is designed to eliminate regions where CO and HC consumption reactions may be quenched; (2) the Recuperative Cooled Liner concept, which achieves reduced CO and HC levels by increasing the combustor primary zone inlet air temperature; and (3) the Catalytic Converter concept, which uses a catalyst to permit more rapid and complete consumption of residual CO and HC. Basic operating considerations and emissions reduction principles of these concepts are described below.

4.1.1 Hot-Wall Liner Combustor

The first combustor design concept evaluated in the LOPER program featured the use of "hot wall" cooling liners as a means of reducing CO and HC emission levels. These liners differ from conventional combustor liners in that the cooling air film normally used to protect the interior surfaces of the combustor is eliminated, and a refractory coating is applied to these surfaces.

It has been deduced from previous low-emissions combustor experience that large proportions of the CO and HC emitted from combustors at low-power operating conditions are the result of inhibition of the combustion reactions on and adjacent to the film cooled surfaces of the combustor dome and liner walls. With conventional film cooling arrangements, the cooling air must be uniformly distributed over the interior surfaces of the combustor and the amount of cooling flow must be large enough to protect the metal liner surfaces at high-power operating conditions where the cooling air temperature may be greater than 800 K. To provide adequate protection at these conditions, the amount of cooling air required is usually 25 to 30% of the total combustor airflow. At low-power operating conditions, the film cooling air, with a temperature of only 350 to 500 K, forms a blanket of cool air near the combustor liner walls that quenches reacting fuel-air mixtures entering these regions. Also, liquid fuel droplets that land on the cool wall surfaces at the low-power conditions evaporate slowly, and the resulting rich fuel-air mixtures are swept along by the film cooling air into the secondary dilution region of the combustor, with a large proportion of the mixture remaining unreacted or partially reacted.

By eliminating or greatly reducing film cooling air in the combustor, and by significantly increasing the interior surface temperature of the combustor walls at the low-power operating conditions, these wall quenching effects should be largely eliminated, resulting in significantly reduced CO and HC emissions levels.

In the hot-wall liner combustor concept, shown in Figure 1, all primary zone film cooling is eliminated by the use of impingement cooling. A double-wall liner is used in this cooling scheme. The inner impingement-cooled liner, which is exposed to the combustion gases, is cooled by an array of air jets provided by perforations in the outer support liner. Spent cooling air is then ducted between the impingement and support liners and is admitted to the combustor either through annuli surrounding the primary and secondary dilution holes, or through film cooling slots at the aft end of the combustor.

In order to provide high wall temperatures while protecting the impingement-cooled liners, a ceramic "thermal barrier" coating is used in this concept. By selection of appropriate coating thickness and thermal conductivity, and by the application of an appropriate coating thickness and thermal conductivity, and by the application of an appropriate quantity of impingement cooling air to the impingement-cooled liner, the surface temperature of the thermal barrier coating can be controlled to provide good performance and long service life.

4.1.2 Recuperative-Cooled Liner Combustor

The second combustor concept evaluated in this program featured provisions to preheat the air entering the primary combustion zone as a means of reducing CO and HC levels.

The strong dependence of CO and HC emissions on combustor inlet temperature has been well documented. Any means of increasing this temperature should provide large reductions in CO and HC levels. One method for increasing combustor inlet temperature is through the use of recuperative cooling of the combustor liners. In this approach, the hot combustor liners are used to heat the air entering the combustor primary zone.

The recuperative-cooled liner combustor concept is shown in Figure 2. In this design approach, an impingement liner-cooling scheme similar to that employed in the hot-wall liner concept is used. However, instead of routing the spent impingement cooling air to the aft end of the combustor, the cooling air is brought forward between the impingement and support liners. This heated cooling air is then used as the primary zone combustion air, including both swirler and primary dilution flows.

In the conceptual design shown in Figure 2, the combustor geometry used is conventional except that the inlet cowl is closed off so that all swirler air is supplied from the liner cooling passages. Maximum recuperative temperature rise is obtained by eliminating all film cooling. With this approach, approximately 50% of the total combustor pressure drop is used to obtain good impingement-cooling heat transfer. The remaining pressure drop is taken across the swirler and primary dilution holes. Some control over recuperative temperature rise can be obtained with this configuration by varying the proportion of pressure drop taken across the impingement cooling holes; however, this option is limited by swirler and primary dilution pressure drop limitations which are dictated by combustor mixing and fuel atomization requirements.

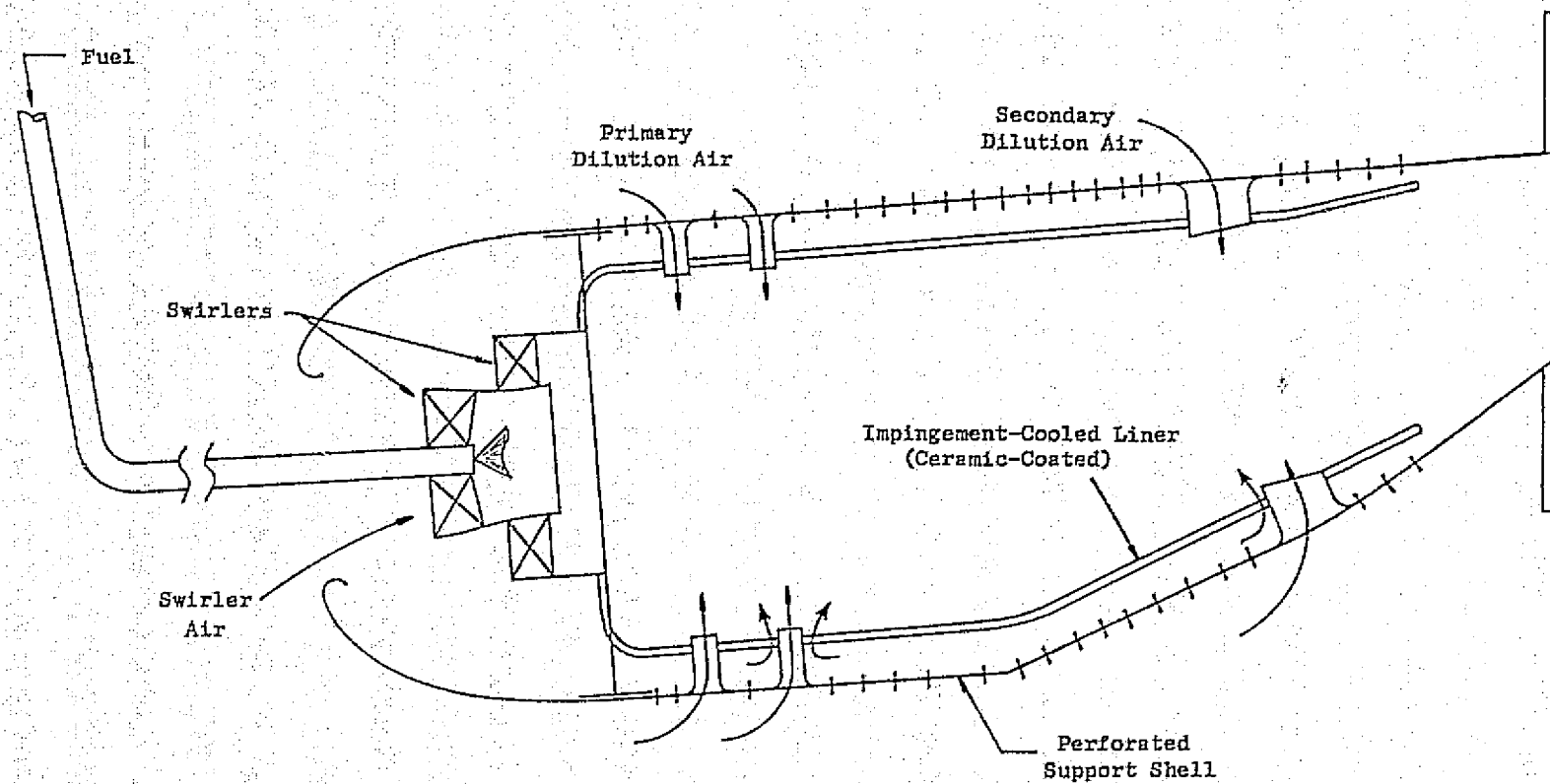


Figure 1. Hot-Wall Liner Combustor Concept.

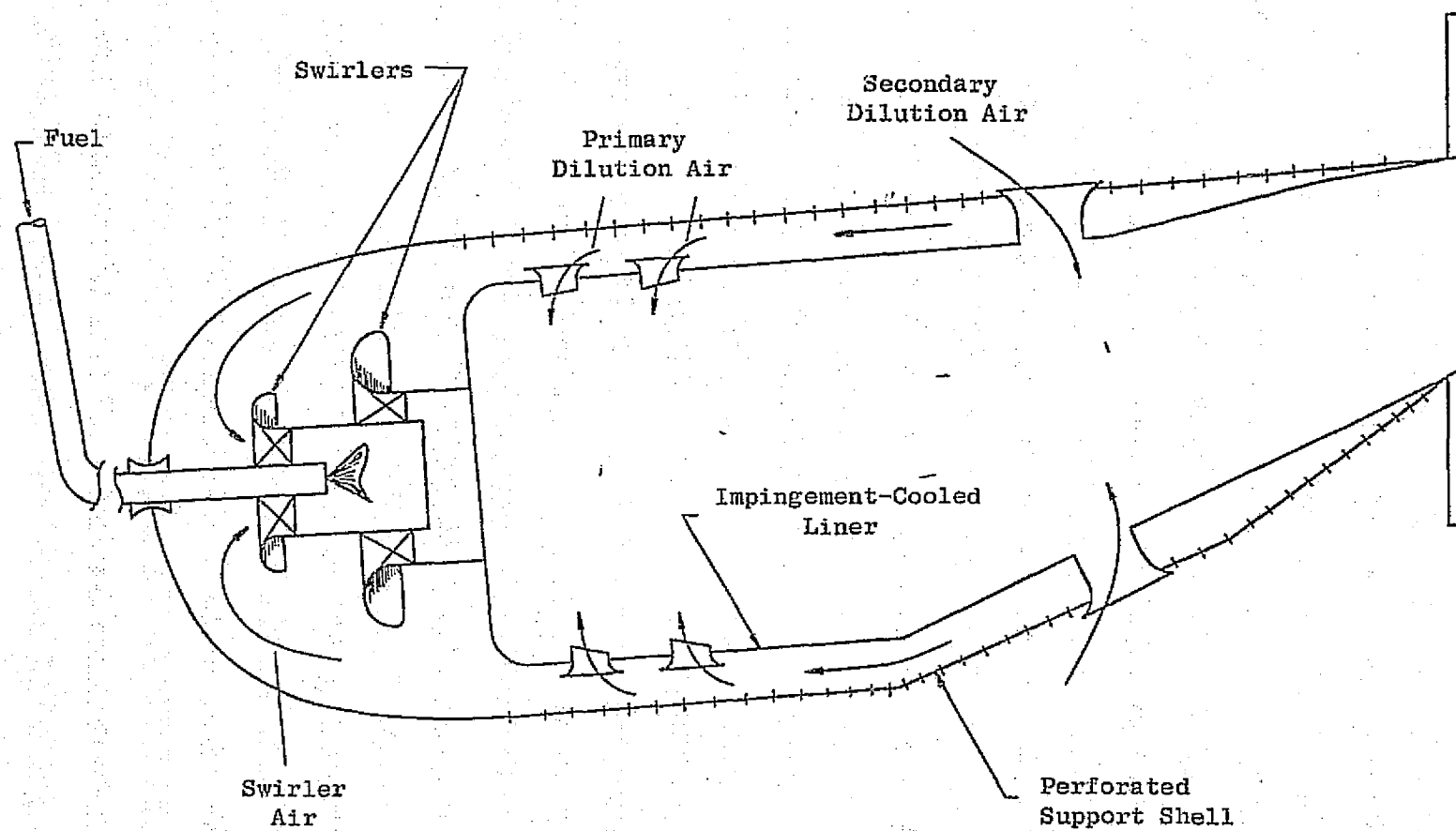


Figure 2. Recuperative-Cooled Liner Combustor Concept.

Additional control over recuperative temperature rise can be obtained by modifying combustor geometry to change liner heat transfer characteristics. One such modification is shown in Figure 3. In this design, the velocity of the hot gases within the combustor is increased by decreasing the cross-sectional area in the high-temperature region of the combustor, thus increasing the hot-side heat transfer coefficient. Recuperative air temperature can be further increased either by using convoluted impingement-cooled liners or by inserting a centerbody into the hot gas flowpath.

4.1.3 Catalytic Converter Combustor

The third combustor concept evaluated in the LCPER program featured the use of a catalytic reactor as a means of reducing CO and HC emissions levels.

The use of catalytic combustion techniques has been shown to be a potentially attractive means of obtaining ultralow pollutant emissions levels (References 6 and 7). For the most part, however, the investigations regarding the use of a catalytic combustion process in turbine engine combustors have been directed to higher engine power operating conditions, where very low NO_x emissions levels have been obtained by using catalytically supported combustion of very lean fuel-air mixtures. With present catalyst technology, a different catalyst operating mode is required at low power conditions, because typical combustor inlet air temperatures at these conditions are below levels required to maintain catalyst activity. For example, catalytic ignition tests of a typical Engelhard combustion catalyst using JP-4 fuel showed an ignition temperature of about 522 K, which is above the typical engine idle inlet temperatures of 350 to 500 K.

To permit the use of a catalytic combustion process at the low-power mode of aircraft turbine engines, at least partial precombustion of the fuel is necessary. With the use of a precombustion step followed by a catalytic combustion cleanup step, it is anticipated that very low CO and HC emission levels can be obtained at low-power operating conditions. Perhaps the simplest approach of this kind would be total combustion of the fuel followed by catalytic cleanup of the exhaust gases just ahead of the turbine inlet. Alternatively, the catalytic reactor could be placed between the secondary combustion and the dilution zone, with about 40 to 50% of the air bypassing the catalytic reactor.

Although positioning the catalytic reactor at the combustor exit to provide catalytic cleanup of the entire hot gas stream is the simplest design, it is not a practical approach since the hot gas velocities at this axial station are generally higher than the velocities that can be accommodated by catalytic reactors. At these very high velocities, even for substantial catalytic reactor axial lengths (say, 15 cm), catalytic conversion efficiency is unlikely to exceed 75%. In addition, the resulting pressure losses would range from 13 to 50%.

More satisfactory results are obtained by placing the catalytic reactor between the secondary and dilution zones. In this case, which has been

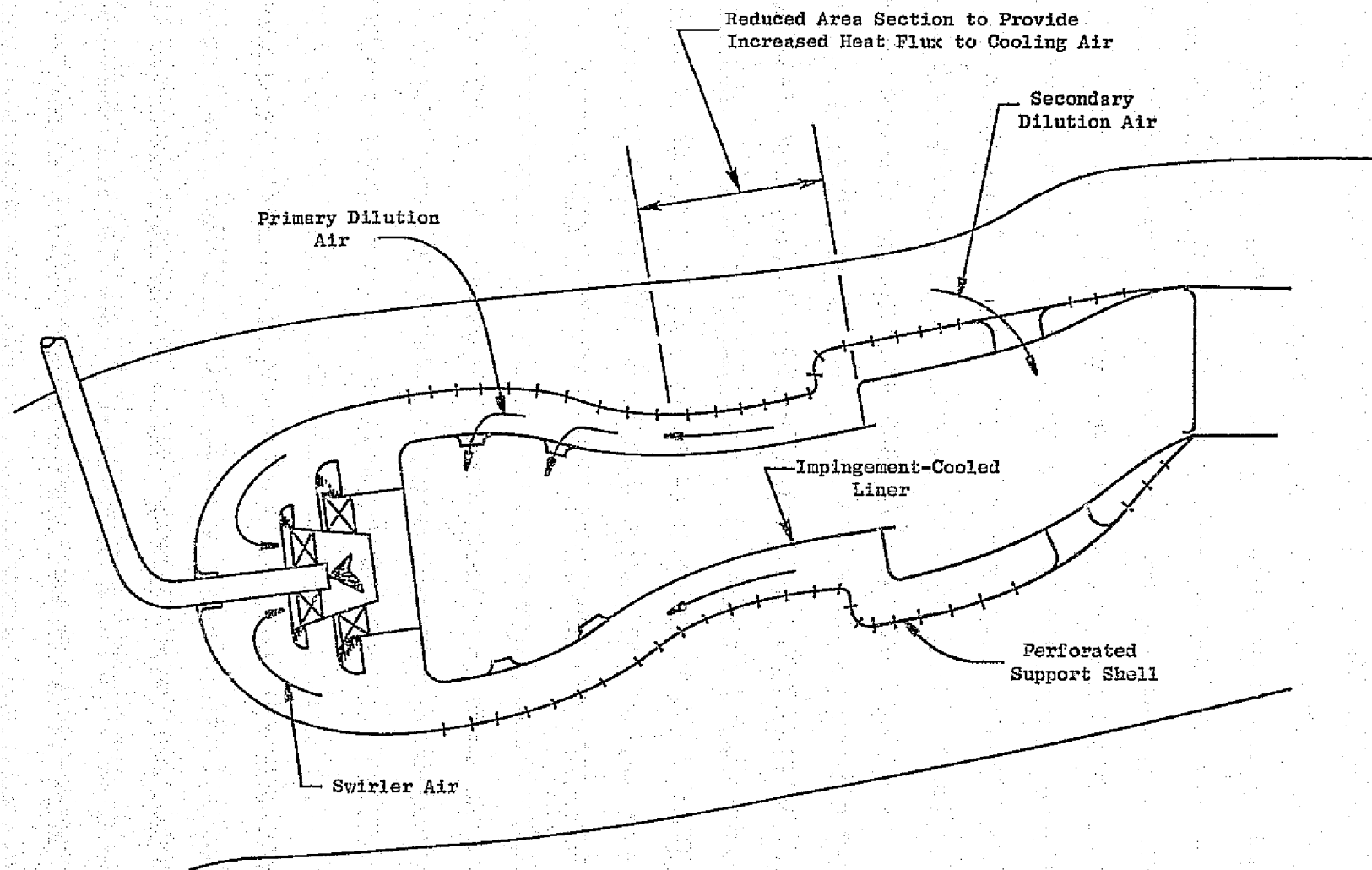


Figure 3. Recuperative Cooled Liner Combustor Concept Variation.

demonstrated in small-scale laboratory combustor tests (Reference 8), catalyst inlet velocities are reduced and catalyst operating temperatures are increased by bypassing about 50% of the combustor airflow around the catalytic reactor. The resulting reduced velocities and increased temperatures allow catalytic reactor length and pressure drop to be reduced.

The centrally mounted reactor catalytic combustor concept is shown applied to a typical annular aircraft combustor flowpath in Figure 4. The combustor is nominally designed to operate with 50% of the total airflow introduced into the catalytic reactor through the swirlers and primary dilution holes. Approximately half of the available combustor pressure drop is taken across the oversize swirlers and primary zone dilution holes, with the remaining pressure drop taken across the catalytic reactor. In the conceptual drawing shown, double-wall liner construction with impingement cooling is shown, but conventional film cooling could be equally effective in this concept.

Design variables which can be adjusted to tailor the catalytic combustor concept to any given application include variations in catalytic reactor airflow, pressure drop, and length. For operation at very low combustor inlet temperatures and fuel-air ratios, catalyst airflow could be decreased below 50% to increase catalyst inlet temperature and provide increased catalytic conversion. Catalytic conversion could also be increased by increasing catalytic reactor pressure drop and/or length. In either case, the extent to which these parameters can be increased would be limited by the requirements of the precombustion zone, which must have sufficient pressure drop to provide good fuel atomization and mixing, and sufficient length for mixing and combustion.

4.1.4 Combustor Airflow Circuits

Airflow circuits for the three low-emission combustor concepts are compared to a conventional combustor airflow circuit in Figure 5. An electrical circuit analogy has been used in this figure. Flow restrictions, such as swirlers and dilution holes where airflow is metered and pressure drop occurs, are represented as resistances. These circuits have been simplified somewhat by neglecting minor pressure drops due to combustor passage friction loss and heat addition pressure loss.

A feature common to all of the low-emissions concepts is the series/parallel impingement cooling circuit, in which cooling flow is first routed through an impingement baffle restriction, then through an annular dilution restriction. This is the only difference between the hot-wall and conventional combustor circuits. Both the recuperative and catalytic concept flow circuits are considerably more complex.

The distinguishing feature of the recuperative flow circuit is the fact that all swirler airflow is first routed through impingement cooling restrictions. Since heat transfer effectiveness of cooling air depends on the pressure drop across the impingement baffles, this pressure drop must be a significant portion of total pressure drop to provide adequate liner cooling and recuperative temperature rise. This means that reduced swirler pressure drop is available to promote fuel atomization and mixing in the primary zone.

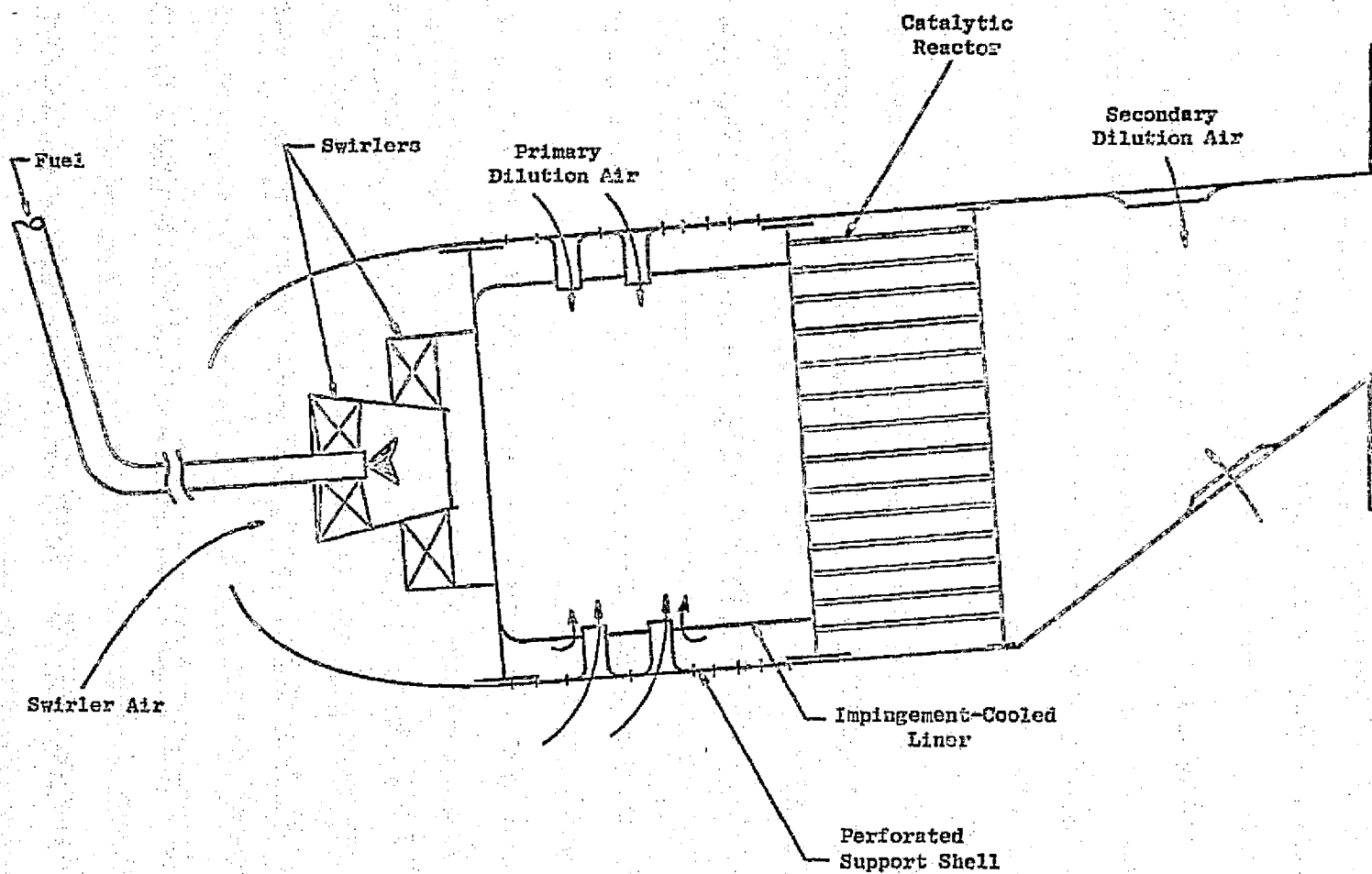


Figure 4. Catalytic Converter Combustor Concept.

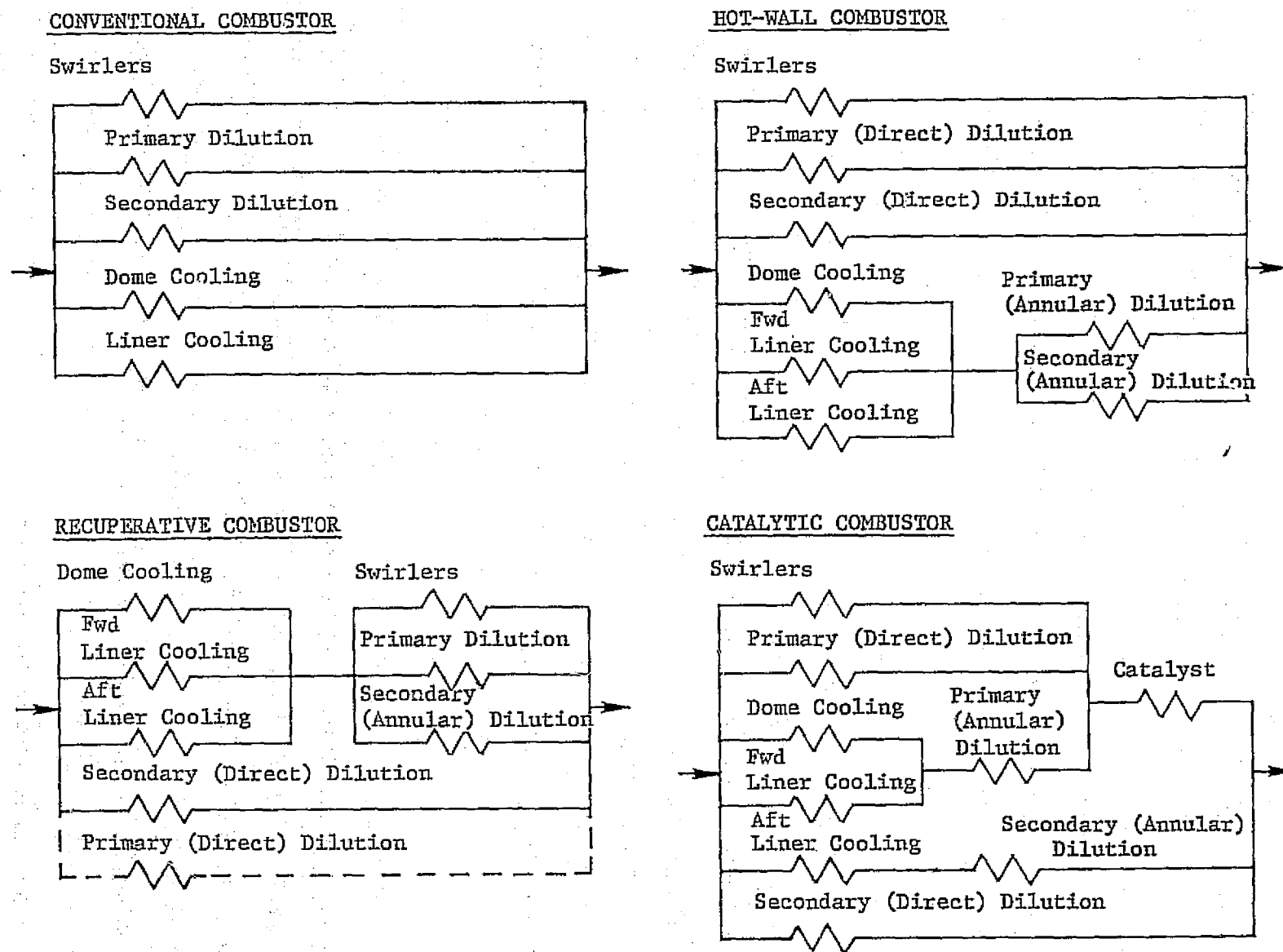


Figure 5. Combustor Airflow Circuits.

Available swirler pressure drop is also decreased in the catalytic combustor. In this case, the pressure drop reduction results from the requirement for a series pressure drop across the catalyst, which affects catalytic conversion.

4.1.5 High-Power Operating Considerations

All of the low-emissions concepts described above are intended specifically for low-power operation, and each of these concepts has certain limitations which preclude operation over the full engine power range without the addition of provisions to ensure adequate combustor durability at high-power conditions. With the hot-wall and recuperative-cooled liner concepts, maximum allowable inlet temperature and fuel-air ratio are limited by liner life considerations as a result of the use of reduced quantities of liner cooling flow. Similarly, high-power operation using the catalytic converter concept is limited by maximum allowable catalyst use temperature.

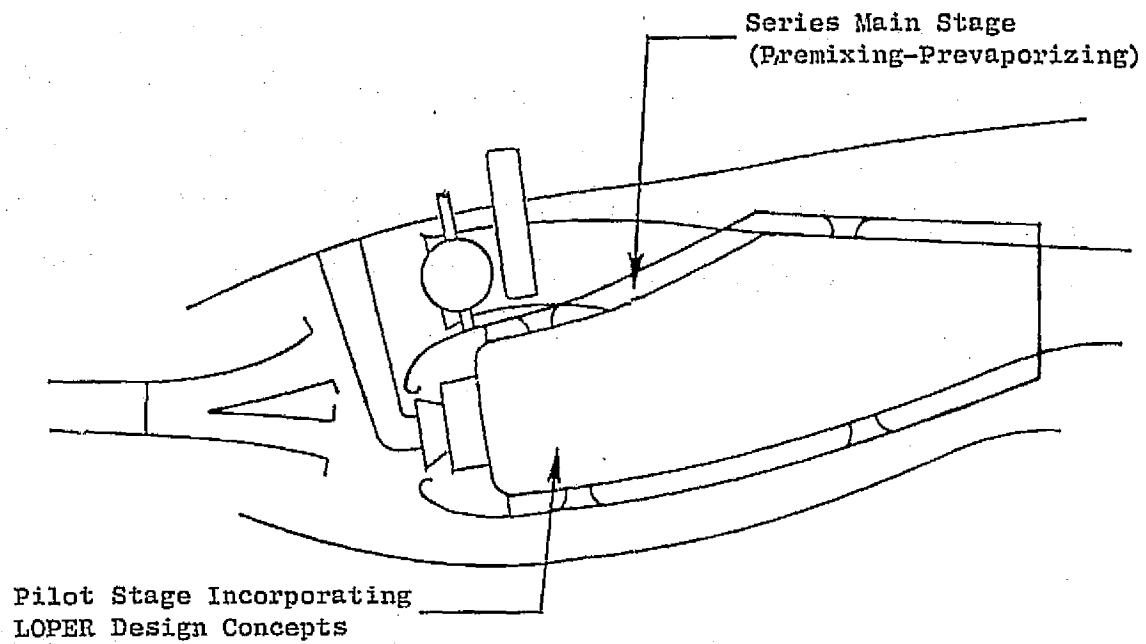
One possible technique that would enable high-power operation is the use of variable geometry to increase liner cooling flow levels during high-power operation with the hot-wall and recuperative concepts, and to reduce catalyst inlet temperature in the catalytic converter concept by increasing catalytic reactor airflow.

An alternative technique would be the use of combustion staging. In this technique, the combustion system would consist of two stages: a pilot stage incorporating one of the low-emissions concepts, and a main stage specifically designed for high-power operation. At idle conditions, only the pilot stage would be fueled, providing low idle emissions. As power would be increased, an increasing proportion of engine fuel flow would be routed to the main stage until, at the highest power operating conditions, almost all of the fuel would be burned in the main stage, with only enough fuel to maintain combustion supplied to the pilot stage. Two possible staged combustion system configurations, in which the pilot stage is mounted (a) in series with and (b) parallel to the main stage, are shown in Figure 6. The use of these combustion staging techniques has been shown to be an effective and practical method for reducing emissions using current combustor concepts; they would be particularly appropriate for use in advanced combustion systems incorporating lean premixing-prevaporizing or catalytic combustion concepts to reduce main stage emissions at high power.

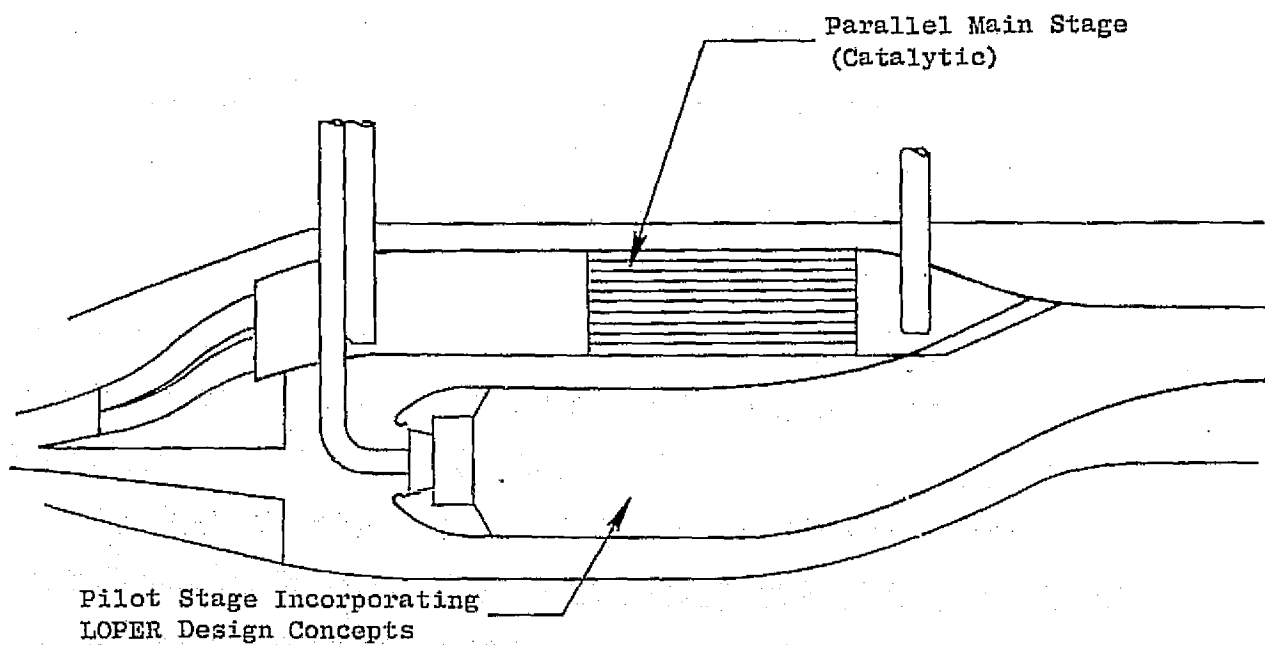
Demonstration of high-power operation was beyond the scope of the LOPER experimental program. Therefore, no attempt was made to incorporate any of the above high-power operating features into the test hardware described in the following section.

4.2 BASELINE COMBUSTOR DESCRIPTIONS

In translating the three low-emissions combustor conceptual designs into test hardware, a conscious effort was made to ensure that the resulting 60-degree-sector test combustor designs would be typical of combustors used in



(a) Series-Staged Combustion System



(b) Parallel-Staged Combustion System

Figure 6. Staged Combustion Systems.

current large turbofan engine combustors. To this end, all of the baseline designs were sized to fit within the combustor envelope of the current CF6-50 turbofan engine, which is currently used in several wide-body commercial aircraft applications. The overall dimensions and configuration of the combustor flowpath used are shown in Figure 7. This flowpath is very similar to that of the CF6-50 combustor, except that a straight wall design was used to simplify fabrication of test combustor components and installation of the honeycomb catalyst bed used in the catalytic combustor. During combustor tests, a good simulation of flow conditions within a typical engine was provided by mounting the combustors within a CF6-50 60-degree-sector combustor test vehicle.

Key idle design parameters for the selected flowpath are compared with those of several current production aircraft combustors in Table III. In this table, values for the LOPER sector have been presented on a full annular basis. Both the overall volume and values of combustor reference velocity and residence time for the LOPER flowpath are representative of current combustor designs.

Details of the three baseline low-emissions combustor designs, including common design features as well as those features unique to the hot-wall, recuperative, or catalytic combustors, are discussed below.

4.2.1 Common Design Features

In order to provide the best possible comparison among the three low-emissions combustor designs, common design features were incorporated into the three baseline designs wherever practical. Comparative cross-sectional views of the three baseline combustors are shown in Figure 8. As shown, common design features include the use of impingement cooling throughout each combustor, the location of primary and aft dilution holes, and the overall combustor external dimensions.

Because of the above similarities, it was possible to use common dome and aft section hardware in each concept. Only the central combustor region, with appropriate emissions reduction features, and details of dome and aft section configuration were varied in the individual concepts.

A photograph of the basic dome assembly is shown in Figure 9. The following comprise the key features provided on this combustor dome design:

- An enclosed impingement cooling baffle, to cool the surface of the splash plates. This baffle is fed by a plenum within the dome, which in turn is fed by a tube extending upstream of the dome cowls. The extended feed tube was necessitated by the recuperative concept, in which the cowl opening is sealed off.
- A flat cowl surface, to facilitate sealing of the cowl opening in the recuperative concept. Figure 10 shows the dome with the cowls and recuperative cover plate installed.

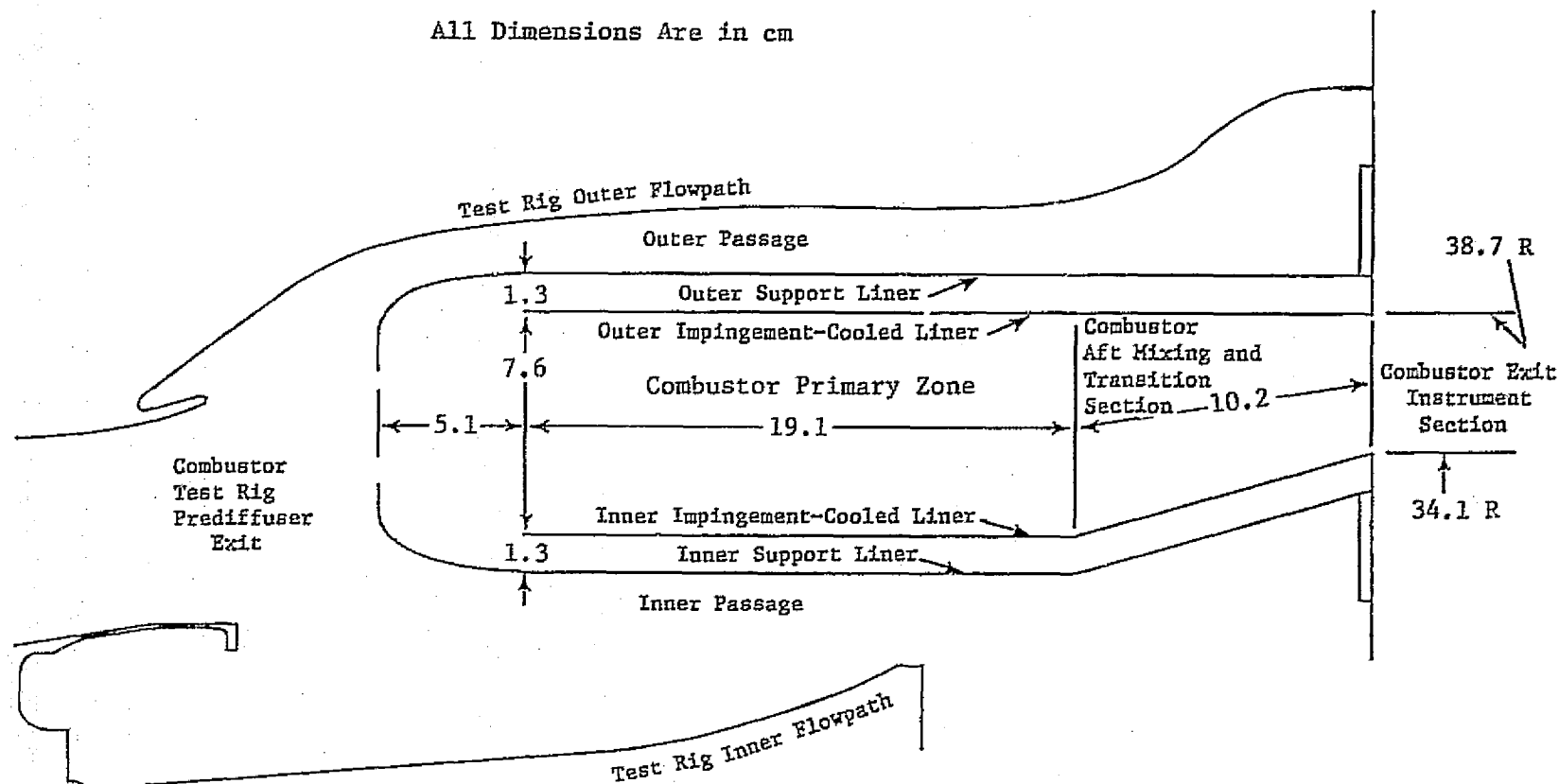


Figure 7. Baseline Combustor Flowpath.

Table III. Combustion Design Parameters.

Combustor Parameter	CF6-6	CF6-50	CFM56	LOPER*
Combustor Airflow (W_{36}), kg/s	10.34	13.81	5.67	9.61
Combustor Inlet Pressure (P_3), kPa	281	295	272	304
Combustor Inlet Temperature (T_3), K	435	429	417	422
Combustor Inlet Density, (ρ_3), kg/m ³	2.25	2.37	2.27	2.51
Dome Reference Area (A_D), m ³	0.223	0.224	0.150	0.167
Reference Velocity ($W_{36}/\rho_3 A_D$), m/s	20.6	23.9	16.7	22.9
Combustor Volume (V_c), m ³	0.0745	0.0578	0.0219	$\leq 0.0457^{**}$
Combustor Resistance Time ($\rho_3 V_c / W_{36}$), ms	16.2	9.9	8.8	$\leq 11.9^{**}$

* Based on full annular combustor.

** Values reduced by catalyst blockage in catalytic combustor.

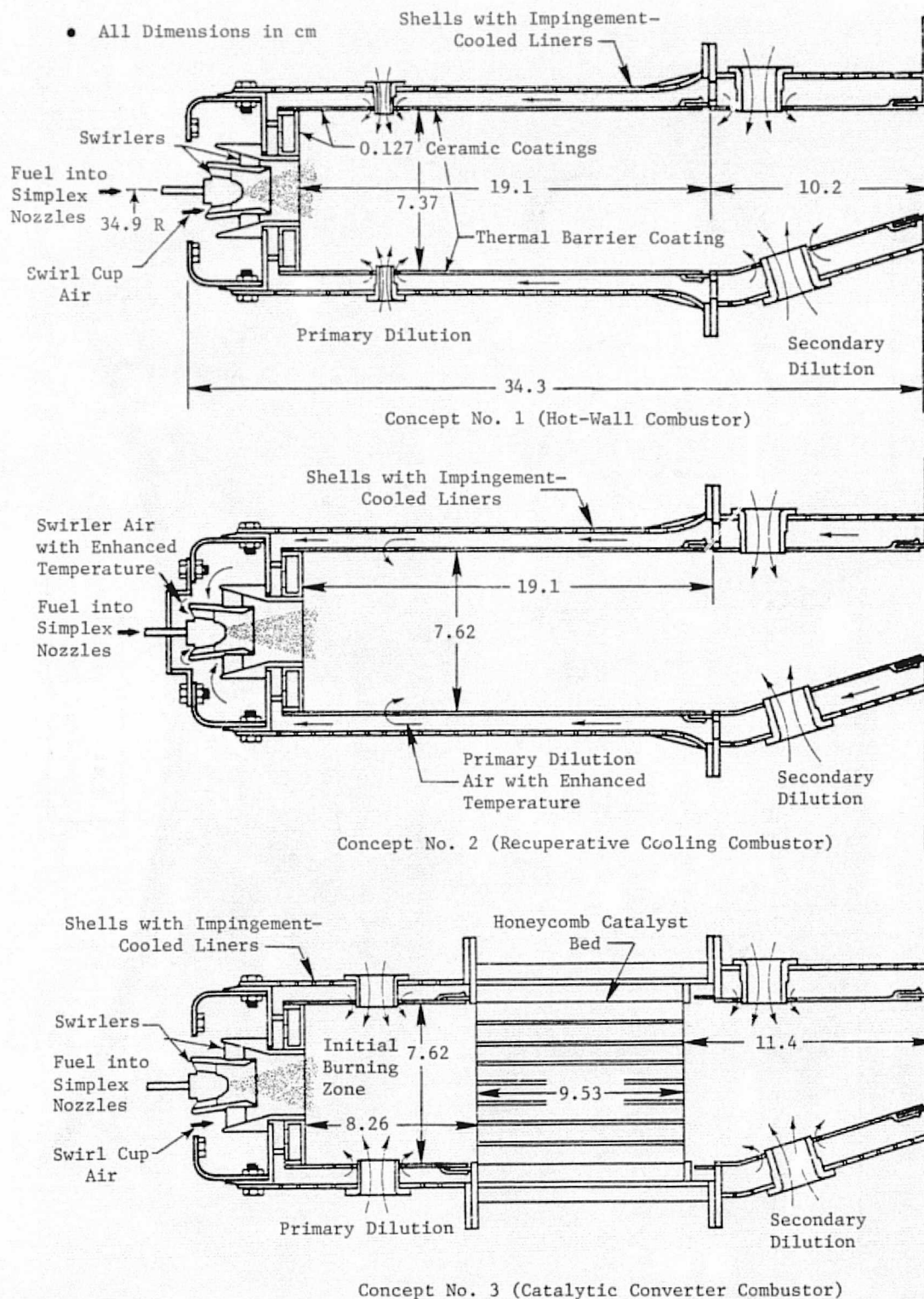


Figure 8. Baseline Combustor Designs.

ORIGINAL PAGE IS
OF POOR QUALITY

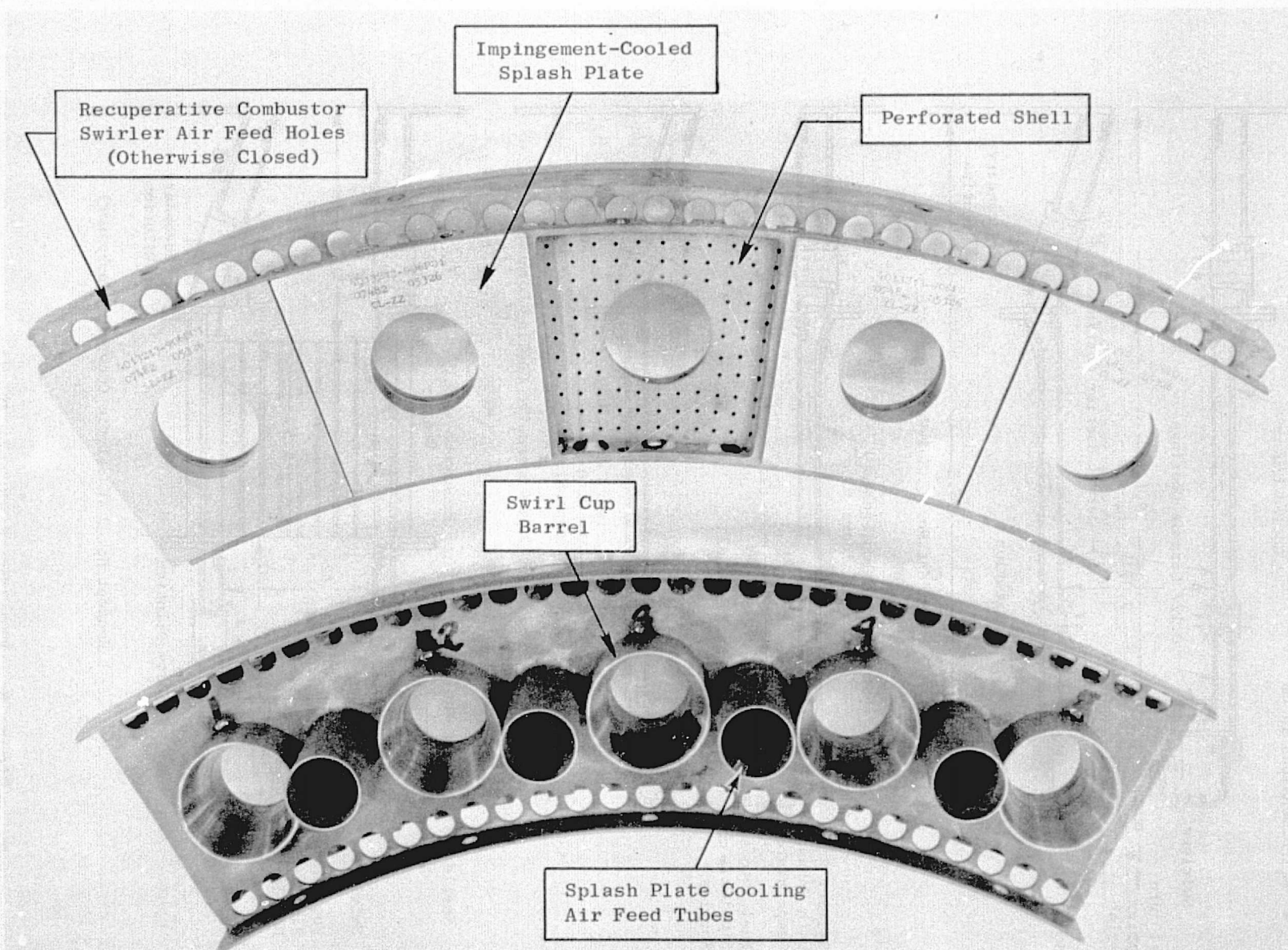


Figure 9. Common Dome Construction Details (Inlet Cowl and Swirlers Not Installed).

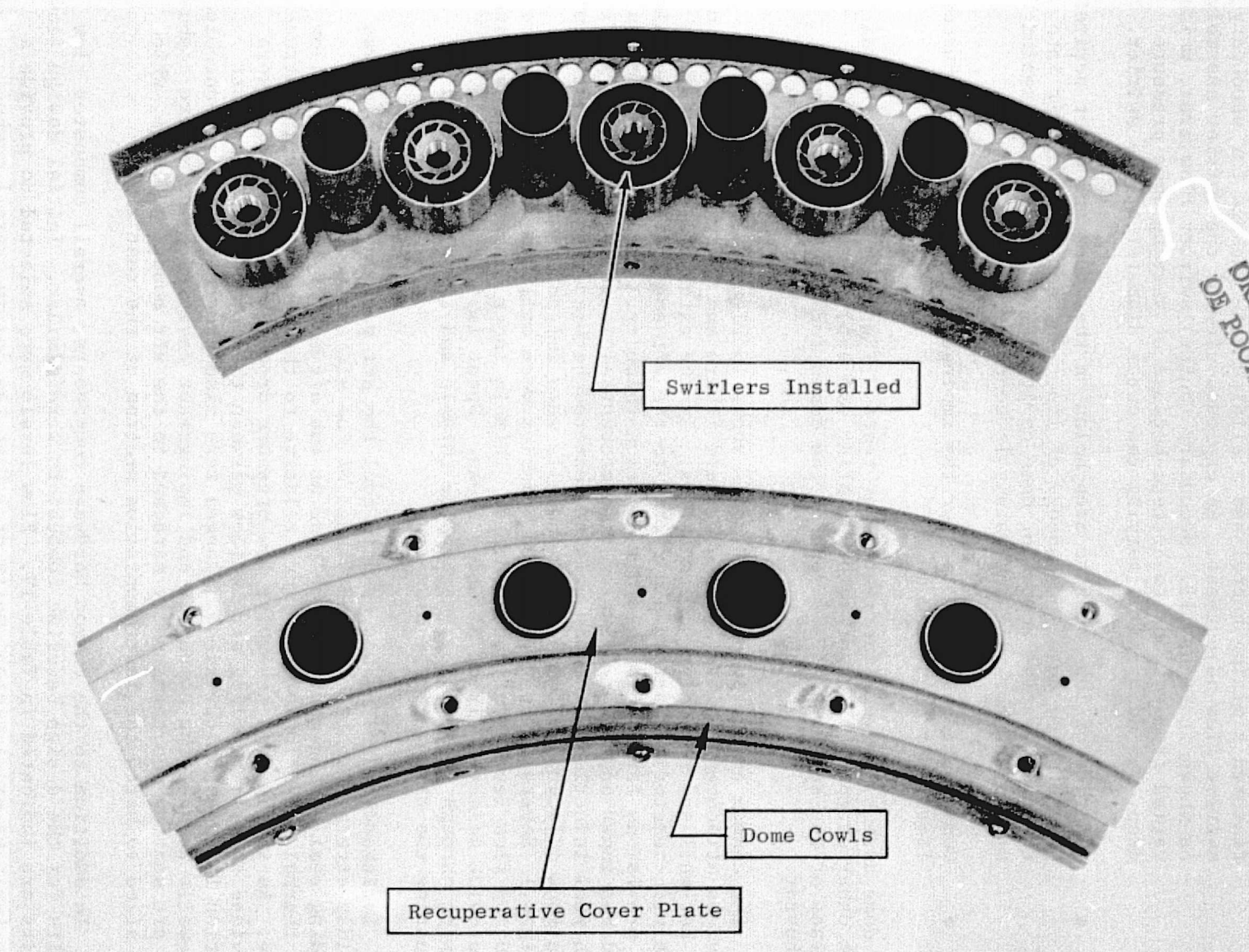


Figure 10. Common Dome Assembly Details.

- Axial flow swirl cups with coaxial counterrotating swirlers, to provide good fuel atomization characteristics. These swirl cups featured a mixing barrel and a sliding vane package for secondary swirler flow adjustment. An exploded view of the swirler assembly is shown in Figure 11. Secondary (outer) swirler flow area, which varied from concept to concept because of varying dome pressure drop, was adjusted by varying the outer diameter of the swirler.
- A series of low-pressure drop holes on the inner and outer perimeter of the dome, to allow passage of liner and dome cooling air into the recuperative combustor dome cavity. These holes were sealed off in the hot-wall and catalytic concepts.
- Common attaching points, for the impingement baffles and combustor liners for each concept.

Two dome assemblies were fabricated for tests. These domes were identical to each other except that a refractory coating was applied to the hot-side surface of the splash plates on one of the domes for use in the hot-wall combustor.

The common combustor aft section is shown in Figure 12. This design provides attachment points for the forward liners and impingement baffles of the hot-wall and recuperative combustors. In the catalytic combustor, the catalytic reactor was attached directly to the aft section. This design also has provisions for mounting 18 aft dilution thimbles. The dilution pattern used has inner and outer dilution circumferential locations, directly in line with fuel injection points as well as centered between them. (Partial dilution locations adjacent to the sector sidewalls were omitted in the baseline designs.) Several sets of dilution thimbles were utilized to provide selected dilution flow levels for each concept. Thimble inner diameters were adjusted to provide selected direct dilution flows. Spent impingement cooling air flowing through the annulus between the thimble and liner was metered by adjusting the thimble outer diameter.

Impingement cooling was used to cool the aft section liner, which was rigidly attached to the forward flange of the aft section assembly. A sliding seal arrangement was employed at the aft end of the liner to allow for thermal expansion of the liner relative to the cooler supporting structure. As in the dome assembly, low pressure drop flange bleed holes were provided to allow cooling air to flow between the forward liner and aft section impingement cavities. Flanges were also provided for flat, uncooled sidewalls to seal the combustor and impingement cavities. The entire combustor aft section was permanently attached to the aft mounting flange, which was sized to match the instrumentation section of the test rig.

In addition to the common hardware components, overall combustor flow splits for the design baseline combustors were similar. Initial design flow splits are indicated in Table IV. Flow levels were selected to provide a dome (swirler exit) stoichiometry of 1.0 at the design overall combustor fuel-air ratio of 10.5 g/kg. This initial stoichiometry was selected to promote

ORIGINAL PAGE IS
OF POOR QUALITY

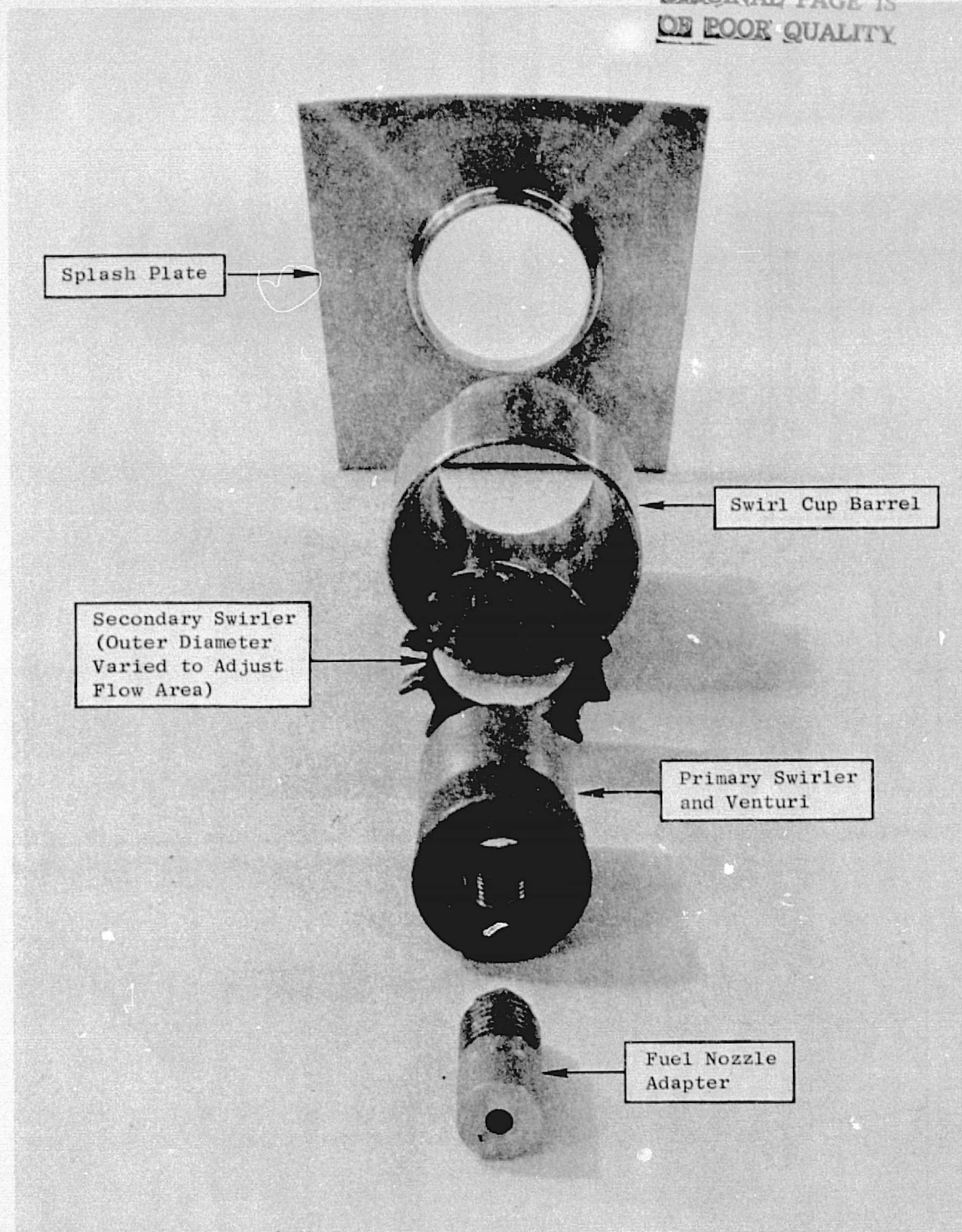


Figure 11. Swirler Assembly.

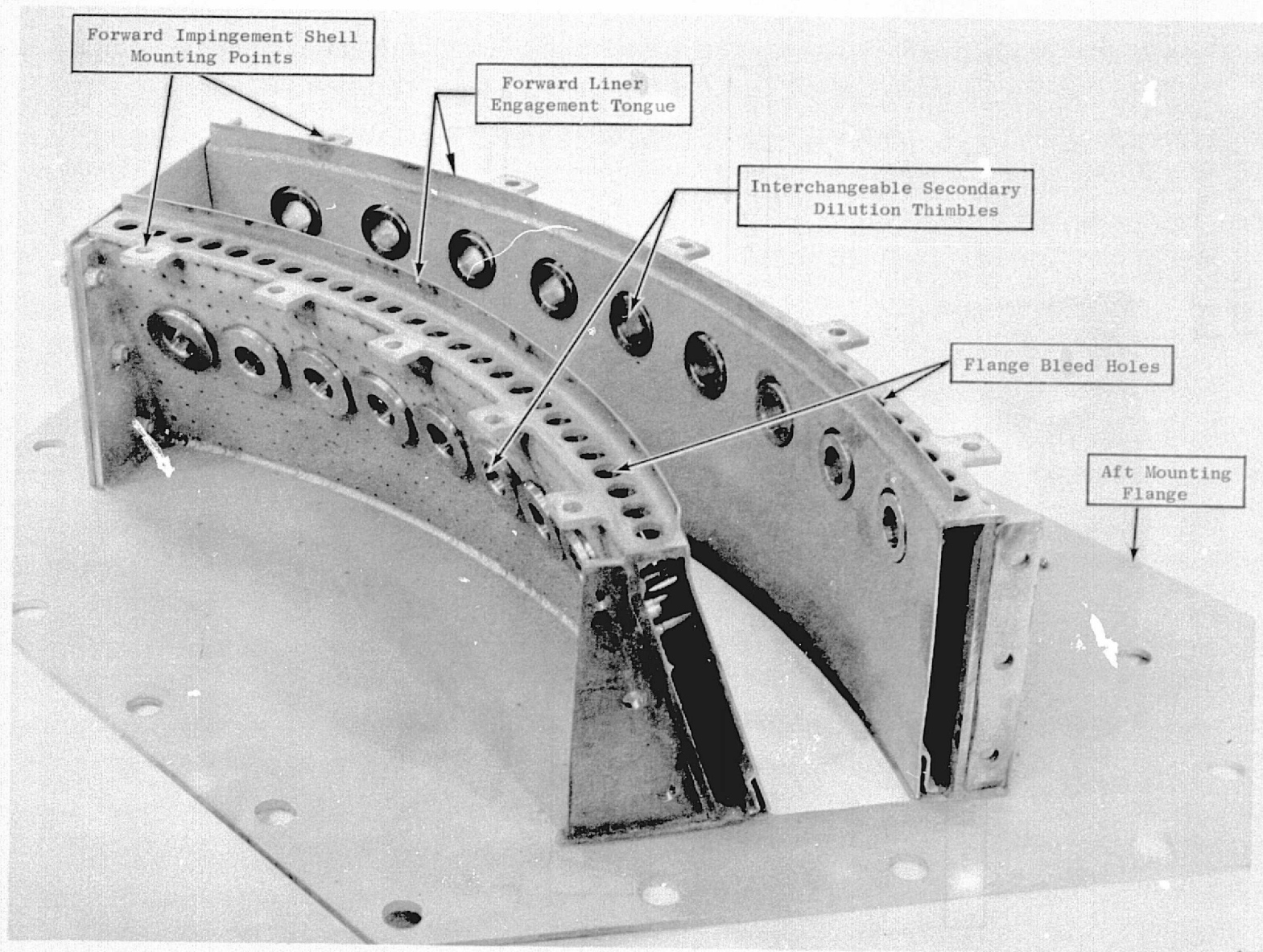


Figure 12. Common Combustor Aft Section (Sideplate Removed).

Table IV. Baseline Combustor Airflow Distributions.

Percent of Total Combustor Airflow			
	Concept I	Concept II	Concept III
	Hot-Wall Baseline	Recuperative Baseline	Catalytic Baseline
<u>Dome</u>			
Swirler			
Primary	6.1	(3.3)	3.3
Secondary	9.3	(12.1)	12.1
Total	15.4	15.4	15.4
Impingement Cooling	5.8	5.8	4.4
<u>Main Combustor</u>			
Impingement Cooling			
Inner	6.8	6.8	3.1
Outer	8.5	8.5	3.9
Total	15.3	15.3	7.0
Dilution			
Central Jet	6.0	(10.2)	23.2
Coannular	(4.2)	0	(11.4)
Total	10.2	10.2	34.6
<u>Aft Combustor Section</u>			
Impingement Cooling			
Inner	4.0	4.0	4.0
Outer	4.6	4.6	4.6
Total	8.6	8.6	8.6
Dilution			
Central Jet	48.9	70.3	41.4
Coannular	(25.5)	(4.1)	8.6
Total	74.4	74.4	50.0
Total	100.0	100.0	100.0

Note: Numbers in parentheses are flows fed by another quoted source and are not included in total (bottom line).

rapid hydrocarbon decomposition reactions. The dome mixture was then diluted to approximately 0.6 equivalence ratio by the primary dilution flow. As shown in Figure 13, equivalence ratios in this range provided the most rapid consumption of the CO produced in the dome region. An exception to this primary dilution flow level was made in the catalytic combustor design, where higher flow levels were required upstream of the catalytic reactor (nominally 50% of combustor airflow) to provide the design catalyst inlet temperature.

4.2.2 Hot-Wall Combustor

A cross-sectional view of the hot-wall baseline combustor, showing the design flow splits and pressure distribution, is shown in Figure 14. These flow splits varied slightly from the design values presented in Table IV due to manufacturing tolerances and preferential cooling added in preliminary checkout tests. As indicated in this figure, the ceramic-coated surfaces included the combustor dome and the forward liners, extending from the dome to the aft section. A total hot-wall burning length of 19.1 cm was provided with this design.

The thermal barrier coating used was a plasma-sprayed three-layered system having a total thickness of 1.3 mm. This system consisted of a 0.1-mm layer of Nichrome plus 6.0% aluminum bond coat, followed by a 0.5-mm layer composed of 30% by weight of bond coat material mixed with 70% calcia stabilized zirconia (87% stabilizer by weight), and a final 0.8-mm layer of yttria stabilized zirconia (12% stabilizer by weight). etc.

With this thermal barrier coating, one-dimensional heat transfer analysis indicated an average ceramic surface temperature of approximately 840 K, with a base metal liner temperature of about 700 K.

The forward ends of the forward liners were rigidly attached to the dome assembly. As in the aft duct assembly, sliding seals were provided at the aft end of the impingement-cooled liner to allow for thermal growth. Flat, uncooled sidewalls were also mounted as in the aft section.

In the Hot-Wall concept, spent dome and liner impingement cooling flows were introduced into the combustor as annular dilution, as shown in Figure 14. Details of the dome configuration and impingement cooling circuit used in the hot-wall combustor are shown in Figure 15.

4.2.3 Recuperative Combustor

A cross-sectional view of the recuperative baseline combustor with its flow splits and pressure distribution is shown in Figure 16. In this combustor, the dome cowl opening was sealed off and the low pressure drop dome feed holes were opened to allow spent impingement cooling air to feed into the swirlers. Details of the dome geometry and cooling circuit are shown in Figure 17. Spent cooling air was also used for the forward dilution. A minimum aft section annular dilution area was used to allow a large proportion

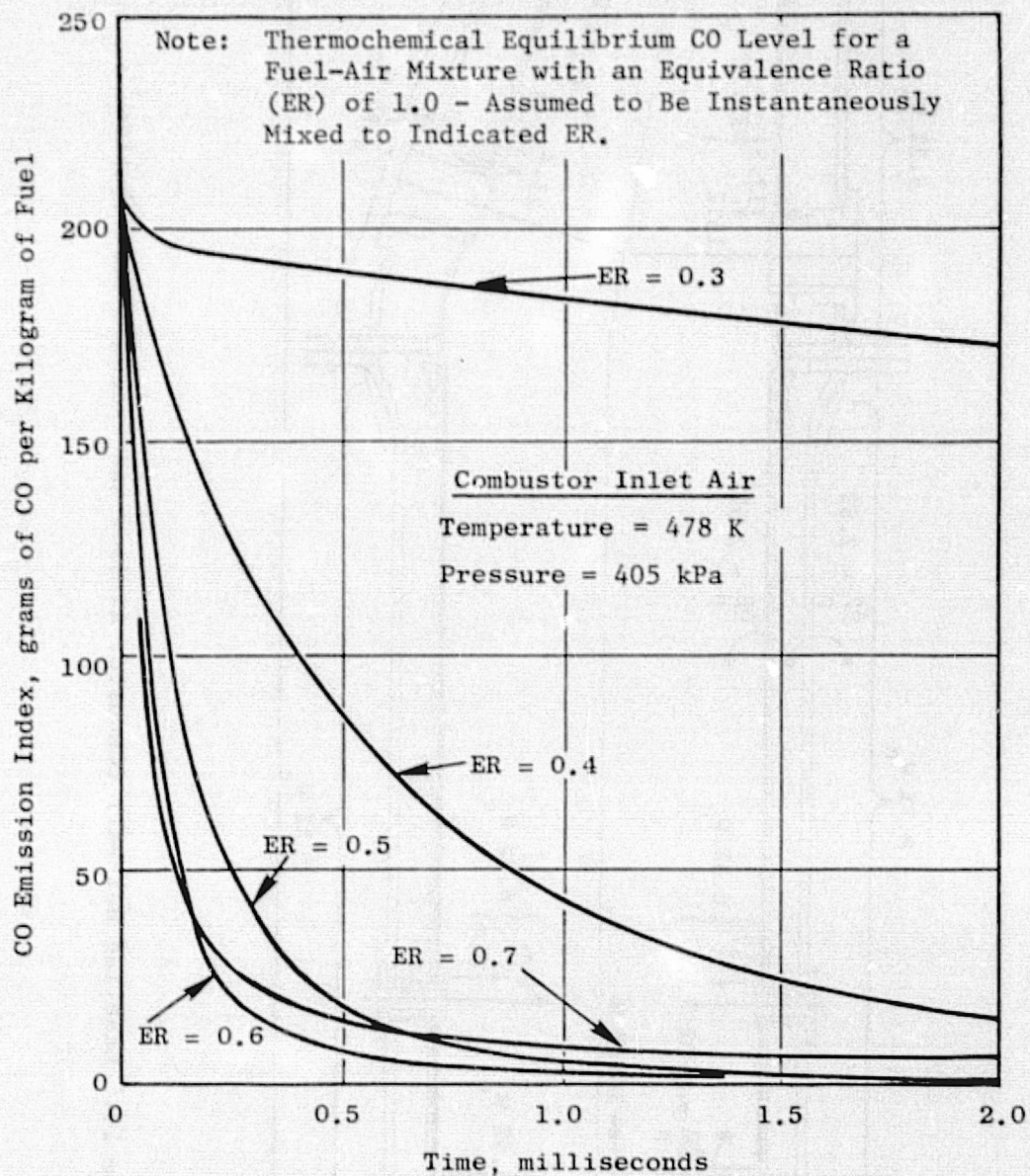


Figure 13. CO Consumption Rates at Low-Power Operating Conditions.

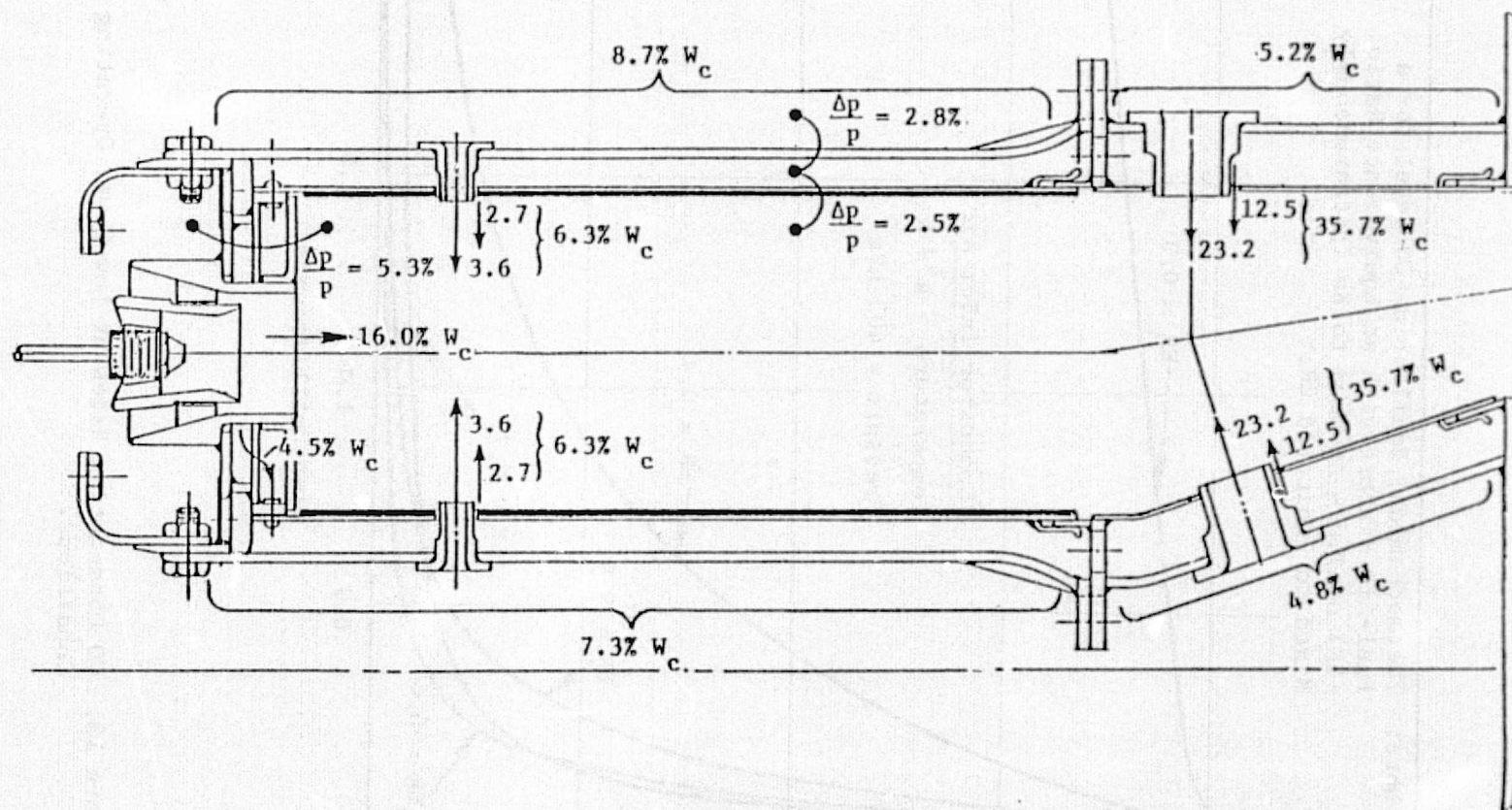


Figure 14. Baseline Hot-Wall Combustor Airflow and Pressure Distribution.

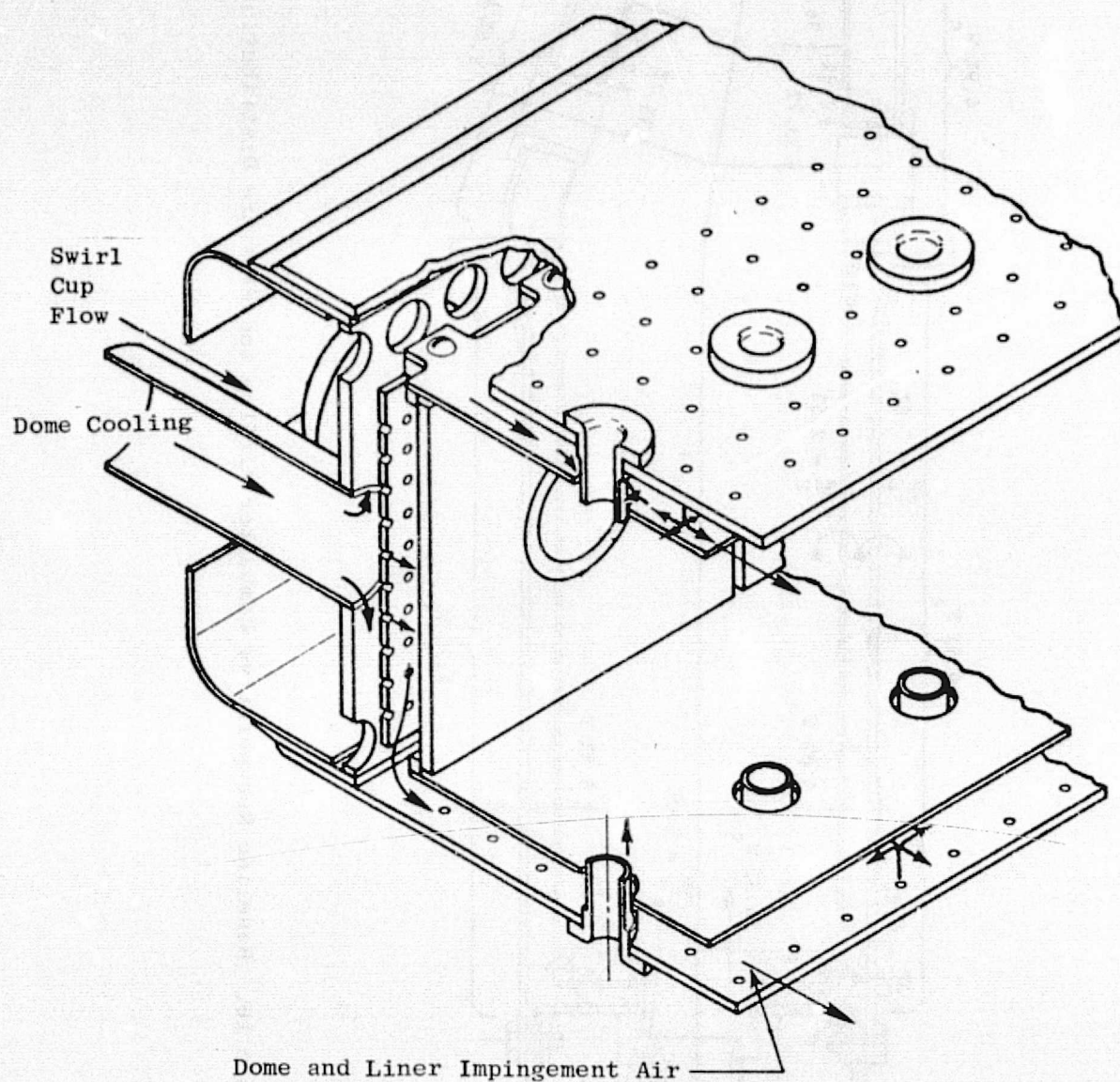


Figure 15. Hot-Wall Combustor Cooling Circuit.

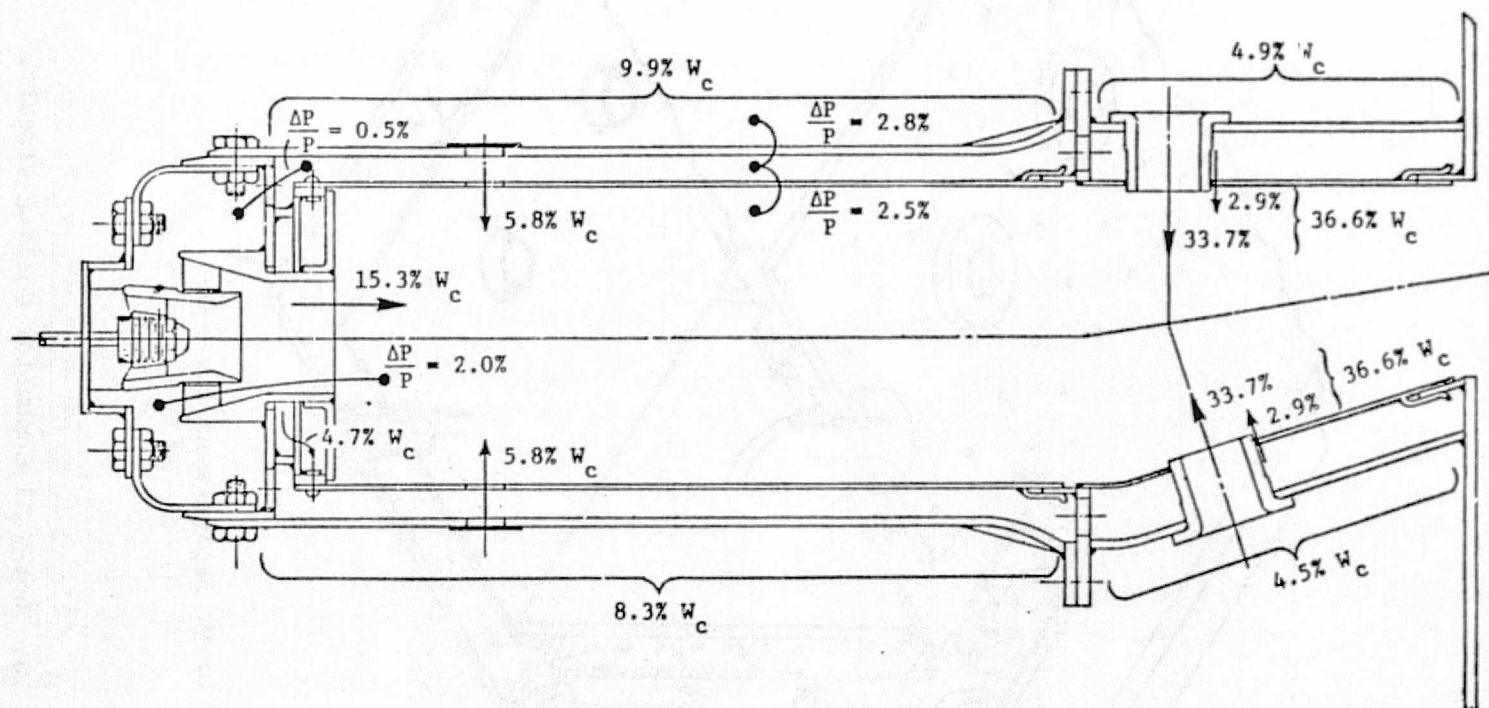


Figure 16. Baseline Recuperative Combustor Airflow and Pressure Distribution.

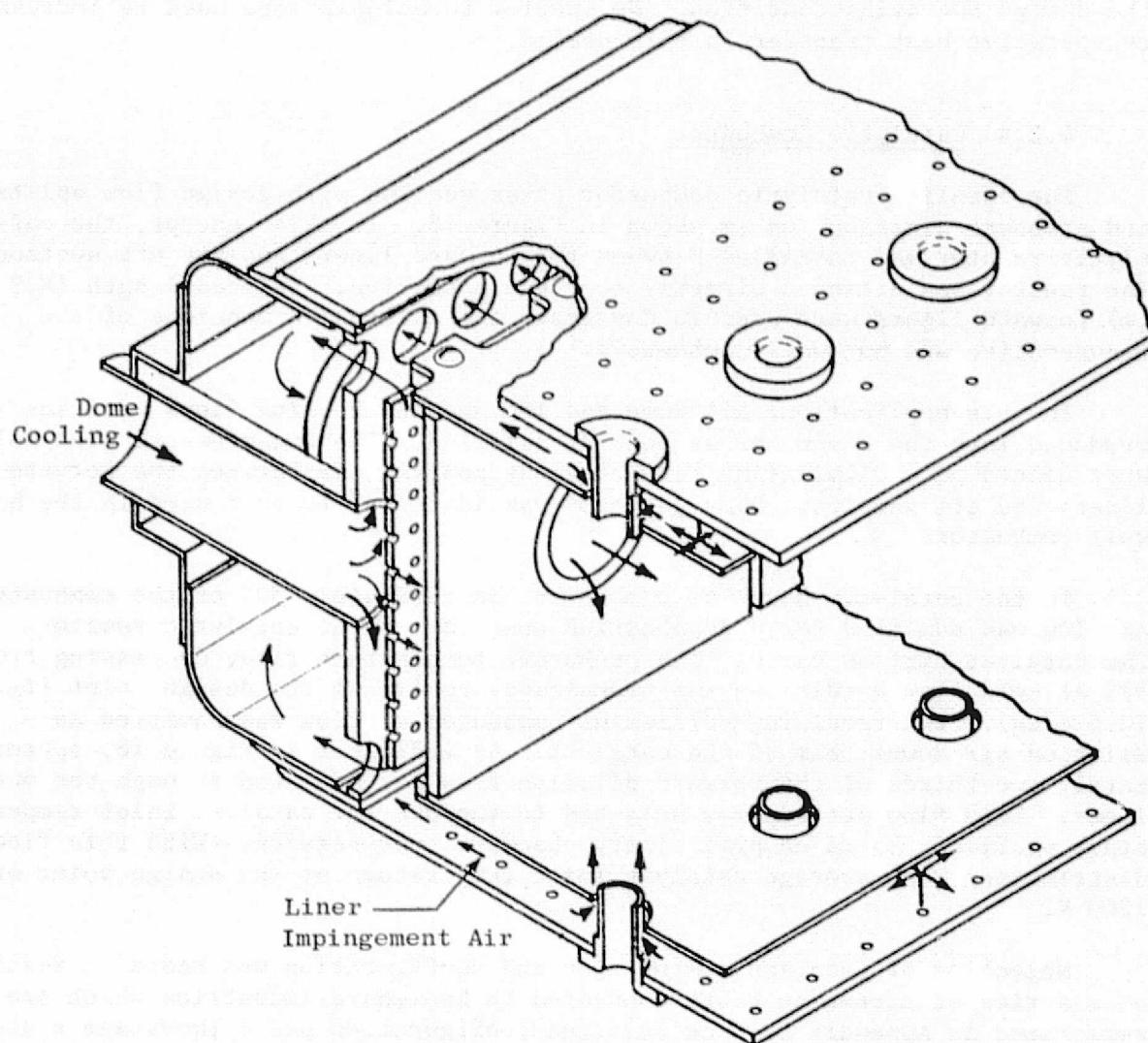


Figure 17. Recuperative Combustor Cooling Circuit.

of impingement air to feed the dome and forward dilution. A small aft annular dilution gap (0.5-mm diametrical clearance) was left to allow for thermal expansion while minimizing leakage.

One-dimensional heat transfer studies conducted for the baseline configuration indicated a recuperative temperature rise of approximately 100 K at the design operating condition. No special techniques were used to increase recuperative heat transfer in this design.

4.2.4 Catalytic Combustor

The baseline catalytic combustor cross section with design flow splits and pressure distribution is shown in Figure 18. In this concept, the catalytic reactor was installed between the forward liners and the aft section. The reactor was attached directly to the aft section. Reduced-length (8.9 cm) forward liners were used to duplicate the external dimensions of the recuperative and hot-wall combustors.

In this application, all dome and impingement cooling flows were introduced into the combustor as annular dilution. The low-pressure feed holes were closed off, eliminating flow of spent cooling air between the forward liners and aft section. Dome geometry was identical to that used in the hot-wall combustor.

In the catalytic baseline combustor, approximately 50% of the combustor airflow was admitted for precombustion upstream of the catalytic reactor. The catalyst airflow varied with preburner temperature rise, decreasing from 57% at cold flow conditions (no preburning) to 49% at the design point ($f_m = 10.5$ g/kg). The remaining portion of combustor airflow was admitted as dilution air downstream of the catalyst. As indicated in Figure 18, approximately two-thirds of the forward dilution flow was admitted through the outer liner. This flow pattern was selected to improve the catalyst inlet temperature profiles, based on preliminary checkout test results. With this flow distribution, the average catalyst inlet temperature at the design point was 1200 K.

Selection of catalyst composition and configuration was based on results of a series of screening tests conducted by Engelhard Industries which are summarized in Appendix G. The selected configuration was a two-stage system composed of series-mounted 5.1 and 3.8 cm lengths of Engelhard DXD-222 catalyst, separated by a 0.6-cm space. The selected catalyst support configuration was a corrugated honeycomb having a sine wave cell shape as shown in Figure 19. This configuration provided a cell density of 39 holes/cm², with a hydraulic diameter of 0.975 mm, and 65.5% open area. Catalyst loading and type are proprietary to Engelhard Industries.

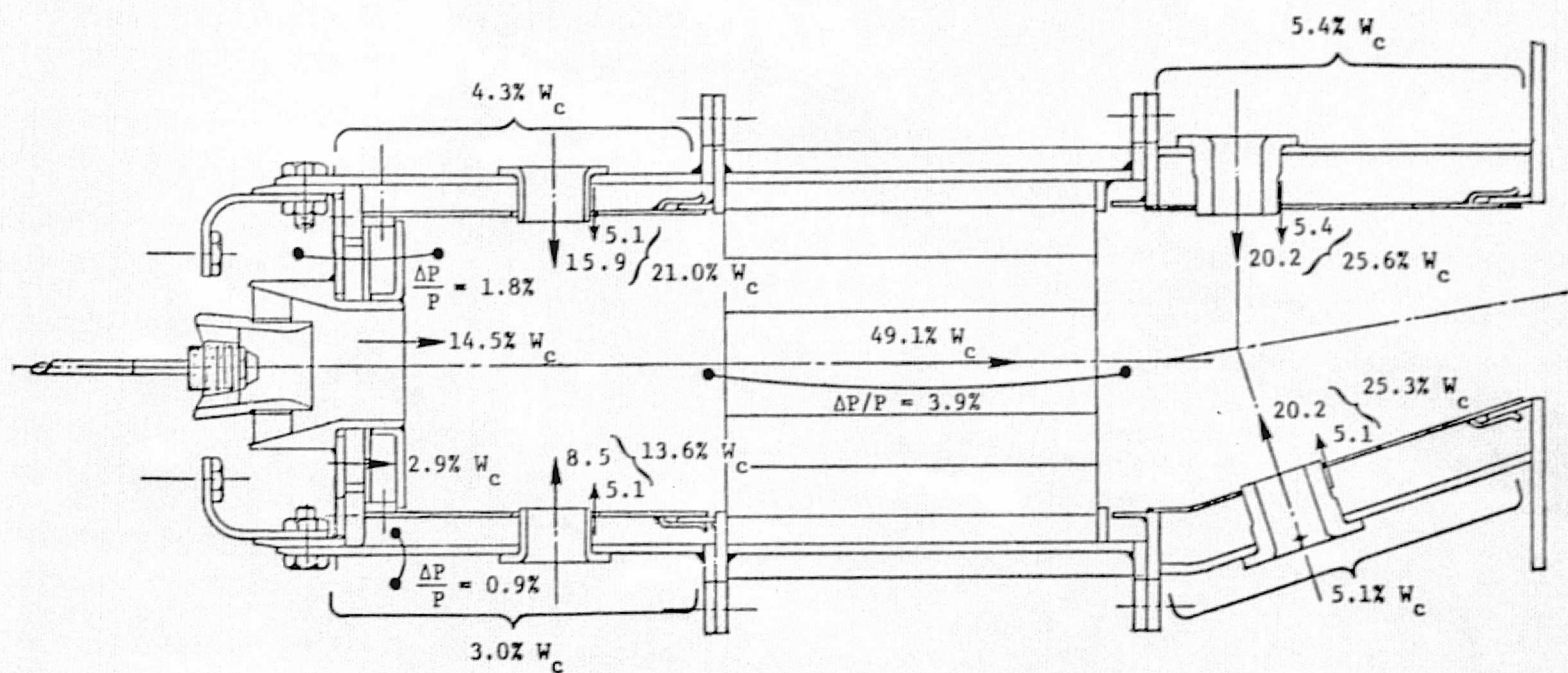


Figure 18. Baseline Catalytic Combustor Airflow and Pressure Distribution.

ORIGINAL PAGE IS
OF POOR QUALITY

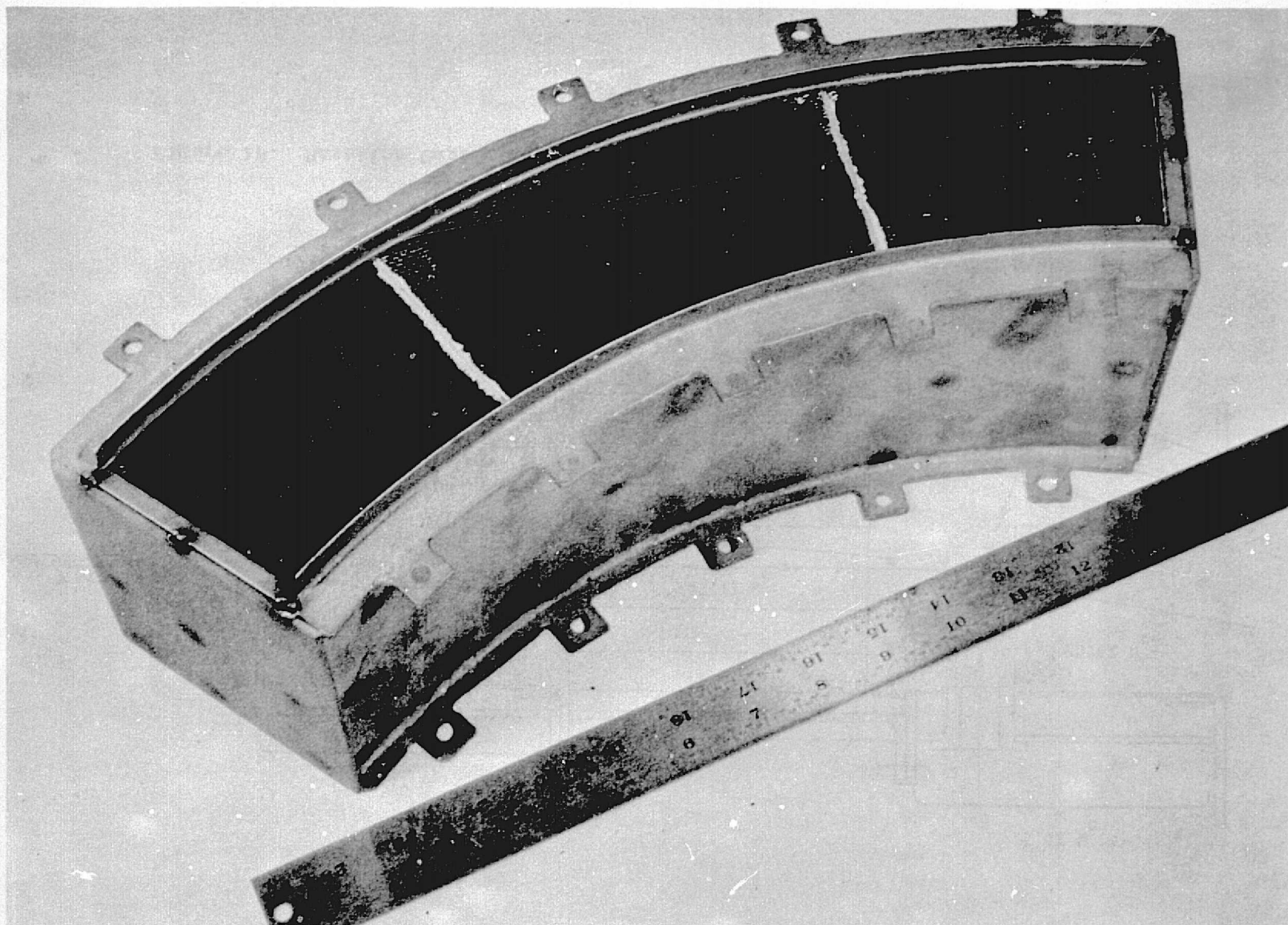


Figure 19. Catalytic Reactor.

4.3 TEST RIG AND FACILITIES

4.3.1 Combustor Rig

The 60-degree sector, CF6-50 test rig assembly shown in Figure 20 was utilized for combustor tests. This rig assembly consists of an inlet plenum, a combustor housing containing the diffuser and combustor casing, an exit instrumentation section, and an exit plenum. The diffuser and combustor housing were constructed from segments of a CF6-50 compressor rear frame, which contains the complete inlet diffuser assembly and outer combustor casing; and a matching segment of the engine seal bearing assembly, which comprises the inner wall of the combustor housing. Flat plates welded to these casings form the sidewalls of the test rig. For the LOPER tests, a port was provided on one sideplate for mounting a hydrogen torch igniter. The 60-degree compressor rear frame segment has provisions for five swirl cup fuel nozzle assemblies.

The LOPER combustors utilized a liner aft-flange mounting design similar to the method employed in F101 and CFM56 engines. The combustor was completely supported from the aft flange, providing a positive flow seal at this station.

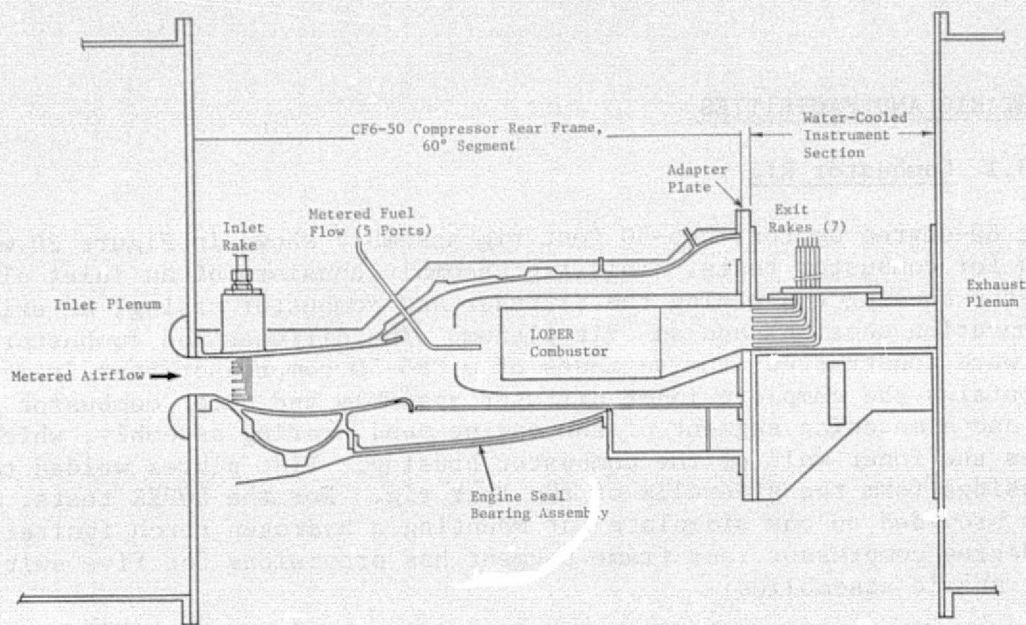
In order to accommodate the straight-wall combustor design selected for the LOPER combustor concepts, it was necessary to lower the exit instrumentation section approximately 3.2 cm relative to the combustor casing. This was accomplished by installing an adapter plate with offset bolt patterns between these components.

Combustor exit instrumentation was located in the water-cooled exit instrumentation section. This assembly contains seven equally spaced ports for mounting gas sample/thermocouple rakes.

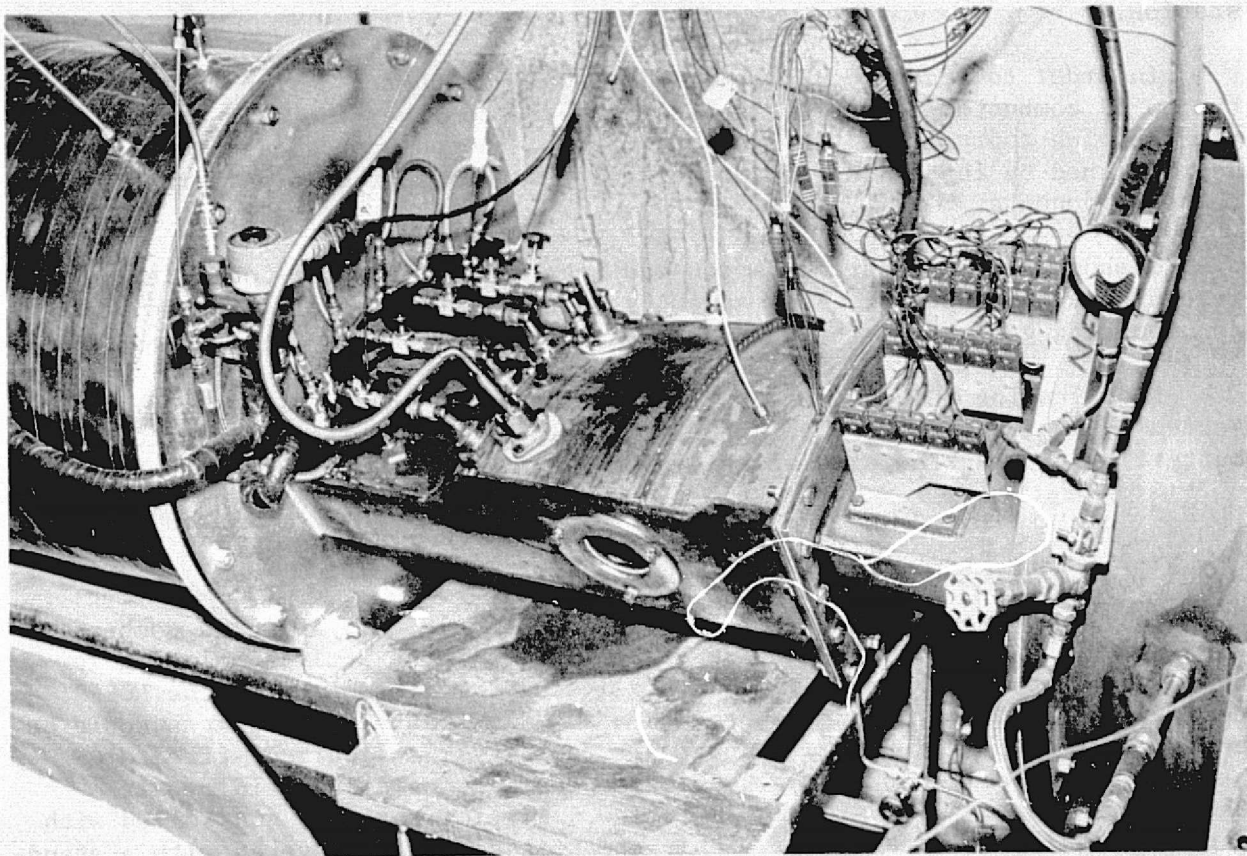
Flow leaving the instrumentation section was quenched with water injected through spraybars within the exit plenum. A pneumatically actuated butterfly valve at the exit of this plenum was used to control rig pressure.

4.3.2 Combustor Test Facility

Tests were conducted in the Building 306 Small-Scale Advanced Combustion Laboratory. This facility provided capabilities for exactly simulating low-power combustor inlet conditions in small-scale rig tests. With the LOPER test setup, air at pressures up to 2 MPa and flow rates up to 5 kg/s could be continuously supplied from a central air facility. An indirect-fired preheater located adjacent to the test cell provided nonvitiating inlet air temperature up to 500 K at 5 kg/s airflow. Airflow rate was controlled with a pneumatically actuated valve within the test cell, and metered with a standard ASME orifice located upstream of this valve. A second airflow measurement obtained with an orifice located downstream of the preheater was used to verify airflow rate and to detect possible leaks within the preheater system.



(a) Test Rig Schematic



(b) Photograph of the Test Rig

JP-5 fuel was supplied from tanks located next to the test cell. Boost pumps located in the cell provided fuel injection pressures up to 7 MPa. Fuel flow was metered with turbine-type flowmeters.

Additional test facility equipment used included high-pressure steam and water supplied for required component and instrumentation heating and cooling applications and an instrument air supply for use in pneumatic valves and regulators and for purging of fuel and gas sample lines.

Test rig inlet conditions were controlled and monitored from a console located in the control room adjacent to the test cell (Figure 21). Other permanently mounted control room facilities used in combustor tests included self-balancing potentiometers and digital recorders to monitor and record thermocouple outputs, and an array of manometers and gages to monitor system pressures. Emissions analysis instrumentation and associated readout equipment were also located within this control room.

4.3.3 Emissions Sampling and Analysis System

Gas samples for emissions analysis were withdrawn from the combustor exit through a fixed array of seven combination temperature/total pressure/gas sampling rakes mounted in the exit instrumentation section. Each of these rakes had five sampling orifices, as shown in Figure 22. The thermocouples mounted within the sampling orifices were aspirated by the sample flow, allowing simultaneous acquisition of gas samples and exit temperatures. Total exit pressure was obtained by shutting off rake flow and reaching system pressure. No probe cooling was necessary for sample quenching or protection of the rakes in this application because of the low exit temperatures encountered within the LOPER test matrix.

Alignment of the sampling rakes relative to the fuel injector centerlines is shown in Figure 23. Because of the instrumentation system offset discussed above, the rake centerlines did not exactly coincide with fuel injector centerlines.

Samples from the rake were routed to the emissions analysis section (CAROL) as shown in Figure 24. With this system, any ganged sample or combination of ganged samples could be analyzed. Sample vents were provided to ensure continuous sample flow throughout the system except during total pressure readings. Sampling system pressure was maintained at 170 kPa by a dump valve at the inlet to the emissions analysis section. All sample lines within this system were steam traced and system temperatures were monitored to maintain sample temperatures close to 422 K.

The emissions analysis section consisted of instrumentation for the measurement of CO, CO₂, HC, and NO_x. The gas analysis instruments utilized in this system were Beckman Model 315B and 864 nondispersive infrared analyzers for CO and CO₂, respectively; a Beckman Model 402 flame ionization detector for HC; and a Beckman Model 951 unheated chemiluminescence analyzer

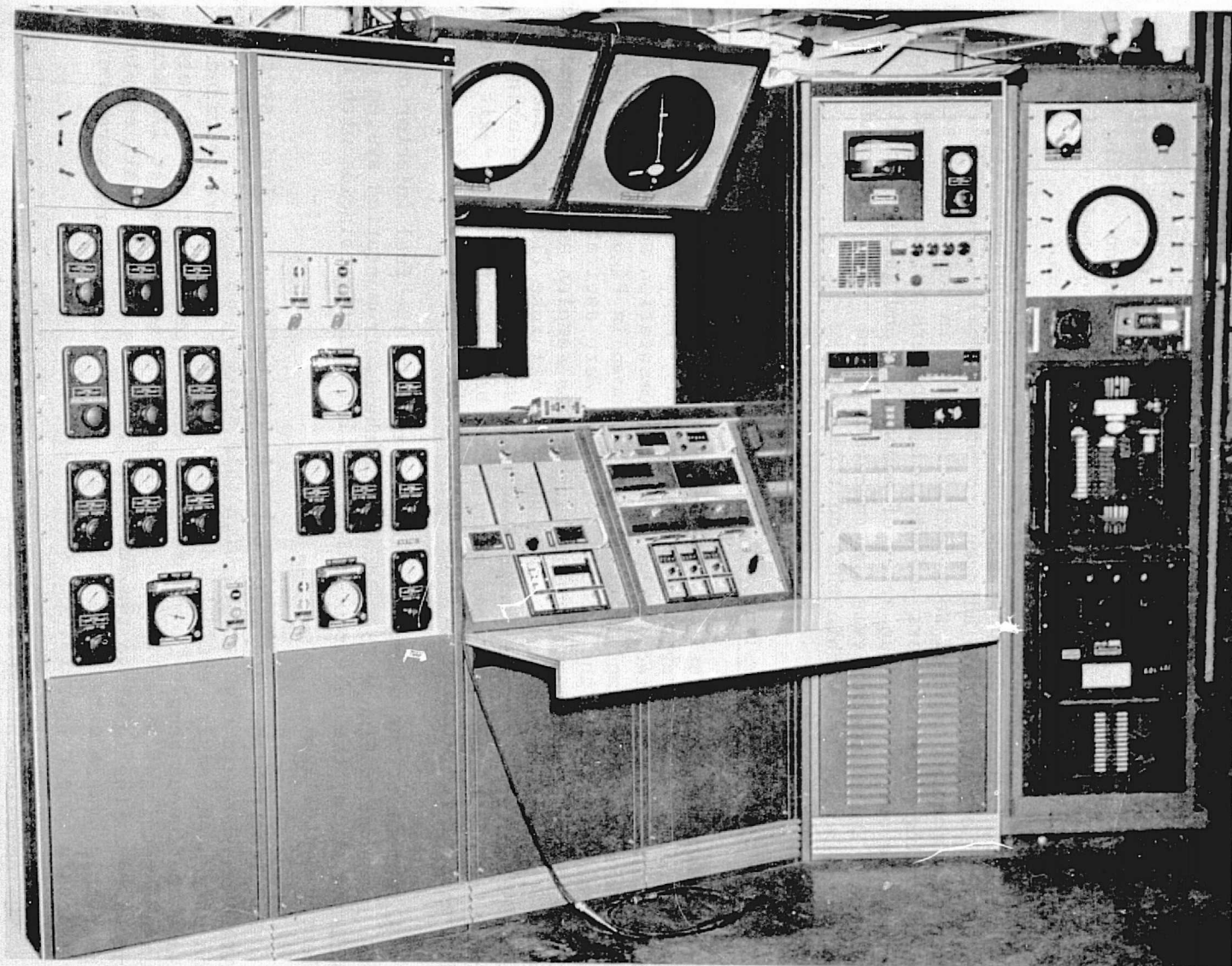


Figure 21. Control Console, Building 306 Advanced Combustion Laboratory.

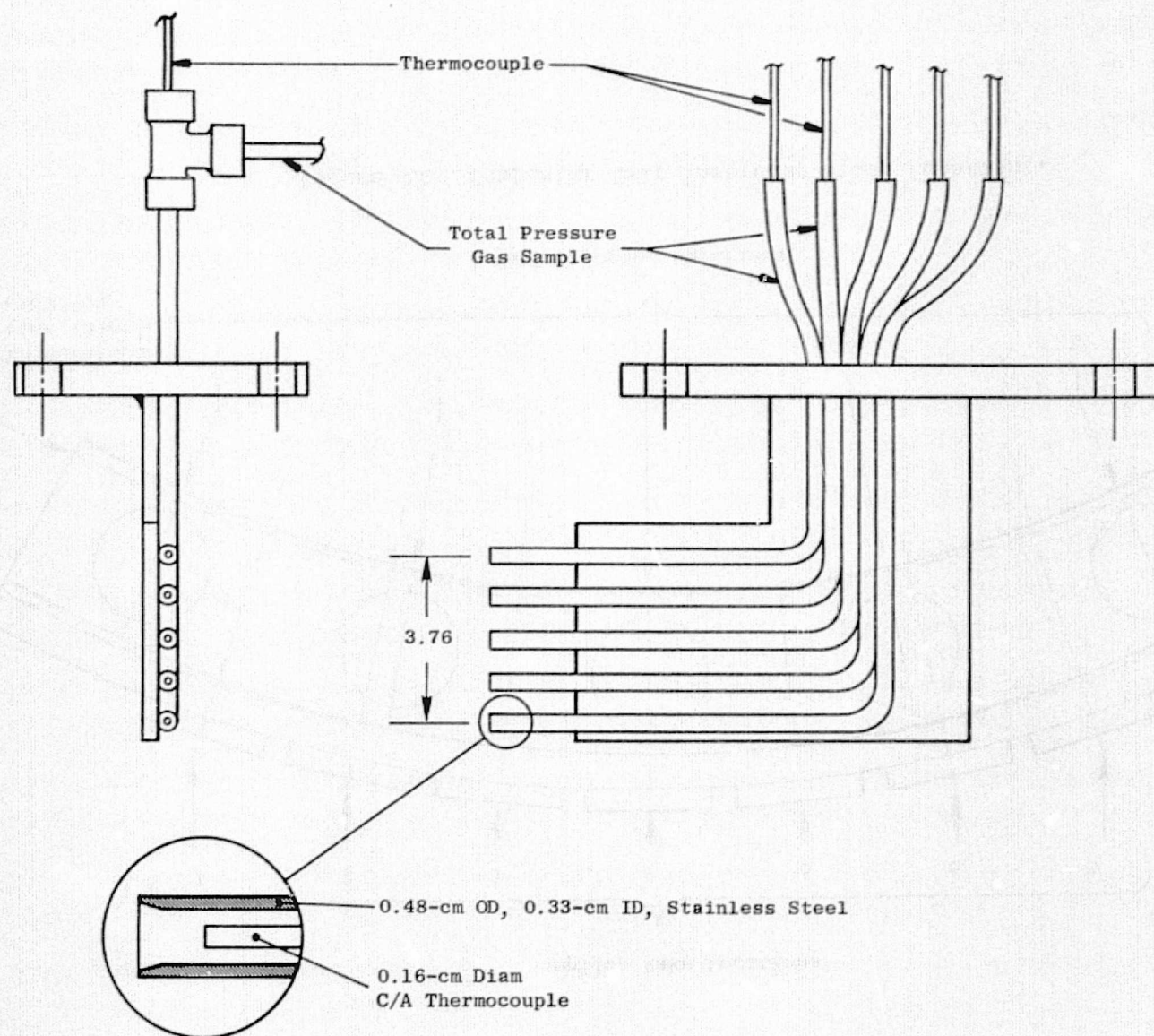


Figure 22. Combination Thermocouple/Gas Sample/Total Pressure Rake.

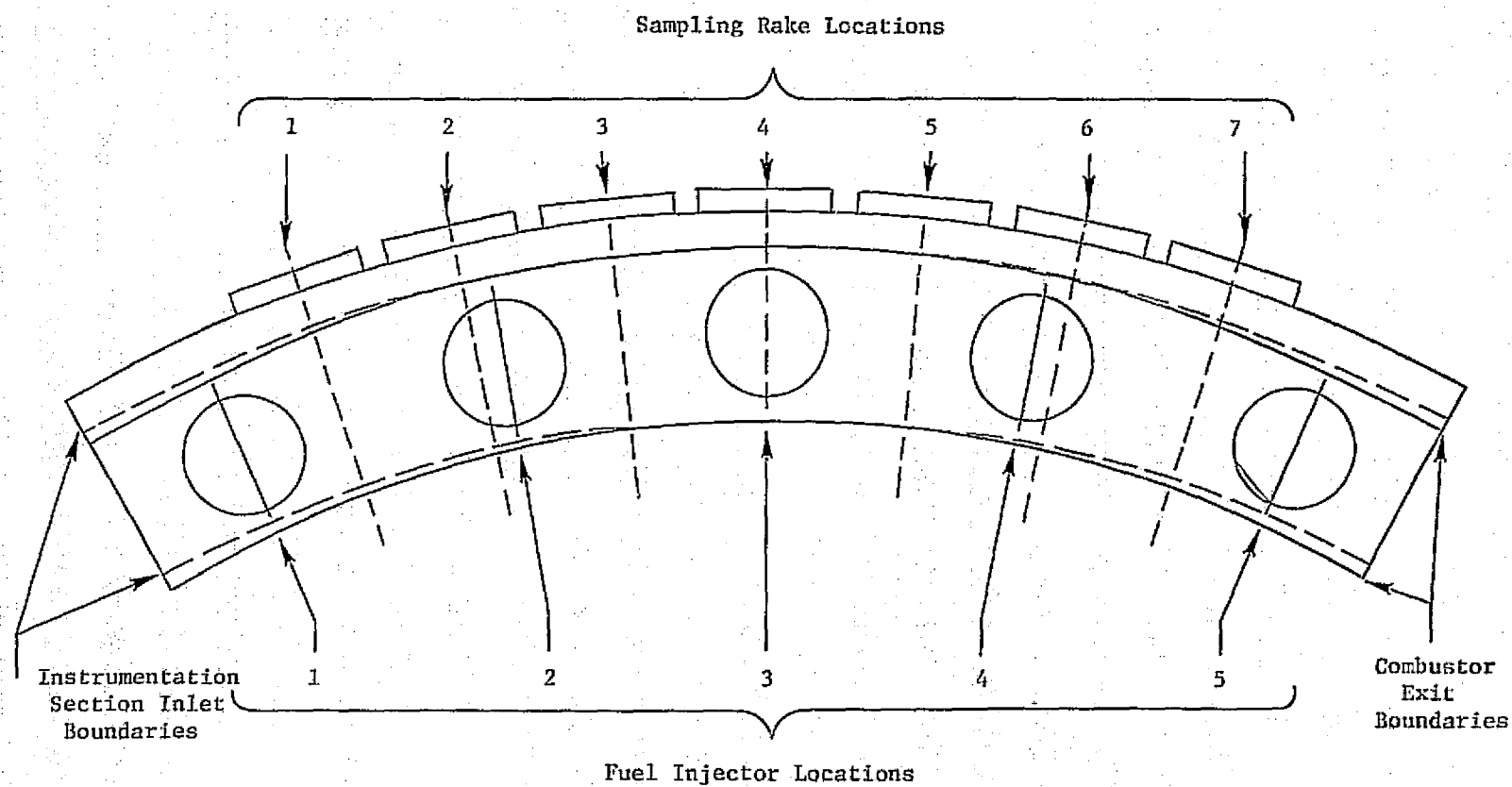
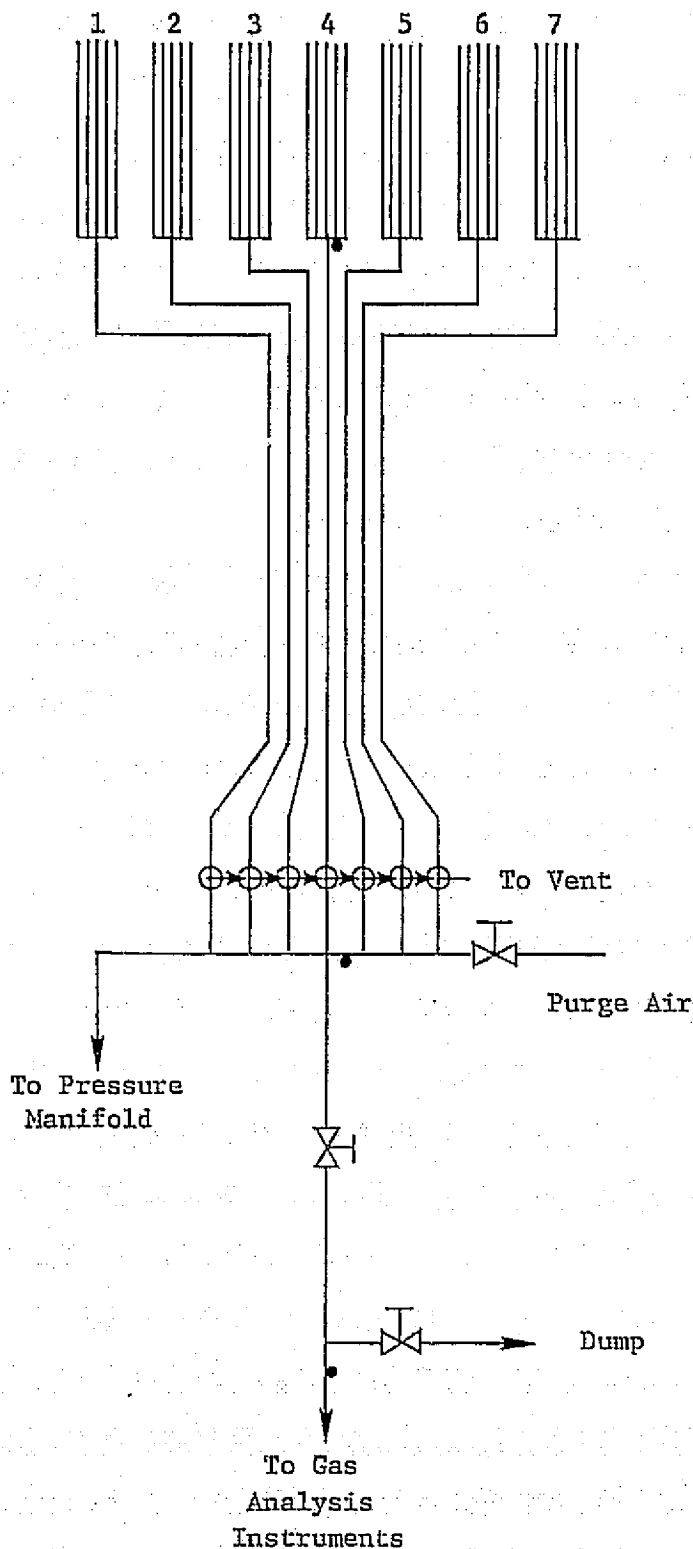


Figure 23. Combustor Exit Instrumentation Locations.



Gas Samples Withdrawn Through Seven 5-Element Temperature/Pressure/Gas Sample Rakes.

Rake Elements Manifolded at Rig Interface (Insulated, Steam Traced).

Sample Transit to Control Room Through Two 5-Element Dekoron Tube Bundles (Steam Heated Internally). Approximately 12 Meters in Length.

Sample Selection Valves and Manifold at CAROL Gas Analysis Interface (Insulated, Steam Traced).

Sample Shutoff Valve (Open for Gas Sample, Closed for Total Pressure).

Sample Dump Valve for CAROL Flow Control.

• = Thermocouple Locations

Figure 24. Gas Sample/Exit Pressure Manifolding Diagram.

for NO_x. Ranges and calibration gases used with each of these analyzers are shown in Table V. The zeros on the NDIR and chemiluminescence analyzers were set with dry nitrogen. The FID zero was set with ultra-pure (hydrocarbon-free) breathing air. Traps maintained at 273 K were installed upstream of the NDIR instruments to provide dry samples for analysis. A trap maintained at 255 K was used to remove water upstream of the unheated chemiluminescence analyzer.

Output of each of the emissions analyzers was monitored and continuously recorded on strip chart recorders. Analyzer outputs indicated at each test point were also hand-logged for subsequent data reduction.

4.3.4 Combustor Performance Instrumentation

Combustion system performance instrumentation consisted of equipment required to monitor temperatures and pressures within the inlet diffuser and combustor, and at the combustor exit. The CF6-50 test rig assembly used in this program had been designed to provide access for extensive internal instrumentation. Test rig instrumentation selected for this program is shown schematically in Figure 25.

Diffuser inlet (compressor exit) conditions were measured with the total pressure and temperature rake shown in Figure 25. This rake had five total-pressure elements and two chromel-alumel temperature elements spaced radially across the diffuser inlet. Inlet temperatures at two other circumferential locations were obtained with thermocouple probes mounted within the diffuser. Diffuser inlet static pressure was obtained from two static taps located on the diffuser wall at the same axial plane as the rake. An additional inlet pressure measurement was obtained with a static tap located in the inlet plenum.

Combustor instrumentation common to all three concepts consisted of 2 total pressure elements, 12 static pressure taps, 9 liner temperature thermocouples, and 2 air temperature thermocouples. An additional thermocouple and static pressure tap were used to measure fuel inlet conditions. The locations of the above devices are shown in Figure 25.

Static pressure taps located in the outer passages and in the liner and dome cavities were used to verify design pressure drops and to estimate any deviation in flow splits from the design values. Dome pressure drop was obtained from total pressure elements located at the cowl lip and a static tap inserted through the combustor sidewall immediately downstream of the dome. A second static tap located in the sidewall of the aft duct was utilized to determine the pressure drop across the catalyst in the catalytic combustor configuration.

Air temperature within the dome cavity, a parameter which was of particular significance in the recuperative combustor configuration, was measured using two chromel-alumel thermocouples located as shown in Figure 25.

Table V. Emission Instrument Calibration Gases.

Gas Constituent	Instrument Range	Nominal Full-Scale Reading	Span Gases			
			1	2	3	4
CO ₂ , %	3	10	00.618	1.97	6.19	8.52
CO, ppm	3	1000	103	208	953	---
	2	2500	103	208	953	2120
HC ^(a) , ppm	3	350	73.3	247	---	---
	4	1750	73.3	247	471	1380
NO _x ^(b) , ppm	3	125	29.8	68	---	---
	4	300	29.8	68	286	---

(a) Calibrated in ppm CH₄ using C₃H₈ span gas.

(b) Calibrated with NO span gas.

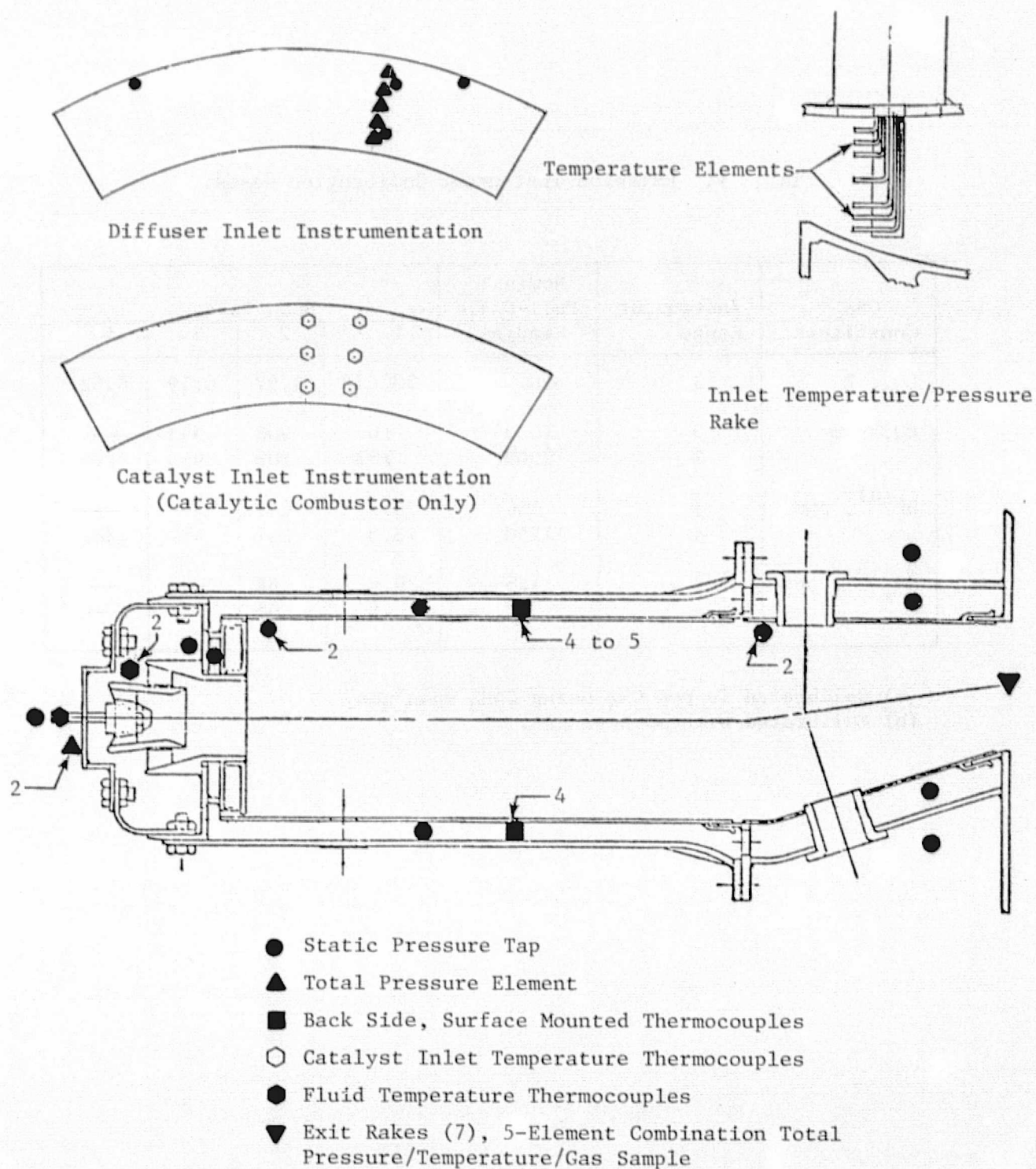


Figure 25. Combustor Performance Instrumentation.

To prevent combustor overtemperature, liner metal temperatures were monitored using eight to nine surface-mounted thermocouples. The locations of these thermocouples were selected based on results of preliminary checkout tests. Locally hot areas were identified in these tests through the use of temperature-sensitive paint applied to the back side of the liners. Thermocouples for the long (hot-wall, recuperative) and short (catalytic) liners were located as shown in Table VI. During runs with the catalytic combustor, an additional array of six thermocouples mounted immediately upstream of the catalyst was used to monitor catalyst inlet temperature.

Combustor exit temperature profiles were obtained with aspirated thermocouples mounted within the exit rake sampling orifices. Exit total pressure was measured by momentarily shutting off flow from the rakes and recording sampling system pressure under no-flow conditions.

4.4 TEST CONDITIONS AND PROCEDURES

4.4.1 Screening Test Point Matrix

Combustor screening tests were conducted over a range of combustor inlet conditions typical of aircraft engine idle conditions. The design value and planned range of variation of inlet conditions are shown in Table II. Specific planned combustor screening test points are listed in Table VII. Test points are coded with three-digit point numbers to indicate inlet temperature/pressure level, reference velocity, and fuel-air ratio. This test point matrix was used as a guideline during tests, but testing was also conducted at fuel-air ratios and reference velocities outside of this matrix, sometimes in order to fully define combustor emissions characteristics and other times to avoid combustion instability, as discussed in the following chapter.

4.4.2 Test Procedures

In combustor screening tests, a minimum number of test points were obtained to characterize combustor emissions and operating characteristics as a function of inlet temperature and pressure, reference velocity, and fuel-air ratio. A typical screening test consisted of 8 to 15 test points selected from Table VII. Test points were selected to give at least two levels of inlet temperature/pressure and two reference velocities. At each set of inlet conditions, fuel flow was varied over a sufficient range to define the characteristic variation of HC and NO_x with fuel-air ratio, and to establish the fuel-air ratio for minimum CO levels. Three to five different fuel flows were generally required to establish these characteristics.

In initial tests of each configuration, operation was first established at the design inlet temperature and pressure (2XX series test points), with reference velocity as required for stable combustion. If, after determining the emissions characteristics as a function of fuel-air ratio, the emissions

Table VI. Combustor Liner Thermocouple Locations.

<u>Liner Type, Location</u>	<u>Axial Location, cm^(a)</u>	<u>Circumferential Locations, °ALF^(b)</u>
Hot-Wall/Recuperative -		
Outer Liner	6.5	342, 354, 6
	9.5	342, 354
Inner Liner	6.5	336, 348, 0, 12
Catalytic -		
Outer Liner	2.0	0, 12, 24
	3.8	21
Inner Liner	2.0	336, 348, 0, 12

(a) Measured from swirler exit.

(b) Center cup at 0° aft looking forward.

Table VII. Combustor Screening Test Point Matrix.

Test Point Number	Inlet Total Pressure, kPa	Inlet Total Temperature, K	Reference Velocity, m/s	Fuel-Air Ratio, g/kg	Expected Total Pressure Loss, %	Combustor Airflow, kg/s
111	203	366	15.2	8.0	2.56	0.82
112				10.5		
113				13.0		
114				15.5		
121			22.9	8.0	5.76	1.23
122				10.5		
123				13.0		
124				15.5		
131			30.5	8.0	10.24	1.64
132				10.5		
133				13.0		
134				15.5		
211	304	422	15.2	8.0	2.22	1.07
212				10.5		
213				13.0		
214				15.5		
221			22.9	8.0	5.00	1.60
222				10.5		
223				13.0		
224				15.5		
231			30.5	8.0	8.89	2.13
232				10.5		
233				13.0		
234				15.5		
311	405	478	15.2	8.0	1.96	1.26
312				10.5		
313				13.0		
314				15.5		
321			22.9	8.0	4.42	1.88
322				10.5		
323				13.0		
324				15.5		
331			30.5	8.0	7.86	2.51
332				10.5		
333				13.0		
334				15.5		

levels closely approached or met program goals, additional testing was conducted at lower temperatures (1XX points). If emissions were well above the goals, inlet temperature was increased for further testing. Additional testing at the second inlet temperature level included attempts to acquire data at a minimum of two different levels of reference velocity.

In later screening tests, where relatively minor modifications were evaluated, the primary objective was to compare the subject combustor to the most similar previous configuration. In these tests, the best comparison was obtained by duplicating the test points which had been run with the previous configuration.

In parametric tests, where the primary objective was to further document the emissions obtained in screening tests, all test points shown in Table VII were attempted. Operating limitations encountered in parametric tests are discussed in a later section.

4.4.3 Data Acquisition Procedures

Emissions data, detailed combustor pressures, and combustor operating parameters were manually recorded on three operator's logs at each operating condition. Exit temperatures and liner skin temperatures were automatically recorded on paper tape with a digital printer.

The data acquisition sequence was as follows:

1. Back purge the sampling system with instrument air.
2. Adjust combustor inlet temperature, pressure, airflow, and fuel flow to selected conditions.
3. Turn off purge. Initiate sample flow (ganged sample) and adjust sample dump valve as required to establish sample system pressure of 170 kPa. Monitor emissions and exit temperatures to determine steady-state conditions.
4. Record emissions, exit temperatures, and combustor operating conditions.
5. Obtain individual- or paired-rake gas samples as required.
6. Shut off sample flow. Read exit total pressure (all rakes ganged).
7. Turn on back purge; adjust operating conditions.

In initial tests, the gas sampling sequence consisted of five separate samples as follows:

<u>Sample Mode</u>	<u>Rake(s)</u>	<u>Position</u>
1	All	Average
2	4	Cup Centerline
3	3 and 5	Between Cups
4	2 and 6	Cup Centerline
5	1 and 7	Between Cups

With this sequence, it was possible to observe circumferential variations and end-wall influences on emissions. Initial results indicated that there were no systematic circumferential variations in emissions or strong end-wall effects.

In later tests, ganged samples were obtained at all test points. Individual rakes were also sampled at selected points to spot check exit emissions profiles and assure that representative samples were obtained.

4.5 DATA REDUCTION PROCEDURES

The overall data reduction flowpath is shown in Figure 26. Emissions data were reduced by means of an existing data reduction program and were input along with combustor operating conditions to a master data reduction program,, which printed out a test data summary.

4.5.1 Emissions Data Processing Procedures

Prior to each combustor test, a complete calibration of the CO, CO₂, HC, and NO_x analyzers was conducted as indicated in Table V. The calibration data were hand-logged and manually input to a computer program (CALIB) which generates a curve fit of pollutant concentration as a function of analyzer range and deflection.

During the tests, analyzer range and deflection and sampling system temperatures and pressures were hand-recorded at each test point. Following the completion of the test, these data were input with calibration curve fits from the CALIB program to another computer program (KAROL) which calculates the exhaust emissions concentrations, emissions indices, combustion efficiency, and fuel-air ratio of each gas sample at every test point.

The KAROL output format is shown in Table VIII. The equations used in this data reduction program are basically those of SAE ARP 1256, and include corrections for water removed in the CO, CO₂, and NO_x analysis systems. In the output, HC emission index is expressed as grams fuel (CH_{1.92}) in the exhaust gases per kilogram fuel supplied to the combustor. Combustion

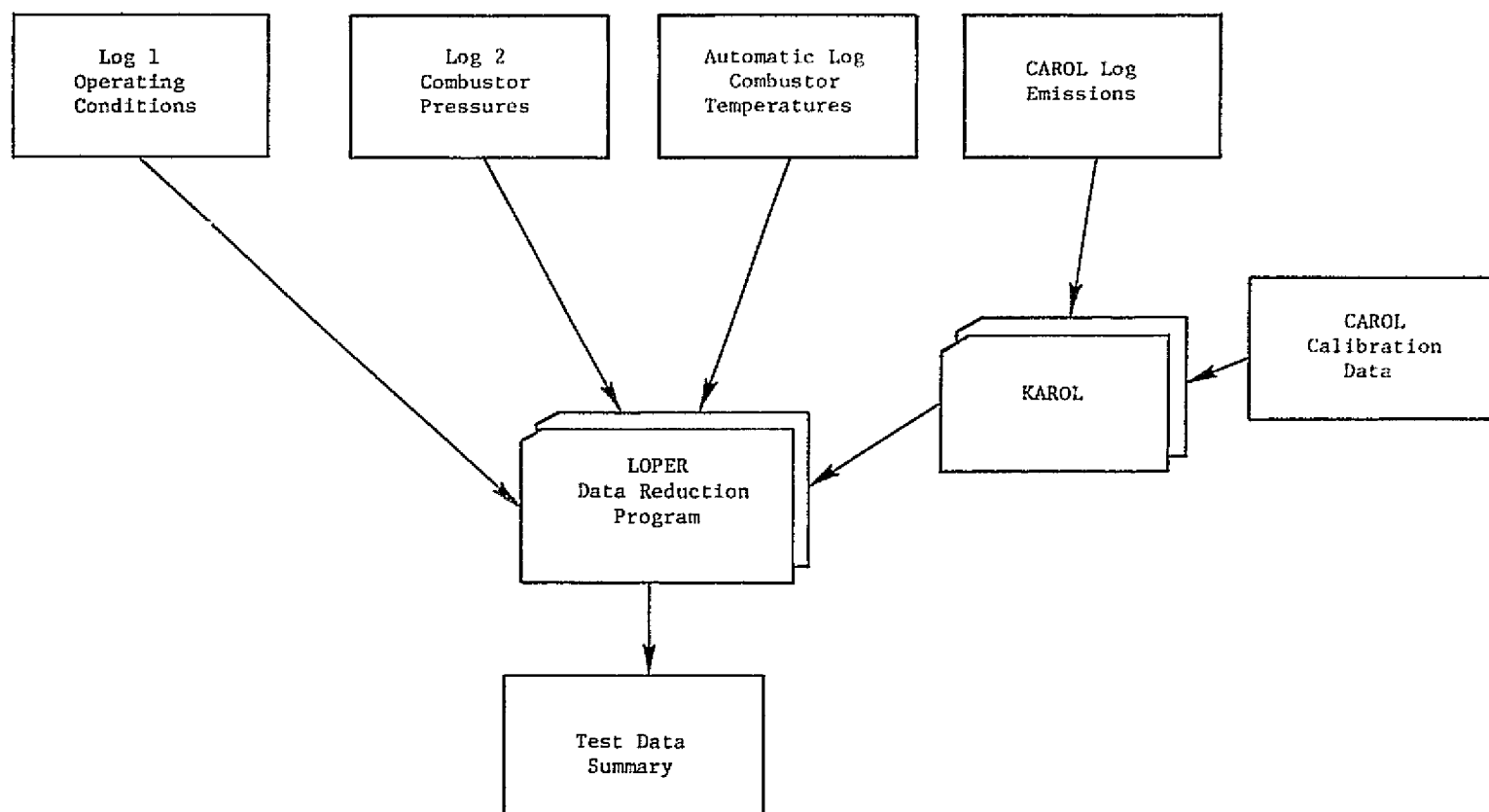


Figure 26. LOPER Data Reduction Flowpath.

Table VIII. Emissions Data Output Format.

TEST - LOPER PARAMETRIC TEST # DATE - 4/13/78
 CELL - 306 RUN - 28 FUEL - JP-5
 CAL TIME = 1030 HUM = 11.2 FUEL H/C = 1.92

RDG 2 POINT 211

SAMPLE LINE TEMPERATURES, K- 422 397 447

		ACTUAL GAS ANALYSIS					SMOKE NUMBER
RAKE PSAMP,	KPA	CO	CO2	HC	NO	NOX	
		SEMI-DRY (PPM)	SEMI-DRY (PCT)	WET (PPM)	DRY (PPM)	DRY (PPM)	
G 0	170.	35.5	1.82	13.4		36.7	
AVG		35.5	1.82	13.4		36.7	

		CALCULATED EMISSIONS LEVELS					COMB EFF
RAKE PSAMP,	KPA	CO	HC	NO	NOX	F/A SAMPLE	
		*****	GROSS FUEL		*****		
G 0	170.	3.9	0.7		6.6	0.00875	99.83
AVG		3.9	0.7		6.6	0.00875	99.83

OVERALL AVG		3.9	0.7		6.6	0.00875	99.83
-------------	--	-----	-----	--	-----	---------	-------

efficiency calculations also assume that all unburned hydrocarbons appear as fuel. The NO_x emission index is reported as grams NO₂ per kilogram fuel.

4.5.2 Operating and Performance Data Processing

Following each run, raw data from the operator's logs, temperature data output from the digital printer, and reduced emissions data output from the KAROL program were input to the LOPER data reduction program. This program employed standard reduction techniques to reduce the raw test data concerning basic combustor operation. Combustor fuel and airflows and the various test rig temperature and pressure measurements were computed and converted to SI units.

Exit temperature data obtained from the aspirated thermocouple rakes were converted without conduction or radiation corrections since these were small at the idle combustor operating conditions studied. Combustor exit temperature pattern factor was calculated using the following formula:

$$PTF = \frac{T_{4 \text{ peak}} - T_{4 \text{ avg}}}{T_{4 \text{ avg}} - T_3}$$

where

PTF = pattern factor

T_{4 peak} = maximum individual exit temperature reading

T_{4 avg} = average exit temperature

T₃ = combustor inlet temperature

Combustion efficiency based on exit temperature was calculated based on a curve fit of ideal temperature rise as a function of inlet temperature and equivalence ratio.

The final output from this data reduction program was a data summary for the configuration tested. The format of this summary is shown in Table IX.

Table IX. Sample Test Summary Format.

Test Summary, Combustor Configuration R5, Run 16

Reading	Test Point	Inlet Total Pressure, kPa	Inlet Total Temperature, K	Inlet Humidity, g H ₂ O/kg Air	Combustor Air Flow, kg/s	Reference Velocity, m/s	Fuel Flow, g/s	Metered Fuel-Air Ratio, g/kg	Sample Fuel-Air Ratio/Metered Fuel-Air Ratio	Thermocouple Combustion Efficiency, %	Sample Combustion Efficiency, %	CO Emission Index, g/kg	HC Emission Index, g/kg	NO Emission Index, g/kg	CO ₂ Volume, %	Thermocouple Average Exit Temperature, K	Pattern Factor	Maximum Liner Temperature, K	Total Pressure Loss, K	Dome Pressure Loss, K	Fuel Nozzle Pressure Drop, kPa	Avg. Catalyst Inlet Temp. (Catalytic), K	Swirl Inlet Temp. (Precombustive), K	or Avg. Liner Temp. (Hot Wall), K
1 111	202.	368.	1.9	0.78	14.7	6.6	8.2	0.89	89.5	97.7	25.6	16.8	2.5	1.53	673.	0.32	969.	2.65	0.59	216.	543.			
2 112	202.	369.	1.9	0.78	14.5	8.6	11.1	0.88	92.3	99.0	14.7	6.7	3.9	2.03	774.	0.33	1034.	2.71	0.58	460.	404.			
3 113	204.	367.	1.9	0.78	14.4	10.6	13.7	0.86	92.2	98.6	36.2	5.3	4.2	2.40	859.	0.32	1043.	2.30	0.58	606.	475.			
4 121	202.	371.	1.9	1.22	23.0	9.9	8.1	0.88	94.2	99.6	7.8	1.8	3.6	1.48	678.	0.26	981.	6.14	1.59	518.	458.			
5 122	204.	368.	2.0	1.22	22.6	12.9	10.6	0.87	93.3	99.4	19.0	1.3	3.6	1.91	760.	0.32	1000.	5.40	1.49	875.	456.			
6 123	202.	367.	1.9	1.22	22.9	15.8	12.9	0.86	92.8	98.9	43.6	0.9	3.5	2.28	837.	0.35	982.	5.11	1.51	1291.	450.			
7 120	203.	366.	1.8	1.22	22.7	8.0	6.6	0.90	94.5	99.1	24.6	2.9	2.9	1.21	616.	0.26	974.	6.12	1.50	325.	441.			
8 131	203.	366.	2.0	1.62	30.1	13.0	8.1	0.88	90.3	99.6	7.9	2.2	3.1	1.47	659.	0.31	1021.	10.53	2.92	869.	447.			
9 210	304.	424.	1.9	1.03	14.8	7.6	7.4	0.93	94.7	99.8	3.4	1.6	5.2	1.43	701.	0.28	1082.	2.27	0.50	397.	512.			
10 211	304.	424.	1.7	1.04	14.9	9.7	9.4	0.93	95.9	99.8	4.5	1.2	5.9	1.82	779.	0.40	1118.	2.27	0.50	513.	526.			
11 216	303.	422.	1.5	1.04	14.9	5.8	5.6	0.94	93.6	93.4	40.8	6.2	3.0	1.07	634.	0.15	883.	1.82	0.50	170.	487.			

ORIGINAL PAGE IS
OF POOR QUALITY

5.0 EXPERIMENTAL TEST RESULTS

5.1 OVERALL TEST SUMMARY

The LOPER experimental program consisted of (1) 18 screening tests in which 6 configurations of each low-emissions combustor design concept were tested to determine the effect of minor modifications on emissions and performance characteristics; and (2) 3 parametric tests, in which the most promising configuration of each concept was tested over a range of parametric test conditions to more completely document these characteristics. Several atmospheric checkout tests, flow calibration tests, and swirl cup fuel spray visualization tests were conducted in support of these tests.

In this chapter, key emissions and operating characteristics observed in the screening tests are described, and final results of parametric tests are briefly discussed and assessed. Additional descriptions of the configurations tested, together with summaries of key emissions and performance data obtained with each of these configurations, are presented in Appendices A and B.

A summary of the configurations evaluated in the screening and parametric tests is presented in Table X, which shows airflow distributions based on effective areas obtained in flow calibration tests and pressure drops based on the average of all measured test data corrected to the design operating point. The axial location of primary and secondary dilution (measured from the swirler exit) has been normalized by combustor dome height ($H_d = 7.6$ cm).

Each configuration tested incorporated one or more minor modifications. These modifications fall into two general categories: (1) general modifications which apply to all concepts, and (2) specific modifications that apply to only one of the three combustor concepts. General modifications included a fuel nozzle change (configurations H2-H7, R2-R7, and C5-C7); a decrease in secondary swirler barrel length-to-diameter ratio (H3-H7, R7, and C5-C7); and variations in swirler flow (H2, R3, and R6), primary dilution flow (R6), and primary dilution pattern (H3-H7, R4-R7, and H4-H7). Specific modifications include a decrease in recuperative combustor primary dilution temperature (R5) and an increase in catalytic combustor primary zone length (C5-C7) and catalyst airflow (C2 and C4).

In conducting the screening tests, any general modification resulting in improved emissions or performance in one concept was normally incorporated into all subsequent configurations of all concepts. In this way, a maximum transfer of technology from concept to concept was achieved.

As a result of technology transfer described above, each of the parametric test configurations incorporated similar modifications of the baseline design. These similarities included the use of low-flow fuel nozzles, decreased secondary swirler barrel length, and the relocations of at least part of the primary dilution to a position downstream of the original position.

Table X. Combustor Design Parameter Summary.

Screening Test Configurations

Configuration/ Test Sequence	AIRFLOW DISTRIBUTION, % WC											Pressure Drop % at		Fuel Nozzle g/s at 690 kPa	Swirler Secondary Barrel Lb/D _B (b)
	Swirlers	Dome Dilution	Primary Dilution at L/H _d = (a)			Secondary Dilution at L/H _d = (a)			Cooling			Design Point Overall	Dome		
			0.5	1.0	1.7	1.5	2.8	4.4	Dome	Fwd Liners	Aft Liners				
H1/3	16.0	---	12.6	---	---	---	71.4	---	4.5	16.0	10.0	5.49	4.93	2.9	0.61
H2/8	22.4	---	11.6	---	---	---	66.0	---	4.2	14.7	9.2	4.73	4.18	2.1	0.88
H3/13	16.0	---	---	12.6	---	---	71.4	---	4.5	16.0	10.0	5.08	4.98	2.1	0.14
H4/14	16.0	---	5.6	7.2	---	---	71.4	---	4.5	16.0	10.0	5.38	4.80	2.1	0.14
H5/15	15.4	---	7.0	8.0	---	---	69.6	---	4.2	15.0	9.2	4.92	4.36	2.1	0.14
H6/16	15.3	5.2	2.4	8.0	---	---	69.2	---	4.2	14.8	9.2	4.13	4.09	2.1	0.14
R1/4	15.3	---	11.6	---	---	---	73.1	---	5.1	18.2	9.4	4.80	1.37	2.9	0.88
R2/5	15.3	---	11.6	---	---	---	73.1	---	5.1	18.2	9.4	5.19	1.07	2.1	0.88
R3/9	11.7	---	12.8	---	---	---	75.5	---	4.8	17.4	8.8	5.52	2.01	2.1	0.61
R4/10	15.3	---	---	11.6	---	---	73.1	---	5.1	18.2	9.4	5.41	1.64	2.1	0.88
R5/11	15.0	---	---	13.0	---	---	72.0	---	4.8	17.2	9.0	5.05	1.29	2.1	0.88
R6/12	22.1	---	---	3.6	---	---	74.3	---	5.3	19.1	9.9	8.72	3.55	2.1	0.88
C1/1	14.5	---	34.6	---	---	50.9	---	---	2.9	7.3	10.5	4.89	2.25	2.9	0.88
C2/2	14.6	---	57.7	---	---	27.7	---	---	3.0	7.3	13.0	7.51	2.62	2.9	0.88
C3/6	14.5	---	34.6	---	---	---	50.9	---	2.9	7.3	10.5	5.09	2.16	2.9	0.88
C4/7	14.6	---	57.7	---	---	---	27.7	---	3.0	7.3	13.0	7.53	2.48	2.9	0.88
C5/17	15.2	---	---	11.3	22.6	---	---	50.8	3.6	12.8	10.6	5.02	2.03	2.1	0.13
C6/18	15.2	---	---	11.3	22.6	---	---	50.8	3.6	12.8	10.6	5.02	2.03	2.1	0.13

Parametric Test Configurations

H7/20	16.0	---	5.6	7.2	---	---	71.4	---	4.5	16.0	10.0	4.93	4.84	2.1	0.14
R7/21	15.6	---	---	11.4	---	---	73.0	---	5.1	18.3	9.4	5.42	1.82	2.1	0.13
C7/19	16.2	---	---	12.1	24.3	---	---	47.4	3.8	13.7	10.0	4.63	2.51	2.1	0.13

(a) L/H_d = Axial Position/Dome Height(b) Lb/D_b = Barrel Length/Barrel Diameter

Ultra-low CO and HC emissions levels, below the program goals of 10-g/kg CO and 1-g/kg HC at the design inlet temperature and pressure levels, were obtained in the course of screening and parametric tests of all three concepts. These emissions necessitated only minor modifications on the hot-wall and recuperative baseline combustors. Modifications to the catalytic combustor were more involved, since it was found that additional primary zone length was required with the LOPER dome geometry to provide catalyst inlet temperatures and pollutant concentration profiles sufficiently uniform to meet program emissions goals. In the hot-wall and catalytic combustors, the low CO and HC levels were obtained with no appreciable increase in NO_x relative to conventional combustors. NO_x was increased above the program goal of 4 g/kg with the recuperative combustor as a result of the increased temperature of the recuperative primary zone airflow.

Overall combustor performance, including combustion efficiency, pressure drop, and exit temperature profiles were satisfactory; however, recurring problems with combustion instability (audible resonance) were evident in tests of all three concepts. This resonance severely limited the range of operation of all configurations tested.

Details of emissions and performance results obtained in the screening and parametric tests are given in the following sections.

5.2 SCREENING TEST EMISSIONS RESULTS

CO and HC emissions levels meeting or very closely approaching the program goals were obtained in the course of screening tests of all three low-emissions combustor concepts. Design point NO_x emissions were also below the program goal with both the hot-wall and catalytic combustor concepts, but were increased with the recuperative concept.

Key emissions trends observed as a result of minor modifications to the hot-wall, recuperative, and catalytic combustor concepts are described in the following paragraphs.

5.2.1 Hot-Wall Combustor

Table XI summarizes the design variables investigated, as well as the resulting changes in emissions and operating characteristics, for the six screening test configurations of the hot-wall combustor. Representative emissions levels for these configurations at the design point and at the lowest inlet temperature/pressure level (more severe conditions for CO and HC emissions) are presented in Table XII. The key emissions-oriented modifications evaluated in these tests were swirler flow rate, swirler secondary barrel length, and primary dilution pattern. Configurations H5 and H6 incorporated additional performance (resonance)-oriented modifications which are discussed in a later section.

Table XI. Hot-Wall Combustor Configurations.

<u>Configuration/ Test Sequence</u>	<u>Modification</u>	<u>Intent</u>	<u>Results</u>
H1/3	Baseline ($T_{\text{wall}} \sim 840 \text{ K}^*$)	Baseline data	Met CO and NO _x goals, resonance damage
H2/8	High-flow swirlers, low-flow fuel nozzles (from R2)	Lean dome evaluation	All emissions shifted to higher f_m
H3/13	*Nondrool swirlers, late primary dilution (from R4)	HC reduction	Step decrease in HC (~60%), NO _x increased above goals
H4/14	"Staggered" primary dilution	NO _x resonance reduction	No resonance change, NO _x below program goals
H5/15	Two rows primary dilution, sidewall acoustic treatment	Resonance reduction	No change in resonance CO, HC increased
H6/16	Dome dilution, plenum mount	Resonance reduction	No change in resonance CO, HC decreased

*Features incorporated into all remaining hot-wall configurations

Table XII. Hot-Wall Combustor Emissions Summary.

Configuration	Representative Emissions										
	at Design Point (422 K, 304 kPa, 22.9 m/s)							at Most Severe Condition (367 K, 203 kPa, 30.5 m/s)			
	Design f/a (10.5 g/kg)			f/a for Minimum CO				f/a for Minimum CO			
	COEI	HCEI	$\text{NO}_x \text{EI}^{(a)}$	f/a	COEI	HCEI	$\text{NO}_x \text{EI}^{(a)}$	f/a	COEI	HCEI	$\text{NO}_x \text{EI}^{(a)}$
H1 - Baseline	2.6	2.3	3.1	10.5	2.6	2.3	3.1	10.4	10.8	1.4	1.4
H2 - Lean Dome ^(b)	4.0	1.7	2.0	11.1	1.8	1.3	2.0	13.8	13.3	5.6	1.9
H3 - Modified Swirler, Late Dilution	1.7	0.4	4.4	10.5	1.7	0.4	4.4	10.5	7.0	0.4	2.2
*H4 - "Staggered" Dilution	1.3	0.5	2.7	10.1	1.3	0.5	2.5	10.5	6.7	0.6	1.4
H5 - Double Dilution	1.5	0.7	2.9	10.0	1.4	0.7	2.6	12.7	13.1	1.1	1.9
H6 - Dome Silution	3.1	0.4	3.0	10.5	3.1	0.4	3.0	12.0	7.5	0.5	2.0

(a) $\text{NO}_x \text{EI}$ corrected to standard humidity $K_H = \exp\left(\frac{H-6.29}{53.2}\right)$

(b) Points run at low reference velocity (10-15 m/s) to avoid resonance

* Configuration selected for parametric tests.

ORIGINAL PAGE IS
OF POOR QUALITY

Hot-wall baseline combustor emissions characteristics as a function of fuel-air ratio, inlet temperature/pressure level, and reference velocity are presented in Figure 27. As shown in this figure, CO levels were minimized at the design fuel-air ratio. This was expected based on swirler and forward dilution flow levels, which were tailored to provide optimum stoichiometry for CO burnout at this fuel-air ratio. At increased reference velocity, CO tended to increase more rapidly as the fuel-air ratio was increased or decreased from the design value, but the minimum level was not strongly affected. Design point CO and NO_x emissions levels with the baseline configuration were below program goals. Therefore, the primary aim of subsequent modifications was to reduce HC levels in this concept.

The effect of increased swirler airflow was investigated with configuration H2. This combustor incorporated the larger swirlers normally used in the recuperative and catalytic combustors, which resulted in a swirler flow increase of approximately 40% relative to the hot-wall baseline combustor. The intent of this modification was to determine whether the characteristic HC emissions curve as a function of fuel-air ratio could be shifted relative to CO and NO_x curves. If this was possible, design point HC levels could be reduced relative to CO and NO_x by revising the split between swirler and forward dilution flows.

The desired shift in HC relative to CO and NO_x was not obtained with the "lean dome" configuration. All measured emission curves were uniformly shifted to higher fuel-air ratios, the magnitude of the shift being approximately proportional to the swirler flow rate. This effect is shown in Figure 28, where lean dome emissions are compared to those of the baseline combustor, as a function of swirler equivalence ratio (the fuel-air ratio based on swirler airflow divided by the stoichiometric fuel-air ratio). With both configurations, CO was minimized at a swirler equivalence ratio slightly less than one, and both CO and HC emissions rose rapidly as swirler equivalence ratio was decreased below the range of 0.6 to 0.8, depending on combustor inlet temperature/pressure level. Although direct comparison is difficult because of the low reference velocities run with the lean dome configuration (necessary to avoid resonance), absolute emissions levels for the two combustors are similar.

Following tests with configuration H2, atmospheric spray visualization tests were conducted which would provide improved fuel atomization to reduce HC emissions. In these tests, one swirler was removed from the dome and mounted in an apparatus which allowed visual observation of the fuel spray. Initial viewing of the baseline swirler indicated that a small portion of the fuel exiting the primary swirler venturi was impinging on the wall of the secondary swirler barrel. This fuel was collecting on the bluff swirler exit and shedding off in large droplets, as shown in part (a) of Figure 29. This "drooling" was eliminated by shortening the secondary barrel and increasing the immersion of the primary swirler as shown in part (b) of Figure 29. With this short-barrel configuration, no wetting of the secondary barrel was observed.

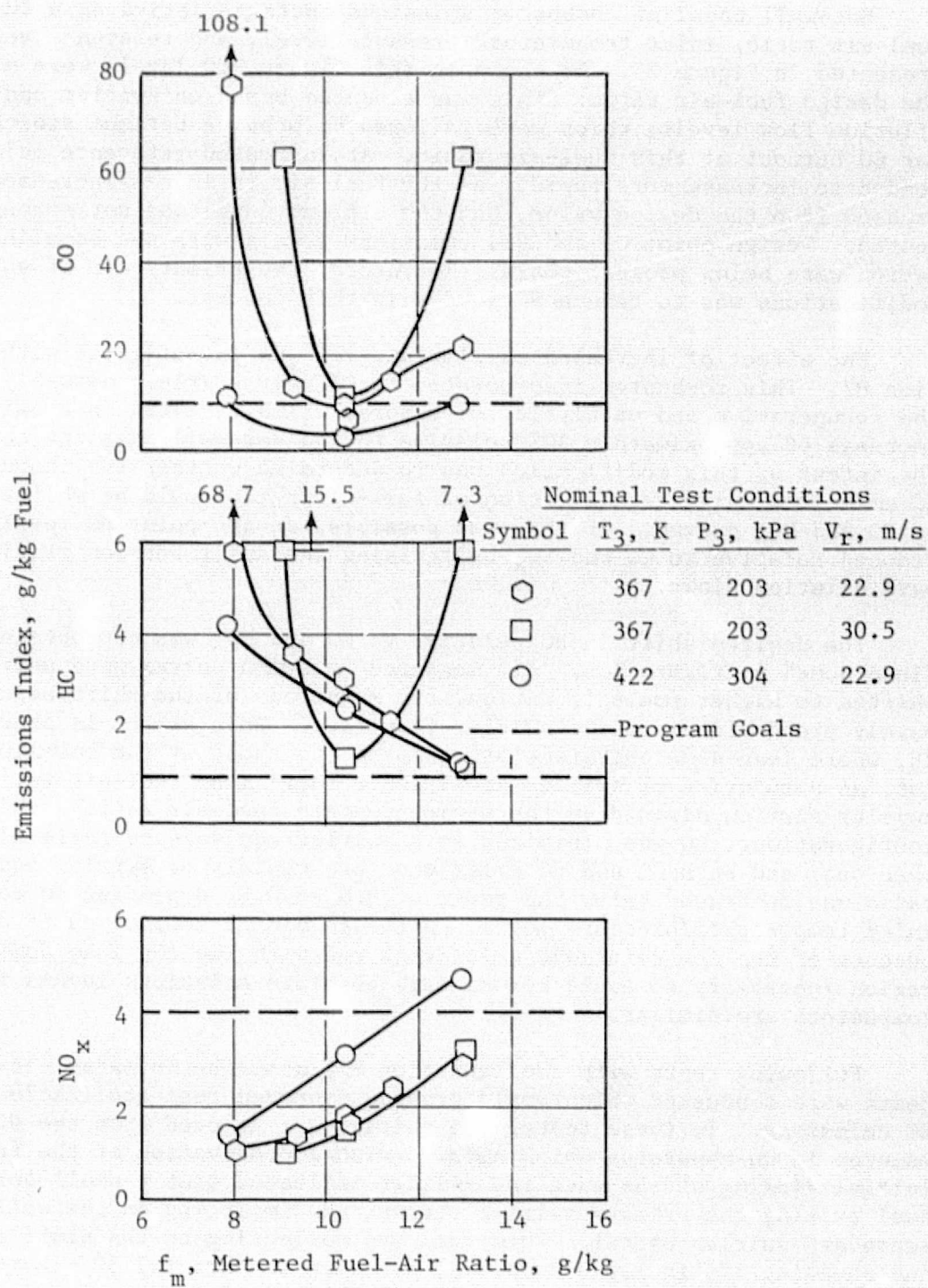


Figure 27. Baseline Hot-Wall Combustor Emissions Characteristics.

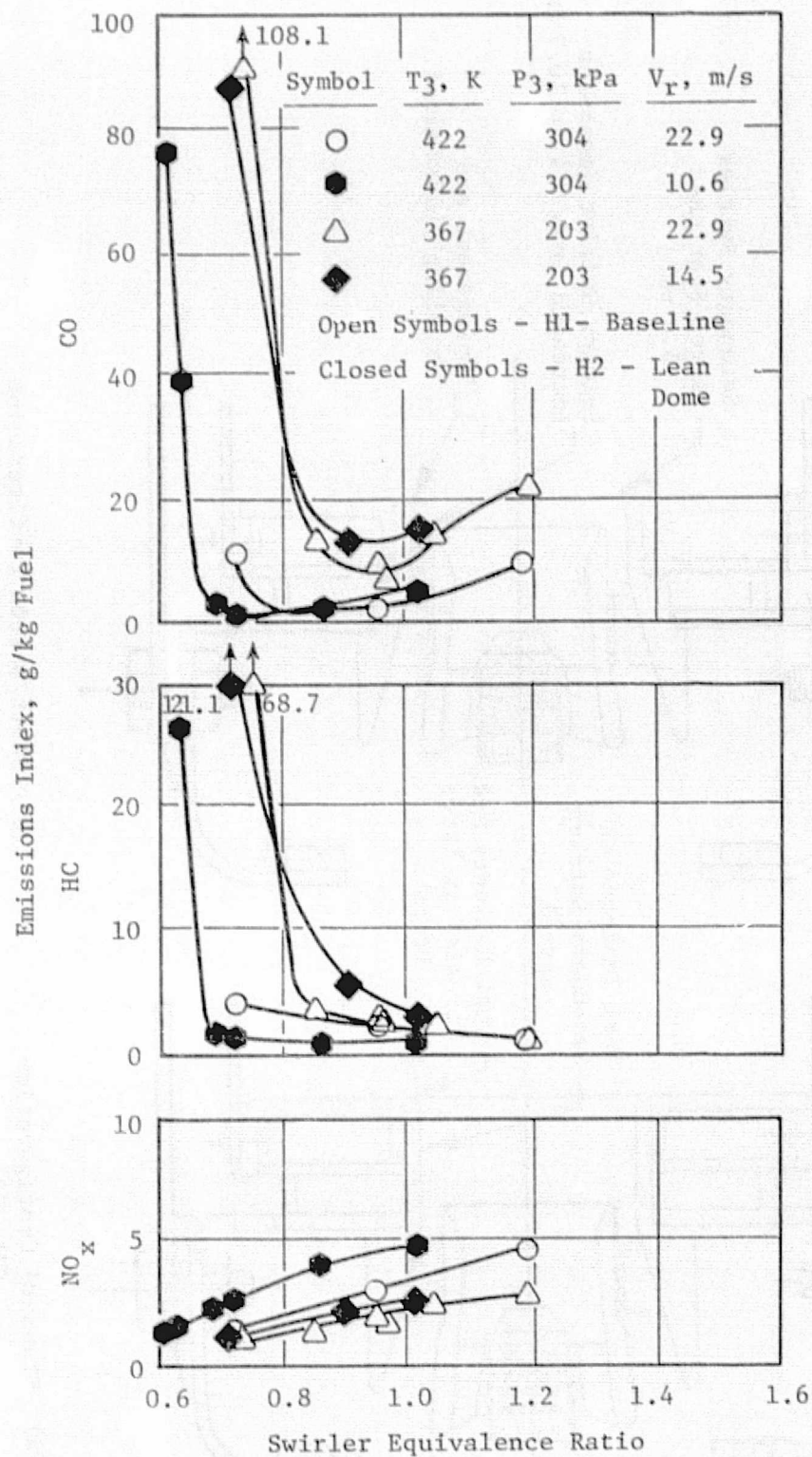


Figure 28. Effect of Swirler Airflow on Hot-Wall Combustor Emissions.

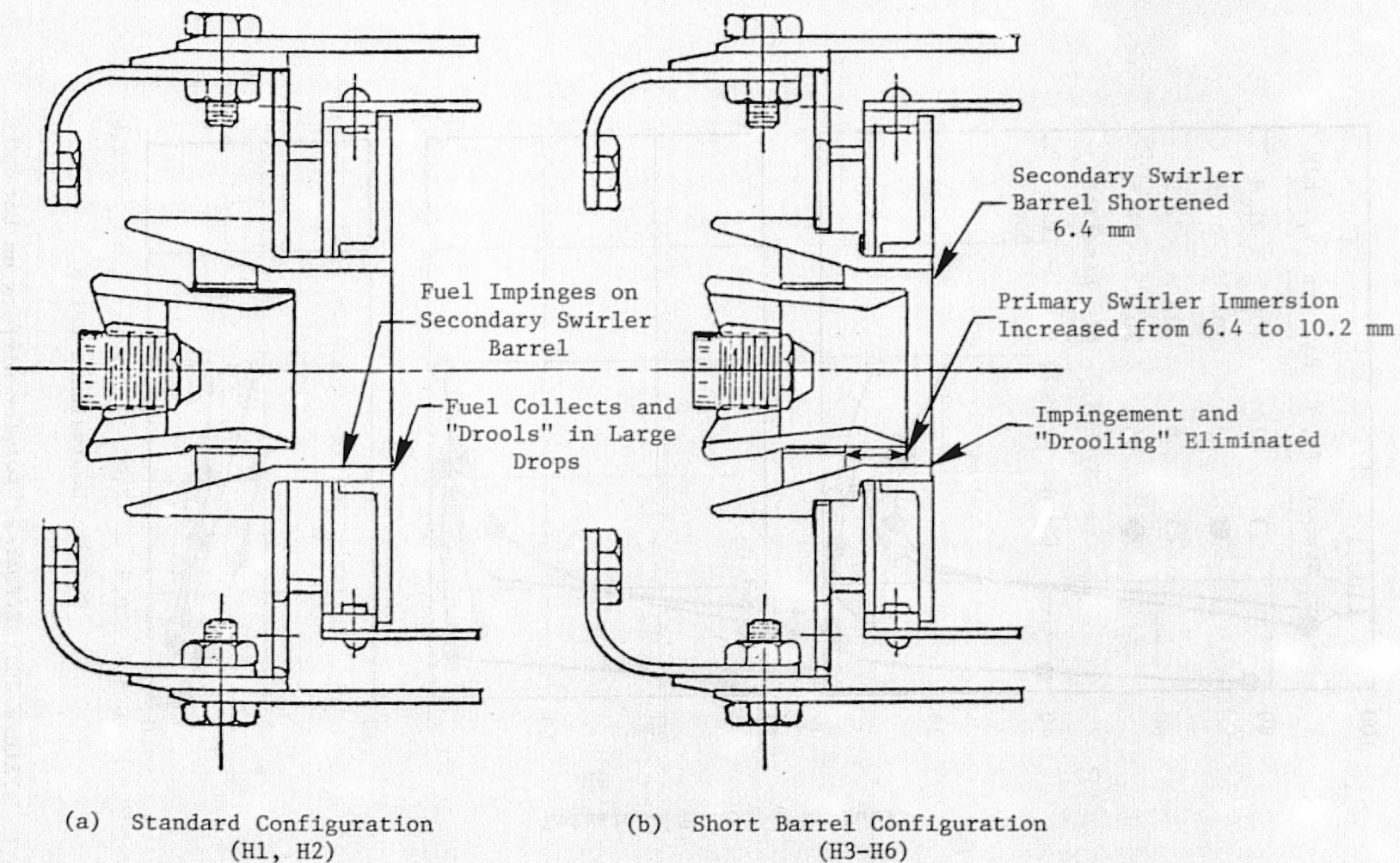


Figure 29. Hot-Wall Combustor Swirler Modifications.

In configurations H4-H6, the effects of the swirler modification and of the location and number of primary dilution holes were investigated. The use of the nondrooling swirler resulted in a reduction of approximately 60% in HC emissions, to levels comfortably below the program goal at the design point. The effects of primary dilution location were generally weak, as shown in Figure 30. A trend toward increasing CO and HC, and decreasing NO_x was noted as liner dilution was moved forward or increased, indicating more rapid quenching of the dome reactions. This quenching effect appeared to be reduced when dilution was moved from the liner to the dome, where dilution air was injected parallel to the direction of combustor flow. Of the four variations in dilution pattern, configuration H4 provided the best balance between CO and NO_x emissions. With this combustor, all emissions were below program goal, both at the design point and at the low-inlet-temperature, high-velocity operating conditions.

Based on the results of hot-wall screening tests, configuration H4 was selected for further parametric testing. This configuration incorporated (1) the nondrooling swirlers, which provided reduced HC emissions, and (2) the "staggered" primary dilution pattern, which provided the best trade off between CO and NO_x emissions at design point. No further modifications were added prior to screening tests.

5.2.2 Recuperative Combustor

The six recuperative combustor screening test configurations are described in Table XIII. Key design variables evaluated in these configurations included fuel nozzle atomization, swirler flow rate, primary dilution location and temperature, and redistribution of swirler and forward dilution flows. Representative emissions levels obtained with these configurations are compared in Table XIV.

The effect of improved fuel nozzle atomization was investigated with configuration R2. In this combustor, the baseline fuel nozzles were replaced with nozzles having smaller metering orifices, which provided improved atomization and increased the spray cone angle. The improved fuel nozzle atomization had little effect on gaseous emissions. This was not unexpected, since fuel atomization with the counterrotating swirl cups used in the LOPER combustors is achieved primarily by the interaction of the fuel film leaving the primary venturi with the shear region created by the converging primary and secondary swirler flows. However, the use of the low-flow nozzles did eliminate heavy carboning of the combustor dome and liners, which had been noted in tests with configuration R1. For this reason, these fuel nozzles were used in all subsequent tests of the hot-wall and recuperative combustors.

The effect of variation of swirler airflow was investigated with configuration R3, in which swirler flow was reduced approximately 24% by installing smaller swirlers. As in similar tests with the hot-wall combustor, the effect of swirler flow variation was to uniformly shift all emissions curves relative to overall fuel-air ratio. This shift was eliminated by plotting against swirler equivalence ratio, as shown in Figure 31.

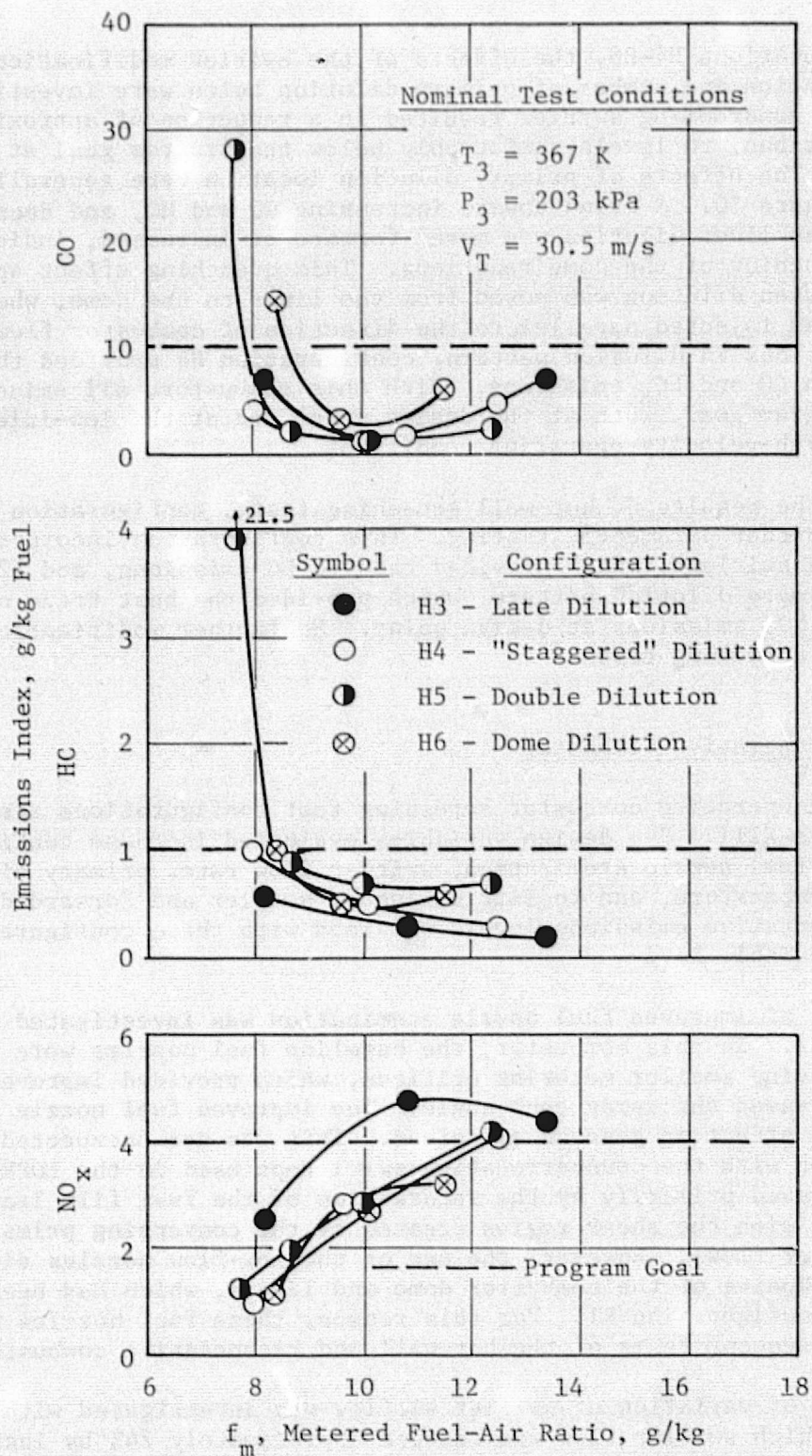


Figure 30. Effect of Primary Zone Dilution Pattern on Hot-Wall Combustor Emissions.

Table XIII. Recuperative Combustor Configurations.

<u>Configuration/ Test Sequence</u>	<u>Modification</u>	<u>Intent</u>	<u>Results</u>
R1/4	Baseline (~100 K temperature rise*)	Baseline data	Met CO goals. Encountered resonance, combustor carboning
R2/5	Low-flow fuel nozzle* (improved atomization)	Reduce carboning, CO, HC	Carboning reduced
R3/9	Low-flow swirlers	Rich dome evaluation	Emissions shifted to lower f_m
R4/10	Late primary dilution	Resonance reduction, delay quenching	CO, HC reduced, emissions shifted to lower f_m
R5/11	Cold primary dilution	Reducing NO_x	CO increased, NO_x reduced slightly
R6/12	Increased swirler flow and pressure drop	Shift CO minimum to design f_m	Emissions shifted and increased slightly

*Features incorporated into all remaining recuperative configurations

Table XIV. Recuperative Combustor Emissions Summary.

Configuration	Representative Emissions										
	at Design Point (422 K, 304 kPa, 22.9 m/s)							at Most Severe Condition (367 K, 203 kPa, 30.5 m/s ^(a))			
	Design f/a (10.5 g/kg)			f/a for Minimum CO				f/a for Minimum CO			
	COEI	HCEI	NO _x EI ^(b)	f/a	COEI	HCEI	NO _x EI ^(b)	f/a	COEI	HCEI	NO _x EI ^(b)
R1 - Baseline	8.0	1.1	6.3	8.5	4.0	2.5	3.5	9.5	16.0	5.0	2.7
R2 - Improved Atomization	7.0	1.4	7.0	8.9	3.0	3.9	---	---	---	---	---
R3 - Rich Dome	15.1	1.2	6.6	6.4	1.7	1.7	2.7	8.0	15.0	7.0	2.2
R4 - Late Dilution	4.0	0.9	6.1	7.3	1.5	1.5	4.2	8.3	5.0	1.5	2.7
R5 - Cold Dilution	6.5	0.9	5.1	7.4	3.4	1.5	4.0	8.1	7.9	2.2	2.9
R6 - Lean Swirler	4.0	1.1	4.4	10.4	4.0	1.1	4.4	10.5	7.3	1.6	1.8

(a) Configurations R1 and R3 data extrapolated from lower reference velocity based on configuration R4 trends.

(b) NO_xEI corrected to standard humidity.

ORIGINAL PAGE IS
OF POOR QUALITY

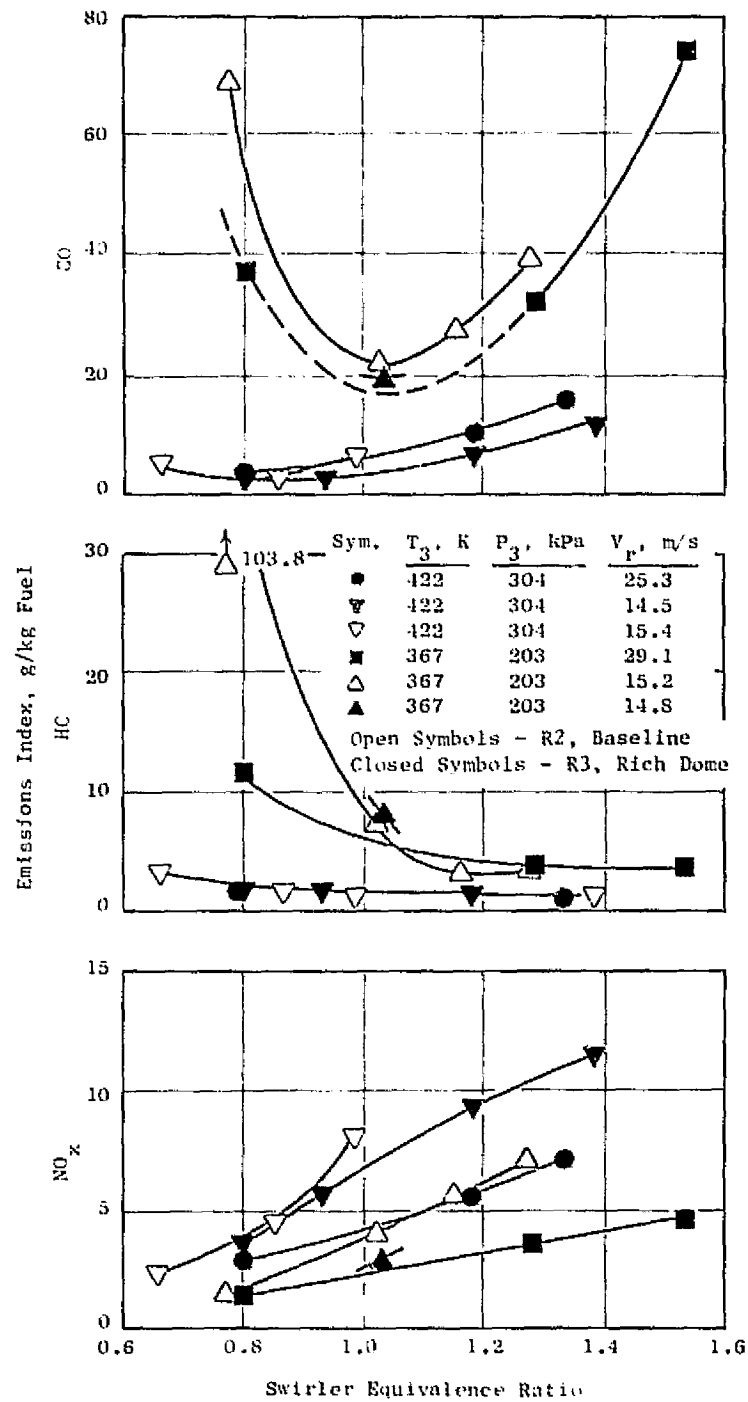


Figure 31. Effect of Swirler Airflow on Recuperative Combustor Emissions.

The effect of primary dilution axial position was evaluated in configuration R4. In this combustor, the primary dilution holes were moved to a location 7.6-cm downstream of the dome. This modification resulted in a significant decrease in CO and HC emissions at the lower fuel-air ratios, particularly at the low-temperature conditions, as shown in Figure 32. This reduction was apparently due to the increased distance between the dome and forward dilution stations, which provided additional residence time and mixing length in the dome region. For lean dome (swirler) mixtures ($f_m < 10.5$ g/kg), where no additional air was required to complete the combustion process, CO and HC were reduced because quenching by the primary dilution jets was delayed. For rich dome mixture, where primary dilution was required to complete combustion, CO and HC levels were not strongly affected by dilution location.

The strong reference velocity dependence of recuperative combustion CO and HC emissions is also apparent in Figure 32. In several previous combustor system tests (Reference 5), CO and HC emissions have been shown to be approximately proportional to reference velocity. This behavior has generally been attributed to residence time effects, with residence time increasing as velocity is decreased, resulting in more complete combustion of CO and HC. In the recuperative combustor, however, significant reductions in CO and HC were observed as reference velocity was increased from 15.2 m/s, indicating that the beneficial effects of improved fuel atomization and mixing under these conditions are stronger than the adverse effects of reduced residence time.

The use of reduced forward dilution temperature as a means of reducing recuperative combustor NO_x emissions was investigated with configuration R5. Flow splits for this combustor were similar to those for R4, but this time cold (nonrecuperative) forward dilution was used. This was accomplished by installing primary dilution thimbles similar to those used in the hot-wall combustor. The use of nonrecuperative primary dilution led to increased CO and HC levels with only a slight decrease in NO_x levels. This approach was therefore abandoned.

One effect of the change in forward dilution position in configurations R4 and R5 was to decrease the fuel-air ratio at which the CO minimum occurred. In configuration R6, swirler flow was increased and primary dilution flow was simultaneously decreased in an attempt to shift the CO minimum back to the design point. In order to obtain the required increase in swirler flow without fabricating larger swirlers, it was necessary to close off four of the aft dilution holes. This modification increased design point pressure drop to approximately 8.6%.

Emissions allowed with configuration R6 are compared with R4 characteristics in Figure 33. Although minimum CO levels were increased slightly, the minimum was successfully shifted to the design fuel-air ratio, resulting in a significant reduction in CO emissions at this point. The increased swirler flow also resulted in a significant reduction in NO_x emissions at the design point.

Based on the results of recuperative combustor screening tests, both configurations R4 and R6 were very promising in terms of emissions reduction

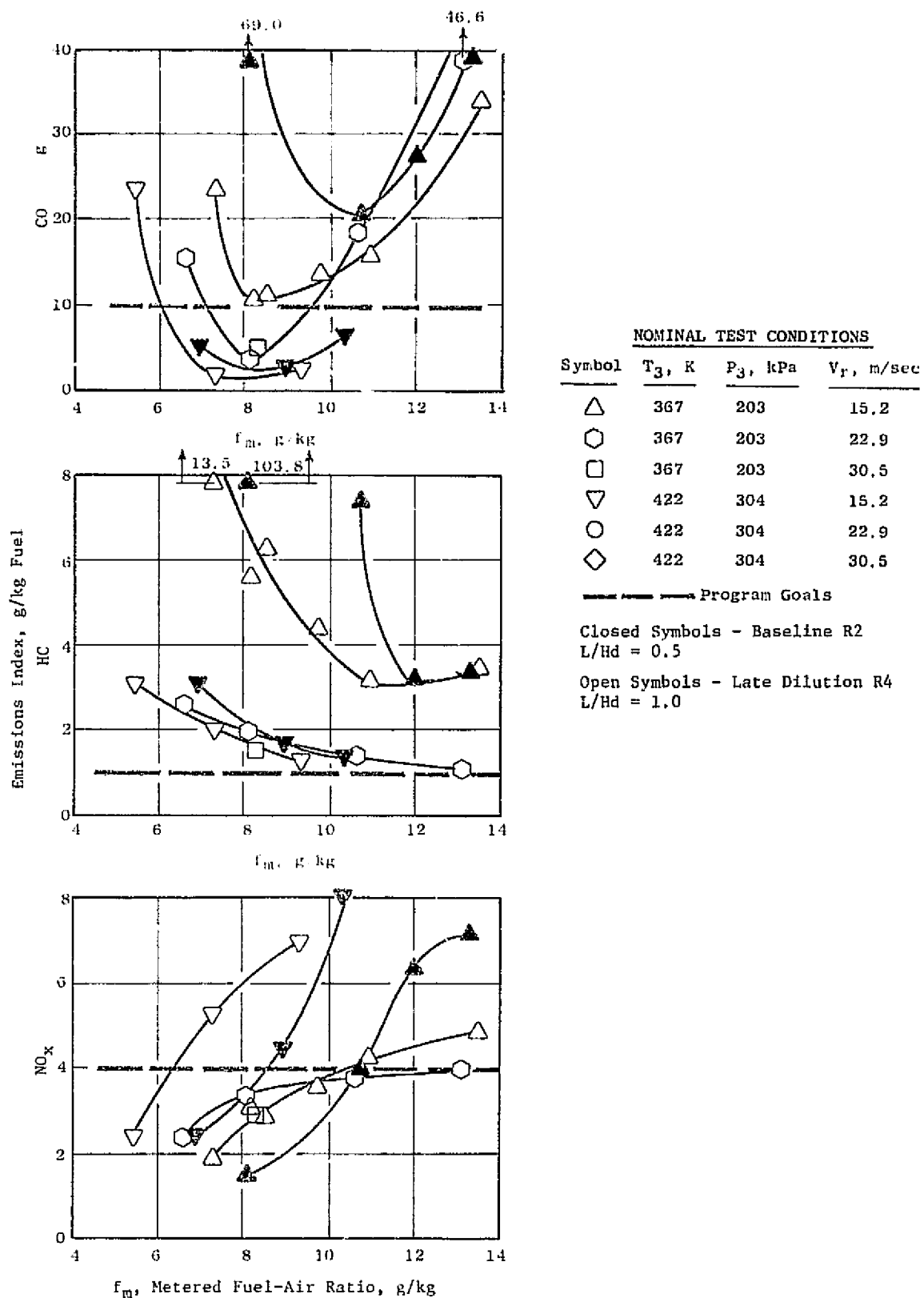


Figure 32. Effect of Primary Zone Dilution Location on Recuperative Combustor Emissions.

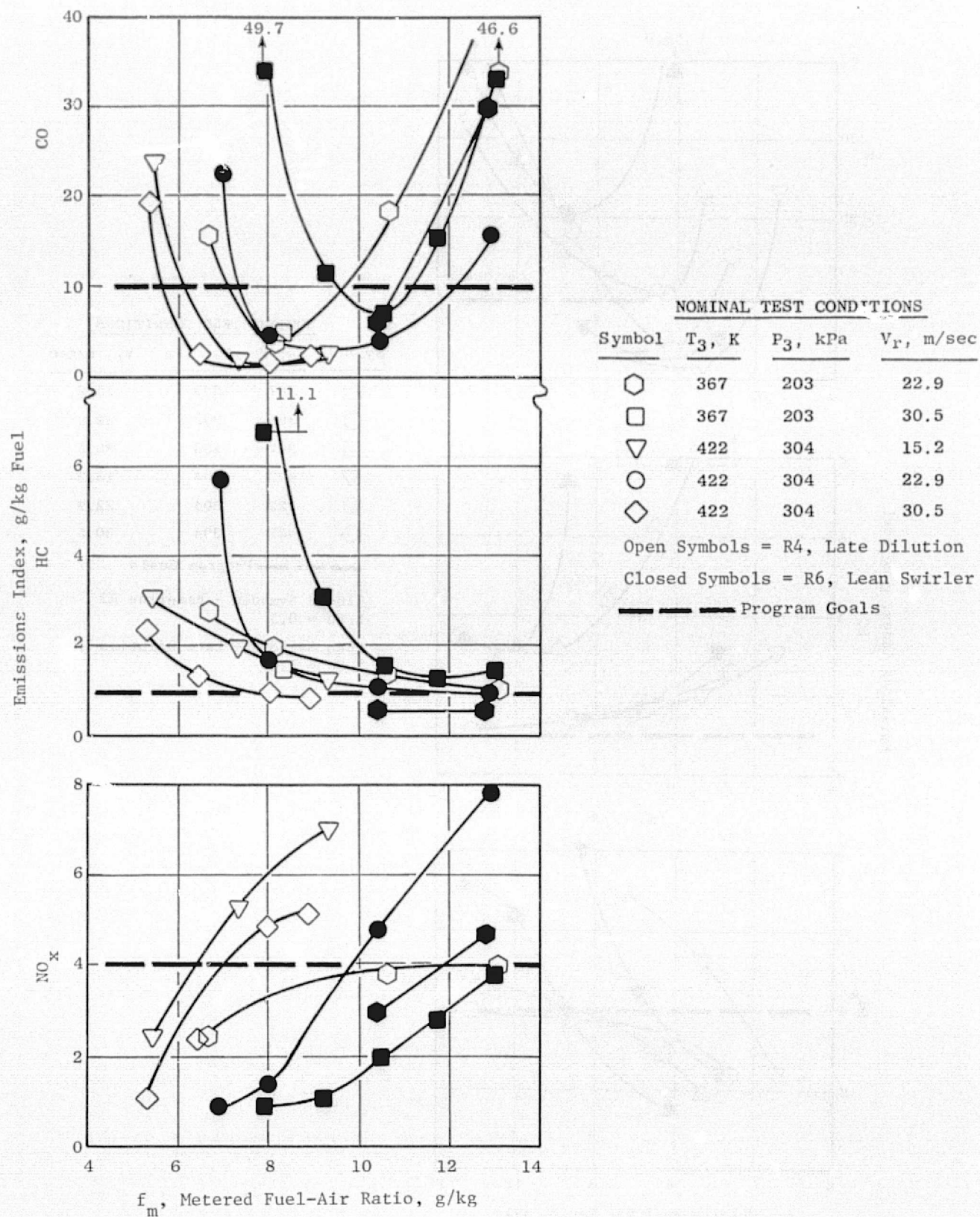


Figure 33. Effect of Airflow Distribution Variations on Recuperative Combustor Emissions.

potential. Of the two, configuration R4 was selected for further parametric testing, primarily based on performance (pressure drop) considerations; however, it is anticipated that with a small amount of further development, the favorable emissions characteristics of configuration R6 could be obtained without increased pressure drop. In addition to the low-flow fuel nozzles and late primary dilution features identified in recuperative combustor screening tests, the final recuperative combustor parametric test configuration incorporated a swirler modification which had shown good potential for HC emissions reduction in hot-wall and catalytic combustor screening tests. Details of this modification are discussed in the following section on catalytic combustor screening test results.

5.2.3 Catalytic Combustor

The six catalytic combustor screening test configurations are described in Table XV. The primary design variables investigated in this test series were catalyst activity, catalytic reactor airflow, and combustor primary zone length. Emissions results obtained with configurations are presented in Table XVI.

As shown in Figure 34, combustors tested in this series were of three different lengths. In configurations C1 and C2, a perforated Hastelloy X catalyst-simulation plate was installed in place of the catalytic reactor in order to obtain zero activity emissions data and to establish catalytic combustor operating procedures. The size and number of perforations in this plate were selected to simulate the effective blockage of the catalytic reactor. In configurations C3 and C4, catalytic conversion was observed by removing the catalyst-simulation plate and installing the catalytic reactor. In configurations C5 and C6, the length of the combustor primary zone was increased to provide additional mixing length, in order to improve catalyst inlet temperature and emissions profiles. This additional primary zone length was obtained by using forward liner components from the recuperative combustor.

The effects of catalyst activity at two different levels of catalyst airflow are shown in Figure 35. By comparing CO and HC levels obtained with the catalytic reactor installed (configuration C3) to those obtained with the simulation plate installed (configuration C1), apparent catalytic CO and HC conversion efficiencies between 50 and 70% were calculated for the baseline combustor. These levels were slightly below the Engelhard Industries predictions of 75 to 85% conversion for purely heterogeneous reaction (with no additional thermal reaction within the catalyst). With catalyst airflow increased to 75% of combustor airflow (configurations C2 and C4), apparent conversion efficiencies were reduced to the 40 to 50% range. NO_x emissions did not appear to be affected by catalyst activity.

The impact of variation in catalyst airflow is shown in Figure 36. When compared at constant combustor fuel-air ratio (part (a) of Figure 36), the increase in catalyst airflow resulted in significant increases in CO and HC and a corresponding reduction in NO_x . These results were due to the combined effects of reduced catalyst inlet temperature (which tends to decrease both primary zone combustion efficiency and catalytic conversion) and increased

Table XV. Catalytic Combustor Configurations.

<u>Configuration/ Test Sequence</u>	<u>Modification</u>	<u>Intent</u>	<u>Result</u>
C1/1	Baseline (50% W_c through catalyst), catalyst simulation plate	Procedure development, inlet profile measurement, zero activity emissions	80-98% efficiency, catalyst pattern factor ~0.35
C2/2	Mod 1 (75% W_c through catalyst), catalyst simulation plate	Catalyst airflow variation, zero activity emissions	80-98% efficiency, catalyst pattern factor ~0.35
C3/6	Baseline - catalyst installed	Baseline data, catalytic conversion	50-70% conversion, resonance encountered, catalyst cracked, discolored
C4/7	Mod 1 - catalyst	Catalyst airflow variation, catalytic conversion	40-50% conversion, hole burned in catalyst
C5/17	Extended length primary zone, *nondrool swirlers	Improve catalyst inlet temperature/emissions	Catalyst failure (collapse), met program emissions goals
C6/18	Extended length primary zone	Catalyst activity	High hydrocarbons (results inconclusive)

* Feature incorporated into configuration C6

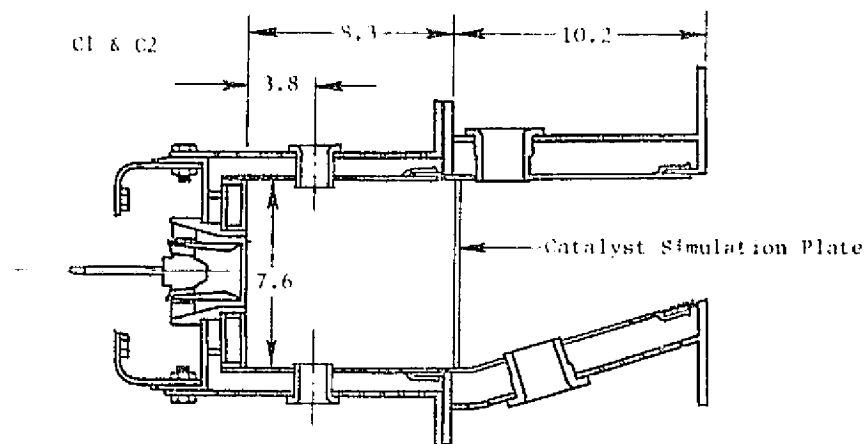
Table XVI. Catalytic Combustor Emissions Summary.

<u>Configuration</u>	<u>Representative Emissions</u>					
	<u>at Design Point^(a)</u>			<u>at Least Severe Condition</u>		
	(422 K, 304 kPa, 15.2 m/s, 9.0 g/kg)			(477 K, 405 kPa, 15.2 m/s, 9.0 g/kg)		
	<u>COEI</u>	<u>HCEI</u>	<u>NO_xEI^(b)</u>	<u>COEI</u>	<u>HCEI</u>	<u>NO_xEI^(b)</u>
C3 - Baseline (50% W _C)	24	30	1.8	16	6	3.1
C4 - Mod 1 (75% W _C)	32	52	0.9	30	28	2.6
C5 - Extended Primary	5.5	1.2	3.7	- - -	Not Measured	- - -
C6 - New Catalyst	6.5	9.5 ^(c)	3.3	- - -	Not Measured	- - -

(a) Reduced reference velocity and fuel-air ratio to avoid resonance

(b) NO_xEI corrected to standard humidity

(c) High HC possibly due to fuel leak



• All Dimensions are cm

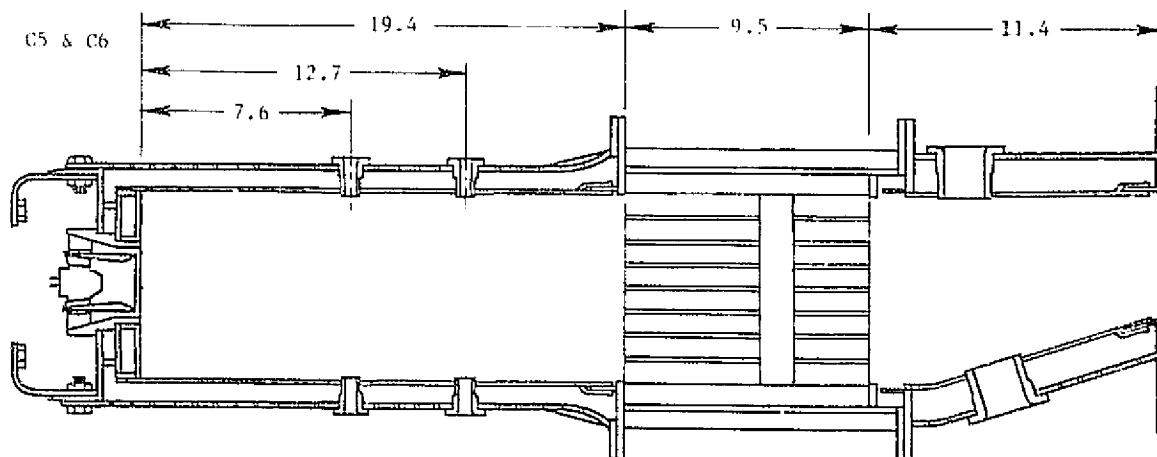
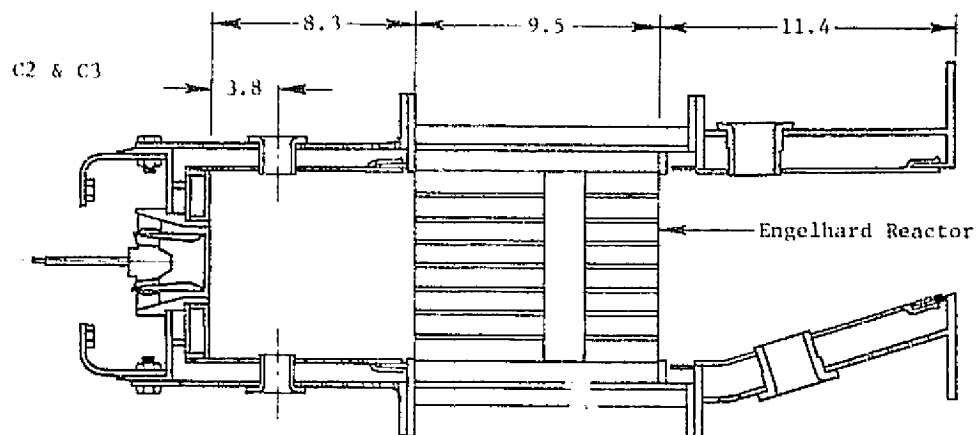


Figure 34. Catalytic Combustor Configurations.

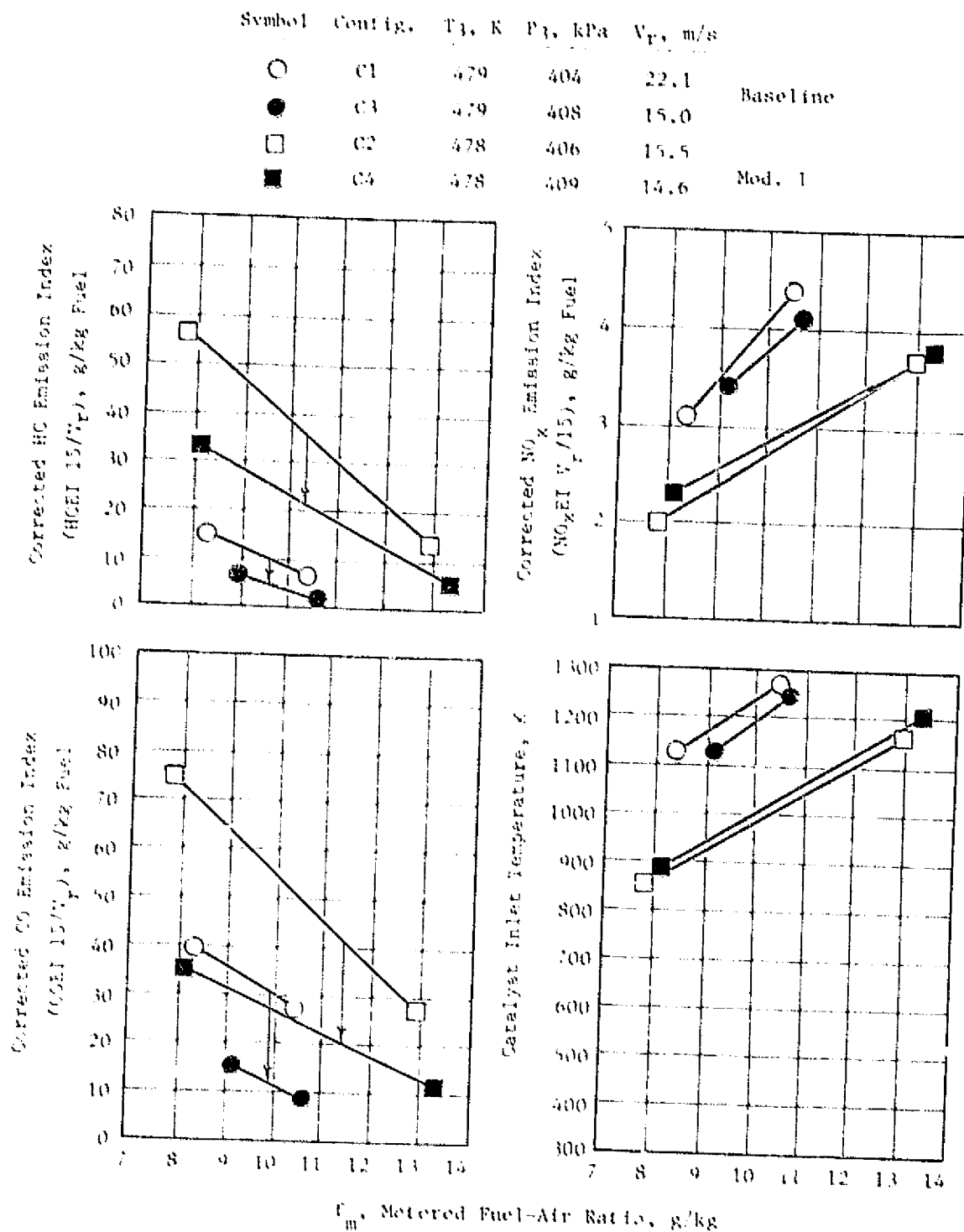


Figure 35. Catalytic Reactor Effectiveness.

Symbol	T_3 , K	P_3 , kPa	V_r , m/s
--------	-----------	-------------	-------------

\triangle	478	304	15-18
-------------	-----	-----	-------

\diamond	478	410	15
------------	-----	-----	----

Open - Baseline - 50% W_c Through Catalyst

Closed - Mod 1 - 75% W_c Through Catalyst

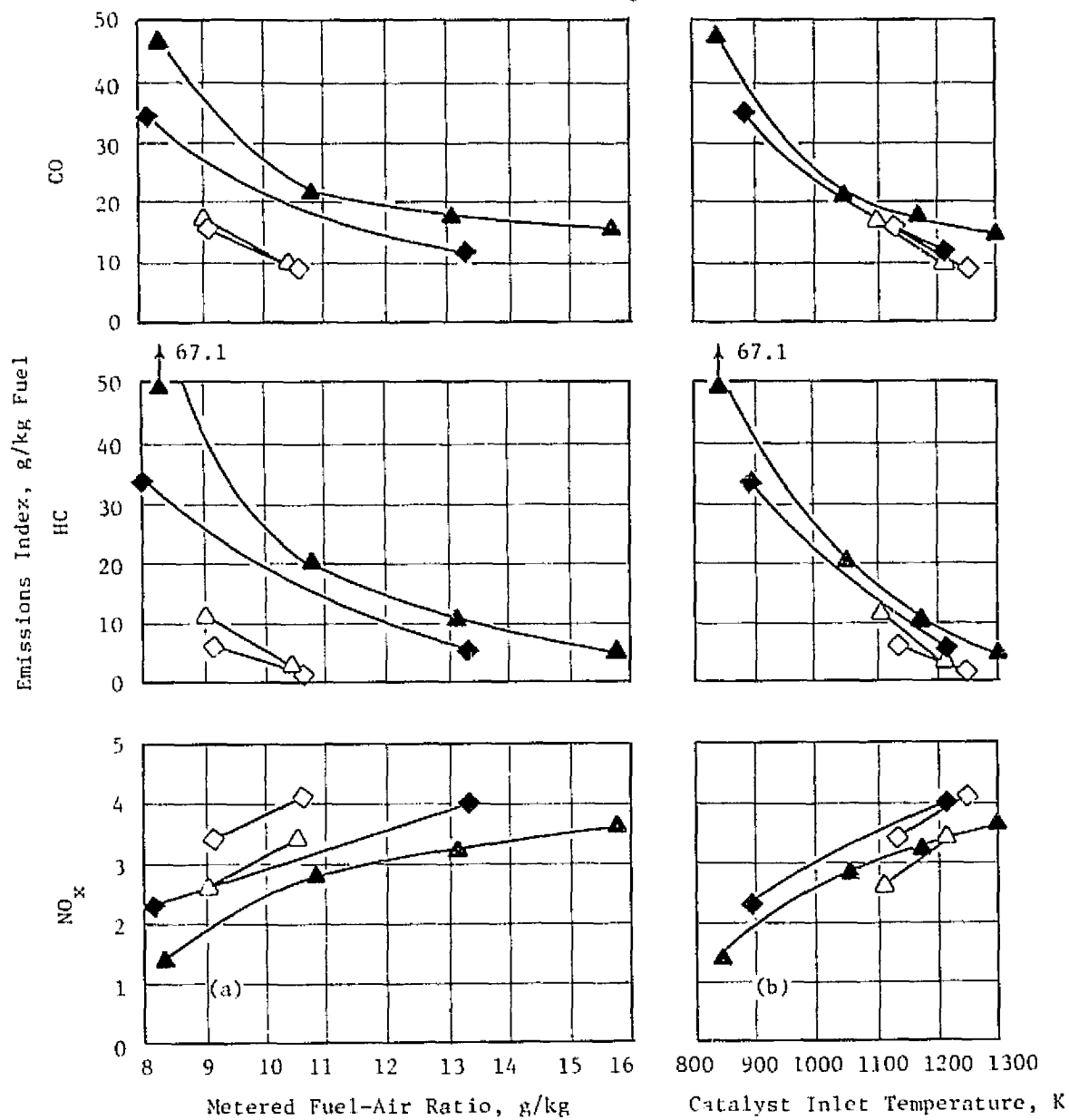


Figure 36. Effect of Airflow Distribution on Catalytic Combustor Emissions.

catalytic throughput velocity at the higher reactor flow level. As shown in part (b) of Figure 36, better agreement in emissions levels is obtained by correlating emissions against measured catalyst inlet temperature. This relationship indicates a fairly weak tendency toward increasing CO and HC as velocity is increased. Based on these tests, it was concluded that CO and HC emissions from the catalytic reactor could be minimized by selecting catalytic reactor airflow such that the peak reactor inlet temperature was equal to the maximum-use temperature of the catalyst. Since this criterion was closely approached with the baseline catalyst flow level, all subsequent configurations utilized a nominal value of 50% flow through the catalyst.

Design point CO and HC emissions from the baseline catalytic combustors were well above program goals. Because improvement in catalytic conversion was limited by catalyst inlet temperature and pressure drop requirements, further emissions reduction required that primary zone performance be improved. This improvement was obtained in configuration C5 by extending the primary zone to provide additional length for combustion upstream of the catalyst. In conjunction with this increase in primary zone length, the primary dilution pattern was modified to conform to the pattern used in recuperative configuration R4. In this modified pattern, two rows of primary dilution were used. The first row was configured to closely simulate the axial position and flow levels used in configuration R4 forward dilution. Additional primary zone airflow required to provide 50% of the combustor airflow through the catalyst was admitted through a second row of primary dilution holes. Catalytic combustor configuration C5 also incorporated the modified swirler configuration shown in Figure 37. This modification was identified in spray visualization tests as a means to prevent fuel from impinging on these secondary barrels and subsequently forming into coarse drops (drooling) and is similar to the modifications which reduce HC emissions in the hot-wall configuration.

As shown in Figure 38, CO and HC emissions were significantly improved by the use of the extended primary zone and nondrooling swirlers. At the design inlet conditions (except for reduced reference velocity), all gaseous emissions were below program goals. No emissions data were obtained at lower temperature because of a failure of the catalyst, which had previously been damaged during tests of configurations C3 and C4.

Because of the favorable emissions results obtained prior to the catalyst failure with configuration C5, the only change in configuration C6 was to install a new catalytic reactor. Interpretation of emissions results with this final configuration was complicated by high HC measurements, which were apparently due to a leak in the internal fuel manifold; but CO and NO_x emissions levels did not appear to be affected by the use of the new reactor.

Based on catalytic-combustor screening-test emissions results, low-flow fuel nozzles, the extended length primary zone, and nondrooling swirlers (as used in configurations C5 and C6) were incorporated into the parametric test configuration. In addition to these features, a modified method of mounting the catalyst within the catalytic reactor was utilized in catalytic combustor

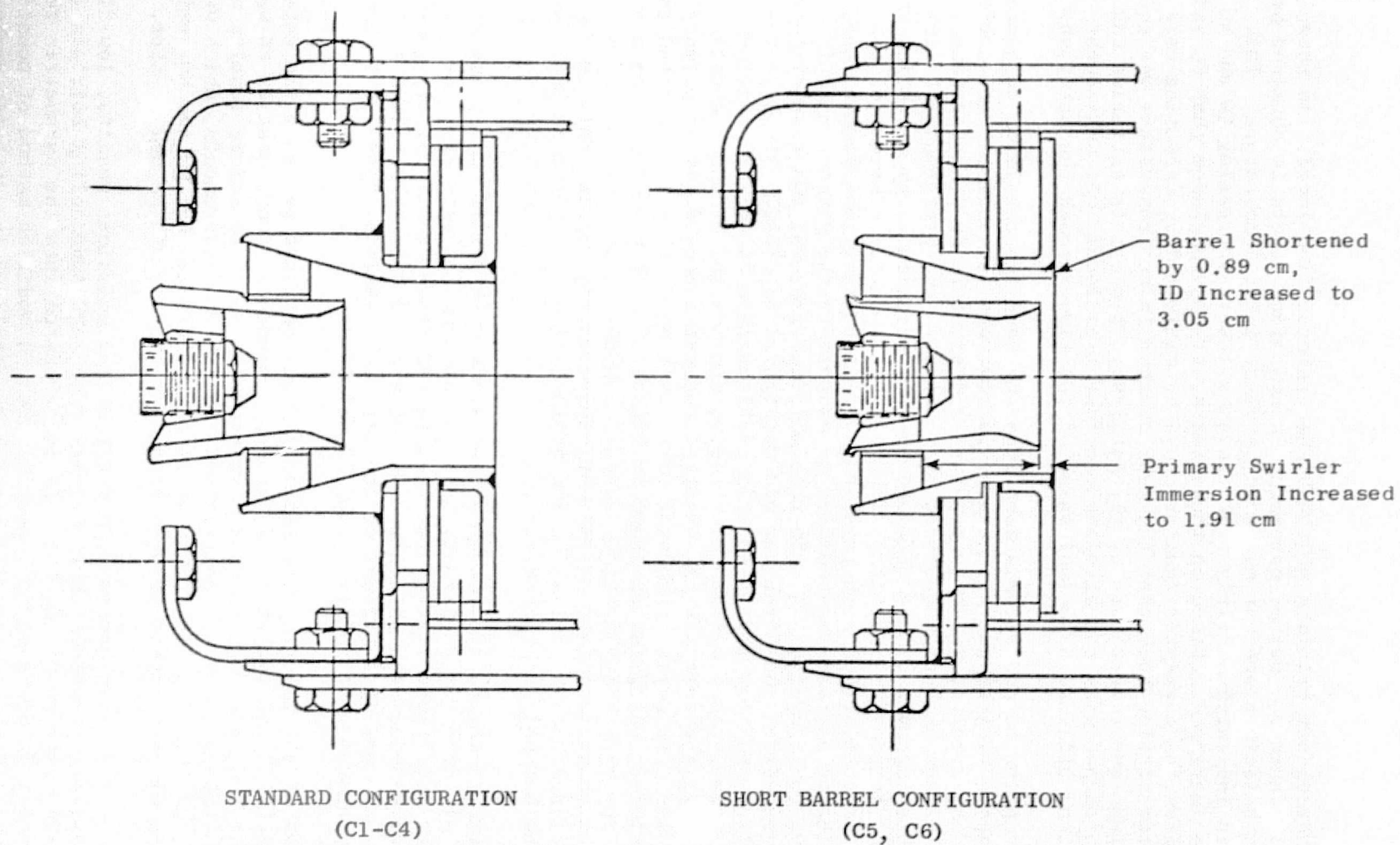


Figure 37. Catalytic Combustor Swirler Modification.

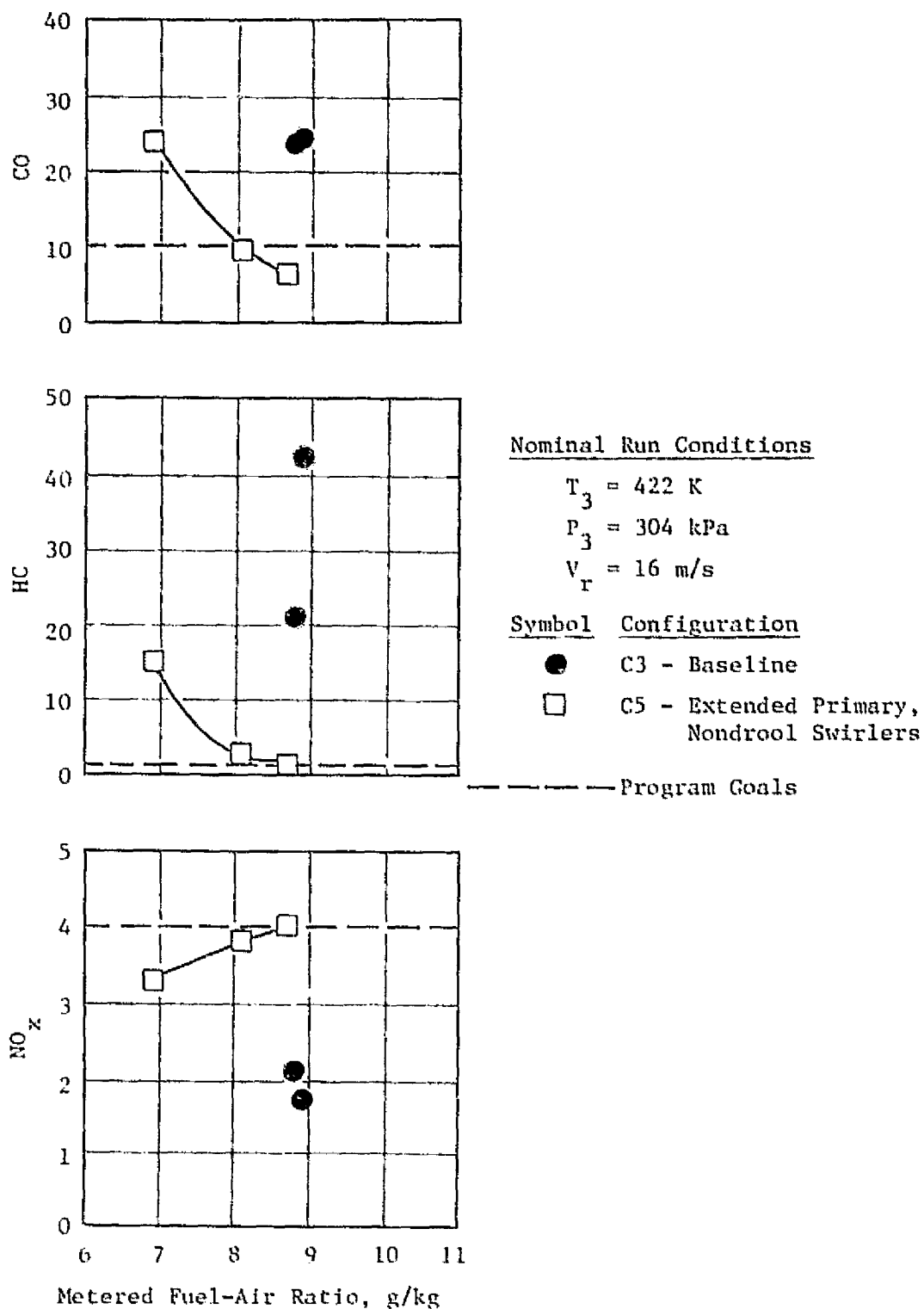


Figure 38. Effect of Increased Primary Zone Length and Swirl Modification on Catalytic Combustor Emissions.

parametric tests. This reactor modification, which was intended primarily to improve catalyst durability, is described in the following section on screening test performance results.

5.3 SCREENING TEST PERFORMANCE RESULTS

5.3.1 General Performance

Several aspects of combustor performance, including combustor pressure drop, combustion efficiency, exit temperature distribution, ignition, combustor stability, and liner life, were similar for all three of the low-emissions combustor concepts. General screening test performance results were as follows:

Combustor Pressure Drop - The measured combustor pressure drop, corrected to the design point operating condition (previously shown in Table X) was generally within 0.5% of the 5.0% design value, except in configurations where pressure drop was intentionally increased as a convenient means for redistributing combustor airflow. Increased pressure drop was utilized in configurations C2 and C4 to increase catalyst airflow, and in configuration R6 to increase swirler airflow. There was no indication of a need for increased pressure drop to improve emissions or performance with any of the low-emissions combustor concepts.

Combustion Efficiency - Design point (idle) combustion efficiencies above the 99.7% level implied by the CO and HC emissions goals were obtained in screening tests of all three concepts.

Exit Temperature Distribution - Measured combustor exit pattern factors were generally below 0.35 at all conditions tested. This level is typical of the idle performance of conventional combustors. However, the shapes of the radial exit temperature profiles were significantly different from those of conventional designs. Because of the absence of a film cooling layer, peak temperatures with the LOPER combustors occurred near the inner and outer liners, rather than near the middle of the annulus. No exit temperature distribution goals were specified, and no attempt was made to trim the exit profiles.

Ignition - All screening test configurations were ignited with a hydrogen torch at elevated combustor inlet temperatures (367 to 422 K). Under these conditions, light off was obtained as soon as fuel flow was increased above the lean flammability limit. No simulated ground start or altitude relight tests were conducted.

Liner Life - Satisfactory liner cooling and mechanical performance were obtained with all concepts. Except for damage as a result of resonance in configuration H1, no liner failures occurred during screening tests. Slight distortion was noted in the vicinity of forward and aft dilution holes, apparently resulting from hot spots caused by locally high heat transfer in regions where flow within the combustor was accelerated by

the blockage of the dilution jets. Minor distortion also occurred in the vicinity of the slip joint at the aft end of the forward liner. This distortion appeared to be caused by nonuniform circumferential growth between the hot impingement-cooled liner and the cooler support liner.

Peak liner temperatures monitored with surface-mounted thermocouples on the impingement-cooled liners were generally below 1200 K, and did not exceed 1300 K during screening tests. Based on inspection of temperature-sensitive paint applied to the back side of the impingement-cooled liners, average primary zone liner temperatures were estimated to be below 1075 K for all configurations tested. The temperature-sensitive paint also clearly indicated temperature gradients in the vicinity of each impingement cooling jet, and local hot spots near the primary dilution jets. Except for the addition of a small amount of preferential cooling adjacent to the dilution jets during atmospheric checkout tests, no adjustment of impingement cooling flows was required to obtain adequate liner performance over the range of conditions tested.

Combustion Stability - Audible resonance was encountered in screening tests of all concepts. Strong resonance was first noted in tests of configuration H1, which was the third of the 18 screening configurations to be tested. Posttest inspection of this combustor revealed resonance-induced damage to the aft portion of the forward liner, as shown in Figure 39. In order to prevent further damage, combustion operation in all subsequent tests was limited to conditions which did not produce audible resonance.

Typical resonance limits with respect to combustor inlet temperature/pressure level, fuel-air ratio, and reference velocity are shown in Figure 40. The limits shown indicate the locus of points at which light or intermittent resonance was encountered. The amplitude of resonance increased toward the central portion of the resonance region. A hysteresis effect was also apparent. After continuous audible resonance had been established, it was necessary to move slightly beyond the indicated limits to reestablish nonresonant operation.

Several screening test modifications were evaluated to determine their effect on resonance limits. Modifications described in the preceding section include variations in swirler configuration (H3-H6, C5-C6), swirler flow rate (H2, R3, R6), and forward dilution position (H3-H6). Of these modifications, only swirler flow variation had a strong effect on resonance limits. Resonance limits with respect to both reference velocity and fuel-air ratio increased when swirler flow was increased. The tendency generally tended to increase as swirler equivalence ratio approached unity.

In addition to the above modifications, configurations H5 and H6 incorporated modifications aimed specifically at resonance reduction. In configuration H5, an acoustic treatment consisting of two tuneable 2.36-cm ID quarter-wave tubes mounted on the combustor sidewalls was evaluated. In this test,

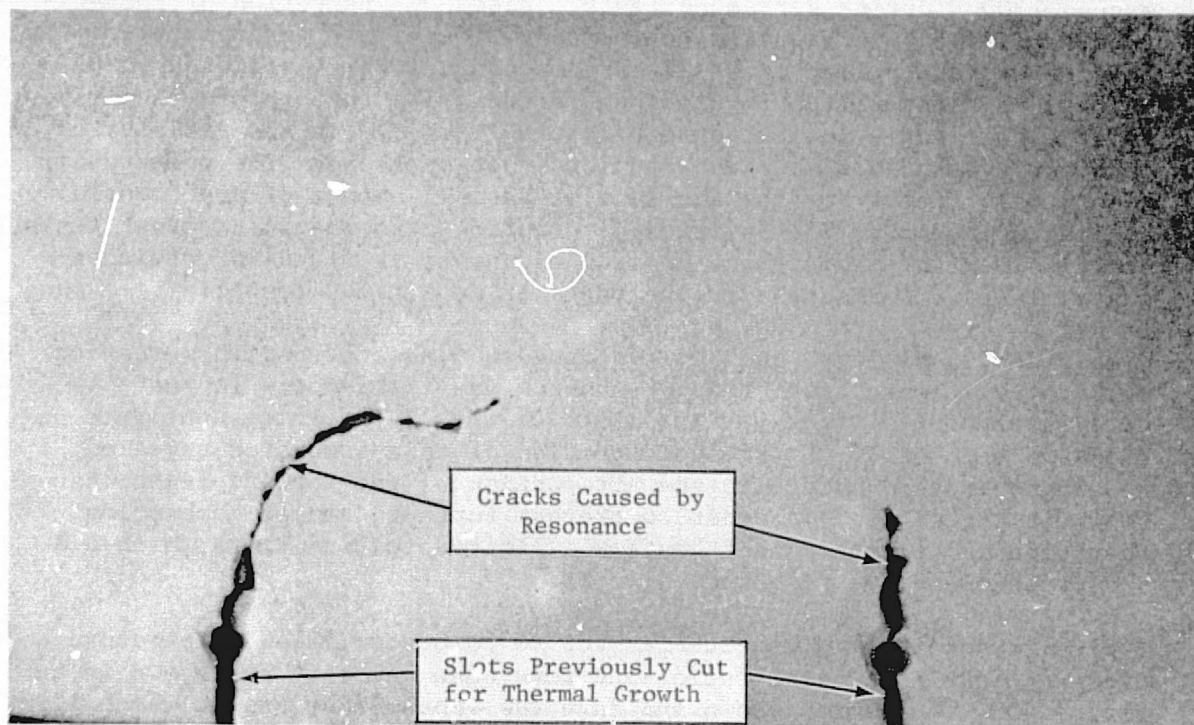


Figure 39. Resonance Damage to Forward Combustor Liner, Configuration H1.

ORIGINAL PAGE IS
OF POOR QUALITY

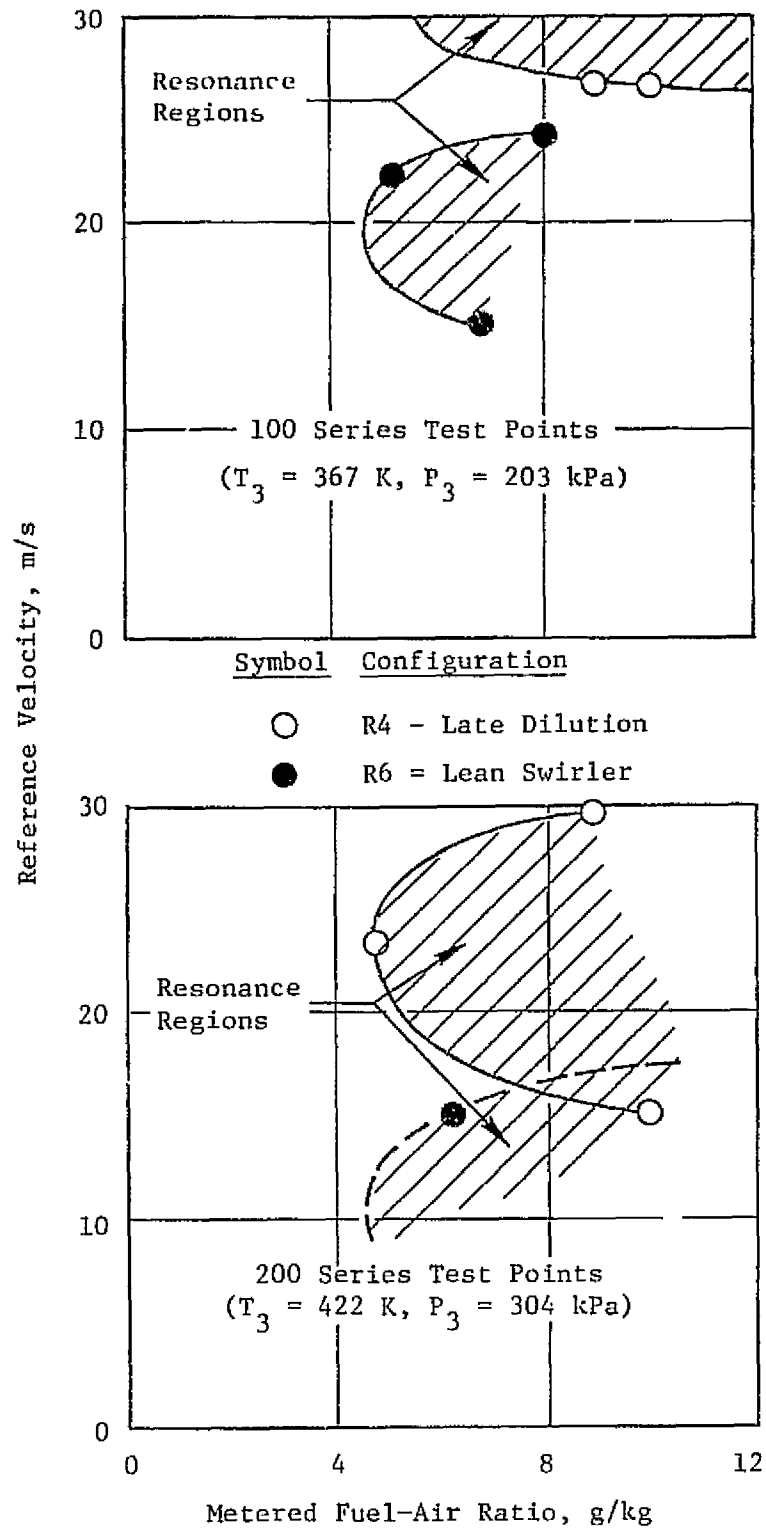


Figure 40. Typical LOPER Resonance Limits.

dynamic pressure measurements were obtained which indicated resonant frequencies of 324 to 340 Hz at $T_3 = 367$ K, and 360 to 368 Hz at $T_3 = 422$ K. Adjustment of the sidewall tubes to these frequencies did not appreciably affect the amplitude of the resonance. Acoustic analysis of the combustor and rig indicated that the most probable sources of this frequency were axial modes either in the rig inlet plenum or in the passage formed by the combustor and exit instrumentation section. In configuration H6, these resonance modes were investigated by modifying rig inlet geometry and combustor flow patterns. Rig inlet geometry was varied by mounting the combustor directly within the inlet plenum, eliminating the diffuser and combustor housing flowpath. Dome dilution was added to modify flow patterns within the combustor. Neither of these modifications affected resonance characteristics.

5.3.2 Low-Emissions Concept Performance

In addition to the general aspects of performance discussed above, each of the low-emissions combustor concepts contained unique design features that could affect overall combustor performance. Specific performance results obtained with these unique design features were as follows:

Hot-Wall Combustor - Liner temperature estimates based on temperature patterns observed with temperature-sensitive paint, and peak liner temperatures measured during tests with the baseline configuration, indicated an average ceramic surface temperature of about 1030 K at the design point, with a temperature rise of approximately 100 K across the thermal barrier. These levels are representative of all hot-wall configurations, since liner cooling flow was not varied during screening tests.

Satisfactory durability was obtained with the thermal barrier coating. The surface of this coating remained intact throughout the screening tests except for some chipping incurred during machining operations to add provisions for additional primary and dome dilution, and during repair of resonance damage to the liners. In the latter case, the coating was successfully repaired by grit-blasting the affected area and recoating it. Liner temperature patterns were generally more uniform with the refractory coating than with the uncoated liners, and liner distortion was also decreased in the coated liners.

Recuperative Combustor - The use of impingement cooling proved to be an effective method for obtaining recuperative temperature rise. As shown in Figure 41, design-point temperature rise approached the predicted value with all configurations tested. As indicated by the correction factor used in this figure, temperature rise was found to be approximately proportional to the -0.5 power of combustor reference velocity. No significant problems were encountered in operation of the recuperative design feature, and no adjustment of cooling features was required to obtain satisfactory temperature rise.

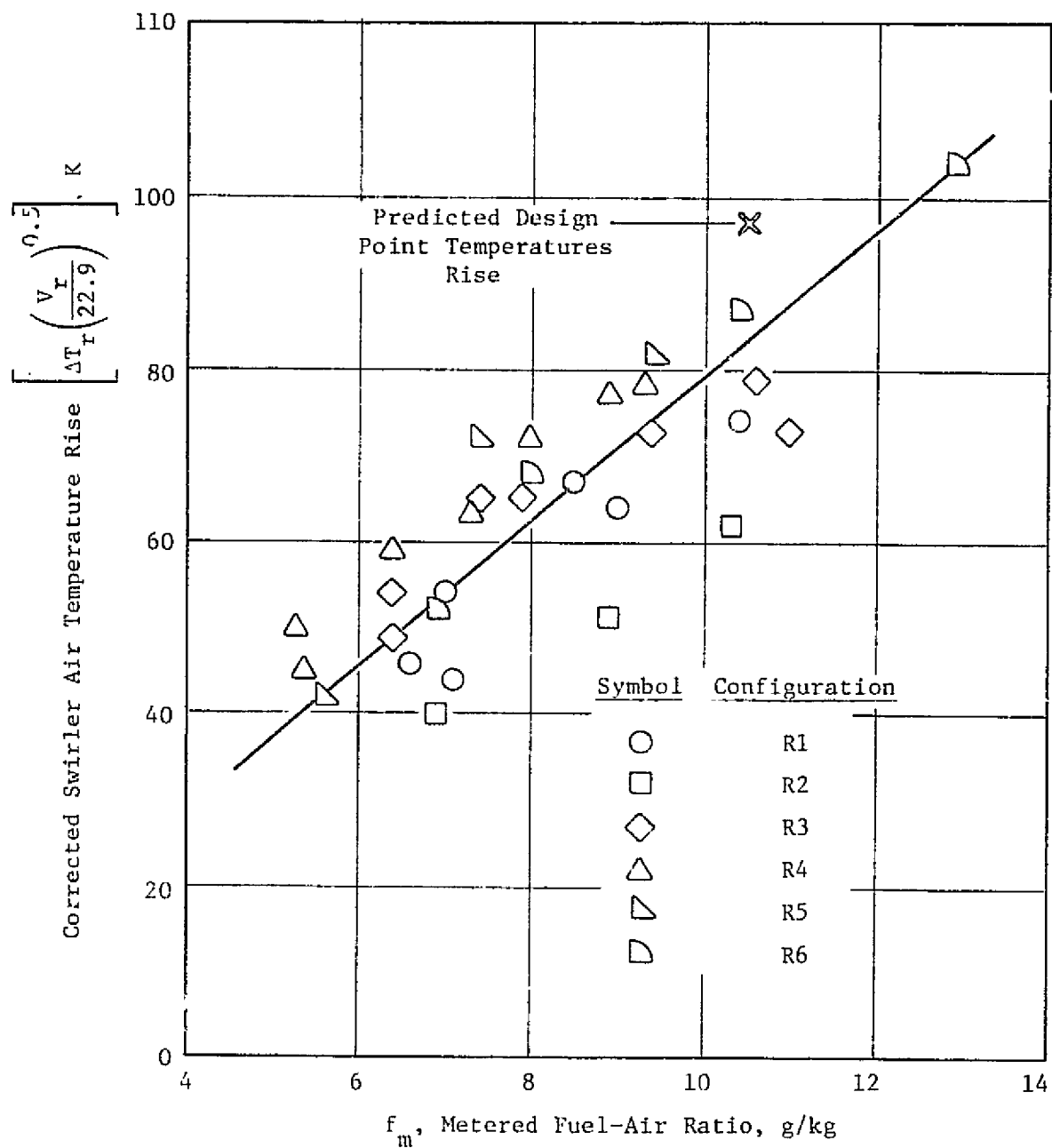


Figure 41. Recuperative Combustor Swirler Air Temperature Rise Correlation.

Catalytic Combustor - Catalytic durability was a prime concern in screening tests of the catalytic combustor. During operation of this concept, peak-indicated catalyst inlet temperature was limited to 1500 K. Based on tests with the catalyst-simulation plate installed (C1 and C2), this limitation should have been sufficient to prevent local temperature excursions from exceeding the 1590 K maximum operating temperature specified by the manufacturer (Engelhard Industries). However, in tests of configuration C3, the inlet surface of the catalyst was discolored in the corners of the catalyst and adjacent to the inner and outer liners. A radial crack in the central position of the catalyst was also observed. Further deterioration was observed after tests with configuration C4, including the appearance of a hole in one corner of the sector (Figure 42). This deterioration was apparently caused by reaction in locally rich regions next to the sidewalls and liners. These regions were not noted with the catalyst simulation plate installed, indicating that the high temperatures obtained with the catalyst installed (estimated to be above 1900 K) were a result of catalytically supported reactions in locally rich regions.

In configuration C5, the catalyst inlet temperature fuel-air ratio profile was improved by extending the length of the primary zone and adding primary dilution holes adjacent to the combustor sidewalls. However, the catalyst (which had also been used in configurations C3 and C4) collapsed, apparently as a result of thermal shock and resonance damage aggravated by distortion of the metallic retainer strips used to hold the catalyst in place. A photograph of the catalyst remnants is shown in Figure 43.

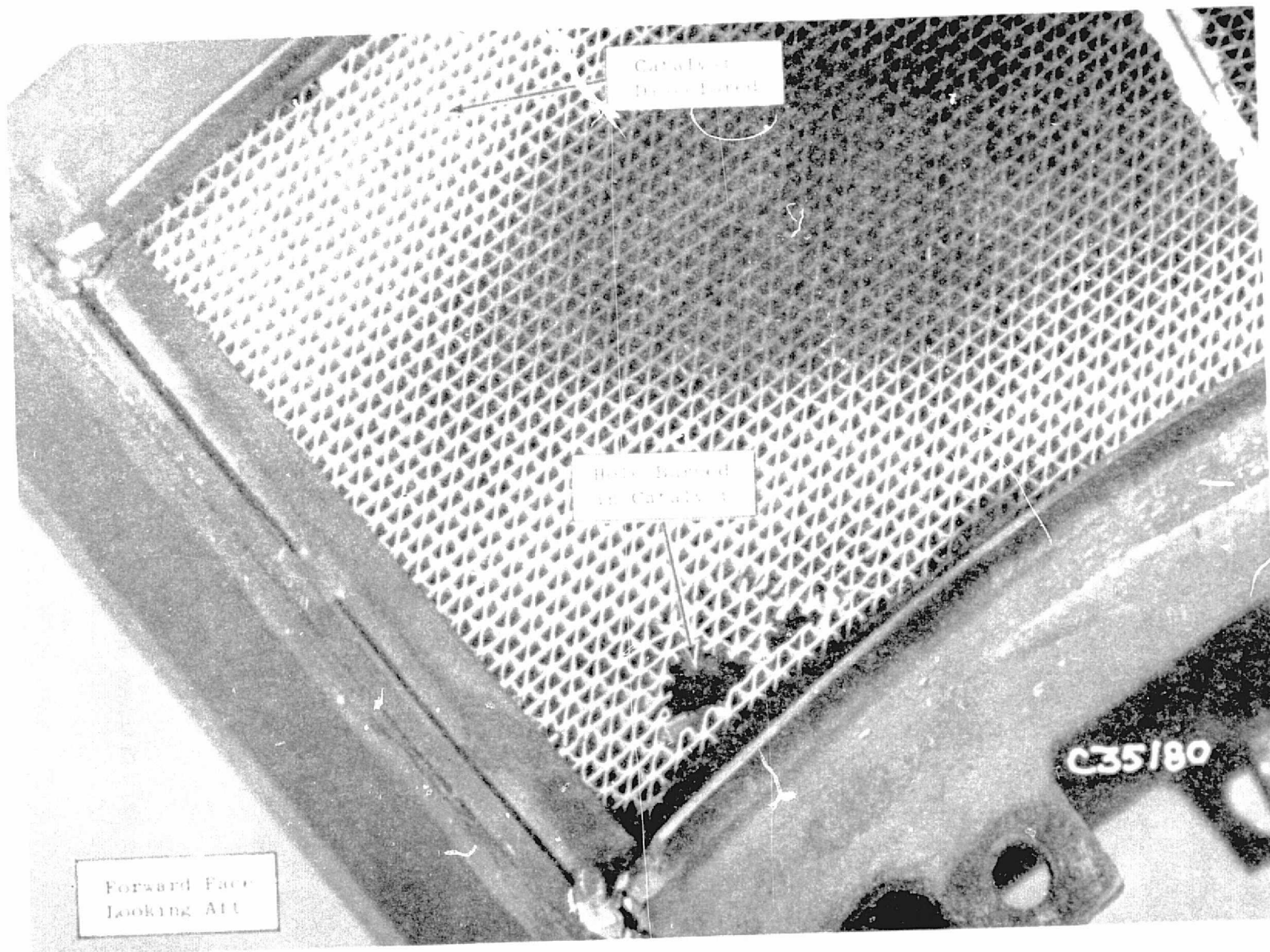
Catalyst durability was more encouraging in configuration C6, which was identical to C5 except for the installation of a new catalytic reactor. Minimal discoloration of the catalyst inlet face was obtained with this configuration; however, one radial crack did appear in the forward catalyst stage.

Based on screening test results, it was clear that an improved catalyst mounting method would be required to obtain satisfactory catalyst durability. Therefore, prior to parametric tests, the reactor was modified by Engelhard Industries. The modified reactor, shown in Figure 44, featured the use of a single-stage catalyst, soft mounting methods, and catalyst holder reinforcements to reduce the probability of damage due to thermal shock, catalyst holder distortion, and resonance. Favorable results obtained with these modifications are discussed in the following section.

5.4 PARAMETRIC TEST RESULTS

The three combustor configurations selected for parametric tests were based on the most promising hot-wall, recuperative and catalytic combustor screening test configurations. In the recuperative and catalytic parametric

C-2



ORIGINAL PAGE IS
OF POOR QUALITY

Figure 42. Localized Catalyst Damage, Configuration C4.

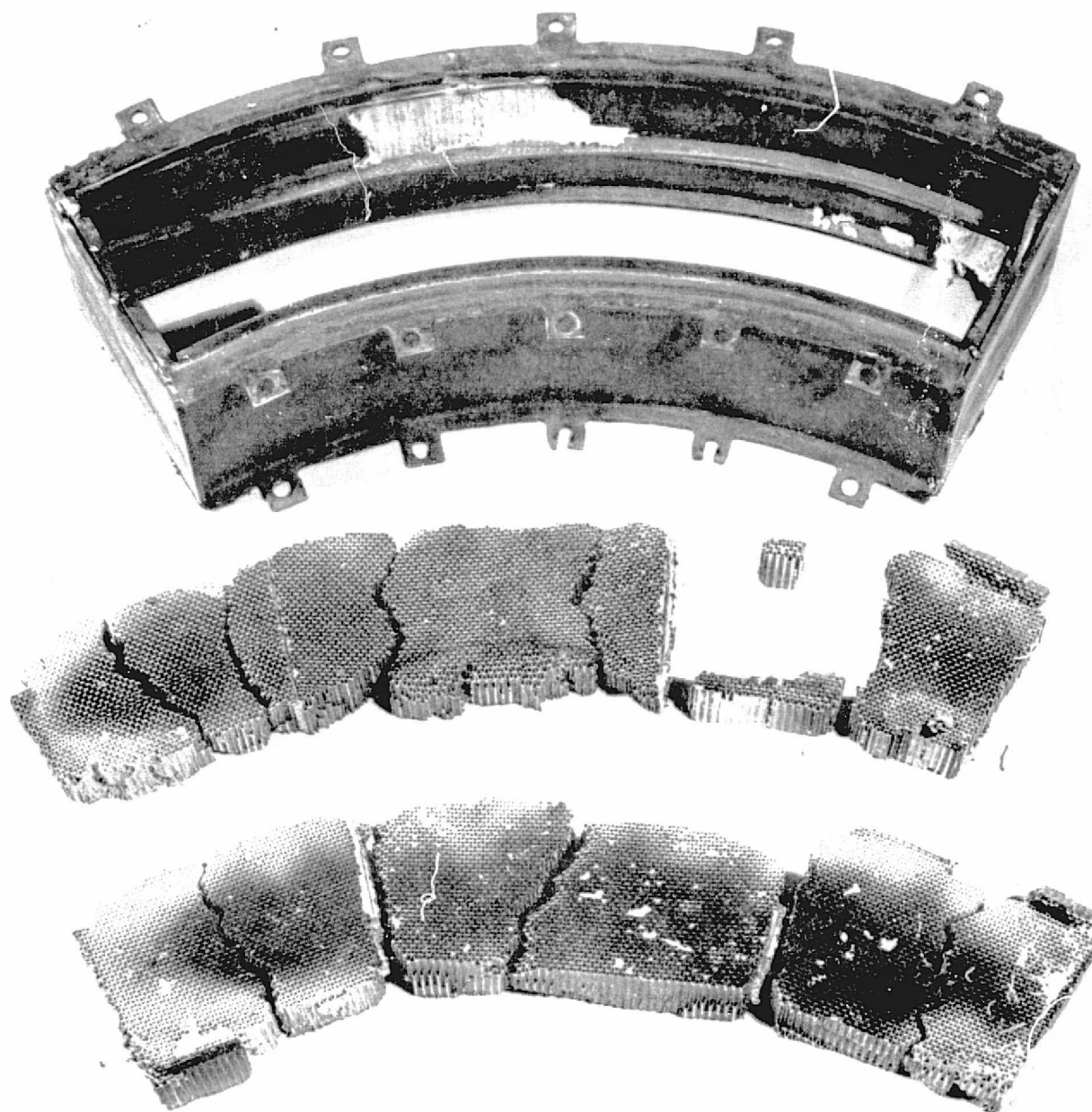
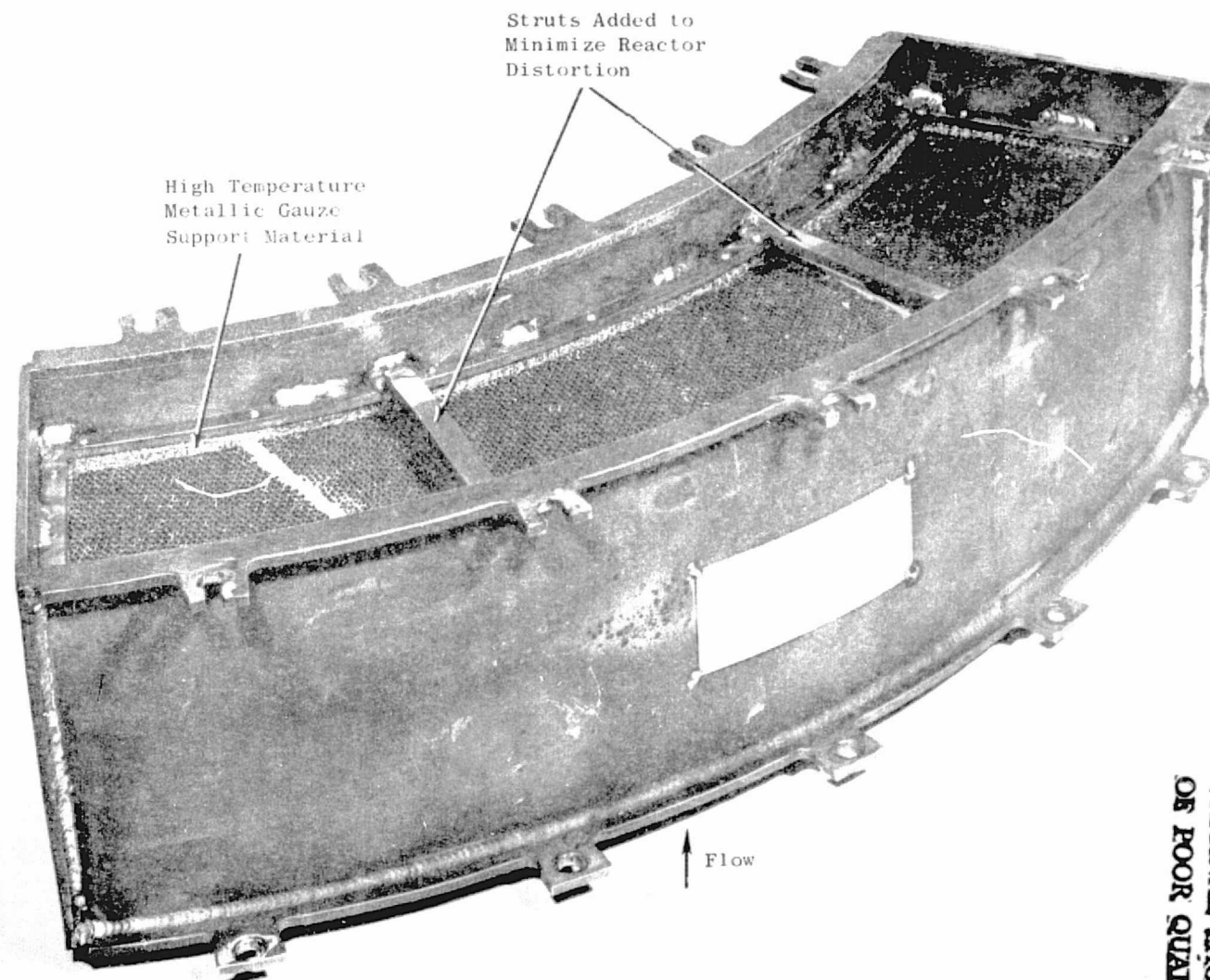


Figure 43. Catalyst Remnants After Collapse, Configuration C5.

ORIGINAL PAGE IS
OF POOR QUALITY



ORIGINAL PAGE IS
OF POOR QUALITY

Figure 44. Modified Catalyst Mounting Scheme.

test configurations, additional modifications were incorporated to improve emissions or performance. The relationship between the three parametric test configurations and the three most similar screening test configurations were as follows:

<u>Parametric Test Configuration</u>	<u>Relationship to Most Similar Screening Test Configuration</u>
Hot-Wall (H7)	Configuration H4, unmodified
Recuperative (R7)	Configuration R4 incorporating nondrooling swirler modification
Catalytic (C7)	Configuration C5/6 incorporating catalyst "soft mounting" modification

The parametric test configurations of each of the three concepts incorporated similar modifications relative to the respective baseline combustor designs. These common modifications included: (1) the use of similar short-secondary barrel, nondrooling swirler configurations, (2) the relocation of at least half of the primary dilution holes to a location 7.6-cm downstream of the swirler exits, and (3) the use of reduced-flow fuel nozzles.

In the configurations selected for parametric tests, the largest deviation from the baseline combustor designs was in the use of the extended-length primary zone in the catalytic combustor. This modification resulted in an 11.1-cm increase in the overall length of the catalytic combustor. External dimensions of the hot-wall and recuperative test configurations were identical to the baseline designs.

Complete test data summaries for each of the parametric test configurations are presented in Appendix B of this report. As in the screening tests, the range of operation of all three concepts was limited to a large extent by audible resonance. Therefore, it was not possible to obtain complete parametric variations in inlet temperature pressure, reference velocity, and fuel-air ratio over the ranges specified in the original test point matrix. However, sufficient data were obtained to define representative emissions at key points within the test point matrix, and to identify general trends resulting from changes in the various combustor inlet conditions.

Emissions and performance trends observed in the parametric tests are described below.

5.4.1 Emissions Results

Pollutant emissions characteristics of each of the parametric test configurations were generally in good agreement with screening test results. CO and HC levels safely below the applicable program goals were obtained with all concepts.

A comparison of emissions obtained near the design point with the hot-wall parametric (H7) and screening (H4) test configurations is shown in Figure 45. All emissions levels are in good agreement at the design fuel-air ratio; however, CO and HC levels rose more rapidly as fuel-air ratio was decreased below the design value in the parametric test build. The observed change in emissions characteristics, which was magnified by the strong dependence of emissions on fuel-air ratio at these conditions, was apparently related to a change in resonance limits, which required that slightly higher velocities be run with the parametric test configuration in order to avoid audible resonance. These changes were attributed to a slight change in flow characteristics resulting from the accumulated effects of several modifications to, and demodifications of, the combustor hardware components during the course of screening tests. Because of the change in resonance characteristics, no emissions measurements could be obtained at the low inlet temperature/pressure level during parametric tests of the hot-wall combustor. However, emissions at these conditions had been well characterized during screening tests of configurations H4 through H6. Parametric variations in combustor inlet temperature and pressure and reference velocity were also limited by resonance.

Recuperative combustor parametric test emissions characteristics at the lowest temperature conditions are compared with levels obtained with screening test configuration R4 in Figure 46. As indicated in this figure, a sharp reduction in HC levels was obtained through the use of the modified, non-drooling swirler configuration. This result was expected because of the large HC reduction obtained with a similar swirler modification in hot-wall screening tests. The improvement in fuel-air mixing obtained with these swirlers also appeared to reduce NO_x levels slightly.

Emissions measured in catalytic combustor parametric tests are compared with levels obtained in screening tests of configuration C5 in Figure 47. All measured emissions were in good agreement, indicating that the modified catalyst mounting technique used in the parametric tests had little effect on catalytic conversion. This was of some concern because total catalyst bed length in the modified reactor had been reduced from 8.9 cm to 7.6 cm.

Emissions obtained with the three parametric test configurations at the design inlet temperature and pressure levels are compared in Figure 48. Because of operating limitations required to avoid resonance, the data shown for the hot-wall and catalytic concepts were obtained at a nominal reference velocity of 26.5 m/s. For comparison, recuperative concept emissions at reference velocities of 22.9 and 30.1 m/s are shown. As indicated in this figure, absolute emissions levels were similar for all three concepts; however, the characteristic emissions curves of the three concepts appeared to be shifted with respect to fuel-air ratio. With the hot-wall combustor, the CO level approached a minimum very close to the design fuel-air ratio (10.5 g/kg), as was expected from primary zone stoichiometry considerations. With the recuperative and catalytic combustors, however, CO approached minimum values at fuel-air ratios of approximately 7.5 and 8.3 g/kg, respectively.

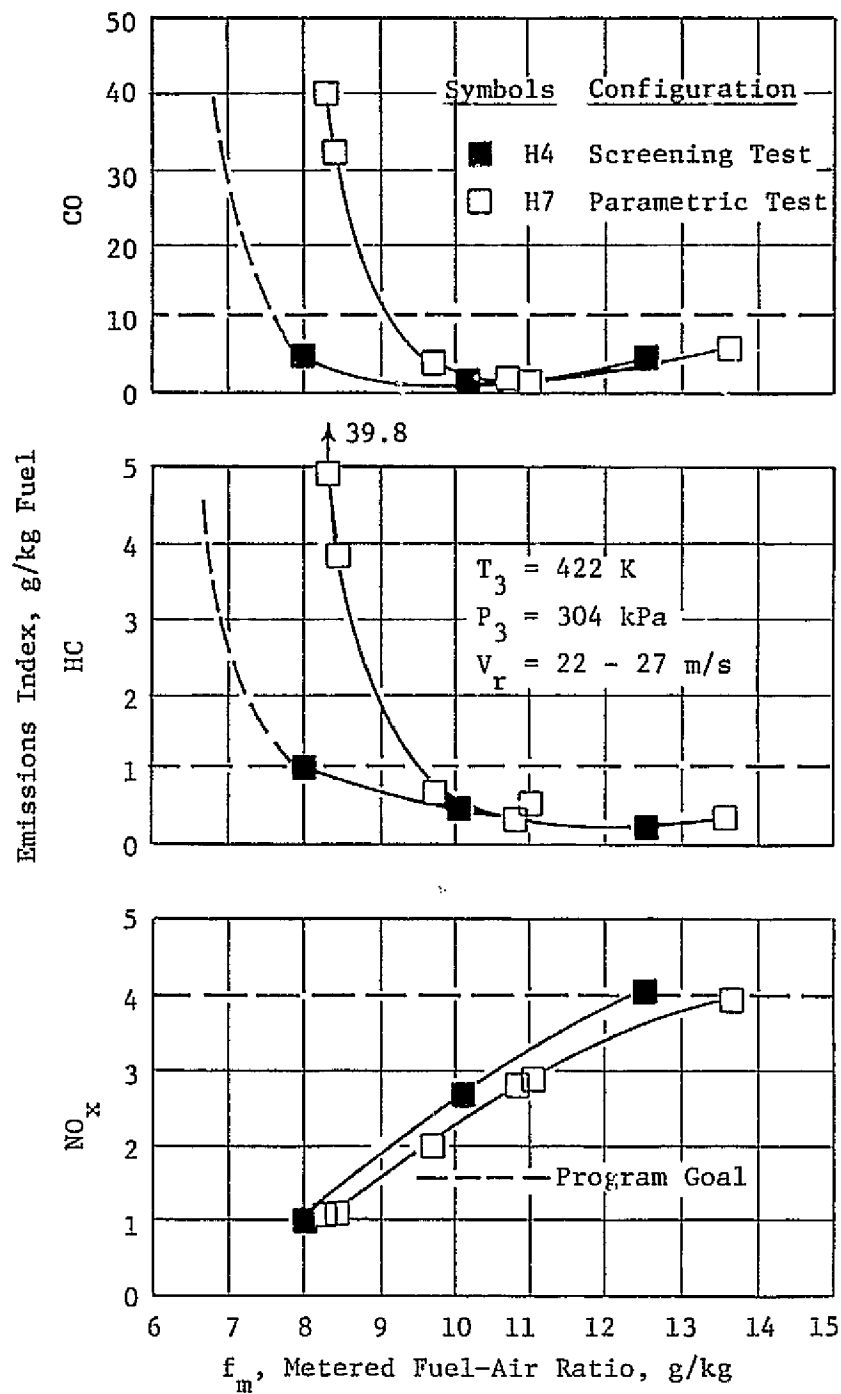


Figure 45. Comparison of Hot-Wall Combustor Screening and Parametric Emission Test Results.

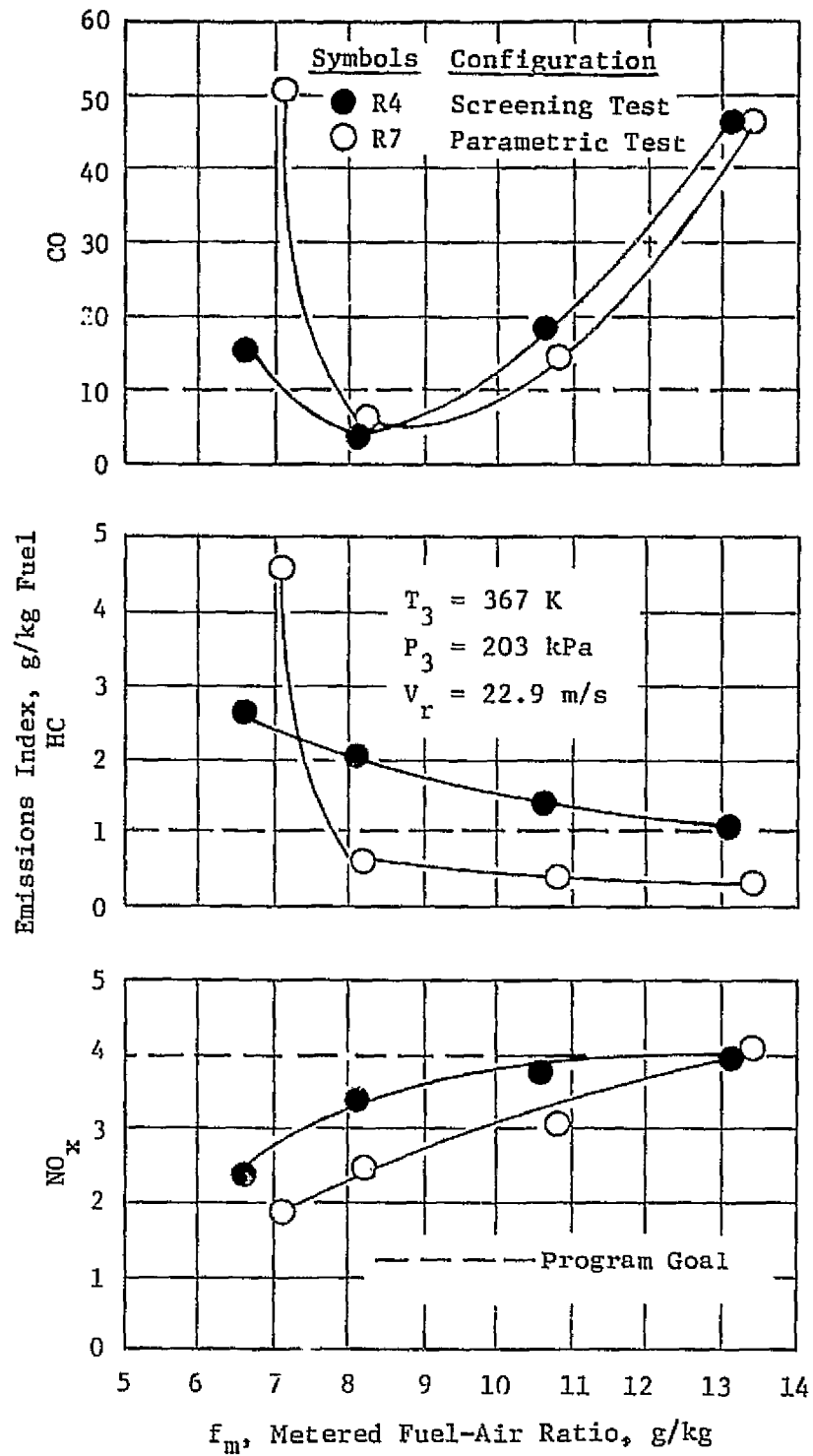


Figure 46. Comparison of Recuperative Combustor Screening and Parametric Emission Test Results.

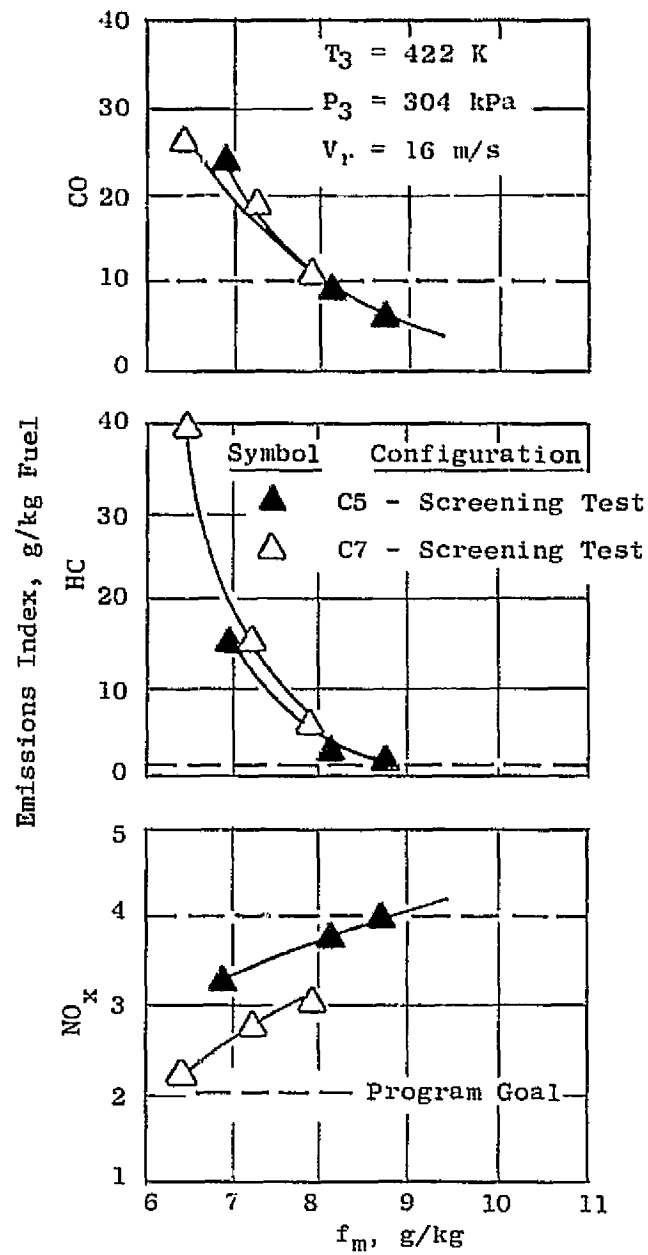


Figure 47. Comparison of Catalytic Combustor Screening and Parametric Emission Test Results.

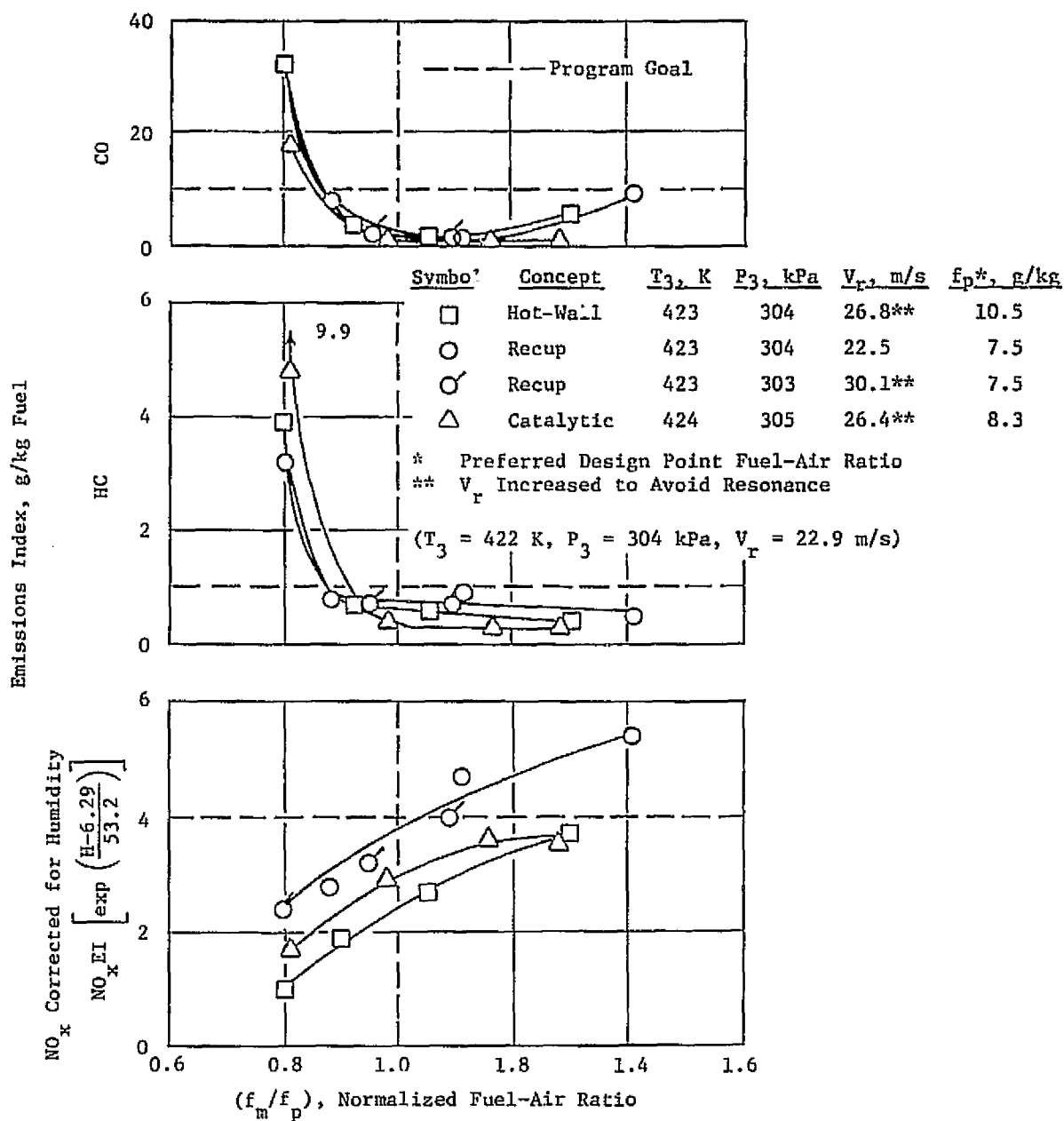


Figure 48. Parametric Test Results, Comparison of Emissions at Design Point Inlet Conditions.

The above shift in emissions relative to fuel-air ratio was similar to an effect observed in screening tests, where it was found that the fuel-air ratios for minimum CO varied in proportion to swirler flow. The possibility that this effect was responsible for the shift observed in parametric tests was investigated with an examination of average swirler and primary dilution airflows for each of the parametric test configurations. These calculations were based on average measured dome pressure drop corrected to the design-point operating conditions, and effective swirler and primary dilution areas measured in flow calibration tests.

As shown in Table XVII, recuperative swirler and primary dilution flows were 10 to 15% lower than hot-wall flows, which accounts for about half of the observed 30% shift in CO emissions with respect to fuel-air ratio. The remaining shift was apparently a result of decreased mixing efficiency due to reduced pressure drop across the recuperative swirlers. As noted in screening tests, with reduced mixing effectiveness primary zone stoichiometry appeared to be controlled by local fuel-air mixing downstream of the swirlers rather than by the bulk mixing which applied to the hot-wall design. This effect tended to increase effective primary zone stoichiometry since most building occurred in fuel-rich eddies.

Calculated primary zone flows for the catalytic configuration were from 7 to 14% higher than hot-wall flows. This increase in primary zone flow would normally be expected to result in a proportionate increase in the fuel-air ratio for minimum CO; however, two factors tended to decrease the position of the CO minimum in this concept. The first of these factors was the mixing effect observed with the recuperative combustor. As with the recuperative combustor, catalytic swirler pressure drop was reduced to about half of total combustor pressure drop. A second factor which would cause an apparent shift in CO levels is the effect of catalytic conversion, which would tend to give an apparent shift in CO and HC levels by decreasing these levels at high fuel-air ratios. This effect was evidenced by the fact that catalytic combustor CO levels tended to approach a minimum and remain close to that minimum up to the catalyst inlet temperature limit (which limited maximum fuel-air ratio). With the hot-wall and recuperative combustors, a definite increase in CO was observed at higher fuel-air ratios.

To facilitate emissions comparisons between the three concepts, emissions are presented as a function of normalized fuel-air ratio in Figures 48 and 49. The normalization factor used in this figure, f_p , corresponds to the point at which CO levels approach a minimum value as fuel-air ratio is increased.

Design point CO and HC emissions were very similar for all concepts. Lowest levels were obtained with the extended-length catalytic combustor, but all concepts were competitive and were comfortably below program goals over a wide range of fuel-air ratios. As in screening tests, NO_x emissions were consistently higher with the recuperative concept because of increased primary zone inlet temperature. These increased NO_x levels narrowed the range of fuel-air ratios over which all emissions goals were met relative to the hot-wall and catalytic concepts.

Table XVII. Primary Zone Airflow Comparison, Parametric Test Configurations

Concept	fp	fp/10.5	Swirler Flow, %W _c			Forward Dilution, %W _c			Total Primary Zone		
			Design	Test	Design Test	Design	Test	Design Test	Design	Test	Design Test
Hot-Wall	10.5	1.00	16.0	15.5	0.97	12.6	12.2	0.97	28.6	27.7	0.97
Catalytic*	8.3	0.79	16.2	17.6	1.09	12.1	13.1	1.08	28.3	30.7	1.08
Recuperative**	7.5	0.71	15.6	14.0	0.90	11.4	9.8	0.86	27.0	23.8	0.88

* Does not include additional precatalyst dilution.

** Assumed recuperative ΔT of 62 K (average of all R7 readings) for flow calculations.

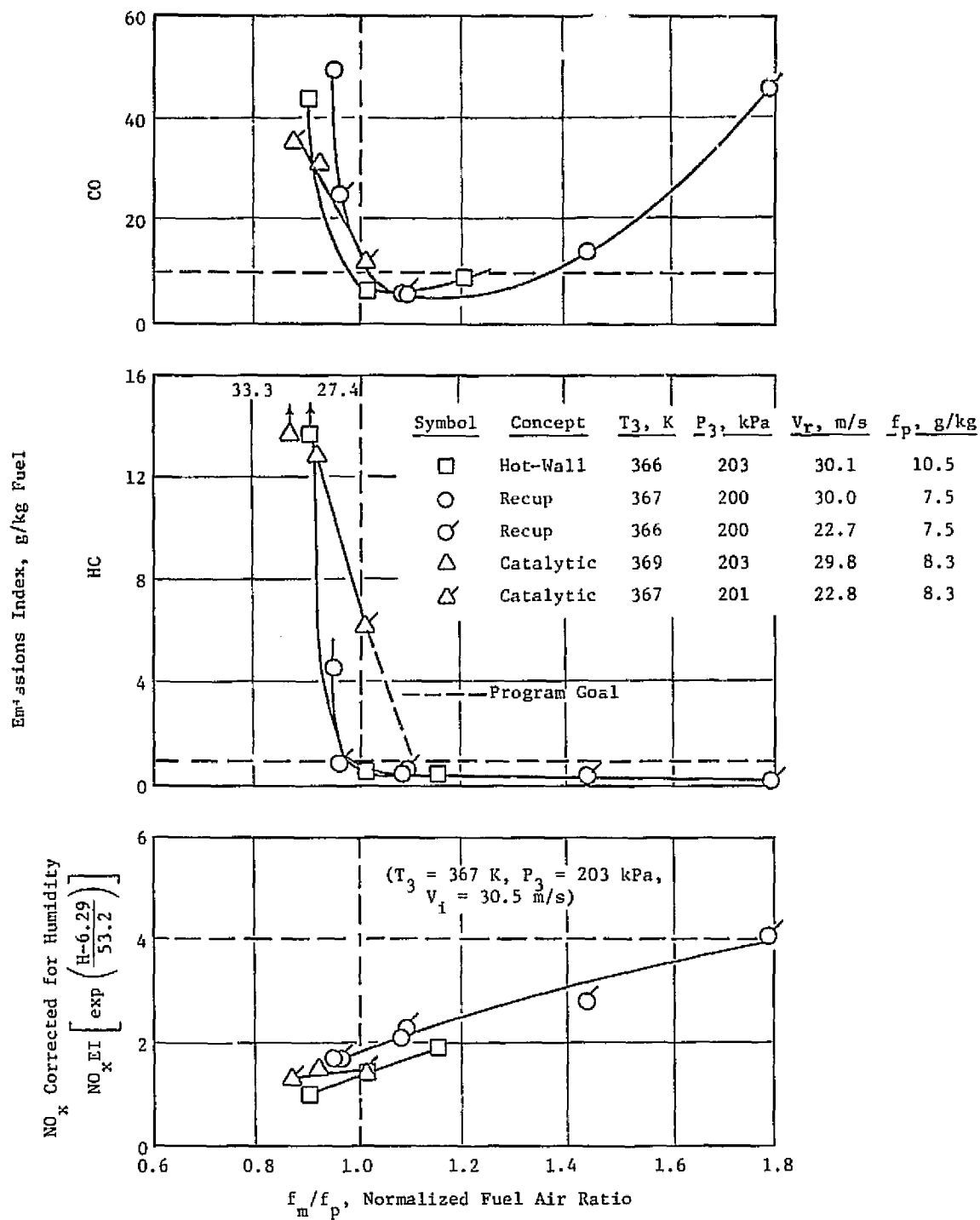


Figure 49. Parametric Test Results, Comparison of Emissions at Most Severe Inlet Conditions.

At the lowest inlet temperature/pressure levels and highest reference velocities (the more severe operating condition for CO and HC emissions), both the hot-wall and recuperative concepts met all emissions goals over a limited range of fuel-air ratios. Catalytic combustor operation at these conditions was limited by resonance and nonuniform catalyst inlet temperature profiles, but parametric test trends indicate that the emissions goals would have been met at increased fuel-air ratios. NO_x emissions were well below the program goal with all three concepts at these operating conditions.

Independent variations in inlet temperature, pressure, and reference velocity were attempted in each of the parametric tests, with varying degrees of success. The extent to which these parameters could be varied was extremely limited because of audible resonance, and correlation of the effects of variation in these parameters was difficult, both because of the emissions' strong sensitivity to fuel-air ratio and because of the low emissions levels measured.

The widest range of parametric variations was obtained with the recuperative combustor. Trends observed as a result of independent variations in combustor inlet temperature and pressure with this burner, which were typical of results obtained with the hot-wall and catalytic combustors, are shown in Figure 50. At low fuel-air ratios, as the lean stability limits were approached, CO and HC emissions were reduced appreciably by increases in combustor inlet temperature and/or pressure. At fuel-air ratios in the vicinity of the CO minimum, the dependence of CO emissions on inlet temperature and pressure continued to be strong, but HC levels appeared to become almost independent of variation in these parameters. At fuel-air ratios well above the CO minimum, both CO and HC demonstrated a much weaker dependence on inlet temperature and pressure.

The effect of reference velocity on recuperative combustor emissions was quite strong, particularly at the lowest temperature conditions. This effect is shown in Figure 51. Very little change in emission characteristics was obtained over the higher range of reference velocities, but when reference velocity was reduced to the 15.2-m/s value, CO and HC emissions were significantly increased. Although fewer data were obtained at low reference velocities with the catalytic combustor because of resonance limitation, a similar increase in emissions at low reference velocity was observed. However, the limited data obtained in screening tests of the hot-wall combustor indicated only a slight dependence of reference velocity at these conditions. Thus, this behavior appeared to be a direct result of decreased fuel atomization and fuel-air mixing effectiveness due to decreased swirler pressure drop in the recuperative and catalytic concepts.

5.4.2 Performance Results

Parametric test performance results were similar to those obtained in screening tests. Overall combustor pressure drop for all three concepts was within 0.5% of the 5.0% target value. Combustion efficiencies above 99.7%

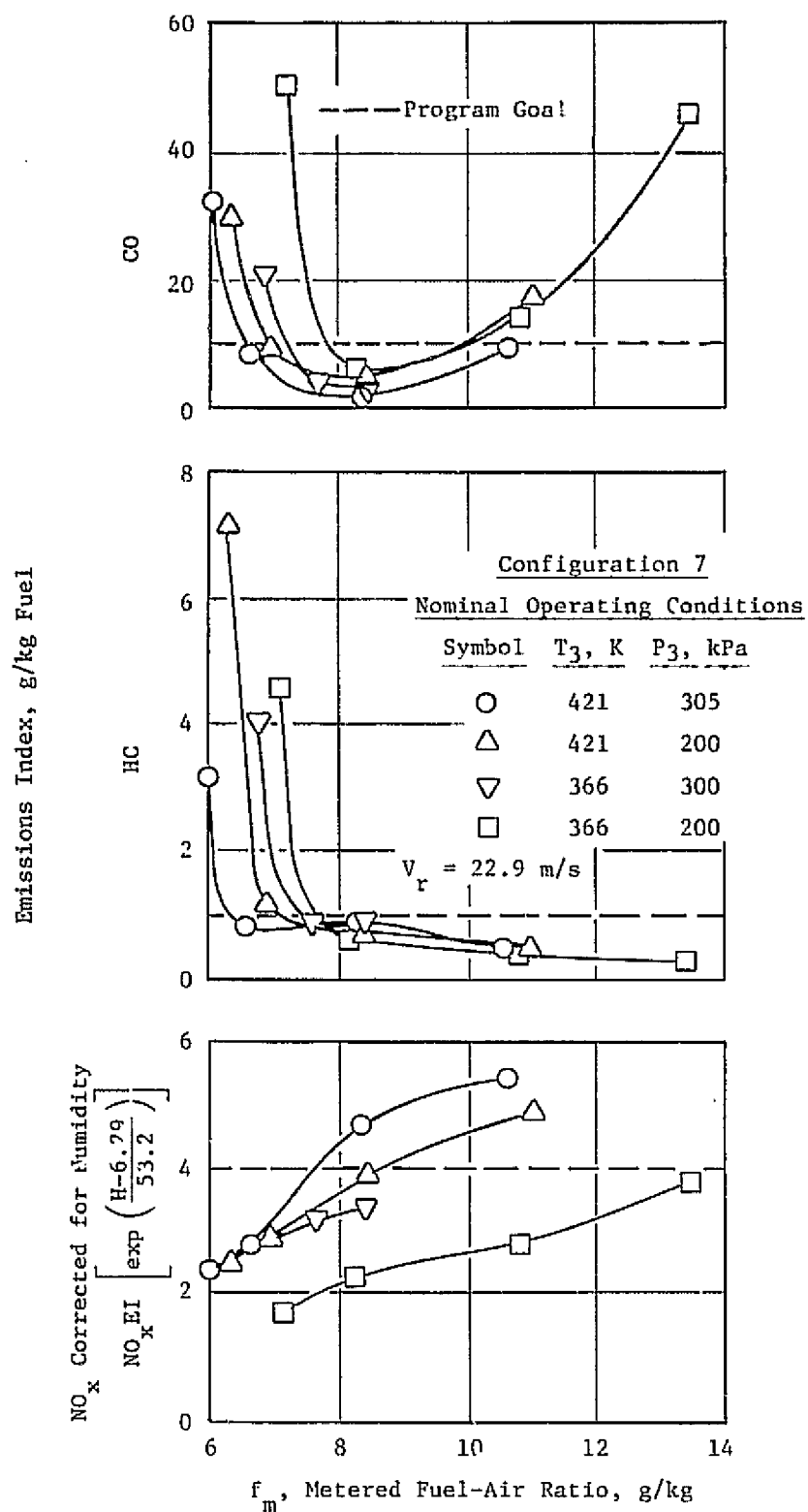


Figure 50. Parametric Test Results, Effect of Inlet Temperature and Pressure on Recuperative Combustor Emissions.

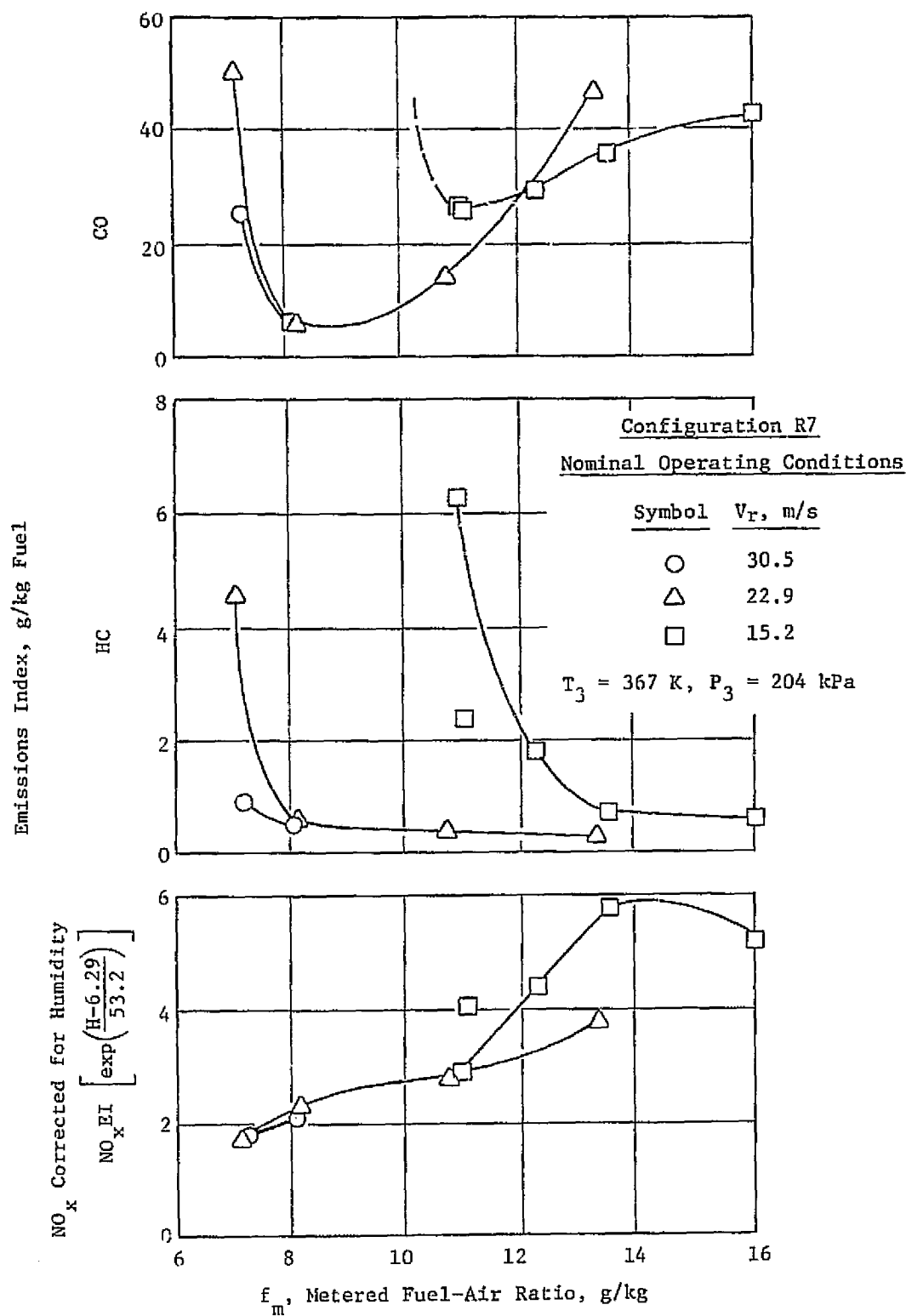


Figure 51. Parametric Test Results, Effect of Reference Velocity on Recuperative Combustor Emissions.

(based on emissions measurements) were also obtained with all concepts. As shown in Figure 52, exit temperature profiles were quite uniform, with peak temperatures occurring adjacent to the inner and the outer liners.

A major performance problem with all of the parametric test configurations was the occurrence of audible resonance. The resonance limits encountered within the planned test point matrix are indicated in Table XVIII. At several of the indicated conditions, operation was not attempted either because emissions characteristics (specifically the CO minimum) had already been defined, or because of peak liner or (in the case of the catalytic combustor) catalyst inlet temperature limitations. A general trend observed with all combustors was a decrease in the reference velocity at which resonance was most prevalent as inlet temperature was increased. Resonance generally occurred at lowest velocities in the hot-wall combustor, and at highest velocities in the recuperative combustor. But no definitive relationship between combustor operating parameters (for example, dome pressure drop) and resonance limits was identified.

One significant improvement in performance which was obtained in parametric tests was in the durability of the catalytic reactor assembly used in the catalytic combustor. Catalyst damage to this reactor was limited to very slight discoloration of the inlet face of the catalyst. Catalyst cracking, which had been a problem in all catalytic combustor screening tests, was not observed in parametric tests.

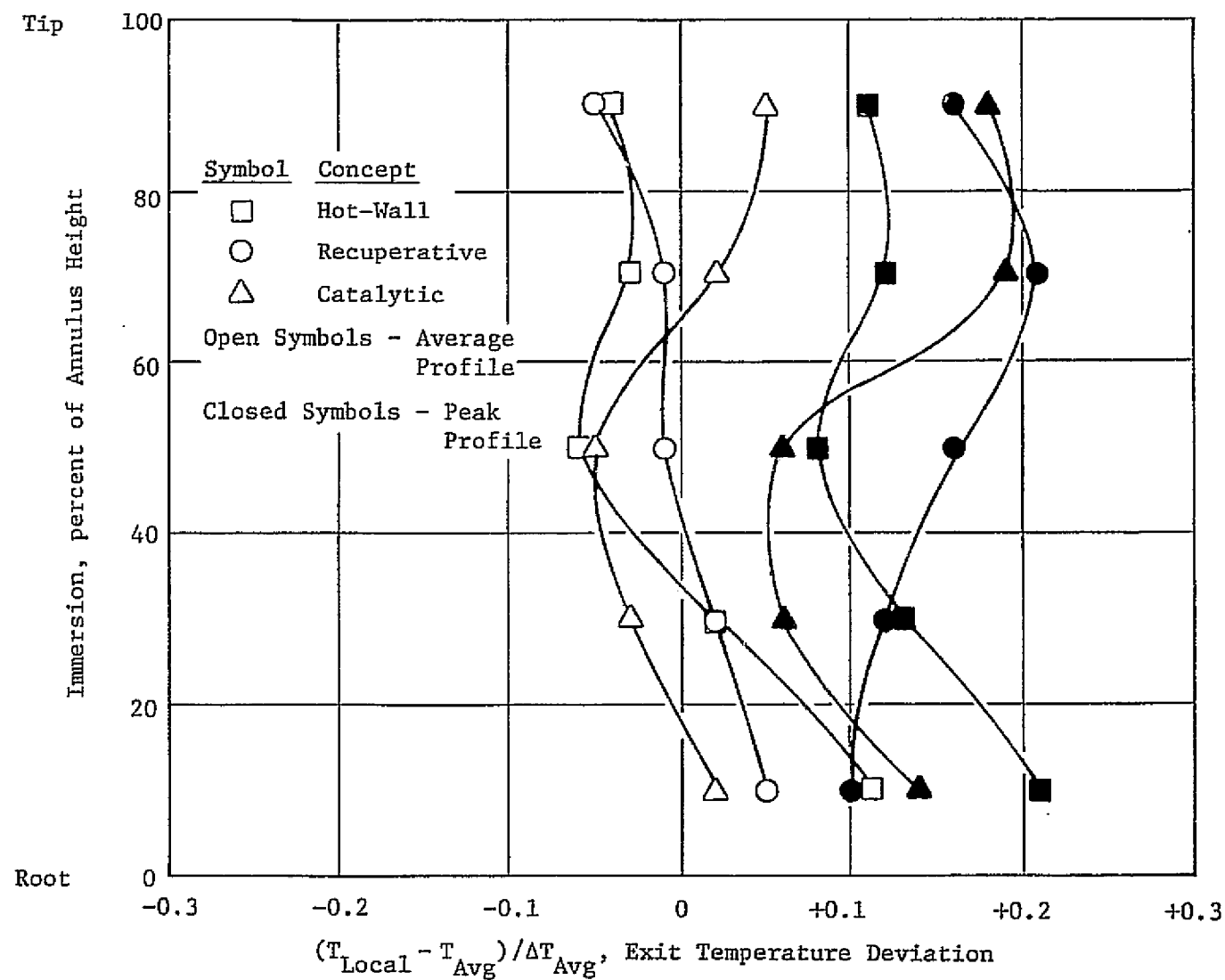


Figure 52. Parametric Test Results, Comparison of Combustor Exit Temperature Profiles.

Table XVIII. Resonance Limits, Parametric Test Configurations.

Test Point Series	T ₃ , K	P ₃ , kPa	V _r , m/s	Observed Maximum Fuel-Air Ratio for Nonresonant Operation, g/kg		
				Configuration		
				H7	R7	C7
110	367	203	15.2	A	N/L (16.1)	N/L (10.0)
120	367	203	22.9	A	N/L (13.4)	8.4
130	367	203	30.5	10.9	8.1	7.6
*140	367	203	35.9	12.2	---	---
210	422	304	15.2	A	11.0	8.5
220	422	304	22.9	8.3	10.6	8.4
230	422	304	30.5	N/L (13.5)	8.2	---
*240	422	304	26.7	N/L (13.6)	---	N/L (10.6)
310	478	405	15.2	A	N/L (8.2)	6.1
320	478	405	22.9	9.3	N/L (6.2)	9.5
330	478	405	30.5	N/L (11.0)	---	---

A - Resonance at all fuel-air ratios

N/L - No fuel-air ratio limit encountered up to indicated value of f_n

--- Operation not attempted at indicated conditions

* - Reference velocity adjusted to avoid resonance

6.0 ASSESSMENT OF RESULTS

6.1 EMISSIONS RESULTS

Representative emissions levels obtained with the most promising configuration of each of the three LOPER low-emissions combustor concepts are compared in Table XIX. In this table, emissions have been compared at preferred design point fuel-air ratios for each concept, as discussed in the previous chapter. The use of these fuel-air ratios was not meant to imply that engine fuel-air ratio must conform to the preferred level, which would clearly be impossible since engine fuel-air ratio is fixed by the engine cycle, but was instead intended to reflect trends observed in screening tests, which indicate that these levels are representative of emission levels achievable at the design point fuel-air ratio with a small amount of further development to "tune" combustor airflow distribution. The change in emissions resulting from this tuning process would be expected to be, at most, proportional to the change in primary zone airflow. Thus, the 20 to 30% increase in airflow required to adjust the preferred fuel-air ratio of the recuperative and catalytic combustor concepts to the design value would be expected to increase design point CO and HC emissions by less than 0.6 and 0.3 g/kg, respectively.

As indicated in Table XIX, the lowest design-point emission levels were obtained with the catalytic combustor concept, closely followed by the recuperative and hot-wall concepts. This order was not unexpected, since the beneficial effects of catalytic conversion and increased inlet temperature have been clearly documented in previous test programs. However, the similarity of CO and HC emissions from the three concepts was at first surprising, since the potential benefits of the hot-wall feature were previously unproven.

A comparison of the LOPER combustors to more conventional combustor concepts reveals several possible reasons for the similarity in emissions. As shown in Table XX, each of the LOPER combustors shared two common features which would be advantageous to the reduction of CO and HC emissions. These features were the elimination of primary zone film cooling, which was a specific feature of the hot-wall concept that was incorporated into all three combustor designs; and the use of long, well-sheltered combustion zones, which resulted from the selected baseline flowpath. Furthermore, there are inherent disadvantages which must be accepted in order to incorporate the recuperative and catalytic features. In either case, swirler pressure drop is reduced (at the possible expense of reduced fuel atomization and fuel-air mixing effectiveness) because of the requirements for flow restrictions in series with the swirler (impingement cooling and/or catalyst pressure drop). In the catalytic concept, additional primary zone airflow must also be added (at the expense of increased quenching tendencies and extended mixing length requirements) to keep peak catalyst temperatures below the maximum use temperature. Thus, the strong emissions-reduction potentials of the recuperative and catalytic concepts are offset to some degree by these inherent disadvantages.

Table XIX. Comparison of Emission Levels, Most Promising Configurations.

Condition	Concept	$f_p^{(a)}$	Emissions at $f/f_p = 1$, (g/kg Fuel)			Range of f/f_p to Meet All Emissions Goals ^(c)
			COEI	HCEI	NO _x EI ^(b)	
Design Point ^(d)	Hot-Wall	10.5	2.5	0.6	2.4	0.87 (CO Limit) to 1.40 (CO Limit)
	Recuperative	7.5	2.0	0.7	3.8	0.87 (CO Limit) to 1.04 (NO _x Limit)
	Catalytic	8.3	1.4	0.4	3.0	0.92 (HC Limit) to 1.30 (Catalyst Temperature Limit)
Most Severe Point ^(e)	Hot-Wall ^(f)	10.5	7.5	0.7	1.4	0.98 (CO Limit) to 1.22 (CO Limit)
	Recuperative	7.5	13.0	0.6	1.8	1.02 (CO Limit) to 1.36 (CO Limit)
	Catalytic	8.3	14.5	6.9	1.5	--- Not Determined ---

(a) - Preferred design point fuel-air ratio

(b) - Corrected to 6.29-g/kg humidity

(c) - See Figures 48 and 49

(d) - $T_3 = 422$ K, $P_3 = 304$ kPa, $V_T = 22.9$ m/s(e) - $T_3 = 367$ K, $P_3 = 203$ kPa, $V_T = 30.5$ m/s

(f) - Configuration H4 screening test data

Table XX. Assessment of LOPER Idle Emission Reduction Design Features.

<u>Concept</u>	<u>Advantages</u>	<u>Disadvantages</u>
Hot-Wall	Primary Zone Wall Temperature Increased Primary Zone Cooling Film Eliminated Long, Sheltered Combustion Zones	None
Recuperative	Primary Zone Inlet Temperature Increased Primary Zone Cooling Film Eliminated Long, Sheltered Combustion Zones	Swirler Pressure Drop Reduced
Catalytic	Catalytic Conversion Added Primary Zone Cooling Film Eliminated Long, Sheltered Combustion Zones	Swirler Pressure Drop Reduced Additional Primary Zone Dilution Added

In spite of the trade offs mentioned above, emissions obtained with all of the LOPER combustors were significantly lower than levels which have been obtained with conventional combustion technology. This point is graphically illustrated in Figure 53, where design-point emissions levels of the three LOPER combustors are compared with levels obtained at similar low-power conditions with advanced combustor designs developed in the NASA Experimental Clean Combustor Program (ECCP). In that program, conventional combustor design technology was utilized in concert with combustion staging concepts to tailor combustor flows for low idle emissions. Also shown in this figure are emissions levels of the production CF6-50 and JT9D engines, for which the ECCP designs were intended. Compared to the ECCP results, all three of the LOPER combustors provided up to an order-of-magnitude decrease in CO and HC emissions, with only a small increase in NO_x emissions.

6.2 PERFORMANCE RESULTS

Because of the similarity of emissions results obtained with the three LOPER low-emissions concepts, the relative performance of each concept is an important factor in determining its overall suitability for use in advanced combustor applications.

In Table XXI, the three LOPER low-emissions combustor concepts are rated in terms of design risk with respect to several key aspects of combustor performance. These ratings apply to the use of the LOPER concepts within the pilot stage of a practical combustion system capable of full-range operation. Since these ratings are based on sector combustor tests, the rating "least design risk" implies the possibility of a requirement for considerable development effort over and above that required for a more conventional combustor stage.

Overall emissions performance of the three combustor concepts is rated low risk based on emissions results obtained in the combustor rig tests. The only area of concern in this category is the increase in NO_x emissions observed in tests with the recuperative combustor.

Overall aerothermal performance of all of the low-emissions concepts was good. Combustion efficiency, pressure drop, lean blowout, and exit temperature profiles were comparable to those generally obtained with conventional concepts. However, additional design risks were identified with respect to some other aspects of aerothermal performance.

A primary area of concern is resonance, which was apparent in all three combustor concepts and did not respond to changes in combustor or test rig geometry. Although the resonance encountered in rig tests could possibly have been due to details of combustor design (i.e., the flat dome surface), or to characteristics of the test facility piping, there is also a strong possibility that the tendency to resonate was increased by the elimination of film cooling holes from the combustor liners, making the combustor walls acoustically "hard". If this is the case, additional development would be

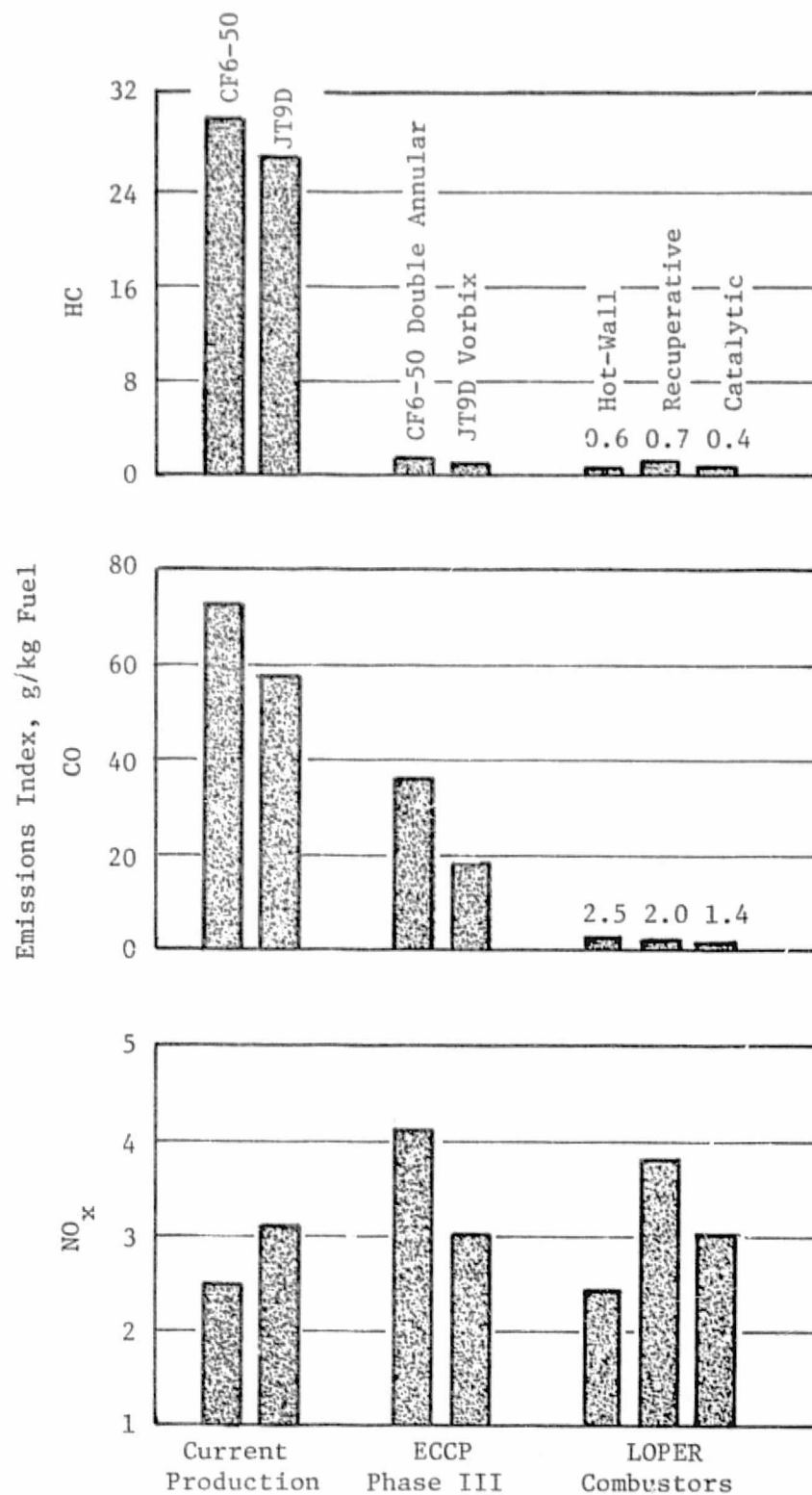


Figure 53. Comparison of Current Production, ECCP, and LOPER Combustor Idle Emission Levels.

Table XXI. Assessment of LOPER Combustor Design Concepts.

<u>Performance Parameter</u>	<u>Combustor Concept</u>		
	<u>Hot-Wall</u>	<u>Recuperative</u>	<u>Catalytic</u>
<u>Emissions</u>			
CO	1	1	1
HC	1	1	1
NO _x	1	2	1
<u>Aerothermal Performance</u>			
Combustion Efficiency	1	1	1
Pressure Drop	1	1	1
Ground Start	1	1	2
Lean Blowout	1	1	1
Altitude Relight	1	2	3
Exit Temperature Profile	1	1	1
Transient Operation	1	1	2
Resonance	2	2	2
<u>Mechanical Layout/Performance</u>			
Combustor Length	1	2	3
Weight	2	1	3
Liner Cooling	2	2	2
Durability of Emissions Reduction Feature	3	1	3

1 - Least Design Risk

2 - Moderate Design Risk

3 - Greater Design Risk or Unknown Risk

required to implement appropriate acoustic features into an impingement-cooled liner. Another aspect of aerothermal performance which is of some concern in the recuperative and catalytic concepts is ignition. No problems were encountered with ignition during screening or parametric tests of the LOPER concepts; in these tests, however, conditions were not typical of engine operation, since ignition was accomplished at elevated inlet temperature with a hydrogen torch.

Additional risk has been noted with respect to both the recuperative and catalytic combustors because of reduced swirler pressure drop, which could result in excessive ignition delay due to poorer fuel atomization and mixing at light-off conditions. Concern is especially acute regarding catalytic-concept light off because of the possibility of catalyst damage from the accumulation of fuel on the surfaces of the catalyst prior to ignition. This effect was observed in tests of a similar catalytic combustor concept described in Reference 8. In those tests, several catalysts were destroyed by the near-stoichiometric burning of fuel which had collected on the catalyst surface during the ignition delay period. The design risk with respect to transient operation is also increased with the catalytic concept because of potential catalyst damage due to overtemperature. Particular attention to acceleration fuel scheduling would be required in the implementation of the catalytic concept because of the increased fuel-air ratios at these conditions.

Increased design risk is apparent in all areas of mechanical performance. With respect to combustor length, both the recuperative and catalytic concepts indicated increased design risk. Based on screening test results with the recuperative concept, the sensitivity of emissions to forward dilution position indicated that the flame was elongated relative to the hot-wall combustor. This flame elongation appeared to be related to decreased mixing rates resulting from the reduced swirler pressure drop in this concept. With the catalytic concept, a further increase in length is probably required as a result of reduced swirler pressure drop, and also because of the need to introduce and thoroughly mix an increased quantity of primary dilution flow in order to obtain acceptable catalyst inlet temperature profiles. In the area of combustor weight, both the hot-wall and catalytic concepts require the use of ceramic materials (thermal barrier and catalyst substrate) in addition to the normal combustor components.

All three of the combustor concepts pose an increased design risk because of the use of impingement cooling. Although satisfactory results were obtained with impingement cooling in all screening and parametric tests, this cooling concept has not been used in actual engine applications. As in the introduction of any new concept, it is anticipated that fairly extensive development of impingement cooling will be required.

The final area of combustor mechanical performance rated in Table XX is the durability of the specific emissions-reduction feature used in each concept. In this area, the hot-wall combustor has been rated a high design risk primarily because of the limited experience which has been obtained

with ceramic coatings in combustion systems. Similarly, the catalytic combustor design risk is increased because of the question of catalyst durability. Although these features were rated as high risk, results of the LOPER test program were encouraging in that no significant durability problems were encountered with the thermal barrier coating, and catalyst durability problems were apparently resolved by the use of a modified catalyst-mounting technique in the final catalytic combustor test configurations.

APPENDIX A

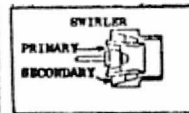
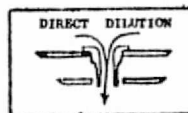
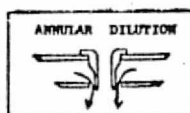
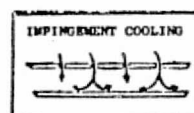
COMBUSTOR TEST CONFIGURATIONS

Detailed area/airflow distributions for each of the screening and parametric test configurations are presented in Tables XXII through XXIV. Axial locations of forward and aft dilution holes, measured from the swirler exit, are indicated below each table. Except as noted, dilution flow was equally distributed among nine dilution holes in both inner and outer liners, as shown in Figure 54.

Table XXII. Hot-Wall Combustor Area/Airflow Distributions.

CONFIGURATION	H1		H2		H3		H4		H5		H6		H7	
	A_e, cm^2	$W_e, \text{kg/s}$	A_e, cm^2	$W_e, \text{kg/s}$	A_e, cm^2	$W_e, \text{kg/s}$	A_e, cm^2	$W_e, \text{kg/s}$	A_e, cm^2	$W_e, \text{kg/s}$	A_e, cm^2	$W_e, \text{kg/s}$	A_e, cm^2	$W_e, \text{kg/s}$
IMPINGEMENT COOLING														
Dome	3.9	4.5	3.9	4.2	3.9	4.5	3.9	4.5	3.9	4.2	3.9	4.2	3.9	4.5
Fwd Outer Liner	7.7	8.7	7.7	8.0	7.7	8.7	7.7	8.7	7.7	8.2	7.7	8.1	7.7	8.7
Fwd Inner Liner	6.4	7.3	6.4	6.7	6.4	7.3	6.4	7.3	6.4	6.8	6.4	6.7	6.4	7.3
Aft Outer Liner	3.8	5.2	3.8	4.8	3.8	5.2	3.8	5.2	3.8	4.8	3.8	4.8	3.8	5.2
Aft Inner Liner	3.5	4.8	3.5	4.4	3.5	4.8	3.5	4.8	3.5	4.4	3.5	4.4	3.5	4.8
ANNULAR DILUTION (a)														
Fwd Outer - Row 1	2.5	2.7	2.5	2.5	0.0	0.0	1.1	1.2	1.0	1.2	1.0	1.2	1.1	1.2
- Row 2	0.0	0.0	0.0	0.0	2.5	2.7	1.4	1.5	0.4	0.5	0.4	0.5	1.4	1.5
Fwd Inner - Row 1	2.5	2.7	2.5	2.5	0.0	0.0	1.1	1.2	1.0	1.2	1.0	1.2	1.1	1.2
- Row 2	0.0	0.0	0.0	0.0	2.5	2.7	1.4	1.5	0.4	0.5	0.4	0.5	1.4	1.5
Aft Outer	11.2	12.5	11.2	11.6	11.2	12.5	11.2	12.5	11.2	12.5	11.2	12.5	11.2	12.5
Aft Inner	11.2	12.5	11.2	11.6	11.2	12.5	11.2	12.5	11.2	12.5	11.2	12.5	11.2	12.5
DIRECT DILUTION (a)														
Dome	0.0	0.0	0.0	0.0	0.0	0.0	0.0	0.0	0.0	0.0	3.1	5.2	0.0	0.0
Fwd Outer - Row 1	2.0	3.6	2.0	3.3	0.0	0.0	0.9 (b)	1.6 (b)	1.4	2.3	0.0	0.0	0.9 (b)	1.6 (b)
- Row 2	0.0	0.0	0.0	0.0	2.0	3.6	1.1 (c)	2.0 (c)	2.0	3.5	2.0	3.5	1.1 (c)	2.0 (c)
Fwd Inner - Row 1	2.0	3.6	2.0	3.3	0.0	0.0	0.9 (b)	1.6 (b)	1.4	2.3	0.0	0.0	0.9 (b)	1.6 (b)
- Row 2	0.0	0.0	0.0	0.0	2.0	3.6	1.1 (c)	2.0 (c)	2.0	3.5	2.0	3.5	1.1 (c)	2.0 (c)
Aft Outer	13.2	23.2	13.2	21.4	13.2	23.2	13.2	23.2	13.2	22.3	13.2	22.1	13.2	23.2
Aft Inner	13.2	23.2	13.2	21.4	13.2	23.2	13.2	23.2	13.2	22.3	13.2	22.1	13.2	23.2
SWIRLER														
Primary	3.6	6.2	3.6	5.8	3.6	6.2	3.6	6.2	3.6	6.0	3.6	6.0	3.6	6.2
Secondary	5.6	9.8	10.3	16.6	5.6	9.8	5.6	9.8	5.6	9.4	5.6	9.3	5.6	9.8
TOTALS														
Swirler		16.0		22.4		16.0		16.0		15.4		15.3		16.0
Fwd Dilution		12.6		11.6		12.6		12.6		15.0		14.6		12.6
Aft Dilution		71.4		66.0		71.4		71.4		69.6		69.2		71.4

- (a) Dilution Hole Axial Positions: Fwd Row 1, $L = 3.8 \text{ cm}$ ($L/H_d = 0.5$); Fwd Row 2, $L = 7.6 \text{ cm}$ ($L/H_d = 1.0$); Aft Dilution, $L = 21.6 \text{ cm}$ ($L/H_d = 2.8$)
 (b) Circumferential Position in Line with Fuel Injectors
 (c) Circumferential Position Between Fuel Injectors



ORIGINAL PAGE IS
OF POOR QUALITY

Table XXIII. Recuperative Combustor Area/Airflow Distributions.

CONFIGURATION	X1	X2	X3	X4	X5	X6	X7	X8	X9	X10	X11	X12	X13	X14	X15	X16	X17
	A_0, cm^2	A_0, cm^2	A_0, cm^2	A_0, cm^2	A_0, cm^2	A_0, cm^2	A_0, cm^2	A_0, cm^2	A_0, cm^2	A_0, cm^2	A_0, cm^2	A_0, cm^2	A_0, cm^2	A_0, cm^2	A_0, cm^2	A_0, cm^2	A_0, cm^2
RECUPERATIVE COOLING																	
Down	2.9	2.1	2.9	2.9	2.9	2.9	2.9	2.9	2.9	2.9	2.9	2.9	2.9	2.9	2.9	2.9	2.9
Fed Outer Liner	7.7	9.9	7.7	7.7	7.7	7.7	7.7	7.7	7.7	7.7	7.7	7.7	7.7	7.7	7.7	7.7	7.7
Fed Inner Liner	2.4	2.3	2.4	2.4	2.4	2.4	2.4	2.4	2.4	2.4	2.4	2.4	2.4	2.4	2.4	2.4	2.4
Air Outer Liner	2.8	4.5	2.8	2.8	2.8	2.8	2.8	2.8	2.8	2.8	2.8	2.8	2.8	2.8	2.8	2.8	2.8
Air Inner Liner	2.5	4.5	2.5	2.5	2.5	2.5	2.5	2.5	2.5	2.5	2.5	2.5	2.5	2.5	2.5	2.5	2.5
APICAL DILUTION (a)																	
Fed Outer - Row 1	4.7	5.2	4.7	4.7	4.7	4.7	4.7	4.7	4.7	4.7	4.7	4.7	4.7	4.7	4.7	4.7	4.7
Fed Outer - Row 2	0.0	0.0	0.0	0.0	0.0	0.0	0.0	0.0	0.0	0.0	0.0	0.0	0.0	0.0	0.0	0.0	0.0
Fed Inner - Row 1	4.7	5.2	4.7	4.7	4.7	4.7	4.7	4.7	4.7	4.7	4.7	4.7	4.7	4.7	4.7	4.7	4.7
Fed Inner - Row 2	0.0	0.0	0.0	0.0	0.0	0.0	0.0	0.0	0.0	0.0	0.0	0.0	0.0	0.0	0.0	0.0	0.0
Air Outer	2.4	2.9	2.4	2.4	2.4	2.4	2.4	2.4	2.4	2.4	2.4	2.4	2.4	2.4	2.4	2.4	2.4
Air Inner	2.4	2.9	2.4	2.4	2.4	2.4	2.4	2.4	2.4	2.4	2.4	2.4	2.4	2.4	2.4	2.4	2.4
EXHAUST DILUTION (a)																	
Down	0.0	0.0	0.0	0.0	0.0	0.0	0.0	0.0	0.0	0.0	0.0	0.0	0.0	0.0	0.0	0.0	0.0
Fed Outer - Row 1	0.0	0.0	0.0	0.0	0.0	0.0	0.0	0.0	0.0	0.0	0.0	0.0	0.0	0.0	0.0	0.0	0.0
Fed Outer - Row 2	0.0	0.0	0.0	0.0	0.0	0.0	0.0	0.0	0.0	0.0	0.0	0.0	0.0	0.0	0.0	0.0	0.0
Fed Inner - Row 1	0.0	0.0	0.0	0.0	0.0	0.0	0.0	0.0	0.0	0.0	0.0	0.0	0.0	0.0	0.0	0.0	0.0
Fed Inner - Row 2	0.0	0.0	0.0	0.0	0.0	0.0	0.0	0.0	0.0	0.0	0.0	0.0	0.0	0.0	0.0	0.0	0.0
Air Outer	12.2	23.7	12.2	12.2	12.2	12.2	12.2	12.2	12.2	12.2	12.2	12.2	12.2	12.2	12.2	12.2	12.2
Air Inner	12.2	23.7	12.2	12.2	12.2	12.2	12.2	12.2	12.2	12.2	12.2	12.2	12.2	12.2	12.2	12.2	12.2
EXHAUST																	
Primary	2.6	3.2	2.6	2.6	2.6	2.6	2.6	2.6	2.6	2.6	2.6	2.6	2.6	2.6	2.6	2.6	2.6
Secondary	10.5	11.4	10.5	10.5	10.5	10.5	10.5	10.5	10.5	10.5	10.5	10.5	10.5	10.5	10.5	10.5	10.5
TOTAL FLUXES																	
Exhaust	15.3	15.3	15.3	15.3	15.3	15.3	15.3	15.3	15.3	15.3	15.3	15.3	15.3	15.3	15.3	15.3	15.3
Fed Dilution	11.0	11.0	11.0	11.0	11.0	11.0	11.0	11.0	11.0	11.0	11.0	11.0	11.0	11.0	11.0	11.0	11.0
Air Dilution	72.3	72.3	72.3	72.3	72.3	72.3	72.3	72.3	72.3	72.3	72.3	72.3	72.3	72.3	72.3	72.3	72.3

(a) Dilution Ratio: Fed Row 1, $L = 2.5$ cm ($L/H = 0.5$); Fed Row 2, $L = 7.5$ cm ($L/H = 1.5$); Air Dilution, $L = 21.5$ cm ($L/H = 2.5$)

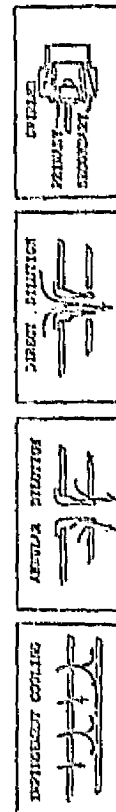
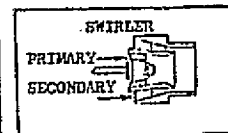
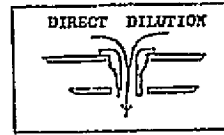
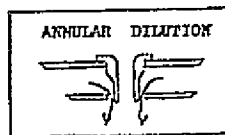
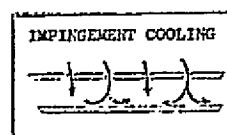


Table XXIV. Catalytic Combustor Area/Airflow Distributions.

CONFIGURATION	C1		C2		C3		C4		C5/6		C7	
	A_e, cm^2	$W_x, \% W_c$	A_e, cm^2	$W_x, \% W_c$	A_e, cm^2	$W_x, \% W_c$	A_e, cm^2	$W_x, \% W_c$	A_e, cm^2	$W_x, \% W_c$	A_e, cm^2	$W_x, \% W_c$
<u>IMPINGEMENT COOLING</u>												
Dome	3.9	2.9	3.9	3.0	3.9	2.9	3.9	3.0	3.9	3.6	3.9	3.8
Fwd Outer Liner	5.7	4.3	5.7	4.3	5.7	4.3	5.7	4.3	7.7	7.0	7.7	7.5
Fwd Inner Liner	4.0	3.0	4.0	3.0	4.0	3.0	4.0	3.0	6.4	5.8	6.4	6.2
Aft Outer Liner	3.8	5.4	3.8	6.7	3.8	5.4	3.8	6.7	3.8	5.4	3.8	5.1
Aft Inner Liner	3.5	5.1	3.5	6.3	3.5	5.1	3.5	6.3	3.5	5.2	3.5	4.9
<u>ANNULAR DILUTION^(a)</u>												
Fwd Outer - Row 1	7.0	5.1	7.1	5.2	7.0	5.1	7.1	5.2	1.0	0.5	1.0	0.5
- Row 2	0.0	0.0	0.0	0.0	0.0	0.0	0.0	0.0	14.3	7.7	14.3	8.2
Fwd Inner - Row 1	7.0	5.1	7.0	5.2	7.0	5.1	7.0	5.2	1.0	0.5	1.0	0.5
- Row 2	0.0	0.0	0.0	0.0	0.0	0.0	0.0	0.0	14.3	7.7	14.3	8.2
Aft Outer	4.6	5.4	4.7	6.7	4.6	5.4	4.7	6.7	4.6	5.4	4.6	5.1
Aft Inner	4.6	5.1	4.7	6.3	4.6	5.1	4.7	6.3	4.6	5.2	4.6	4.9
<u>DIRECT DILUTION^(a)</u>												
Fwd Outer - Row 1	15.2	15.9	32.9	31.2	15.2	15.9	32.9	31.2	4.9	5.2(b)	4.9	5.6 (b)
- Row 2	0.0	0.0	0.0	0.0	0.0	0.0	0.0	0.0	3.5	3.7(b)	3.5	4.0 (b)
Fwd Inner - Row 1	8.0	8.5	15.2	16.1	8.0	8.5	15.2	16.1	4.9	5.2(b)	4.9	5.5 (b)
- Row 2	0.0	0.0	0.0	0.0	0.0	0.0	0.0	0.0	3.5	3.7(b)	3.5	3.9 (b)
Aft Outer	10.9	20.2	3.3	7.4	10.9	20.2	3.3	7.4	10.9	20.1	10.9	18.8
Aft Inner	10.9	20.2	3.3	7.4	10.9	20.2	3.3	7.4	10.9	20.1	10.9	18.8
<u>SWIRLER</u>												
Primary	3.6	3.7	3.6	3.8	3.6	3.7	3.6	3.8	3.6	3.8	3.6	3.8
Secondary	10.3	10.8	10.3	10.8	10.3	10.8	10.3	10.8	10.8	11.4	10.8	12.2
<u>TOTAL FLOWS</u>												
Swirler		14.5		14.6		14.5		14.6		15.2		16.2
Fwd Dilution		34.8		57.7		34.8		57.7		33.9		36.4
Aft Dilution		50.9		27.7		50.9		27.7		50.8		47.6
Total Catalyst		49.1		72.3		49.1		72.3		49.1		52.8

(a) Dilution Axial Positions as Shown in Figure 34
 (b) 0.5% W_c Added Adjacent to Sidewalls



ORIGINAL PAGE IS
OF POOR QUALITY

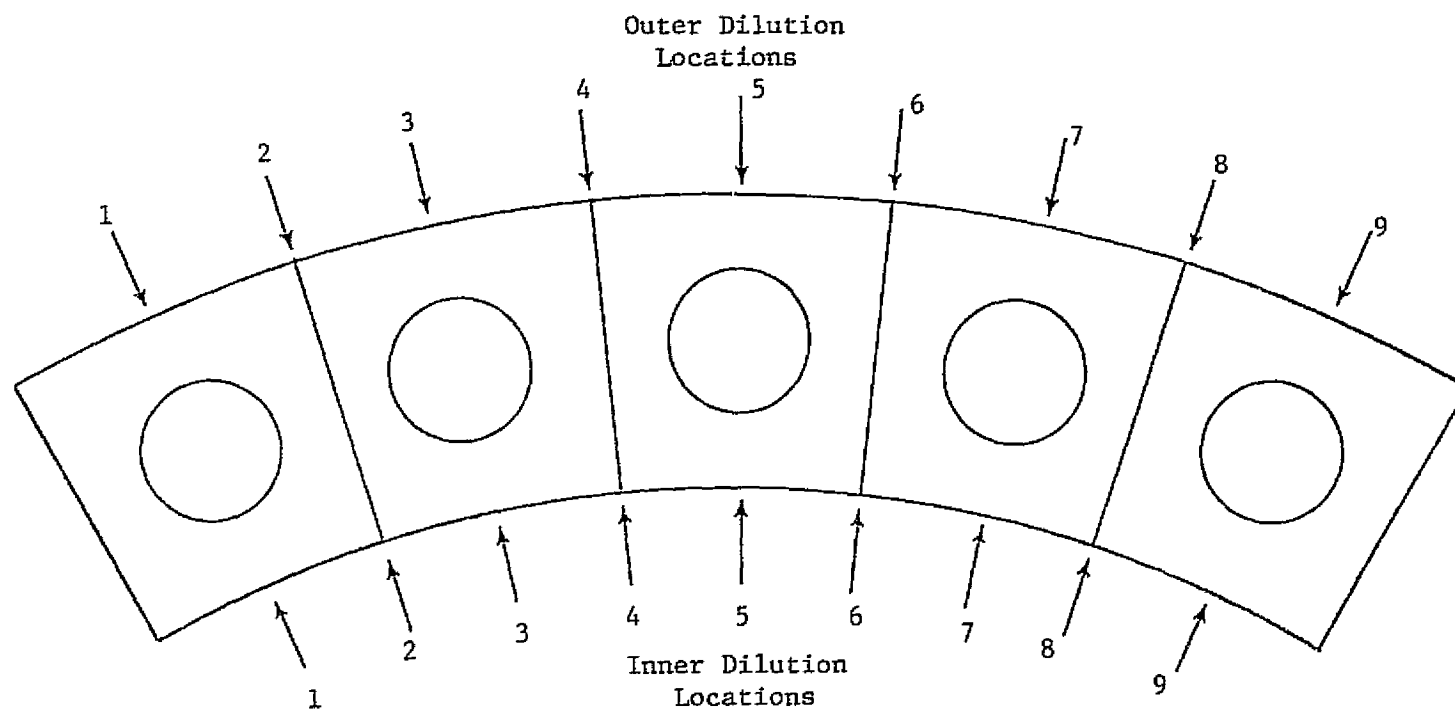


Figure 54. Dilution Hole Circumferential Locations.

APPENDIX B

COMBUSTOR TEST RESULTS

Hot-wall combustor screening and parametric test results are presented in Tables XXV through XXXI; recuperative combustor test results are summarized in Tables XXXII through XXXVIII; and catalytic combustor test results are found in Tables XXXIX through XLV.

Table XXV. Test Summary, Combustor Configuration H1, Runs 4 and 5.

Reading	Test Point	Inlet Total Pressure, kPa	Inlet Total Temperature, K	Inlet Humidity, g H ₂ O/kg Air	Combustor Air Flow, kg/s	Reference Velocity, m/s	Fuel Flow, g/s	Heated Fuel-Air Ratio, g/kg	Sample Fuel-Air Ratio/Heated Fuel-Air Ratio	Thermocouple Combustion Efficiency, %	Sample Combustion Efficiency, %	CO Emission Index, g/kg	HC Emission Index, g/kg	NO _x Emission Index, g/kg	CO ₂ Volume, %	Thermocouple Average Exit Temperature, K	Pattern Factor	Maximum Liner Temperature, K	Total Pressure Loss, %	Demo Pressure Loss, %	Fuel Nozzle Pressure Drop, kPa	Avg. Catalyst Inlet Temp. (Catalytic), K Swirl Inlet Temp. (Reoperative), K or Avg. Liner Temp. (Hot Wall), K*
1	221	363.	425.	4.3	1.61	23.2	12.8	7.9	0.90	97.5	99.3	11.0	4.2	1.4	1.48	733.	0.24	932.	4.54	4.58	493.	785.
2	222	366.	422.	4.3	1.60	22.8	16.6	10.4	0.92	93.8	99.7	2.6	2.4	3.1	1.78	803.	0.18	1247.	5.19	5.10	815.	725.
3	223	365.	422.	4.3	1.60	22.6	20.6	12.9	0.89	93.1	99.6	9.7	1.3	4.7	2.39	808.	0.21	1095.	5.88	5.28	1291.	1016.
4	121	263.	366.	4.3	1.23	23.0	9.8	8.0	0.90	90.2	90.6	108.1	88.7	1.1	1.32	658.	0.31	904.	5.78	5.26	239.	737.
5	122	263.	365.	4.4	1.23	22.8	12.9	10.5	0.76	90.7	99.6	6.9	2.5	1.7	1.66	743.	0.26	931.	6.42	5.99	496.	916.
6	123	262.	368.	4.4	1.24	23.2	16.1	13.0	0.74	90.6	99.4	22.0	1.2	2.9	2.00	831.	0.28	932.	7.50	6.53	767.	932.
7	125	261.	366.	1.9	1.25	23.5	11.4	9.3	0.84	96.0	99.3	13.6	3.6	1.4	1.62	724.	0.27	372.	7.56	5.57	437.	672.
** 8	122	201.	368.	1.7	1.20	23.4	12.9	10.4	0.81	91.7	99.5	9.5	3.1	1.8	1.74	747.	0.34	903.	6.51	5.81	519.	903.
9	126	202.	368.	1.9	1.24	23.2	14.1	11.4	0.74	90.5	99.4	14.3	2.2	2.8	1.75	775.	0.31	917.	6.83	5.95	615.	917.
10	132	203.	367.	1.6	1.63	30.4	16.9	10.4	0.67	99.4	99.6	10.8	1.4	1.5	1.87	777.	0.26	858.	10.89	9.19	663.	856.
11	131	263.	367.	1.7	1.61	30.6	14.6	9.1	0.91	92.5	97.0	62.9	15.5	1.9	1.64	703.	0.20	754.	9.68	9.01	635.	754.
12	133	265.	366.	1.7	1.61	30.1	21.0	13.0	0.55	91.5	97.8	62.2	7.3	3.2	1.44	842.	0.36	872.	11.57	10.36	1331.	872.

* Avg Liner Temp based on Single Thermocouple Mounted on Outer Liner, between Cups 2 and 3,

5 cm. Aft of Primary Dilution

** Single Ganged Sample, Includes Rakes 1 and 7.

Table XXVI. Test Summary, Combustor Configuration H2, Run 11.

Table XXVI. Test Summary, Combustor Configuration H2, Run 11.																								
Reading	Test Point	Inlet Total Pressure, kPa	Inlet Total Temperature, K	Inlet Humidity, g H ₂ O/kg Air	Combustor Air Flow, kg/s	Reference Velocity, m/s	Fuel Flow, g/s	Metered Fuel-Air Ratio, g/kg	Sample Fuel-Air Ratio/Metered Fuel-Air Ratio	Thermocouple Combustion Efficiency, %	Sample Combustion Efficiency, %	CO Emission Index, g/kg	HC Emission Index, g/kg	NO Emission Index, g/kg	CO ₂ Volume, %	Thermocouple Average Exit Temperature, K	Pattern Factor	Maximum Liner Temperature, K	Total Pressure Loss, %	Dome Pressure Loss, %	Fuel Nozzle Pressure Drop, kPa	Avg. Catalyst Inlet Temp. (Catalytic), K Swirl Inlet Temp. (Recuperative), K or Avg. Liner Temp. (Hot Wall), K	Comments	
1	202	307, 422	1.0	0.75	10.6	8.3	11.1	1.07	107.1	99.8	1.8	1.5	2.7	2.49	886	0.20	1135	1.12	0.88	400	999			
2	202	304, 423	1.7	0.74	10.6	7.8	10.5	1.05	107.1	99.8	3.0	1.5	2.3	2.31	864	0.21	1132	0.91	0.89	340	979			
3	203	305, 423	1.8	0.74	10.6	9.7	13.1	1.04	105.2	99.9	2.6	0.9	4.1	2.86	956	0.23	1132	1.13	0.89	540	1039			
4	204	304, 421	2.4	0.74	10.6	11.4	15.4	1.04	105.0	99.8	5.3	1.0	4.8	3.41	1043	0.18	1068	1.13	0.89	750	956			
5	201	305, 422	2.4	0.74	10.6	6.9	9.3	1.03	95.1	91.1	76.3	71.0	1.3	1.78	770	0.30	807	0.91	0.89	264	623			
6	205	302, 423	2.5	0.74	10.6	7.1	9.7	1.05	100.2	98.4	39.3	26.4	1.6	2.03	804	0.23	879	0.91	0.90	288	664			
7	206	311, 419	2.7	0.87	12.2	9.5	10.9	1.00	102.7	99.4	9.0	3.5	2.0	2.26	856	0.23	1029	0.89	1.09	499	741	Resonance Above f = 11.0 g/kg		
8	207	307, 424	3.6	0.87	12.3	8.6	9.9	1.02	102.3	98.2	28.6	11.4	1.8	2.07	824	0.25	1008	0.90	1.10	421	643			
9	112	203, 370	3.0	0.78	14.5	8.5	10.9	0.95	86.8	85.9	86.9	121.1	1.2	1.81	746	0.30	779	1.70	1.83	400	552			
10	113	204, 369	3.4	0.78	14.5	10.7	13.8	0.95	99.5	99.1	13.3	5.6	2.2	2.70	903	0.17	944	1.69	1.99	627	725			
11	114	212, 366	3.6	0.77	13.8	11.9	15.5	0.86	94.9	99.3	15.3	3.1	2.7	2.79	934	0.18	966	1.63	1.92	785	786	Increased Pressure to Avoid Resonance		

ORIGINAL PAGE IS
OF POOR QUALITY

Table XXVII. Test Summary, Combustor Configuration H3, Run 18.

Reading	Test Point	Inlet Total Pressure, kPa	Inlet Total Temperature, K	Inlet Humidity, g H ₂ O/kg Air	Combustor Air Flow, kg/s	Reference Velocity, m/s	Fuel Flow, g/s	Metered Fuel-Air Ratio Ratio, g/kg	Sample Fuel-Air Ratio/Metered Fuel-Air Ratio	Thermocouple Combustion Efficiency, %	Sample Combustion Efficiency, %	CO Emission Index, g/kg	HC Emission Index, g/kg	NO Emission Index, g/kg	CO ₂ Volume, %	Thermocouple Average Exit Temperature, K	Pattern Factor	Maximum Liner Temperature, K	Total Pressure Loss, %	Dome Pressure Loss, %	Fuel Nozzle Pressure Drop, kPa	Avg. Catalyst Inlet Temp. (Catalytic), K	Swirl Inlet Temp. (Recoverative), K	or Avg. Liner Temp. (Hot Wall), K
1	202	306	425	2.1	0.73	10.4	8.2	11.3	0.98	99.1	99.9	2.3	0.6	4.5	2.32	862	0.19	1143	1.12	1.01	352	1080		
2	201	303	423	2.1	0.73	10.5	6.9	9.4	1.01	99.5	99.9	1.7	0.8	4.0	1.99	793	0.24	1130	0.91	1.02	245	1028		
3	200	309	423	2.1	0.74	10.4	5.9	8.0	0.99	97.9	99.6	11.1	1.5	3.5	1.63	734	0.25	1111	0.89	0.99	171	982		
4	221	307	424	3.6	1.6	22.1	12.8	8.2	0.96	96.3	99.8	7.1	0.6	2.6	1.65	739	0.24	1163	4.71	4.52	834	992		
5	222	306	421	2.7	1.56	22.1	16.7	10.8	0.95	96.3	99.9	1.9	0.3	4.8	2.14	827	0.22	1211	4.74	4.54	1442	1093		
6	223	306	422	2.4	1.56	22.1	20.8	13.4	0.93	91.5	99.8	7.1	0.2	4.4	2.61	894	0.24	1190	4.72	4.54	2304	1109		
7	131	202	368	2.4	1.60	30.1	13.1	8.2	0.92	94.2	98.0	64.2	5.0	1.6	1.51	677	0.21	1045	10.94	10.21	857	915		
8	132	204	366	2.4	1.61	29.8	16.6	10.3	0.92	95.4	99.8	7.4	0.4	2.4	1.97	758	0.19	1139	10.49	10.06	1358	1018		
9	133	201	366	2.3	1.61	30.2	18.7	11.6	0.94	95.7	99.8	8.4	0.4	2.5	2.29	806	0.22	1146	10.98	10.45	1685	1151		
10	135	201	367	2.3	1.60	30.0	14.9	9.3	0.90	94.9	99.6	16.4	0.7	2.0	1.74	721	0.21	1113	10.98	10.28	1085	984		
11	113	202	365	1.6	0.79	14.7	10.7	13.5	0.93	97.1	99.7	12.1	0.5	3.4	2.62	877	0.18	1043	4.77	2.34	601	986		
12	114	200	367	1.4	0.79	14.9	12.1	14.1	0.95	96.9	99.4	24.3	0.4	3.7	3.18	947	0.18	1017	3.11	2.34	532	962		

* REDUCED V_T TO 22.9 m/sec (120 SERIES TEST POINTS), ENCOUNTERED RESONANCE AT < 7.5 g/kg

ORIGINAL PAGE IS
OF POOR QUALITY

RESONANCE
 $V_T > 11$ m/secRESONANCE
 $V_T < 21$ m/secRESONANCE
 $f_M > 12$ g/kgRESONANCE
 $f_M < 13$ g/kg

Table XXVIII. Test Summary, Combustor Configuration H4, Run 19.

Reading	Test Point	Inlet Total Pressure, kPa	Inlet Total Temperature, K	Inlet Humidity, ρ H ₂ O/kg Air	Combustor Air Flow, kg/s	Reference Velocity, m/s	Fuel Flow, g/s	Metered Fuel-Air Ratio Ratio, g/kg	Sample Fuel-Air Ratio/Metered Fuel-Air Ratio	Thermocouple Combustion Efficiency, %	Sample Combustion Efficiency, %	CO Emission Index, g/kg	HC Emission Index, g/kg	NO Emission Index, g/kg	CO ₂ Volume, %	Thermocouple Average Exit Temperature, K	Pattern Factor	Maximum Liner Temperature, K	Total Pressure Loss, %	Door Pressure Loss, %	Fuel Nozzle Pressure Drop, kPa	Avg. Catalyst Inlet Temp. (Catalytic), K	Swirl Inlet Temp. (Re recuperative), K	or Avg. Liner Temp. (Hot Wall), K
1	221	302.	423.	3.0	1.59	23.0	12.8	8.0	1.05	99.2	99.8	4.1	1.0	1.0	1.75	740.	0.30	971.	5.25	4.58	867.	848.	RESONANCE $V_T < 23$ m/sec	
2	222	305.	423.	3.1	1.66	23.7	16.7	10.1	0.99	96.9	99.9	1.3	0.5	2.7	2.09	807.	0.25	1108.	5.21	4.98	1444.	990.		
3	223	305.	423.	2.9	1.64	23.8	20.8	12.5	0.97	94.5	99.9	4.9	0.3	4.1	2.55	882.	0.22	1130.	5.21	5.00	1864.	1031.		
4	232	307.	421.	3.0	2.05	29.0	21.7	10.6	0.94	94.2	99.9	2.5	0.5	2.7	2.07	811.	0.24	1201.	8.30	7.55	1862.	1007.	RESONANCE $f_M > 12.5$ g/kg	
5	132	202.	367.	3.0	1.62	30.3	17.1	10.6	0.99	95.7	99.8	6.7	0.6	1.5	2.18	769.	0.27	1076.	11.27	9.90	1374.	828.		
6	135	203.	366.	3.0	1.61	30.0	15.1	9.4	0.97	90.4	96.2	44.4	27.4	1.1	1.80	705.	0.36	1022.	11.54	9.83	1104.	754.		
7	136	204.	366.	2.6	1.62	30.0	19.5	12.1	0.98	95.5	99.7	9.4	0.4	2.0	2.46	819.	0.26	1030.	10.82	9.80	1751.	813.	RESONANCE $V_T < 27.5$ m/sec	
8	142	205.	368.	2.4	1.50	27.9	15.8	10.5	0.97	96.2	99.9	4.7	0.5	1.7	2.12	769.	0.28	1066.	10.45	8.19	1206.	829.		
9	111	204.	368.	1.9	0.77	14.3	6.7	8.8	1.01	96.5	98.6	30.1	7.0	1.6	1.81	706.	0.36	942.	3.38	2.33	228.	815.	RESONANCE $f_M > 9$ g/kg	

Table XXIX. Test Summary, Combustor Configuration H5, Runs 20 and 21.

Reading	Test Point	Inlet Total Pressure, kPa	Inlet Total Temperature, K	Inlet Humidity, g H ₂ O/kg Air	Combustor Air Flow, kg/s	Reference Velocity, m/s	Fuel Flow, g/s	Metered Fuel-Air Ratio, g/kg	Sample Fuel-Air Ratio/Metered Fuel-Air Ratio	Thermocouple Combustion Efficiency, %	Sample Combustion Efficiency, %	CO Emission Index, g/kg	HC Emission Index, g/kg	NO Emission Index, g/kg	CO ₂ Volume, %	Thermocouple Average Exit Temperature, K	Pattern Factor	Maximum Liner Temperature, K	Total Pressure Loss, %	Dome Pressure Loss, %	Fuel Nozzle Pressure Drop, kPa	Avg. Catalyst Inlet Temp. (Catalytic), K Swirl Inlet Temp. (Re recuperative), K or Avg. Liner Temp. (Hot Wall), K
1	223	303.	422.	1.0	1.69	24.2	20.8	12.4	0.93	96.1	99.9	2.7	0.7	4.2	2.41	883.	0.20	1183.	4.72	4.69	*	1081.
2	222	304.	423.	1.0	1.67	23.9	16.8	10.0	0.95	97.2	99.9	1.4	0.7	2.9	1.99	806.	0.22	1098.	5.41	4.56	1311.	1030.
3	221	304.	421.	1.0	1.67	23.9	12.8	7.7	1.00	96.0	97.2	28.2	21.5	1.3	1.53	715.	0.28	1001.	5.21	4.56	1049.	917.
4	225	304.	421.	1.1	1.67	23.9	14.6	8.7	0.98	99.8	99.9	2.1	0.9	2.0	1.78	767.	0.22	1059.	5.21	4.56	1049.	986.
5	232	302.	425.	1.2	2.03	29.5	21.6	10.6	0.93	94.5	99.9	1.7	0.6	2.8	2.07	819.	0.21	1112.	8.00	7.13	*	1019.
6	111	202.	369.	0.9	0.81	15.2	6.8	8.4	1.03	84.6	84.8	108.6	127.0	1.2	1.47	654.	0.48	963.	1.71	2.18	228.	839.
7	132	202.	366.	0.9	1.63	30.4	17.0	10.5	1.00	97.8	99.4	16.2	2.7	1.4	2.17	772.	0.21	1083.	10.25	8.98	1366.	961.
8	132	201.	368.	0.8	1.65	31.1	17.2	10.4	1.00	96.8	99.3	18.6	2.9	1.5	2.14	768.	0.22	1097.	10.62	9.34	1513.	979.
9	133	205.	370.	1.0	1.67	31.1	21.2	12.7	0.98	96.1	99.6	13.1	1.1	2.1	2.58	847.	0.23	1147.	11.08	9.40	*	1029.
10	134	205.	370.	1.3	1.68	31.1	25.3	15.1	0.96	92.8	99.1	36.7	0.6	2.6	2.98	912.	0.28	1157.	10.41	9.40	*	1047.
11	135	203.	369.	1.3	1.67	31.2	19.1	11.5	0.96	90.3	97.5	32.5	17.6	1.7	2.22	777.	0.33	1059.	11.87	9.49	1407.	961.

* Off Scale

** Low Fuel Pressure, Post Run Inspection Revealed No. 1 Nozzle Leak.

ORIGINAL PAGE IS
OF POOR QUALITY

Table XXX. Test Summary, Combustor Configuration H6, Run 22.

Reading	Test Point	Inlet Total Pressure, kPa	Inlet Total Temperature, K	Inlet Humidity, g H ₂ O/kg Air	Combustor Air Flow, kg/s	Reference Velocity, m/s	Fuel Flow, g/s	Metered Fuel-Air Ratio, g/kg	Sample Fuel-Air Ratio/Metered Fuel-Air Ratio	Thermocouple Combustion Efficiency, %	Sample Combustion Efficiency, %	CO Emission Index, g/kg	HC Emission Index, g/kg	NO Emission Index, g/kg	CO ₂ Volume, %	Thermocouple Average Exit Temperature, K	Pattern Factor	Maximum Liner Temperature, K	Total Pressure Loss, %	Dome Pressure Loss, %	Fuel Nozzle Pressure Drop, kPa	Avg. Catalyst Inlet Temp. (Catalytic), K Swirl Inlet Temp. (Heater), K or Avg. Liner Temp. (Hot Wall), K
1	112	203.	368.	6.1	0.77	14.4	8.7	11.3	0.93	99.9	98.6	26.5	7.7	2.9	2.17	813.	0.24	936.	2.04	1.83	496.	869.
2	222	302.	422.	6.1	1.63	23.4	16.7	10.3	1.02	96.3	99.7	7.2	1.2	2.9	2.21	811.	0.24	1073.	4.34	4.21	1693.	907.
3	223	303.	420.	5.6	1.73	24.7	19.9	11.3	0.95	95.5	99.8	6.2	0.6	3.2	2.29	848.	0.19	1063.	4.55	4.75	*	923.
4	222	307.	422.	5.1	1.74	24.6	16.7	9.6	1.01	96.0	99.9	3.3	0.5	2.9	2.03	786.	0.22	1050.	4.49	4.68	1598.	877.
5	221	303.	421.	4.8	1.75	25.1	14.7	8.4	1.03	98.8	99.6	14.2	1.0	2.2	1.81	752.	0.22	1003.	4.56	4.76	1258.	836.
6	220	302.	423.	4.8	1.73	24.9	13.3	7.7	1.01	92.3	94.2	65.2	42.5	1.8	1.50	766.	0.27	936.	4.57	4.77	1025.	780.
7	232	303.	422.	4.4	2.17	31.2	22.2	10.2	0.92	93.9	99.9	0.7	0.8	2.6	1.97	799.	0.18	998.	7.75	7.78	*	877.
8	233	305.	423.	4.4	2.17	31.1	27.7	12.0	0.95	95.6	99.9	3.1	0.6	3.4	2.54	895.	0.16	1066.	7.92	7.67	*	954.
9	231	305.	423.	4.3	2.17	31.0	16.8	7.7	0.88	95.2	98.6	48.4	3.2	1.6	1.38	715.	0.19	878.	8.13	7.65	1428.	700.
10	132	202.	367.	4.3	1.65	30.9	17.2	10.4	0.84	96.5	99.6	13.7	1.0	1.8	1.83	767.	0.22	914.	8.88	8.89	1469.	808.
11	133	202.	367.	3.8	1.65	30.8	19.7	12.0	0.87	96.3	99.8	7.5	0.5	2.1	2.17	822.	0.19	942.	8.88	8.89	1931.	844.
12	131	202.	367.	3.8	1.64	30.7	14.7	8.4	0.90	97.2	97.9	60.8	6.6	1.7	1.61	715.	0.22	829.	8.88	8.89	1062.	737.
13	102	203.	368.	3.6	0.61	11.4	6.7	10.4	1.01	100.8	77.2	32.3	20.4	1.8	2.23	804.	0.19	959.	1.36	1.25	119.	802.
14	103	201.	368.	3.4	0.61	11.5	8.0	13.2	1.00	101.7	98.0	18.9	15.7	3.0	2.71	891.	0.17	984.	1.72	1.27	249.	891.

* Off Scale

ORIGINAL PAGE IS
OF POOR QUALITY

Table XXXI. Test Summary, Combustor Configuration H7, Run 27.

Reading	Test Point	Inlet Total Pressure, kPa	Inlet Total Temperature, K	Inlet Humidity, g H ₂ O/kg Air	Combustor Air Flow, kg/s	Reference Velocity, m/s	Fuel Flow, g/s	Metered Fuel-Air Ratio, g/kg	Sample Fuel-Air Ratio/Metered Fuel-Air Ratio	Thermocouple Combustion Efficiency, %	Sample Combustion Efficiency, %	CO Emission Index, g/kg	HC Emission Index, g/kg	NO _x Emission Index, g/kg	CO ₂ Volume, %	Thermocouple Average Exit Temperature, K	Pattern Factor	Maximum Liner Temperature, K	Total Pressure Loss, N	Dome Pressure Loss, %	Fuel Nozzle Pressure Drop, kPa	Avg. Catalyst Inlet Temp. (Catalytic), K Swirl Inlet Temp. (Re recuperative), K or Avg. Liner Temp. (Hot Wall), K	Comments (Operating Limits)
1	221	303.	424.	3.6	1.55	22.3	12.9	8.3	0.92	87.6	95.1	40.8	39.6	1.1	1.51	713.	0.34	920.	3.64	4.70	769.	789.	Resonance Vr < 24.5 m/s
2	242	303.	423.	3.3	1.86	26.8	20.5	11.0	0.88	92.1	99.9	2.1	0.6	2.9	2.02	819.	0.18	1031.	5.92	6.60	1796.	920.	
3	241	305.	422.	3.4	1.87	26.7	19.7	8.4	0.92	91.7	98.9	32.2	3.9	1.1	1.58	727.	0.23	877.	6.78	6.55	1056.	802.	
4	245	303.	422.	3.3	1.87	26.8	18.1	9.7	0.93	92.5	99.8	4.1	0.7	2.0	1.87	775.	0.22	972.	6.37	6.60	1410.	869.	
5	243	306.	423.	3.3	1.67	26.7	25.5	13.6	0.92	91.5	99.8	6.3	0.4	3.9	2.61	903.	0.20	1074.	6.99	6.43	1802.	978.	
6	222	301.	424.	3.1	1.70	24.6	18.3	10.8	0.93	91.9	99.9	2.5	0.4	2.8	2.10	811.	0.21	1040.	5.73	5.52	1426.	924.	No Limit Encountered
7	232	303.	423.	3.0	2.05	29.4	22.4	10.9	0.94	91.7	99.9	1.9	0.3	2.6	2.16	814.	0.20	1020.	8.42	7.94	1865.	907.	
8	253	306.	423.	3.0	2.45	29.2	27.7	13.5	0.94	92.4	99.8	5.9	0.2	3.7	2.65	903.	0.22	1076.	8.78	7.85	1802.	965.	
9	231	302.	423.	2.9	2.04	29.5	17.0	8.3	0.89	89.6	90.3	48.7	5.9	1.1	1.51	719.	0.23	863.	8.21	7.96	1252.	767.	
10	321	402.	476.	2.6	1.82	22.1	15.1	8.3	0.97	92.8	99.8	3.7	1.0	2.4	1.69	779.	0.23	975.	3.77	3.79	966.	875.	Resonance fr > 0.3
11	322	397.	477.	2.7	1.81	22.4	16.8	9.3	0.95	92.6	99.9	2.3	0.6	3.4	1.84	812.	0.24	1018.	3.99	3.84	1240.	906.	
12	320	398.	477.	2.5	1.81	22.4	12.7	7.0	1.00	91.4	98.4	50.4	4.1	1.2	1.42	731.	0.28	897.	4.16	3.83	722.	801.	No Limit Encountered
13	332	401.	475.	2.6	2.17	26.5	23.8	11.0	0.96	91.2	99.9	1.3	0.4	4.0	2.21	862.	0.21	1075.	5.50	5.58	1767.	946.	
14	331	400.	478.	2.4	2.17	26.6	19.2	8.4	0.94	92.8	99.9	2.5	0.6	2.4	1.65	783.	0.22	972.	5.69	5.59	1405.	805.	
15	336	403.	476.	2.4	2.16	26.4	14.8	6.9	0.94	89.1	97.8	68.6	6.0	1.2	1.29	720.	0.27	870.	5.65	5.55	938.	782.	No Limit Encountered
16	153	199.	424.	2.6	1.37	30.0	18.5	13.5	0.94	90.6	99.8	9.6	0.3	3.0	2.67	895.	0.21	1079.	8.99	8.49	1479.	1019.	
17	154	199.	423.	2.6	1.37	30.1	21.1	15.3	0.95	90.3	99.5	19.0	0.2	3.4	3.02	952.	0.19	1057.	9.37	8.86	1907.	1015.	
18	152	199.	424.	2.6	1.37	30.1	15.1	11.0	0.95	91.0	99.9	3.5	0.3	1.7	2.19	814.	0.22	1076.	9.37	8.86	983.	951.	
19	132	196.	366.	2.5	1.57	29.9	17.2	10.9	0.97	84.3	92.8	51.5	60.2	1.2	2.02	731.	0.32	986.	9.40	10.09	1273.	784.	
20	143	204.	364.	2.3	1.95	35.9	23.7	12.2	0.98	90.6	99.4	16.9	1.9	1.3	2.49	798.	0.28	916.	16.25	14.80	1964.	816.	Resonance Threshold*

* HUG 19 and 20 Emissions Levels Reflected by Blowout Following Run 18.

Table XXXII. Test Summary, Combustor Configuration R1, Runs 6 and 7.

Reading	Test Point	Inlet Total Pressure, kPa	Inlet Total Temperature, K	Inlet Humidity, g H ₂ O/kg Air	Combustor Air Flow, kg/s	Reference Velocity, m/s	Fuel Flow, g/s	Motored Fuel-Air Ratio, g/kg	Sample Fuel-Air Ratio/Motored Fuel-Air Ratio	Thermocouple Combustion Efficiency, %	Sample Combustion Efficiency, %	CO Emission Index, g/kg	HC Emission Index, g/kg	NO _x Emission Index, g/kg	CO ₂ Volume, %	Thermocouple Average Exit Temperature, K	Pattern Factor	Maximum Liner Temperature, K	Total Pressure Loss, %	Dome Pressure Loss, %	Fuel Nozzle Pressure Drop, kPa	Avg. Catalyst Inlet Temp. (Catalytic), K	Swirl Inlet Temp. (Recuperative), K	or Avg. Liner Temp. (Hot Wall), K
1	220	300.	422.	3.0	1.63	23.6	11.0	7.0	0.96	94.2	99.8	3.5	5.1	2.4	1.38	685.	0.16	916.	5.74	1.69	372.	475.		
2	210	304.	424.	3.4	1.14	16.3	7.5	6.6	0.98	96.8	99.4	7.1	4.6	2.3	1.35	681.	0.14	957.	2.26	0.76	347.	479.		
3	211	304.	424.	3.4	1.14	16.4	9.7	8.5	0.99	98.3	99.7	4.0	2.5	4.4	1.75	757.	0.14	1124.	2.50	0.74	327.	501.		
4	111	292.	367.	2.4	0.81	15.2	6.6	8.1	0.88	89.2	90.0	72.2	74.2	1.4	1.33	659.	0.39	891.	1.71	0.67	119.	426.		
5	113	291.	367.	2.6	0.81	15.3	8.6	10.6	0.67	95.5	98.5	26.4	9.0	3.8	1.48	770.	0.28	1045.	2.40	0.67	209.	461.		
6	113	293.	367.	3.6	0.80	15.0	10.6	13.2	0.61	92.0	96.4	50.0	4.5	6.1	2.17	876.	0.36	1069.	2.72	0.67	361.	463.		
7	114	292.	366.	3.8	0.80	15.0	12.7	15.8	0.75	95.4	98.2	66.9	2.8	5.9	2.39	954.	0.29	1106.	2.73	0.67	481.	457.		
8	121	293.	367.	3.8	1.27	22.7	9.9	8.2	0.81	95.1	98.8	21.7	6.7	1.8	1.34	679.	0.29	895.	5.95	1.30	276.	415.		
9	210	306.	422.	2.0	1.06	15.1	7.5	7.1	0.93	97.7	99.5	6.3	3.3	2.8	1.55	698.	0.19	972.	2.03	0.55	150.	476.		
10	211	302.	421.	2.0	1.07	15.3	9.6	9.0	0.92	96.7	99.7	5.0	1.5	5.0	1.73	767.	0.32	1135.	2.05	0.56	270.	499.		
11	212	303.	423.	1.9	1.07	15.3	11.1	10.4	0.93	96.1	99.7	6.6	1.1	7.5	2.01	815.	0.33	1181.	2.05	0.56	369.	514.		

Table XXXIII. Test Summary, Combustor Configuration R2, Run 8.

Reading	Test Point	Inlet Total Pressure, kPa	Inlet Total Temperature, K	Inlet Humidity, g H ₂ O/kg Air	Combustor Air Flow, kg/s	Reference Velocity, m/s	Fuel Flow, g/s	Metered Fuel-Air Ratio, g/kg	Sample Fuel-Air Ratio/Metered Fuel-Air Ratio	Thermocouple Combustion Efficiency, %	Sample Combustion Efficiency, %	CO Emission Index, g/kg	HC Emission Index, g/kg	NO Emission Index, g/kg	CO ₂ Volume, %	Thermocouple Average Exit Temperature, K	Pattern Factor	Maximum Liner Temperature, K	Total Pressure Loss, %	Dome Pressure Loss, %	Fuel Nozzle Pressure Drop, kPa	Avg. Catalyst Inlet Temp. (Catalytic), K	Swirl Inlet Temp. (Decorative), K	or Avg. Liner Temp. (Hot Wall), K
1 111	200.	366.	3.0	0.81	15.3	6.6	8.1	0.87	84.7	88.0	69.0	103.8	1.5	1.28	643.	0.30	887.	1.89	0.54	234.	412.			
2 112	201.	368.	3.0	0.81	15.2	8.6	10.7	0.85	95.4	98.8	22.0	7.4	4.0	1.88	773.	0.24	1073.	3.77	0.54	423.	458.			
3 113	200.	367.	2.9	0.80	15.1	10.6	13.3	0.85	92.3	98.7	39.5	3.4	7.2	2.31	846.	0.32	1114.	2.76	0.59	652.	468.			
4 115	202.	368.	2.9	0.81	15.1	9.6	12.0	0.88	94.4	99.0	27.7	3.2	6.4	2.17	812.	0.31	1039.	2.91	0.54	526.	466.			
5 210	305.	420.	2.9	1.09	15.5	7.5	6.9	1.00	99.7	99.6	5.3	3.1	2.4	1.42	695.	0.24	954.	2.03	0.44	319.	469.			
6 211	304.	423.	3.3	1.08	15.5	9.6	8.9	0.97	96.4	99.8	3.0	1.7	4.5	1.80	762.	0.19	1027.	2.04	0.45	521.	485.			
7 212	306.	422.	3.0	1.08	15.4	11.1	10.3	0.94	96.4	99.7	6.8	1.4	8.1	2.01	812.	0.34	1125.	2.37	0.44	712.	498.			

THIS PAGE IS
OF POOR QUALITY

ORIGINAL PAGE IS
OF POOR QUALITY

Table XXXIV. Test Summary, Combustor Configuration R3, Runs 12 and 13.

Reading	Test Point	Inlet Total Pressure, kPa	Inlet Total Temperature, K	Inlet Humidity, g H ₂ O/kg Air	Combustor Air Flow, kg/s	Reference Velocity, m/s	Fuel Flow, g/s	Metered Fuel-Air Ratio, g/kg	Sample Fuel-Air Ratio/Metered Fuel-Air Ratio	Thermocouple Combustion Efficiency, %	Sample Combustion Efficiency, %	CO Emission Index, g/kg	HC Emission Index, g/kg	NO _x Emission Index, g/kg	CO ₂ Volume, %	Thermocouple Average Exit Temperature, K	Pattern Factor	Maximum Liner Temperature, K	Total Pressure Loss, %	Dome Pressure Loss, %	Fuel Nozzle Pressure Drop, kPa	Avg. Catalyst Inlet Temp. (Catalytic), K Swirl Inlet Temp. (Re recuperative), K or Avg. Liner Temp. (Hot Wall), K	Comments
1	212	300.	425.	1.9	1.03	15.0	11.3	11.0	0.95	97.2	99.6	12.0	1.5	11.5	2.18	804.	0.45	1243.	1.84	0.78	745.	515.	
2	211	307.	422.	2.4	1.02	14.5	9.6	9.4	0.96	97.8	99.7	6.9	1.5	9.3	1.88	785.	0.41	1190.	2.02	0.75	545.	514.	
3	210	305.	424.	2.5	1.01	14.5	7.5	7.4	0.98	98.8	99.8	2.2	1.7	5.7	1.52	716.	0.36	1079.	2.49	0.76	333.	506.	
4	207	305.	421.	2.4	1.02	14.6	6.5	6.4	1.00	97.4	99.8	2.3	1.6	3.0	1.32	672.	0.36	984.	2.04	0.77	243.	489.	
5	220	312.	424.	2.3	1.77	25.4	11.3	6.4	0.95	94.1	99.5	1.7	1.7	2.9	1.26	669.	0.37	993.	6.40	2.29	716.	481.	
6	222	307.	424.	2.1	1.78	25.3	18.9	10.6	0.86	90.8	99.5	15.9	1.1	7.2	1.88	890.	0.52	1111.	6.06	2.32	2412.	499.	
7	226	317.	424.	2.4	1.78	25.3	11.5	6.4	0.81	92.6	96.8	2.0	31.7	3.0	1.05	663.	0.21	962.	6.95	2.43	765.	471.	*
8	221	306.	423.	2.3	1.78	25.3	14.1	7.9	0.84	93.7	99.3	2.6	6.1	4.1	1.38	719.	0.29	1048.	7.66	2.49	1200.	485.	*
9	223	303.	421.	2.3	1.77	25.4	16.7	9.4	0.79	91.3	99.2	10.3	5.2	5.7	1.54	762.	0.30	1052.	6.37	2.60	1706.	490.	*
10	130	203.	370.	2.3	1.55	29.0	9.0	6.4	0.66	92.0	97.6	37.5	13.5	1.3	1.11	609.	0.25	788.	11.19	3.91	607.	416.	
11	131	201.	360.	2.3	1.55	29.1	15.7	10.2	0.74	91.4	98.9	32.3	3.7	3.7	1.54	736.	0.45	1005.	11.35	4.05	1526.	438.	
12	132	202.	367.	2.3	1.55	29.0	18.9	12.2	0.71	90.6	97.9	74.4	3.8	4.7	1.74	801.	0.44	1069.	11.27	4.03	2311.	444.	
13	111	208.	366.	2.3	0.86	14.8	6.6	8.2	0.90	94.5	98.8	19.2	7.9	2.9	1.51	680.	0.30	925.	2.68	0.99	266.	446.	

* Erroneous HC Readings - Sample Lines Contaminated with Fuel

Table XXXV. Test Summary, Combustor Configuration R4, Runs 14 and 15.

Reading	Test Point	Inlet Total Pressure, kPa	Inlet Total Temperature, K	Inlet Humidity, g H ₂ O/kg air	Compressor Air Flow, kg/s	Reference Velocity, m/s	Fuel Flow, g/s	Heated Fuel-Air Ratio, g/kg	Sample Fuel-Air Ratio, g/kg	Heated Fuel-Air Ratio	Thermocouple Combustion Efficiency, %	Sample Combustion Efficiency, %	CO Extinction Index, g/kg	H ₂ Extinction Index, g/kg	NO Extinction Index, g/kg	CO ₂ Volume, %	Thermocouple Average Exit Temperature, K	Pattern Factor	Maximum Liner Temperature, K	Total Pressure Loss, %	Purge Pressure Loss, %	Fuel Nozzle Pressure Drop, kPa	Avg. Catalyst Inlet Temp. (Catalytic), K	Swirl Inlet Temp. (Re recuperative), K	or Avg. Liner Temp. (Hot Wall), K
1	210	397.	425.	1.9	1.04	16.9	7.4	7.3	0.94	93.7	99.8	1.9	2.0	5.3	1.42	699.	0.19	1090.	2.02	0.66	331.	504.	Resonance $f_m > 10.0$		
2	211	303.	424.	1.9	1.04	15.1	9.7	9.3	0.92	93.2	99.8	2.7	1.3	7.0	1.79	767.	0.18	1153.	1.82	0.67	556.	520.			
3	216	366.	425.	1.9	1.05	15.0	5.6	5.4	1.02	96.3	99.1	23.5	3.1	2.4	1.12	635.	0.12	939.	2.03	0.66	174.	480.			
4	111	202.	366.	1.6	0.78	14.7	6.7	6.5	0.94	90.8	99.1	11.4	6.3	2.9	1.65	678.	0.21	1019.	2.39	0.75	243.	448.			
5	112	205.	367.	1.6	0.78	14.5	8.5	10.2	0.96	92.1	99.3	16.1	3.2	4.3	2.15	763.	0.21	1121.	2.69	0.74	400.	469.	No Resonance		
6	113	204.	368.	1.6	0.78	14.6	10.6	13.5	0.92	90.9	98.9	34.3	3.5	4.4	2.56	847.	0.16	1132.	2.70	0.75	1069.	472.			
7	115	202.	366.	1.6	0.78	14.7	7.6	9.7	0.96	92.3	99.2	13.9	4.4	3.6	1.93	724.	0.19	1103.	3.27	0.75	353.	456.			
8	116	201.	366.	1.6	0.78	14.8	5.7	7.3	0.77	90.5	99.1	23.9	13.5	1.9	1.44	633.	0.19	931.	2.75	0.76	176.	429.			
9	111	203.	369.	1.1	0.81	15.1	6.7	8.2	0.94	94.4	99.2	10.4	5.6	3.1	1.59	681.	0.16	1034.	2.71	0.83	241.	449.	No Resonance		
10	121	203.	366.	1.1	1.22	22.6	9.9	8.1	0.92	93.0	99.7	3.9	2.0	3.4	1.56	671.	0.13	1023.	5.76	1.26	537.	449.			
11	122	202.	369.	1.2	1.22	22.9	12.9	10.4	0.90	92.0	99.4	18.7	1.4	3.8	1.96	754.	0.15	1082.	6.48	1.28	954.	458.			
12	123	203.	368.	1.3	1.21	22.6	15.9	13.1	0.88	91.3	98.8	40.6	1.1	4.0	2.36	836.	0.13	1084.	6.44	1.76	1330.	450.			
13	120	201.	367.	1.3	1.21	22.7	8.0	6.6	0.93	93.2	99.4	15.8	2.4	2.4	1.27	618.	0.14	978.	6.51	1.25	346.	453.	Resonance $f_m > 9$		
14	131	203.	366.	1.5	1.45	26.9	12.0	8.3	0.82	93.5	99.7	5.0	1.5	2.9	1.41	678.	0.14	1076.	9.49	2.25	772.	443.			
15	231	303.	424.	2.6	2.06	29.8	16.4	8.0	0.57	89.3	99.4	1.7	1.0	4.9	1.44	706.	0.18	1066.	8.65	2.28	1334.	427.			
16	232	306.	425.	2.4	2.07	29.6	18.4	8.9	0.65	88.6	99.9	2.4	0.9	5.2	1.59	737.	0.18	1097.	9.01	2.77	1648.	493.			
17	230	303.	424.	2.0	2.07	29.8	13.3	6.4	0.90	90.5	99.8	2.8	1.2	2.4	1.20	658.	0.18	954.	8.26	2.79	278.	476.	Resonance Above Indicated f_m		
18	235	365.	423.	1.7	2.07	29.6	11.1	5.3	0.91	89.6	99.3	19.2	2.4	1.1	1.00	617.	0.17	849.	9.03	2.77	607.	457.			
19	220	301.	429.	0.	1.58	23.3	7.4	4.7																	
20	132	199.	359.	0.	1.44	26.8	14.6	10.0																	

Short Readings to Define Resonance Limits.

ORIGINAL PAGE IS
OF POOR QUALITY

Comments

Table XXXVI. Test Summary, Combustor Configuration R5, Run 16.

Reading	Test Point	Inlet Total Pressure, kPa	Inlet Total Temperature, K	Inlet Humidity, g H ₂ O/kg Air	Compressor Air Flow, kg/s	Reference Velocity, m/s	Fuel Flow, g/s	Metered Fuel-Air Ratio	Sample Fuel-Air Ratio/Metered Fuel-Air Ratio	Thermocouple Combustion Efficiency, %	Sample Combustion Efficiency, %	CO Emission Index, g/kg	HC Emission Index, g/kg	NO _x Emission Index, g/kg	CO ₂ Volume, %	Thermocouple Average Exit Temperature, K	Pattern Factor	Maximum Liner Temperature, K	Total Pressure Loss, %	Dome Pressure Loss, %	Fuel Nozzle Pressure Drop, kPa	Avg. Catalyst Inlet Temp. (Calalytic), K Swirl Inlet Temp. (Recuperative), K or Avg. Liner Temp. (Hot Wall), K
1	111	202.	368.	1.9	0.78	10.7	6.6	8.4	0.89	89.8	97.7	25.6	16.8	2.5	1.53	673.	0.32	969.	2.05	0.59	216.	442.
2	112	204.	369.	1.9	0.78	10.5	8.6	11.1	0.88	92.3	99.0	14.7	6.7	3.9	2.03	774.	0.35	1034.	2.71	0.58	400.	467.
3	113	204.	367.	1.9	0.78	14.8	10.6	13.7	0.86	92.2	98.6	36.2	5.3	4.2	2.40	859.	0.32	1043.	2.30	0.58	600.	475.
4	121	202.	371.	1.9	1.22	23.0	9.9	8.1	0.88	94.2	99.6	7.8	1.8	3.6	1.48	678.	0.26	981.	6.14	1.59	512.	458.
5	122	204.	368.	2.0	1.22	22.6	12.9	10.6	0.87	93.3	99.4	19.0	1.3	3.6	1.91	760.	0.32	1000.	5.40	1.49	875.	456.
6	123	202.	367.	1.9	1.22	22.9	15.8	12.9	0.86	92.8	98.9	43.6	0.9	3.5	2.28	837.	0.35	982.	5.11	1.51	1291.	450.
7	120	203.	366.	1.8	1.22	22.7	6.0	6.6	0.90	94.5	99.1	24.6	2.9	2.9	1.21	618.	0.26	974.	6.12	1.50	325.	441.
8	131	203.	366.	2.6	1.62	30.1	13.0	8.1	0.88	90.3	99.6	7.9	2.2	3.1	1.47	859.	0.31	1021.	10.53	2.92	869.	447.
9	210	304.	424.	1.9	1.03	14.8	7.6	7.4	0.93	94.7	99.8	3.4	1.6	5.2	1.43	704.	0.28	1086.	2.27	0.50	307.	512.
10	211	304.	424.	1.7	1.04	14.9	9.7	9.4	0.93	95.9	99.8	4.5	1.2	5.9	1.82	779.	0.40	1118.	2.27	0.50	513.	526.
11	216	303.	422.	1.5	1.04	14.9	5.8	5.6	0.94	93.6	98.4	40.8	6.2	3.0	1.07	634.	0.15	883.	1.82	0.50	170.	487.

Table XXXVII. Test Summary, Combustor Configuration R6, Run 17.

Reading	Test Point	Inlet Total Pressure, kPa	Inlet Total Temperature, K	Inlet Humidity, g H ₂ O/kg Air	Combustor Air Flow, kg/s	Reference Velocity, m/s	Fuel Flow, g/s	Metered Fuel-Air Ratio Ratio, g/kg	Sample Fuel-Air Ratio/Metered Fuel-Air Ratio	Thermocouple Combustion Efficiency, %	Sample Combustion Efficiency, %	CO Emission Index, g/kg	HC Emission Index, g/kg	NO Emission Index, g/kg	CO ₂ Volume, %	Thermocouple Average Exit Temperature, K	Pattern Factor	Maximum Liner Temperature, K	Total Pressure Loss, %	Domo Pressure Loss, %	Fuel Nozzle Pressure Drop, kPa	Avg. Catalyst Inlet Temp. (Catalytic), K Swirl Inlet Temp. (Recuperative), K or Avg. Liner Temp. (Hot Wall), K	COMMENTS
1	221	308.	426.	1.0	1.61	22.9	17.9	8.0	0.89	96.2	99.7	4.7	1.7	1.4	1.47	732.	0.27	972.	8.05	3.46	854.	694.	*
2	222	304.	422.	1.0	1.60	22.8	16.7	10.4	0.93	94.0	99.8	4.0	1.1	4.8	2.01	807.	0.32	1100.	8.58	3.33	1429.	509.	
3	223	305.	422.	1.0	1.60	22.9	20.8	12.9	0.88	93.4	99.5	16.1	1.0	7.8	2.37	890.	0.30	1163.	8.37	3.22	2278.	526.	
4	220	304.	422.	1.0	1.60	22.9	11.0	6.9	0.92	95.3	98.9	22.0	5.7	0.9	1.29	684.	0.24	842.	8.61	3.51	617.	474.	
5	131	204.	369.	1.0	1.64	30.5	13.0	7.9	0.81	84.8	97.7	49.7	11.2	0.9	1.29	640.	0.11	807.	18.24	7.71	883.	427.	
6	132	206.	367.	1.0	1.64	30.3	17.2	10.5	0.80	88.3	99.7	7.3	1.6	2.0	1.74	734.	0.26	931.	18.57	7.63	1482.	453.	
7	133	205.	366.	1.0	1.64	30.1	21.3	13.0	0.84	86.6	99.1	33.6	1.5	3.8	2.25	807.	0.22	1115.	17.84	7.36	2412.	469.	
8	135	204.	366.	1.0	1.64	30.3	19.2	11.7	0.83	87.2	99.5	15.4	1.3	2.8	2.01	769.	0.24	1088.	18.57	7.46	1668.	462.	
9	136	201.	366.	1.0	1.64	30.8	15.1	9.2	0.86	90.3	99.4	11.9	3.1	1.1	1.62	698.	0.16	979.	18.49	7.62	1147.	443.	
10	123	203.	366.	1.0	1.30	24.2	16.7	12.8	0.81	92.0	99.2	30.3	0.6	4.7	2.13	829.	0.28	1095.	11.52	4.66	1462.	479.	**
11	122	204.	366.	1.0	1.30	24.1	13.6	10.4	0.82	94.3	99.8	6.4	0.6	3.0	1.78	757.	0.32	1046.	10.81	4.64	945.	467.	**

* RESONANCE AT $V_r < 20$ m/sec

** BORDERLINE RESONANCE - INCREASED SHARPLY AT $f_M < 10$ g/kg OR $V_r < 24$ m/sec

Table XXXVIII. Test Summary, Combustor Configuration R7, Run 28.

Reading	Test Point	Inlet Total Pressure, kPa	Inlet Total Temperature, K	Inlet Humidity, g H ₂ O/kg Air	Compressor Air Flow, kg/s	Reference Velocity, m/s	Fuel Flow, g/s	Watered Fuel-Air Ratio, g/kg	Sample Fuel-Air Ratio/ Watered Fuel-Air Ratio	Thermocouple Combustion Efficiency, %	Sample Combustion Efficiency, %	CO Emission Index, g/kg	HC Emission Index, g/kg	NO _x Emission Index, g/kg	CO ₂ Vol %	Thermocouple Average Exit Temperature, K	Pattern Factor	Maximum Liner Temperature, K	Total Pressure Loss, %	Dome Pressure Loss, %	Fuel Nozzle Pressure Drop, kPa	Avg. Catalyst Inlet Temp. (Catalytic), K	Swirl Inlet Temp. (Re recuperative), K	or Avg. Liner Temp. (Hot Wall), K
1	212	302.	423.	1.6	1.03	14.9	11.3	11.0	0.91	92.8	99.7	10.3	0.7	7.5	2.07	822.	0.16	1149.	2.05	0.90	597.	509.		
2	211	304.	424.	1.6	1.02	14.7	9.6	9.4	0.93	94.4	99.8	3.9	0.7	6.6	1.82	774.	0.19	1079.	2.49	0.89	430.	498.		
3	210	302.	423.	1.5	1.02	14.8	7.5	7.3	0.95	95.5	99.8	3.3	1.1	5.2	1.45	703.	0.19	1022.	2.05	0.90	266.	481.		
4	215	301.	422.	1.6	1.02	14.6	5.7	5.6	0.98	95.2	98.9	31.5	3.7	3.2	1.12	638.	0.17	879.	2.06	0.90	157.	459.		
5	216	304.	423.	1.6	1.02	14.7	5.4	5.3	0.99	93.8	97.0	83.4	11.0	2.6	1.03	623.	0.16	845.	2.27	0.89	134.	455.		
6	221	305.	424.	1.9	1.56	22.4	13.0	8.3	0.91	91.9	99.9	1.9	0.9	5.1	1.59	728.	0.21	1038.	4.52	1.78	767.	487.		
7	222	301.	424.	1.9	1.57	22.8	16.7	10.6	0.90	90.1	99.7	9.5	0.5	5.9	1.99	799.	0.18	1103.	4.56	1.80	1253.	498.		
8	220	304.	423.	1.9	1.57	22.6	10.4	6.6	0.94	92.0	99.7	8.4	0.8	3.0	1.28	666.	0.18	1032.	4.54	1.79	527.	471.		
9	225	306.	421.	1.9	1.57	22.3	9.4	6.0	0.96	90.9	98.9	32.5	3.2	2.6	1.16	640.	0.15	975.	4.73	1.77	393.	667.		
10	311	490.	476.	1.8	1.23	15.1	10.1	8.2	0.96	96.1	99.9	1.3	0.5	8.7	1.65	787.	0.24	1222.	1.90	0.68	478.	556.		
11	310	399.	478.	1.8	1.22	15.1	7.6	6.2	0.96	93.8	99.9	1.7	0.6	7.2	1.23	709.	0.21	1059.	1.73	0.68	259.	537.		
12	315	398.	478.	1.8	1.23	15.2	6.1	5.0	1.00	95.1	99.6	13.4	1.0	4.3	1.03	668.	0.18	903.	1.73	0.68	170.	524.		
13	131	199.	367.	1.9	1.58	30.0	12.9	8.1	0.88	89.4	99.8	6.1	0.5	2.3	1.49	660.	0.17	1084.	12.10	3.74	741.	416.		
14	130	200.	367.	1.9	1.59	30.0	11.5	7.2	0.90	89.9	99.3	25.4	0.9	1.9	1.34	631.	0.20	1063.	11.72	3.72	582.	418.		
15	121	198.	366.	1.5	1.20	22.9	9.8	6.2	0.91	90.8	99.8	6.2	0.6	2.5	1.56	666.	0.23	1097.	6.62	2.05	432.	425.		
16	122	200.	366.	1.5	1.20	22.6	12.9	10.8	0.87	88.7	99.6	14.4	0.4	3.1	1.95	744.	0.20	1152.	6.55	2.03	734.	438.		
17	123	199.	366.	1.5	1.20	22.8	16.1	13.4	0.86	88.7	98.9	46.9	0.3	4.1	2.34	831.	0.24	1102.	6.59	2.05	1142.	440.		
18	120	201.	366.	1.6	1.20	22.6	8.5	7.1	0.93	90.0	98.4	50.7	4.6	1.9	1.34	626.	0.23	1017.	6.52	2.02	340.	415.		

Table XXXIX. Test Summary, Combustor Configuration C1, Runs 1 and 2.

Reading	Test Point	Inlet Total Pressure, kPa	Inlet Total Temperature, K	Inlet Humidity, g H ₂ O/kg Air	Combustor Air Flow, kg/s	Reference Velocity, m/s	Fuel Flow, g/s	Metered Fuel-Air Ratio, g/kg	Sample Fuel-Air Ratio/Metered Fuel-Air Ratio	Thermocouple Combustion Efficiency, %	Sample Combustion Efficiency, %	CO Emission Index, g/kg	HC Emission Index, g/kg	NO _x Emission Index, g/kg	CO ₂ Volume, %	Thermocouple Average Exit Temperature, K	Pattern Factor	Maximum Liner Temperature, K	Total Pressure Loss, %	Dome Pressure Loss, %	Fuel Nozzle Pressure Drop, MPa	Avg. Catalyst Inlet Temp. (Catalytic), K	Swirl Inlet Temp. (Recuperative), K	or Avg. Liner Temp. (Hot Wall), K
4	221	287.	422.	3.9	1.53	23.3	14.1	9.2	0.89	82.6	81.6	155.3	147.8	1.0	1.32	721.	0.38	0.	5.05	2.36	592.	1068.		
3	222	294.	423.	4.3	1.53	22.7	16.7	10.9	0.88	84.9	84.2	159.0	120.5	1.3	1.60	765.	0.32	0.	4.93	1.84	806.	1175.		
5	223	308.	421.	3.6	1.55	21.8	18.0	11.7	0.87	89.2	92.9	115.0	44.3	1.3	1.91	826.	0.26	0.	5.16	2.20	951.	1308.		
6	222	304.	426.	4.1	1.53	22.0	16.7	11.0	0.92	87.0	91.8	107.8	57.2	1.7	1.88	792.	0.34	0.	4.87	2.23	830.	1197.		
7	321	404.	480.	3.9	1.80	22.1	15.0	8.3	0.92	92.4	96.5	58.1	21.8	2.1	1.53	782.	0.33	0.	3.75	1.80	682.	1126.		
8	322	403.	478.	3.9	1.80	22.0	18.7	10.4	0.94	93.7	98.1	40.2	9.4	3.0	1.99	854.	0.31	0.	3.25	1.81	1076.	1274.		

ORIGINAL PAGE IS
OF POOR QUALITY

Table XL. Test Summary, Combustor Configuration C2, Run 3.

Reading	Test Point	Inlet Total Pressure, kPa	Inlet Total Temperature, K	Inlet Humidity, g H ₂ O/kg Air	Combustor Air Flow, kg/s	Reference Velocity, m/s	Fuel Flow, g/s	Metered Fuel-Air Ratio, g/kg	Sample Fuel-Air Ratio/Metered Fuel-Air Ratio	Thermocouple Combustion Efficiency, %	Sample Combustion Efficiency, %	CO Emission Index, g/kg	HC Emission Index, g/kg	NO Emission Index, g/kg	CO ₂ Volume, %	Thermocouple Average Exit Temperature, K	Pattern Factor	Maximum Liner Temperature, K	Total Pressure Loss, %	Dome Pressure Loss, %	Fuel Nozzle Pressure Drop, kPa	Avg. Catalyst Inlet Temp. (Catalytic), K Swirl Inlet Temp. (Recuperative), K or Avg. Liner Temp. (Hot Wall), K
1	222	306.	422.	3.4	1.58	22.5	16.7	10.5	0.90	77.9	81.4	173.4	146.0	1.2	1.52	744.	0.30	0.	12.41	2.44	877.	973.
2	222	293.	423.	3.6	1.58	23.5	16.7	10.6	0.98	78.5	79.5	177.5	163.7	1.2	1.62	706.	0.32	0.	8.01	2.72	690.	987.
3	223	304.	423.	3.6	1.56	22.1	20.7	13.2	0.98	85.0	88.0	136.6	87.9	1.4	2.29	856.	0.32	0.	8.27	2.75	1343.	1161.
4	224	293.	423.	3.4	1.57	23.3	24.5	15.6	0.97	84.8	90.0	130.1	69.7	1.4	2.75	928.	0.37	0.	9.64	3.35	1875.	1262.
5	321	406.	476.	3.4	1.87	22.6	15.1	8.1	1.01	90.4	91.3	95.6	64.9	1.4	1.50	763.	0.30	0.	5.77	2.17	735.	926.
6	322	409.	477.	3.4	1.87	22.4	19.0	10.5	1.01	83.2	96.0	54.3	27.6	2.1	2.10	815.	0.23	0.	6.24	2.15	1201.	1111.
7	325	400.	478.	3.4	1.88	23.1	24.3	12.0	0.97	94.5	96.6	56.5	20.9	2.4	2.51	945.	0.29	0.	6.72	2.24	1769.	1191.
8	311	407.	477.	3.1	1.27	15.4	10.0	7.8	0.94	86.0	92.4	76.9	57.6	1.9	1.39	742.	0.28	0.	2.20	0.92	328.	853.
9	313	464.	479.	3.1	1.27	15.5	16.3	12.9	0.93	91.9	97.9	28.4	13.8	3.5	2.46	931.	0.29	0.	3.08	0.92	855.	1165.

ORIGINAL PAGE IS
OF POOR QUALITY

Table XLI. Test Summary, Combustor Configuration C3, Run 9.

Reading	Test Point	Inlet Total Pressure, kPa	Inlet Total Temperature, K	Inlet Humidity, g H ₂ O/kg Air	Combustor Air Flow, kg/s	Reference Velocity, m/s	Fuel Flow, g/s	Motored Fuel-Air Ratio, g/kg	Sample Fuel-Air Ratio/Motored Fuel-Air Ratio	Thermocouple Combustion Efficiency, %	Sample Combustion Efficiency, %	CO Emission Index, g/kg	HC Emission Index, g/kg	NO _x Emission Index, g/kg	CO ₂ Volume, %	Thermocouple Average Exit Temperature, K	Pattern Factor	Maximum Liner Temperature, K	Total Pressure Loss, %	Done Pressure Loss, %	Fuel Nozzle Pressure Drop, kPa	Avg. Catalyst Inlet Temp. (Catalytic), K	Swirl Inlet Temp. (Re recuperative), K	or Avg. Liner Temp. (Hot Wall), K
1	211	397.	426.	3.1	1.09	15.5	9.6	8.9	0.93	93.0	95.2	24.3	42.2	1.7	1.63	752.	0.15	1028.	2.47	0.99	293.	1033.		
2	0	364.	477.	3.1	1.08	17.4	9.7	9.0	0.97	96.2	98.5	17.2	11.2	2.6	1.80	816.	0.15	1124.	2.72	1.12	300.	1103.		
3	1	304.	441.	3.1	1.08	17.6	11.2	10.4	0.93	97.5	99.5	10.0	3.0	3.4	2.01	873.	0.13	1141.	2.95	1.11	368.	1204.		
4	311	408.	478.	3.1	1.24	14.9	11.3	9.1	0.96	99.1	99.0	15.2	6.1	3.4	1.81	831.	0.08	1072.	1.52	0.79	361.	1129.		
5	312	408.	479.	3.1	1.24	15.0	13.1	10.6	1.00	100.4	99.6	8.8	1.7	4.1	2.19	889.	0.10	1161.	1.69	0.79	450.	1240.		
6	211	366.	424.	3.1	1.10	15.6	9.7	8.8	0.98	95.8	97.3	23.9	21.2	2.1	1.75	759.	0.12	1000.	2.70	1.05	263.	1045.		
7	2	308.	366.	3.6	1.09	13.4	9.6	8.8	0.99	75.6	75.8	26.8	235.8	0.6	1.37	633.	0.16	652.	2.02	0.83	254.	534.		

Table XLII. Test Summary, Combustor Configuration, C4, Run 10.

Reading	Test Point	Inlet Total Pressure, kPa	Inlet Total Temperature, K	Inlet Humidity, g H ₂ O/kg Air	Combustor Air Flow, kg/s	Reference Velocity, m/s	Fuel Flow, g/s	Heated Fuel-Air Ratio, g/kg	Sample Fuel-Air Ratio/Heated Fuel-Air Ratio	Thermocouple Combustion Efficiency, %	Sample Combustion Efficiency, %	CO Emission Index, g/kg	HC Emission Index, g/kg	NO _x Emission Index, g/kg	CO ₂ Volume, %	Thermocouple Average Exit Temperature, K	Pattern Factor	Maximum Liner Temperature, K	Total Pressure Loss, %	Dome Pressure Loss, %	Fuel Nozzle Pressure Drop, kPa	Avg. Catalyst Inlet Temp. (Catalytic), K	Swirler Inlet Temp. (Re Recuperative), K	or Avg. Liner Temp. (Hot Wall), K
1	212	304.	423.	3.8	1.06	15.2	11.1	10.5	0.94	94.5	95.7	26.4	36.5	1.6	1.97	811.	0.15	990.	3.63	1.12	348.	935.		
2	213	304.	424.	3.8	1.06	15.3	13.9	13.0	0.88	95.4	98.2	18.9	13.3	2.8	2.35	906.	0.17	1137.	4.08	1.22	547.	1123.		
3	104	410.	423.	3.8	0.99	10.5	16.4	16.6	1.00	100.1	98.8	21.7	7.2	3.1	3.42	1053.	0.18	1222.	2.02	0.45	766.	1261.		
4	103	408.	423.	3.8	0.99	10.5	13.8	14.0	0.98	97.7	97.3	33.3	18.9	2.6	2.80	949.	0.23	1103.	2.03	0.46	547.	1116.		
5	102	410.	423.	3.8	0.99	10.5	11.2	11.3	1.00	97.6	95.0	33.0	41.9	2.1	2.24	854.	0.24	998.	1.35	0.45	356.	968.		
6	303	431.	477.	3.8	1.12	12.8	15.7	14.0	1.00	100.5	99.1	13.9	6.1	4.0	2.92	1012.	0.26	1241.	2.08	0.64	703.	1216.		
7	302	433.	479.	3.8	1.12	12.8	12.4	11.2	0.98	99.4	98.2	21.6	13.0	3.7	2.26	909.	0.26	1113.	2.23	0.64	447.	1199.		
8	301	429.	478.	3.6	1.12	12.9	9.4	8.4	0.98	99.3	95.9	34.2	33.5	2.4	1.63	804.	0.24	934.	2.25	0.65	257.	892.		
9	201	304.	478.	3.9	0.93	15.0	7.7	8.3	0.98	93.6	92.2	47.5	67.1	1.4	1.55	782.	0.23	847.	2.04	0.09	196.	640.		
10	202	304.	476.	3.8	0.93	15.0	10.0	10.8	1.02	100.5	97.5	21.4	19.9	2.8	2.22	894.	0.19	1101.	2.27	0.89	292.	1069.		
11	203	305.	477.	3.8	0.93	14.9	12.2	13.1	0.97	99.6	98.6	17.5	10.3	3.2	2.62	976.	0.15	1209.	2.26	0.89	430.	1172.		
12	204	305.	478.	3.6	0.93	15.0	14.6	15.7	0.98	101.1	99.2	14.3	4.8	3.6	3.26	1077.	0.15	1287.	2.26	0.89	609.	1296.		
13	311	409.	478.	3.6	1.23	14.8	10.0	8.1	0.99	98.3	95.9	34.7	32.6	2.3	1.60	791.	0.23	926.	2.36	0.91	288.	821.		
14	313	419.	478.	3.2	1.22	14.4	16.3	13.3	0.99	99.5	99.2	11.5	5.5	4.0	2.73	982.	0.20	1238.	2.53	0.87	771.	1212.		

Table XLIII. Test Summary, Combustor Configuration C5, Run 23.

Reading	Test Point	Inlet Total Pressure, kPa	Inlet Total Temperature, K	Inlet Humidity, g H ₂ O/kg Air	Combustor Air Flow, kg/s	Reference Velocity, m/s	Fuel Flow, g/s	Metered Fuel-Air Ratio, g/kg	Sample Fuel-Air Ratio/Metered Fuel-Air Ratio	Thermocouple Combustion Efficiency, %	Sample Combustion Efficiency, %	CO Emission Index, g/kg	HC Emission Index, g/kg	NO Emission Index, g/kg	CO ₂ Volume, %	Thermocouple Average Exit Temperature, K	Pattern Factor	Maximum Liner Temperature, K	Total Pressure Loss, %	Done Pressure Loss, %	Fuel Nozzle Pressure Drop, kPa	Avg. Catalyst Inlet Temp. (Catalytic), K	Swirl Inlet Temp. (Recuperative), K	or Avg. Liner Temp. (Hot Wall), K	COMMENTS
1	210	300.	409.	0.6	1.11	15.7	7.6	6.9	1.07	111.9	97.9	24.1	15.1	3.3	1.49	718.	0.15	1107.	2.30	1.02	241.	1048.	Resonance $f_H > 9$ g/kg		
2	211	301.	404.	0.6	1.11	15.5	9.0	8.1	1.08	110.9	99.5	9.7	2.8	3.6	1.80	765.	0.15	1205.	2.29	0.90	303.	1179.			
3	212	305.	406.	0.5	1.12	15.4	9.8	8.7	1.06	109.3	99.7	6.3	1.4	4.0	1.93	785.	0.15	1223.	2.26	0.89	429.	1245.			
4	230	303.	415.	0.6	2.14	30.2	16.3	7.0	1.05	109.2	99.9	2.1	0.8	3.2	1.66	747.	0.18	1132.	9.09	3.69	1257.	1116.	Resonance $f_H > 9.5$ g/kg		
5	231	305.	413.	0.7	2.12	24.6	19.0	9.0	1.07	107.4	99.9	1.5	0.5	3.6	1.99	795.	0.19	1185.	9.51	3.56	1603.	1218.			
6	229	303.	410.	0.8	2.12	29.6	13.6	6.4	1.12	108.5	99.8	4.7	0.9	2.2	1.49	692.	0.23	958.	9.12	3.56	658.	1004.			
7	220	302.	411.	0.8	1.06	22.4	10.0	6.2	1.10	109.5	99.1	14.0	5.8	3.0	1.41	688.	0.16	1062.	4.89	2.02	452.	999.	Resonance $f_H > 6.5$ g/kg		

ORIGINAL PAGE IS
OF POOR QUALITY

Table XLIV. Test Summary, Combustor Configuration C6, Runs 24 and 25.

Reading	Test Point	Inlet Total Pressure, kPa	Inlet Total Temperature, K	Inlet Humidity, g H ₂ O/kg Air	Combustor Air Flow, kg/s	Reference Velocity, m/s	Fuel Flow, g/s	Metered Fuel-Air Ratio, g/kg	Sample Fuel-Air Ratio/Metered Fuel-Air Ratio	Thermocouple Combustion Efficiency, %	Sample Combustion Efficiency, %	CO Emission Index, g/kg	*HC Emission Index, g/kg	NO Emission Index, g/kg	CO ₂ Volume, %	Thermocouple Average Exit Temperature, K	Pattern Factor	Maximum Liner Temperature, K	Total Pressure Loss, %	Domo Pressure Loss, %	Fuel Nozzle Pressure Drop, kPa	Avg. Catalyst Inlet Temp. (Catalytic), K	Swirl Inlet Temp. (Recuperative), K	or Avg. Liner Temp. (Hot Wall), K
1	211	304.	416.	2.1	1.15	16.3	9.0	7.8	1.12	110.4	99.3	4.2	6.0	3.2	1.81	760.	0.18	1153.	2.95	0.89	445.	1142.		
2	210	307.	414.	2.1	1.14	15.8	7.6	6.7	1.11	108.0	96.2	19.8	33.6	2.5	1.49	705.	0.14	1030.	2.47	0.88	311.	972.		
3	211	303.	416.	1.9	1.15	16.2	9.0	7.9	1.10	112.0	98.9	10.3	8.8	3.5	1.78	768.	0.15	1173.	3.41	0.89	445.	1133.		
4	121	203.	362.	1.6	1.27	23.3	9.9	7.8	1.07	107.7	98.6	13.6	11.0	1.4	1.72	701.	0.12	991.	6.78	2.41	504.	1031.		
5	141	205.	359.	1.3	1.04	18.8	9.6	9.2	1.21	102.9	99.2	8.4	5.6	2.3	2.32	762.	0.12	1117.	4.71	1.49	475.	1178.		
6	111	203.	360.	2.1	0.82	15.0	6.6	8.1	1.10	106.8	97.2	19.1	24.0	2.1	1.80	709.	0.11	1077.	3.40	0.84	236.	1076.		
7	112	206.	355.	2.1	0.82	14.5	7.7	9.4	1.05	107.0	98.6	13.8	10.8	1.8	2.02	758.	0.11	1132.	3.01	0.74	301.	1223.		
8	121	205.	368.	2.1	1.25	23.2	9.9	7.9	0.97	105.4	98.1	15.9	15.5	1.2	1.56	705.	0.13	995.	7.07	2.56	496.	1043.		
9	122	203.	367.	0.6	1.25	23.2	10.9	8.7	0.92	104.9	98.7	9.4	10.4	1.9	1.64	733.	0.13	1079.	7.80	2.75	587.	1158.		
10	112	205.	361.	0.6	0.82	14.9	7.7	9.3	1.07	107.5	98.4	17.1	11.7	2.4	2.03	762.	0.13	1116.	3.02	0.74	309.	1159.		
11	211	303.	419.	0.6	1.15	16.3	9.0	7.9	1.11	109.6	98.5	12.1	11.9	3.0	1.80	763.	0.12	1172.	2.51	0.90	419.	1092.		
12	212	303.	421.	0.6	1.14	16.4	9.8	8.5	1.11	108.8	98.8	8.3	9.8	3.3	1.95	790.	0.15	1208.	2.96	0.90	487.	1167.		
13	230	308.	417.	2.3	2.15	30.1	16.2	7.5	1.10	108.8	97.4	10.0	23.2	1.8	1.81	744.	0.20	1093.	8.74	3.80	1227.	1014.		

*High HC Emissions Attributed to Leak in Internal Fuel Manifold.

Table XLV. Test Summary, Combustor Configuration C7, Run 26.

Reading	Test Point	Inlet Total Pressure, kPa	Inlet Total Temperature, K	Inlet Humidity, g H ₂ O/kg Air	Combustor Air Flow, kg/s	Reference Velocity, m/s	Fuel Flow, g/s	Metered Fuel-Air Ratio, g/kg	Sample Fuel-Air Ratio/Metered Fuel-Air Ratio	Thermocouple Combustion Efficiency, %	Sample Combustion Efficiency, %	CO Emission Index, g/kg	HC Emission Index, g/kg	NO _x Emission Index, g/kg	CO ₂ Volume, %	Thermocouple Average Exit Temperature, K	Pattern Factor	Maximum Liner Temperature, K	Total Pressure Loss, %	Dome Pressure Loss, %	Fuel Nozzle Pressure Drop, kPa	Avg. Catalyst Inlet Temp. (Catalytic), K	Swirl Inlet Temp. (Re recuperative), K	or Avg. Liner Temp. (Hot Wall), K	Comments
1	211	395.	395.	0.6	1.09	14.5	9.6	8.8	1.09	106.4	99.9	1.3	0.5	3.4	2.01	769.	0.21	1082.	2.49	2.00	533.	1140.			
2	212	393.	426.	0.6	1.07	15.5	6.9	6.4	1.21	106.3	95.5	25.7	39.1	2.2	1.52	699.	0.27	1011.	2.73	1.12	286.	938.			
3	215	397.	423.	0.6	1.07	15.3	7.7	7.2	1.19	111.1	98.0	19.2	15.3	2.7	1.73	741.	0.22	1075.	2.47	1.10	365.	1029.			
4	216	394.	423.	0.7	1.08	15.5	8.5	7.9	1.15	109.3	99.1	11.9	6.1	3.1	1.88	766.	0.19	1116.	2.27	1.11	423.	1093.			
5	317	431.	478.	0.6	1.28	15.7	7.7	6.1	1.26	115.0	99.9	2.1	0.8	3.4	1.58	755.	0.23	1097.	3.61	1.01	361.	1011.			Resonance, $f_n > 8.5$
6	321	474.	481.	0.6	1.88	23.1	15.1	8.0	1.15	109.5	99.9	0.9	0.4	4.9	1.92	826.	0.27	1110.	3.75	2.22	1240.	1119.			
7	322	401.	482.	0.7	1.88	23.3	17.8	9.5	1.13	108.9	99.9	1.1	0.3	6.2	2.23	883.	0.25	1270.	4.12	2.24	1684.	1229.			Resonance, $f_n > 9.5$
8	242	395.	426.	0.6	1.85	26.6	17.8	9.6	1.10	107.3	99.9	1.2	0.3	4.0	2.21	832.	0.26	1204.	6.10	3.38	1642.	1196.			
9	243	397.	423.	0.6	1.85	26.3	19.7	10.6	1.07	106.3	99.9	1.3	0.3	3.9	2.37	865.	0.24	1235.	6.29	3.37	1862.	1272.			
10	241	397.	424.	0.6	1.85	26.3	15.1	8.1	1.13	111.6	99.9	1.4	0.4	3.2	1.92	785.	0.27	1112.	5.39	3.37	1186.	1094.			Peak Catalyst Temp. Limit, $f_n > 10.6$
11	247	393.	422.	0.6	1.84	26.4	12.3	6.7	1.14	110.4	98.6	12.3	9.9	1.9	1.56	719.	0.29	983.	5.70	3.41	832.	973.			
12	221	397.	425.	0.6	1.57	22.3	13.2	8.4	1.06	106.8	99.9	1.0	0.9	3.4	1.86	782.	0.19	1093.	4.93	2.53	923.	1139.			Resonance, $f_n > 8.4$
13	127	292.	365.	0.6	1.21	22.6	8.7	7.2	1.07	101.3	95.8	35.5	33.3	1.4	1.52	699.	0.25	978.	3.41	3.02	422.	888.			
14	121	290.	368.	0.6	1.21	22.9	10.1	8.4	0.96	102.9	95.1	12.7	6.1	1.	1.65	715.	0.19	1034.	3.79	3.13	576.	1063.			Resonance, $f_n > 8.4$
15	137	291.	369.	0.4	1.59	29.8	12.1	7.6	1.11	106.4	98.0	31.4	12.9	1.7	1.72	697.	0.27	1002.	8.50	5.01	890.	961.			Resonance, $f_n > 7.6$
16	111	199.	368.	0.4	0.80	15.2	6.6	8.3	1.12	103.0	95.5	31.4	37.5	1.5	1.83	710.	0.18	974.	2.43	1.19	260.	949.			
17	112	207.	371.	0.4	0.80	15.0	8.0	10.0	1.10	109.2	99.4	10.0	3.5	2.8	2.29	807.	0.15	1154.	2.37	1.17	365.	1289.			Peak Catalyst Temp. Limit, $f_n > 10.0$
18	141	307.	366.	0.4	1.21	14.9	9.9	8.1	1.10	106.3	97.5	28.3	18.6	2.2	1.81	715.	0.25	1051.	2.02	1.10	545.	974.			
19	142	371.	366.	0.4	1.21	15.1	10.9	9.1	1.09	108.7	99.3	9.7	4.5	3.0	2.03	761.	0.17	1153.	2.06	1.12	674.	1175.			Resonance, $f_n > 9.1$
20	151	293.	422.	0.7	1.58	33.9	13.2	8.3	1.15	108.9	99.5	11.4	1.9	2.1	1.99	783.	0.21	1180.	10.55	5.68	952.	1089.			
21	152	293.	423.	0.7	1.58	34.0	14.4	9.1	1.15	109.2	99.8	5.9	0.8	2.4	2.18	815.	0.24	1221.	10.55	5.68	1111.	1131.			Liner Temp. Limit, $f_n > 9.1$
22	161	199.	395.	0.7	1.62	33.1	13.2	8.1	1.19	111.0	99.2	16.5	3.9	1.9	1.99	756.	0.26	1141.	10.73	5.78	949.	1066.			
23	162	299.	397.	0.7	1.61	33.0	12.2	7.6	1.21	109.7	98.8	23.4	6.8	1.6	1.88	739.	0.27	1124.	10.35	5.76	817.	992.			Resonance, $f_n > 8.1$

ORIGINAL PAGE IS
OF POOR QUALITY

APPENDIX C

CATALYTIC REACTOR DESIGN PROGRAM SUMMARY

The catalytic reactor used in tests of the LOPER catalytic combustor was designed and fabricated by Engelhard Industries under subcontract to General Electric. The catalyst design program* included a series of catalyst screening tests to select a preferred catalyst configuration and to provide a basis for catalyst performance predictions, and a series of parametric tests to determine catalyst performance at conditions representative of the LOPER operating conditions.

Performance Goals

The performance goals for the catalytic reactor were as follows:

- Cleanup capability to maintain combustor emissions less than 10 g/kg for CO and 1.0 g/kg for HC
- A reactor pressure loss of less than 3%
- An overall reactor length of less than 9.5 cm

The above goals applied to the LOPER design operating conditions, assuming a 50% combustor airflow through the catalytic reactor, a precombustion zone combustion efficiency of 98%, and a catalyst approach velocity of 34.8 m/s.

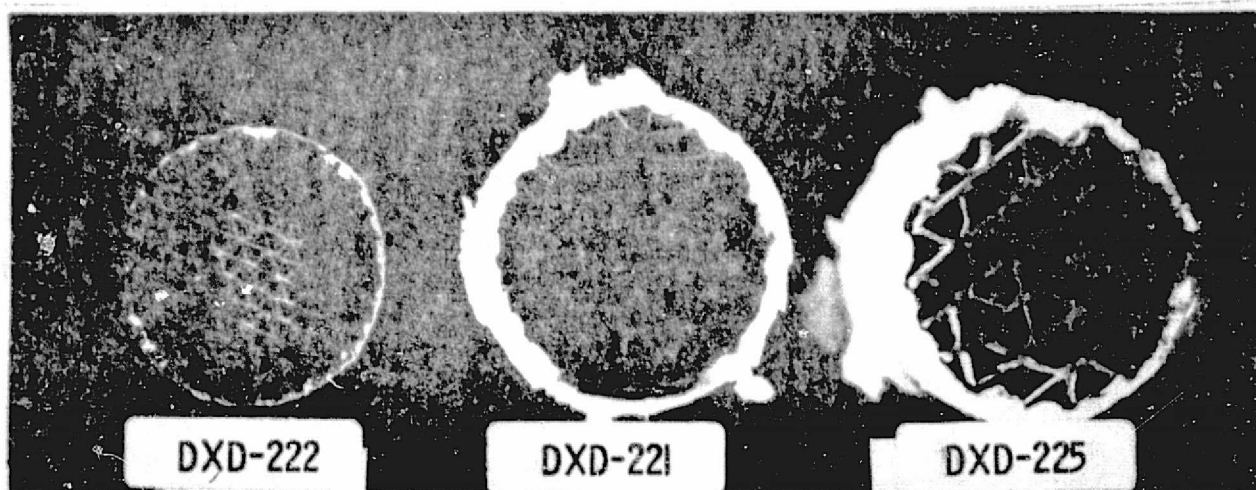
Screening Tests

Laboratory evaluations were conducted on 2.5-cm-diameter test catalysts. Vitiated inlet air with negligible pollutant emissions was provided to simulate LOPER catalyst inlet temperature and oxygen concentrations. This air was seeded with CO and C₃H₆ to simulate incomplete primary zone reactions. The reactor was instrumented to measure test catalyst pressure drop, inlet and exit temperatures, and CO, HC, and NO_x emissions.

Initial screening tests were designed to evaluate the purely catalytic performance of the four catalyst configurations shown in Figures 55 and 56. These catalysts differed only in the cell packing density of the honeycomb support. Catalyst lengths were selected based on equal geometric surface area, with one additional length of catalyst tested to provide additional

* I.T. Osgerby, R.M. Heck, R.V. Carrubba, C. Gleason, and E. Mularz, "Combustion Catalyst Studies for Simulated Aircraft Idle Mode Operation," to Be Submitted for Presentation at the Twenty-fourth Annual ASME International Gas Turbine Conference, March 11-15, 1979.

ORIGINAL PAGE IS
OF POOR QUALITY



	<u>I.D. Code</u>	<u>Cell Density Holes/cm²</u>	<u>Cell Shape</u>	<u>Length, cm</u>	<u>Hydraulic Diameter, cm</u>	<u>Percent Open Area</u>
A.	DXD-222	39	Sine Wave	7.6	0.0975	65.5
B.	DXD-221	14	Sine Wave	11.4	0.1722	54.2
C.	DXD-225	6	Sine Wave	15.2	0.300	73.3
D.	DXD-221	14	Sine Wave	15.2	0.1722	54.2

Note: Catalyst loading and type are proprietary information.

Figure 55. Catalyst Screening Test Configurations.

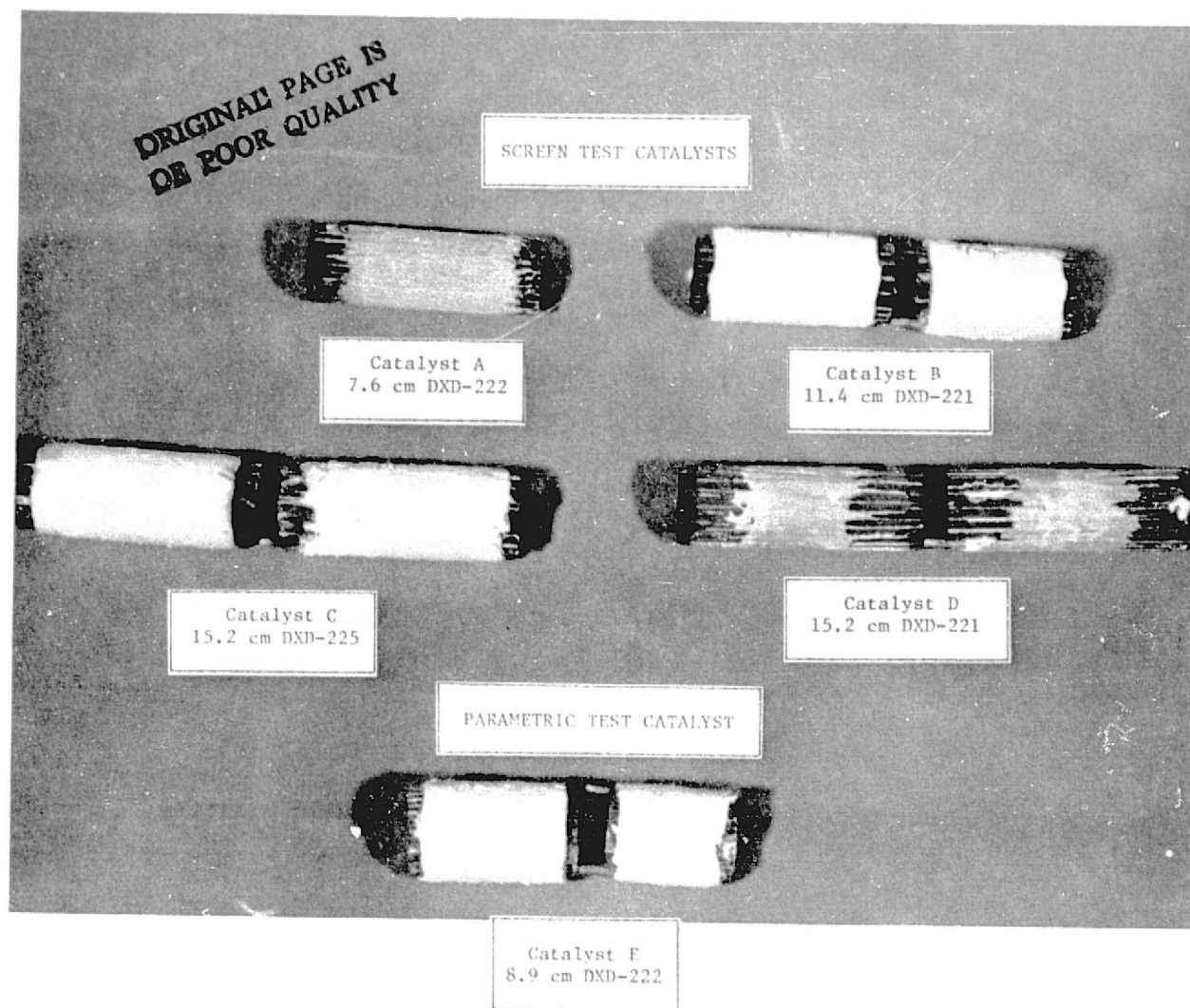


Figure 56. Screening and Parametric Test Catalysts.

information for predictions of catalytic conversion. Screening test conditions (Table XLVI) were selected to preclude homogeneous (thermal) combustion. Catalyst performance was evaluated based on the trade off between catalytic-conversion time-span requirements and pressure-loss time-span restrictions.

Conversion and pressure loss predictions based on screening test results are summarized in Figure 57. None of the configurations tested met both HC and CO conversion goals with purely catalytic reaction, indicating that a homogeneous combustion contribution would be required to meet emissions objectives. Of the configurations tested, Catalyst DXD-222 provided clearly superior conversion characteristics. Pressure loss with this catalyst was also very close to the goal of three percent at the LOPER design inlet pressure and velocity. Based on these results, a configuration consisting of 5.1 cm + 0.6 cm space + 3.8 cm of Catalyst DXD-222 was selected for the LOPER application. This two-stage design was used because no 8.9-cm catalyst support material was available.

Parametric Tests

A limited series of parametric tests was conducted with the selected catalyst to determine the enhancement of CO and HC conversion which could be obtained with additional homogeneous combustion within the catalytic reactor. To promote thermal reaction, tests were conducted at increased catalyst inlet temperatures, as indicated in Table XLVI.

Results of these parametric tests are shown in Figure 58. Predicted catalytic (mass transfer) conversion levels, extrapolated from DXD-222 screening test data, are also shown for two representative velocities. Test points taken early in this series at 36.0 m/s indicated a homogeneous reaction contribution at a temperature of 1233 K. With this contribution, the C_3H_6 conversion goal was very closely approached. No evidence of a significant homogeneous reaction contribution was observed in CO conversion, indicating a higher activation energy for homogeneous combustion of CO than for C_3H_6 .

Data obtained in later test points indicated conversion well below levels predicted by mass transfer considerations. This effect was apparently the result of a deterioration in catalyst activity after the initial high-temperature tests. Posttest inspection of the catalyst indicated that some temperature damage had occurred, possibly from catalyst overtemperature during fuel-air ratio adjustments.

Based on the above tests, it was concluded that both CO conversion and pressure drop goals could be met with the preferred DXD-222 catalyst, and that HC conversion goals could be closely approached with some homogeneous reaction contribution.

Table XLVI. Nominal Catalyst Test Conditions.

<u>Screening Tests</u>				
<u>Pressure,</u> <u>kPa</u>	<u>Catalyst</u> <u>Inlet</u> <u>Temperature, K</u>	<u>Approach</u> <u>Velocity,</u> <u>m/s</u>	<u>Co,</u> <u>ppm</u>	<u>Seed Gases</u> <u>C₃H₆,</u> <u>ppm</u>
203	811	24.4	200/400	200/400
203	811	30.5	200/400	200/400
203	811	36.6	200/400	200/400
203	811	42.7	200/400	200/400
203	1033	24.4	200/400	200/400
203	1033	30.5	200/400	200/400
203	1033	36.6	200/400	200/400
203	1033	42.7	200/400	200/400
<u>Parametric Tests</u>				
203	1256	36.6	600 & 1200	600 & 1200
203	1144	36.6	600 & 1200	600 & 1200
203	1033	36.6	600 & 1200	600 & 1200
203	1256	27.4	600 & 1200	600 & 1200
203	1144	27.4	600 & 1200	600 & 1200

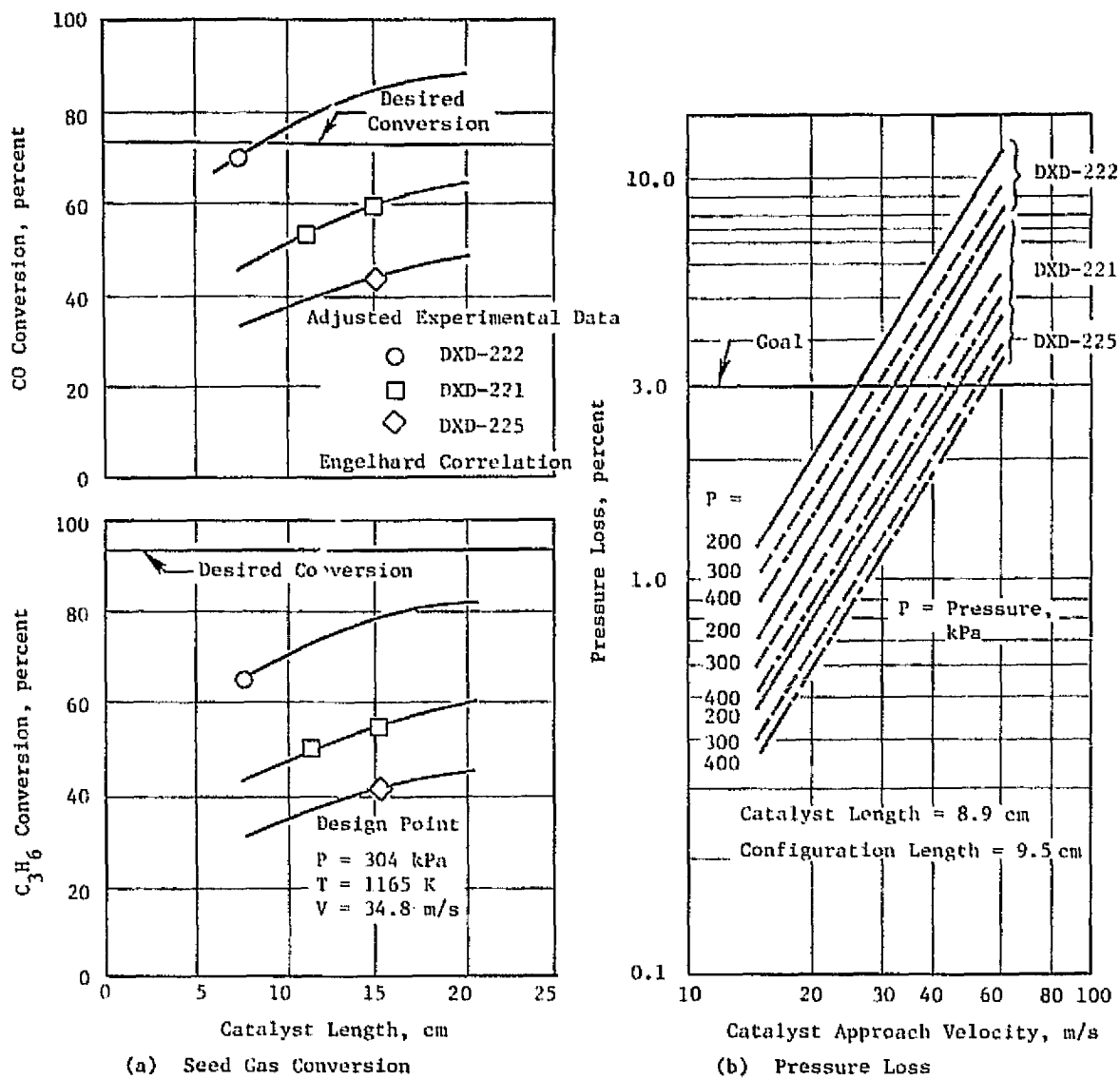


Figure 57. Catalytic Conversion and Pressure Drop Predictions Based on Screening Test Results.

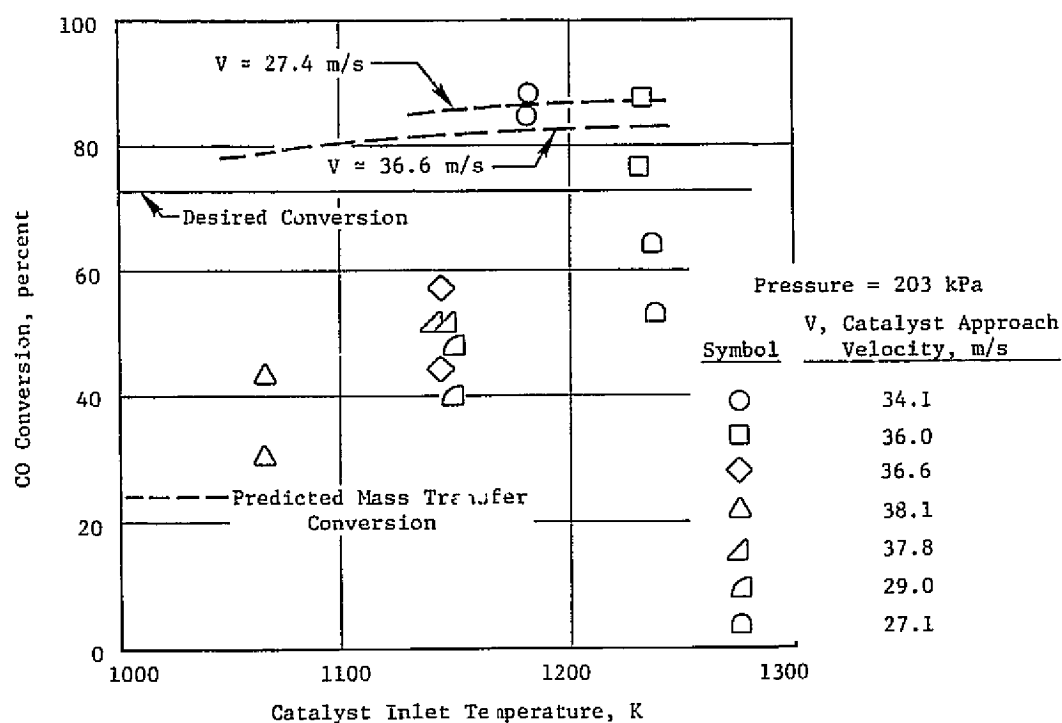
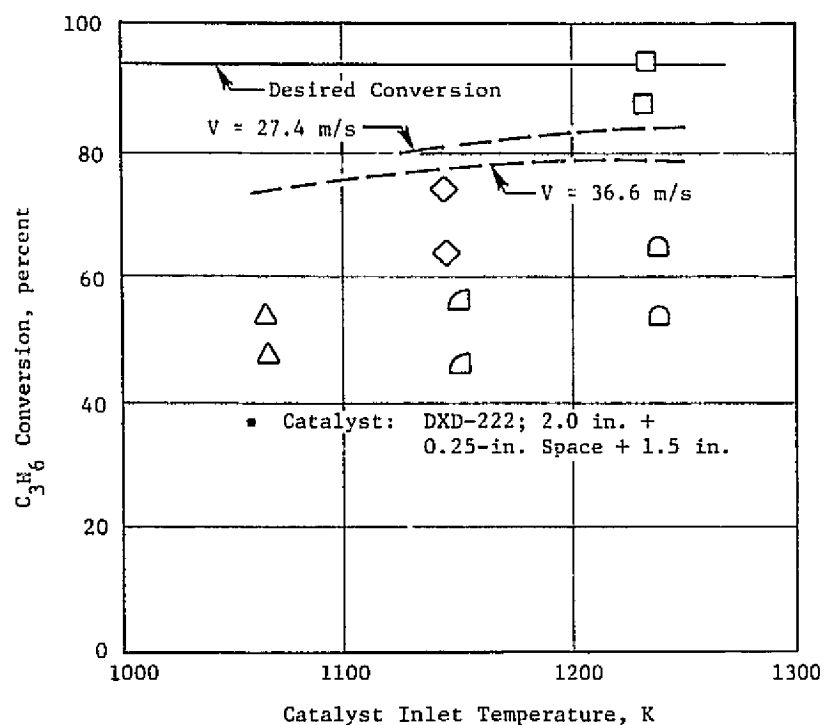


Figure 58. Parametric Test Conversion Performance Catalyst.

APPENDIX D

SYMBOLS

<u>Symbol</u>		<u>Units</u>
A_e	Combustor/Component Effective Flow Area (Geometric Area x Flow Coefficient)	cm^2
A_D	Dome Cross-Sectional Area	m^2
COEI	Carbon Monoxide Emission Index	g/kg
D_b	Secondary Swirler Barrel Diameter	cm
f_m	Metered Combustor Fuel-Air Ratio	g/kg
f_s	Fuel-Air Ratio Calculated from Gas Sample	g/kg
HCEI	Unburned Hydrocarbon Emission Index	g/kg
H_d	Combustor Dome Height	cm
L	Combustor Axial Position Measured From Swirler Exit	cm
L_b	Secondary Swirler Barrel Length	cm
L_c	Total Combustor Length	cm
$\text{NO}_x \text{ EI}$	Oxides of Nitrogen Emission Index	g/kg
P_3	Compressor Discharge (Combustor Inlet) Total Pressure	kPa
P_4	Combustor Exit Total Pressure	kPa
T_3	Compressor Discharge (Combustor Inlet) Total Temperature	K
T_4	Combustor Exit Total Temperature	K
V_c	Total Combustor Volume	m^3
V_r	Combustor Reference Velocity	m/s
W_c, W_{36}	Total Combustor Airflow Rate	kg/s
W_f	Combustor Fuel Flow Rate	g/s
ρ_3	Combustor Inlet Density	kg/m^3

APPENDIX D (Concluded)

<u>Symbol</u>		<u>Units</u>
ΔP_c	Combustor Total Pressure Drop	kPa
ΔP_d	Dome Pressure Drop	kPa